publicaciones técnicas

Thermo-hydro-mechanical characterisation of a bentonite from Cabo de Gata

A study applied to the use of bentonite as sealing material in high level radioactive waste repositories

enresa

publicación técnica 04/2002

Thermo-hydro-mechanical characterisation of a bentonite from Cabo de Gata

A study applied to the use of bentonite as sealing material in high level radioactive waste repositories

María Victoria Villar Galicia
Universidad Complutense de Madrid
Facultad de Ciencias Geológicas
Departamento de Geodinámica

enresa

ENRESA
Dirección de Ciencia y Tecnología
Emilio Vargas nº 7
28043 Madrid - España
Tfno.: 915 668 100
Fax: 915 668 169
www.enresa.es

Diseño y producción: TransEdit
Imprime: GRAFISTAFF, S.L.
ISSN: 1134-380X
D.L.: M-29183-2002
Junio de 2002

This work is a Doctorate Thesis presented to the Department of Geodynamics of the Universidad Complutense de Madrid in September 2000. It has been advised by Dr. Antonio Lloret from the Geotechnical Engineering Department of the Technical University of Catalonia and carried out in the context of the FEBEX Project, financed by ENRESA and the European Commission and coordinated by Fernando Huertas.

The tests have been carried out in the facilities of the Hydrogeochemical Site Characterisation Project of CIEMAT (Centro de Investigaciones Energéticas, Medioambientales y Tecnológicas). Among the persons that have contributed to the design and performance of the tests are Ramón Campos, Alicia Pelayo, Juan Aroz, Joaquín Almendrote and Juan Manuel Durán (CIEMAT), Manuel Cáceres (Mecánica Científica, S.A.), Montserrat Marsal and Dr. José María Manero (Department of Materials Science and Metallurgic Engineering of the Technical University of Catalonia). Joaquín Farias and Miguel Angel Jiménez drew part of the graphical information.

Pedro Rivas, Pedro L. Martín, Pascual Fariña and Dr. Jaime Cuevas have collaborated in the interpretation and analysis of the results, as well as in the revision of the document.

The translation into English has been done by John E. Kennedy – TLS.

página en blanco

Table of contents

Table of contents

Abbreviations and symbols used

Abbreviations and symbols used

AECL	Atomic Energy of Canada Limited
AGP	Almacenamiento Geológico Profundo (*Deep Geological Disposal*)
AITEMIN	Asociación para la Investigación y Desarrollo Industrial de los Recursos Naturales (*Association for the Research and Industrial Development of Natural Resources*) (Madrid)
ANDRA	Agence Nationale pour la Géstion des Déchets Radiactives (*National Radioactive Waste Management Agency*) (France)
ASTM	American Society of Testing Materials
BMT	Buffer Mass Test (Stripa, Sweden)
Boom Clay	Clay formation used as reference host rock in the Belgian disposal concept, constituted by kaolinite/ illite, quartz and inter-stratified.
CEA	Commissariat à l'Énergie Atomique (*Commisariat for Atomic Energy*) (France)
CEDEX	Centro de Experimentación de Obras Públicas (*Civil Works Experimental Centre*) (Madrid)
CIEMAT	Centro de Investigaciones Energéticas, Medioambientales y Tecnológicas (*Centre for Energy, Environment and Technology Research*) (Madrid)
CSIC-Zaidín	Consejo Superior de Investigaciones Científicas – Estación Experimental del Zaidín (*Scientific Research Council – Zaidín Experimental Station*) (Granada)
DOE	Department of Energy (United States of America)
ENRESA	Empresa Nacional de Residuos Radiactivos (*National Radioactive Waste Management Agency*) (Madrid)
EUR	European Commission publication
FEBEX	Full Scale Engineered Barrier Experiment in Crystalline Host Rock
FoCa	French Fourges-Cahaignes smectite, used as the reference material in the ANDRA disposal concept.
G.3S	Groupement pour l'Etude des Structures Souterraines de Stockage (*Underground Disposal Structures Study Group*) (France)
GRS	Gesellschaft für Anlagen-und-Reaktorsicherheit mbH (*German Reactor and Systems Safety Company*)
RH	Relative humidity
RTD	Research and Technological Development
IUPAC	International Union of Pure and Applied Chemistry
LVDT	Linear Variable Differential Transformer
SEM	Scanning Electron Microscopy
NAGRA	Nationale Genossenschaft für die Lagerung Radioaktiver Abfälle *(Swiss radioactive waste disposal agency)*
OECD	Organisation for Economic Cooperation and Development
ONDRAF/ NIRAS	Organisme National pour les Déchets Radioactifs et les matières Fissiles enrichies (*National radioactive waste and enriched fissile materials organisation*) (Belgium)
JNC	Japan Nuclear Cycle Development Institute
HLW	High Level radioactive Wastes
UAM	Universidad Autónoma de Madrid
EU	European Union
ULC	Universidad de La Coruña
UNE	Una Norma Española (*Spanish national technical standard*)
UPC	Universidad Politécnica de Cataluña
UPM	Universidad Politécnica de Madrid
USDA	United States Department of Agronomy
a_s	Specific surface
atm. p.	Atmospheric pressure
C_c	Compression index
C_s	Swelling index
e	Void ratio
I_P	Plasticity index
k	Unsaturated permeability to water
k_g	Permeability to gas
k_{g0}	Permeability to gas of dry soil
k_{ig}	Intrinsic permeability deduced from gas flow measurement
k_{iw}	Intrinsic permeability deduced from water flow measurement

k_r	Relative permeability
k_w	Saturated permeability to water (hydraulic conductivity)
S_r	Degree of saturation
u_a	Air pressure in pores
u_w	Water pressure in pores
w	Water content
w_L	Liquid limit
w_P	Plastic limit
$\in$	Strain
γ_s	Specific gravity
λ	Thermal conductivity
θ	Volumetric water content
ρ_d	Dry density
ρ_w	Density of water
σ	Vertical pressure
σ'_p	Preconsolidation pressure

Resumen

Resumen

El Proyecto FEBEX, iniciado por ENRESA en 1995, es un ensayo de demostración de la posibilidad técnica de construcción e instalación de las barreras de ingeniería de un almacenamiento de residuos de alta actividad en roca cristalina, y de estudio de su comportamiento. El Proyecto consta de un ensayo *in situ* a escala real, en la instalación subterránea de Grimsel (Suiza); de un ensayo en maqueta a gran escala bajo condiciones controladas, en las instalaciones de CIEMAT (Madrid); y de una serie de ensayos de laboratorio que complementan la información de los dos ensayos a gran escala sobre el comportamiento del material de sellado, y soportan los trabajos de modelización que se llevan a cabo simultáneamente.

Este trabajo forma parte del conjunto de ensayos de laboratorio del Proyecto FEBEX, y se centra en la caracterización Termo-Hidro-Mecánica (THM) del material de sellado. Se ha utilizado la bentonita española de referencia, seleccionada por ENRESA a partir de estudios de idoneidad previos, extraída del yacimiento de Cortijo de Archidona en la región de Cabo de Gata (Almería). Se ha tratado de reproducir el comportamiento de la bentonita en condiciones similares a aquéllas en las que se encontrará en la barrera del almacenamiento durante el transitorio de saturación. Para ello se ha trabajado con la bentonita compactada a densidades próximas a las de los bloques de la barrera, se ha sometido el material a diferentes condiciones de saturación, y se ha introducido el factor temperatura en algunos ensayos.

Se ha utilizado la bentonita granulada en fábrica, en la mayor parte de los casos compactada con su humedad higroscópica hasta densidades secas comprendidas entre 1,30 y 1,85 g/cm^3, lo que cubre desde la densidad inicial de los bloques compactados para los ensayos a gran escala del Proyecto FEBEX, hasta la densidad de la barrera una vez saturada en el emplazamiento, incluso con las variaciones locales esperables. Se ha determinado la repercusión de la densidad, del tipo de agua y de la anisotropía en la conductividad hidráulica, en la presión de hinchamiento y en la deformación al saturar. Se han medido la permeabilidad al gas y la conductividad térmica de muestras con diferente grado de saturación. Se ha establecido la curva de retención para diferentes densidades secas en condiciones de volumen libre y confinado, siguiendo trayectorias de secado y humectación, a 20 y a 40 °C. Una parte importante del trabajo contiene los resultados de ensayos edométricos con succión controlada realizados a 20 °C siguiendo diferentes trayectorias de esfuerzos (cargas verticales entre 0,1 y 9 MPa, succiones entre 0 y 550 MPa, por lo que prácticamente todos los estados de hidratación de la bentonita se han explorado). Se incluyen también resultados de ensayos edométricos con succión controlada realizados a 40, 60 y 80 °C.

Se han puesto a punto nuevas técnicas experimentales –como las de medida de la permeabilidad al gas, determinación de la curva de retención a volumen constante y realización de ensayos edométricos con control de succión y temperatura– dado que, debido al comportamiento de este tipo de materiales (alta expansibilidad, muy baja permeabilidad, succiones en el agua muy altas), las técnicas de ensayo habituales en mecánica del suelo son de difícil aplicación.

El análisis de los resultados obtenidos resalta la repercusión de la microestructura en el comportamiento macroscópico del material. Los resultados de los ensayos representan un avance en el conocimiento de las propiedades de las arcillas expansivas y pueden ser de gran utilidad para los investigadores dedicados a los fenómenos de deformación y flujo en los materiales arcillosos utilizados como barreras en almacenamientos de residuos. En particular, en lo que se refiere a la caracterización del comportamiento de un material expansivo, se destacan las siguientes conclusiones:

- Cuando la arcilla se satura a volumen constante, impidiéndose su expansión, el agua que entra adquiere una densidad superior a 1,00 g/cm^3.
- El aumento de densidad seca de la muestra produce una disminución exponencial de la permeabilidad.
- La permeabilidad intrínseca de muestras de igual porosidad varía con el grado de saturación, pudiendo llegar a haber hasta ocho órdenes de magnitud de diferencia entre la muestra seca y saturada.
- La conductividad hidráulica aumenta ligeramente cuando se utiliza como permeante agua salina en lugar de agua granítica o destilada.
- La succión de la bentonita FEBEX es muy elevada y fundamentalmente de tipo matricial, siendo inapreciable la contribución de la succión osmótica.
- La capacidad de retención de agua de la arcilla está muy condicionada por su estado de confinamiento. La diferencia entre las humeda-

des alcanzadas para una misma succión a volumen libre y confinado se hace más notable para succiones por debajo de determinado valor, que depende de la densidad seca y que marca el límite entre succión intra e interagregado.

- La relación entre succión y humedad determinada a volumen libre puede expresarse mediante una ley logarítmica.
- Las curvas de retención a volumen constante presentan histéresis.
- La presión de hinchamiento de la bentonita se relaciona con la densidad seca mediante una ley exponencial.
- Los bloques compactados no muestran anisotropía respecto a la conductividad hidráulica, a la presión de hinchamiento ni a la capacidad de retención.
- El cambio de volumen durante la hidratación –cuya componente es mayoritariamente microestructural–, disminuye de intensidad cuanto mayor es la sobrecarga bajo la que se realiza. La expansión de la microestructura por hidratación bajo una carga pequeña da lugar a una reorganización de la macroestructura, que se hace más porosa, produciéndose un aumento de volumen irreversible. Durante esta expansión microestructural se produce también una disminución de la presión de preconsolidación.
- La presión de hinchamiento de la muestra no saturada aumenta de forma logarítmica en el intervalo de succión comprendido entre los 130 MPa (la succión correspondiente a la humedad higroscópica) y los 10 MPa, pero por debajo de este valor el aumento se atenúa. Para succiones superiores a los 200 MPa apenas se desarrolla presión de hinchamiento.
- El secado de la muestra por reducción de la succión hasta valores próximos a 500 MPa no conlleva prácticamente variación de volumen. Para succiones por encima de este valor, la carga externa tampoco produce consolidación importante en la muestra, que se hace rígida.
- El secado de la muestra por aumento de la succión hasta 500 MPa no modifica su capacidad de hinchamiento durante la hidratación posterior, ni tampoco su presión de hinchamiento una vez saturada.
- El aumento de la temperatura hasta 80 °C en los ensayos edométricos con succión controlada parece inducir una rigidificación del material, aumentando su presión de preconsolidación y limitando su capacidad de hinchamiento.

Por otra parte, las principales conclusiones de este trabajo, en lo que se refiere al uso de bentonita como material de sellado en almacenamientos de residuos radiactivos de alta actividad, son:

- La elevada succión de la bentonita instalada en el almacenamiento en forma de bloques de alta densidad, fabricados a partir del granulado de arcilla con su humedad higroscópica, será el motor fundamental de la saturación de la barrera con el agua proveniente del macizo circundante. Pero, a medida que la arcilla se va saturando, su permeabilidad intrínseca disminuye, al disminuir el tamaño de los canales de flujo, a la vez que disminuye el gradiente de succión, por lo que el proceso de saturación será progresivamente más lento. Esta disminución en el flujo sólo se verá en parte compensada por el aumento de la permeabilidad relativa al aumentar la saturación.
- Simultáneamente a la hidratación tiene lugar la expansión de la bentonita en aquellos lugares donde existe espacio para ello. De esta manera, el hinchamiento y la elevada succión de la bentonita impiden también que las juntas entre bloques se conviertan en canales preferentes para el flujo de agua, puesto que el agua que entra en contacto con la bentonita es inmediatamente absorbida, provocando su expansión y el sellado de cualquier tipo de grieta. Así mismo, el hueco entre los bloques de bentonita y la pared de la galería se cerrará por este mismo proceso. En las zonas donde la bentonita está confinada, la presión de hinchamiento ejercida por la arcilla irá aumentando con la saturación de forma logarítmica, con lo que se produce la compresión de las zonas más secas y el aumento de su densidad.
- Los ensayos edométricos con succión controlada han mostrado que durante la hidratación de la bentonita compactada pueden tener lugar deformaciones irreversibles, que son mayores cuanto menor es la sobrecarga. En la barrera, por estar confinada, la sobrecarga sobre la bentonita será siempre importante, por lo que no es previsible que se produzcan deformaciones irreversibles durante la hidrata-

ción, excepto en las juntas entre bloques y en la periferia, donde el espacio entre la bentonita y la roca puede ser suficiente para permitir la expansión libre de la arcilla. De esta manera, quedaría un anillo exterior en el que la bentonita tendría una densidad seca menor –que ya no se recuperaría– y una humedad más elevada. Este anillo podría constituir un aprovisionamiento de agua y aseguraría su reparto homogéneo sobre toda la superficie de la barrera.

- Por otra parte, el secado de la bentonita que tiene lugar en las proximidades del contenedor debido al aumento de la temperatura, siempre que no produzca una reducción de su humedad por debajo del 4-6 %, no producirá en ella una reducción de volumen significativa, puesto que por encima de la succión correspondiente a la humedad higroscópica, la muestra se hace muy rígida. Esto impedirá que la formación de grietas de retracción y canales de flujo preferentes sea importante.
- La elevada succión generada por el secado, al aumentar los gradientes hidráulicos, puede acelerar la llegada del agua a las partes internas de la barrera. Se ha comprobado que el secado hasta humedades del 4-6 % no reduce la capacidad de hinchamiento de la bentonita, por lo que las propiedades hidro-mecánicas del material no se verán alteradas tras el transitorio, y con la llegada del agua se producirá la expansión de la bentonita y el confinamiento del contenedor.
- Una vez saturada la barrera, y considerando que la densidad seca del conjunto sea de entre 1,60 y 1,65 g/cm^3, la permeabilidad de la barrera estará comprendida entre 10^{-13} y 10^{-14} m/s, y su presión de hinchamiento entre 4 y 10 MPa. El posible aumento de la densidad del agua al ser adsorbida por la bentonita compactada, puede ocasionar que el volumen de agua necesario para saturar la barrera sea hasta un 20 % mayor que el previsto al hacer el cálculo considerando la densidad del agua igual a 1,00 g/cm^3.
- La conductividad térmica de los bloques de bentonita FEBEX saturados –entre 1,2 y 1,3 W/m·K–, es suficiente para favorecer la disipación del gradiente térmico generado por la desintegración del residuo. En cualquier caso, el impacto de la temperatura sobre las propiedades analizadas no parece ser drástico.

página en blanco

Abstract

Abstract

The FEBEX Project, initiated by ENRESA in 1995, is a test designed to demonstrate the technical feasibility of manufacturing and installing the engineered barriers for a high level waste disposal facility in crystalline rock and to study their behaviour. The Project consists of a full-scale *in situ* test, performed at the Grimsel underground facility (Switzerland), of a large-scale mock-up test carried out under controlled conditions at the CIEMAT installations (Madrid) and of a series of laboratory tests designed to complement the information acquired from the two large-scale tests on the performance of the sealing material and provide a basis for the modelling work carried out simultaneously.

This work is part of the set of laboratory tests performed within the FEBEX Project, and focuses on the Thermo-Hydro-Mechanical (THM) characterisation of the sealing material. The Spanish reference bentonite has been used, selected by ENRESA from previous suitability studies and extracted from the Cortijo de Archidona deposit in the Cabo de Gata region (Almería). Attempts have been made to reproduce the behaviour of the bentonite under conditions similar to those that will be found in the disposal barrier during the saturation transient. For this purpose, work has been carried out with the bentonite compacted to densities close to those of the barrier blocks, the material has been subjected to different saturation conditions and the temperature factor has been introduced in certain tests.

The determinations were carried out on the granulated bentonite compacted, in most of the cases with its hygroscopic water content, at dry densities of between 1.30 and 1.85 g/cm^3, this covering from the initial density of the compacted blocks used for the large scale tests of the FEBEX Project to the density of the barrier once saturated at the emplacement, including even the local variations to be expected. The repercussion of material density, water type and anisotropy on hydraulic conductivity, on swelling pressure and on strain upon saturation has been tested. Permeability to gas and thermal conductivity have been measured in samples with different degrees of saturation. The retention curve for different dry densities has been determined under free and constant volume conditions, following drying and wetting paths, at 20 and 40 °C. An important part of the work contains the results of suction controlled oedometric tests performed at 20 °C following different stress paths (vertical loads from 0.1 to 9 MPa, suctions from 0 to 500 MPa, as a result of which practically all the hydration states of the bentonite have been explored). The results of suction controlled oedometric tests performed at 40, 60 and 80 °C are also included.

New experimental techniques have been fine tuned up –like those for measurement of the permeability to gas, determination of the retention curve at constant volume and performance of suction and temperature controlled oedometric tests– as, due to the special behaviour of this type of materials (high expansibility, very low permeability, very high suction), the soil mechanics standard testing techniques are difficult to apply.

The analysis of the results dealt with in this work underline the repercussion of the microstructure on the macrostructural behaviour. The tests results represent an advance in the knowledge of the properties of expansive clays and may be useful for those researching the flow and strain phenomena in the clayey materials used as barriers in waste repositories. In particular, with respect to the characterisation of an expansive material, the following conclusions can be highlighted:

- When the clay saturates at a constant volume, expansion being prevented, the water entering acquires a density in excess of 1.00 g/cm^3.
- The increase of the dry density of the sample gives rise to an exponential decrease in permeability.
- Hydraulic conductivity increases slightly when saline water is used instead of granitic or distilled water as the permeating agent.
- The intrinsic permeability of samples having the same porosity varies with the degree of saturation, with differences of up to eight orders of magnitude between dry and saturated samples.
- The suction of the FEBEX bentonite is very high and fundamentally of the matric type, with the contribution made by osmotic suction being inappreciable.
- The water retention capacity of the clay is conditioned to a large extent by the state of confinement. The difference between the water contents reached for a given value of suction under free volume and confined conditions becomes more appreciable for suctions below a given value, which depends on dry density and indicates the limit between intra and inter-aggregate suction.
- The suction/water content relation determined under free volume conditions may be expressed by means of a logarithmic law.

- The retention curves at constant volume show hysteresis.
- The swelling pressure of bentonite relates to dry density by way of an exponential law.
- The compacted blocks do not show anisotropy with respect to either hydraulic conductivity, swelling pressure or retention capacity.
- The change in volume during hydration –whose main component is microstructural– decreases in intensity the higher the overload under which it occurs. The expansion in the microstructure as a result of hydration under low load gives rise to a reorganisation of the macrostructure, which becomes more porous, an irreversible increase in volume occurring. During this microstructural expansion there is also a decrease in preconsolidation pressure.
- The swelling pressure of the unsaturated sample increases logarithmically in the interval of suctions of between 130 MPa (the suction corresponding to hygroscopic water content) and 10 MPa, although below this value the increase is attenuated. For suctions in excess of 200 MPa, there is hardly any development of swelling pressure.
- The drying of the sample by decreasing suction to values of around 500 MPa involves practically no variation in volume. For suctions above this value, the external load does not cause any important consolidation in the sample, which becomes rigid.
- Drying of the sample by increasing suction to 500 MPa does not modify either its swelling capacity during subsequent hydration or its swelling pressure once saturated.
- The increase in temperature to 80 °C in the controlled suction oedometric tests performed would appear to induce a hardening of the material, increasing its preconsolidation pressure and limiting its swelling capacity.

The main conclusions concerning the use of bentonite as sealing material in HLW repositories are summarised below:

- The high value of suction of the bentonite installed in the disposal facility in the form of high density blocks manufactured from the clay granulate with its hygroscopic water content will be the fundamental force driving the saturation of the barrier with the water from the surrounding massif. However, as the clay saturates, its intrinsic permeability will decrease, as the size of the flow channels becomes smaller, this being accompanied by a decrease in the suction gradient, as a result of which the saturation process will become steadily slower. This reduction in flow will be compensated only in part by the increase in relative permeability occurring with increasing saturation.
- Simultaneously with hydration there will be expansion of the bentonite in those areas in which there is space for this to occur. In this way, the swelling and high level of suction of the bentonite will also prevent the joints between blocks becoming preferential channels for the flow of water, since water coming into contact with the bentonite will be immediately absorbed, causing the latter to expand and to seal any type of joint. Likewise, the gap between the bentonite and the wall of the drift will be closed by this same process. In those areas in which the bentonite is confined, the swelling pressure exercised by the clay will increase logarithmically with saturation, causing compression of the drier areas and an increase in their density.
- The controlled suction oedometric tests have shown that during the hydration of the compacted bentonite irreversible strains may occur, these being larger the lower the overload. In the barrier, and due to its being confined, the overload of the bentonite will in all cases be important, therefore irreversible strains are not expected to occur during hydration, except at the joints between the blocks and at the periphery, where the space between the bentonite and the rock may be sufficient to allow for free expansion of the clay. As a result, there would be an outer ring in which the bentonite would have a lower dry density –which would no longer be recovered– and a higher water content. This ring might constitute a source of water supply and would ensure its homogeneous distribution across the entire surface of the barrier.
- Furthermore, the drying of the bentonite that occurs in the vicinity of the canister due to increasing temperature, as long as water content does not decrease below 4-6 percent, will not cause any significant reduction in volume, since above the value of suction corresponding to hygroscopic water content the sample becomes very rigid. This will prevent the forma-

tion of shrinkage cracks and preferential flow channels from becoming important.

- The high suction generated by drying may, with increasing hydraulic gradients, speed up the arrival of water to the internal areas of the barrier. It has been seen that drying to water contents of 4-6 percent does not reduce the swelling capacity of the bentonite, as a result of which the hydro-mechanical properties of the material will not be altered following the transient period, and with the arrival of water the bentonite will expand and the canister will be confined.
- Once the barrier is saturated, and taking into consideration that the dry density of the assembly is between 1.60 and 1.65 g/cm^3, its permeability will be between 10^{-13} and 10^{-14} m/s, and its swelling pressure between 4 and 10 MPa. The possible increase in the density of the water on being adsorbed by the compacted bentonite may cause the volume of water required to saturate the barrier to increase by up to 20 percent over that foreseen by the calculations considering the density of the water to be equal to 1.00 g/cm^3.
- The thermal conductivity of the saturated blocks of FEBEX bentonite –between 1.2 and 1.3 W/m·K– is sufficient to favour the dissipation of the heat generated by decay of the radioactive wastes. In any case, the impact of temperature on the properties analysed does not appear to be drastic.

página en blanco

1. Introduction

1. Introduction

Deep geological disposal is considered to be a realistic solution for the definitive disposal of long-lived, heat-emitting high level radioactive wastes (HLW). The safety of this disposal concept is based on the existence of a series of superimposed barriers: natural barriers, constituted by the host rock, and artificial barriers, constituted by the solid matrix of the waste itself, the metallic canister and its backfill, the sealing materials placed around the canister and the material backfilling the drifts of the installation.

High level radioactive waste disposal programmes are required to optimise the guarantees of validity of the systems designed and long-term safety. For this purpose, contrasted models are developed and applied that simulate the different phenomena controlling the release and migration of radionuclides from the disposal facility to the biosphere and that predict dose rates to people in the long term. In order to apply these models, accurate data must be available on the different components of the system: the geosphere, *i.e.* the host rock that constitutes the main barrier to the migration of radionuclides to the biosphere; the waste, whose long-term physical and chemical characteristics under different conditions must be known; the engineered barrier, with the different backfill and sealing materials; and the processes that may take place within the environment of the disposal facility, modifying the properties of the barriers and impacting radionuclide migration. The following are among these processes: saturation of the engineered barriers and the dissipation of heat across them, modification of the geochemical environment, corrosion of the canister, gas generation, the alteration/dissolution of the waste, radionuclides release and their diffusion and sorption in the barriers, and incorporation into the underground hydrological system. In order to gain reliable insight into these processes, the following is required: characterisation of the candidate sealing and backfilling materials, validation of the geochemical models describing the behaviour of the radionuclides in the near field, study of gas generation and their migration in the barrier, demonstration of the effectiveness of the sealing material with respect to hydraulic or gas pressures and research into the reaction of the geological medium to increasing temperature and radiation, among others.

Crystalline rocks (granite, basalt), clays and salts have been proposed as the surrounding geological material. The disposal concepts include the placing of a sealing material between the canister and the host rock, this usually being made up for the most part by bentonites, except in the case of the salt option. Bentonites are rocks made up of clay minerals and belonging to the smectites group, formed by the devitrification and accompanying chemical alteration of vitreous igneous materials. Their physical and chemical properties –low permeability, high swelling potential, high retention capacity, plasticity and mechanical resistance– make them ideal for this use. Their acceptable thermal conductivity, which is necessary to contribute to the dissipation of the heat generated by the wastes; good compressibility, guaranteeing the possibility of manufacturing blocks; and longevity in the presence of high temperatures and chemical gradients, are other valued characteristics.

In relation to the granite and clay disposal options, the Spanish deep geological disposal concept for radioactive wastes (AGP) considers the placing of compacted bentonite blocks around the canisters as the sealing material. The layer of bentonite will measure 0.75 m in thickness and the temperature inside will not exceed 100 C. The blocks will be manufactured from a clay granulate material with its hygroscopic water content, as a result of which they will not initially be saturated. In view of the low permeability of the bentonite, the barrier will take a relatively long time to become saturated, and this process will take place in the presence of a thermal gradient. The repercussions of this transient phase on the subsequent behaviour of the clay barrier are still under study.

For technical reasons, and in view of the timescales involved, the mathematical modelling of the Thermo-Hydro-Mechanical (THM) behaviour of the clay is the main tool used to assess the long-term performance of disposal facilities. This modelling must be based on profound knowledge of the basic physical, physico-chemical and mechanical phenomena involved. The numerical simulations of the long-term behaviour of the disposal facility must be guided by experimental research that serve also to validate the models through comparison of the calculations with observations made in the field or laboratory (Hueckel & Peano 1996). The models must be validated on two scales: time and space. The first refers to the extrapolation of the validity of the models beyond the timescale of the tests. The second is related to spatial variability and to lack of homogeneity within the clay barrier, as well as to the representativeness of the volume of clay used in the tests. The question of the timescale is addressed through the study of natural analogues. The problem of the spatial scale is resolved through experimentation on three scale levels: beginning with the small scale,

with laboratory tests on homogeneous samples, followed by tests on an intermediate scale, in which thermohydraulic cells, calibration chambers and large triaxial cells are used, and finishing with large-scale tests, *in situ* second generation tests, among which the FEBEX Project is included.

The FEBEX Project, initiated by ENRESA in 1995, is a test designed to demonstrate the technical feasibility of installing the engineered barriers for a high level waste disposal facility in crystalline rock and to study their behaviour. The Project consists of a full-scale *in situ* test, performed at the Grimsel underground facility (Switzerland), of a large-scale mock-up test carried out under controlled conditions at the CIEMAT installations (Madrid) and of a series of laboratory tests designed to complement the information acquired from the two large-scale tests on the performance of the sealing material and provide a basis for the modelling work carried out simultaneously (ENRESA 2000).

The work presented in this Doctorate Thesis is part of a set of laboratory tests performed within the FEBEX Project, and focuses on the thermo-hydro-mechanical characterisation of the sealing material. The Spanish reference bentonite has been used, selected by ENRESA from suitability studies performed between 1987 and 1991 by various organisations and extracted from the Cortijo de Archidona deposit in the Cabo de Gata region (Almería). CIEMAT participated actively in the characterisation of this material and since 1991 has focused its intervention on the thermo-hydro-mechanical and geochemical aspects of its behaviour. For the FEBEX Project attempts have been made to reproduce the behaviour of the bentonite under conditions similar to those that will be found in the disposal barrier during the saturation transient. For this purpose, work has been carried out with the bentonite compacted to densities close to those of the barrier blocks, the material has been subjected to different saturation conditions and the temperature factor has been introduced in certain tests.

The experimental study of highly compacted and particularly expansive materials poses serious difficulties, and is not a habitual practice in geotechnical laboratories. For this reason, there are no conventional laboratory techniques for their hydromechanical characterisation, which in any case is usually addressed only under saturated conditions. Furthermore, the experimental information on unsaturated materials is limited, especially for the case of expansive clays with a high suction, as is the case of bentonite. Indeed, most of the experimental studies carried out in this area in recent years have taken place within the context of the study of engineered barriers in radioactive waste disposal facilities. For these reasons, the present Doctorate Thesis is encompassed in a novelty area of research that is still in the development phase.

Objectives

In view of what has been said above, the fundamental objective of the work presented below is to establish the basis of knowledge required to understand the behaviour of bentonite as a sealing material for a radioactive waste disposal facility, in order to be able to model its evolution during the operating period of such an installation. This objective has been addressed gradually, by way of a stepwise approach based on the following partial objectives:

- Development and fine tuning of experimental equipment and techniques allowing expansive materials to be studied in the saturated and unsaturated state.
- Determination of the basic physical characteristics of the reference bentonite used in the FEBEX Project as a sealing material.
- Characterisation of the thermo-hydro-mechanical behaviour of the bentonite subjected to the conditions of the barrier.

Structure of the thesis

This Doctorate Thesis has been structured into an INTRODUCTION, seven chapters and two APPENDICES.

The chapter on the BACKGROUND places this work within the context of the research performed nationally and internationally on deep geological disposal. The chapter reviews the main research projects and programmes on clay barriers for high level radioactive waste disposal facilities carried out by the international community. It then goes on to describe the processes of selection and initial characterisation of the Spanish reference sealing material. Finally, the general features of the FEBEX Project are presented, as an advanced milestone in the study of the clay barrier in Spain.

A chapter on the THERMO-HYDRO-MECHANICAL BEHAVIOUR OF EXPANSIVE CLAYS has been in-

cluded, since these are materials that present peculiarities whose study is not normally addressed systematically. The chapter begins with a synthesis of the properties and hydromechanical behaviour of smectites. There is a description also of the configuration of the bentonite in an engineered barrier and of the processes that are expected to take place during the transient saturation phase. Finally, there is a review of the main experimental techniques and developments applied to the study of expansive, unsaturated materials, including the suction control techniques.

The chapter on the MATERIAL describes the geological context of the Cortijo de Archidona deposit from which the bentonite originates, and the processing to which the batch extracted for the FEBEX Project was subjected. The mineralogical and chemical characteristics of this material, determined during the initial phase of the Project, are also summarised in this chapter.

The chapter on METHODOLOGY describes the experimental techniques applied in this work for determination of the basic characteristics of the bentonite, the study of its microstructure and determination of hydraulic conductivity, permeability to gas, swelling pressure, deformation on saturation and thermal conductivity. There is an explanation also of the suction control techniques used and their application in determining the retention curves and in performing the controlled suction oedometric tests.

The RESULTS obtained are classified into four subchapters: basic, hydraulic, mechanical and thermal characterisation. The results tables and figures are included in the text, with the exception of the complete porosimetric analysis and oedometric testing data, which are included in Appendices I and II. The chapter on RESULTS also includes a subchapter in which there is a discussion of the density value of the water in the saturated bentonite, deduced from the results of various tests.

Finally, the CONCLUSIONS of the work are presented classified into four groups: conclusions regarding the experimental procedures and techniques, those referring to the thermo-hydro-mechanical characterisation and behaviour of expansive materials, conclusions regarding the knowledge of the clay barrier and orientations for subsequent research.

Finally, the bibliographic references used in drawing up this report are listed in the chapter BIBLIOGRAPHY.

página en blanco

2. Background

2. Background

The bentonite characterisation studies presented in this work have been performed within a highly precise context: the use of this material as an insulating medium for high level radioactive waste disposal facilities. For this purpose, its characteristics have been analysed from different points of view and under representative conditions that have conditioned the entire research. The following sections establish the functions of the barrier material and explain why bentonites were selected for this purpose and how their study evolved within this context, with special reference to the Spanish case.

The geological disposal of radioactive wastes

Radioactive wastes are considered to be any substance that contains or is contaminated with radionuclides in concentrations higher than those established by the competent authorities and for which no subsequent use is foreseen. Such wastes are produced during the generation of electricity using nuclear means, in the decommissioning of nuclear and radioactive installations and in the use of radioisotopes in industry, medicine, agriculture, research, etc.

From the point of view of definitive disposal, radioactive wastes are generally classified into low and intermediate level wastes and high level wastes. The latter have high specific short-lived emitter activities, contain appreciable concentrations of long-lived alpha-emitting radionuclides and are major heat producers (Echagüe *et al.* 1989).

The solution as regards protecting people and the environment against the radiations emitted by the radionuclides contained in high level wastes consists in isolating them in such a way that throughout the period in which they remain active they cannot be released to the biosphere along any of the possible paths. The generally accepted option for the definitive disposal of high level wastes (HLW) consists in their disposal in stable deep geological formations (500-1000 m) (Goguel *et al.* 1987), as was suggested by the United States National Academy of Science in the 1950's. In order to guarantee isolation, a series of natural and artificial barriers is put into place (Figure 1):

1. The chemical barrier, which is constituted by immobilising the waste in a solid, stable, long-lasting and chemically inert matrix.
2. The physical barrier, which is the high corrosion resistance canister in which the immobilised wastes are confined.
3. The engineered barrier, which is the installation in which the wastes are placed, made up of a series of chambers, shafts and drifts in which the canisters are introduced. The diameter of these excavations is always larger than that of the canister, the remaining space being surrounded by appropriate materials known as sealing materials, the chambers and access shafts being plugged with the so-called backfill material.
4. The geological barrier, constituted by the geological medium housing the installation (salts, granites, clays, basalts or volcanic tuffs) and the surrounding geological formations.

The system of barriers aims to remove the possible escape paths for the radionuclides to the environment, the most important of which is the circulation of groundwaters. In this context, the basic functions of the sealing material are to prevent or limit the entry of water to the wastes and to contribute to radionuclide retention. Other additional functions are to contribute to heat dissipation and to provide mechanical protection for the waste canisters.

Bentonites as backfill and sealing material

Bentonites are rocks made up of crystalline clay minerals formed by the devitrification and accompanying chemical alteration of vitreous igneous materials, normally volcanic tuffs or ashes (Ross & Hendricks 1945). The clay minerals present in bentonites belong to the smectites group, in which montmorillonite is the most common species.

In view of the functions of the sealing material described in the previous section, Pusch (1979) proposed the use of high density compacted sodium bentonite in the form of blocks as a sealing material, since it provides the following characteristics:

- Very low permeability, reducing the percolation of groundwaters, since hydrogeological transport is the main radionuclide transfer mechanism.
- High exchange capacity, and therefore a high capacity for ion adsorption in the event of radionuclide release.

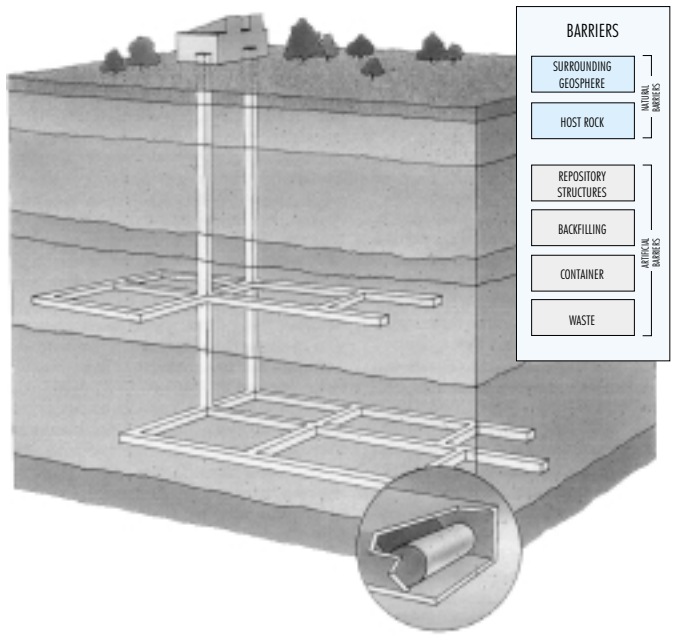

Figure 1. Schematic representation of the concept of multiple barriers in a geological disposal facility.

- Sufficient thermal conductivity, to prevent the generation of excessive thermal gradients.
- Mechanical resistance to withstand the weight of the canister.
- Mechanical properties guaranteeing the homogeneous nature of the barrier, this including plastic behaviour to prevent the formation of fissures as a result of differential displacements or the location of stresses, and swelling potential favouring the self-sealing of existing voids.

Other material requirements of the barrier that have been underlined in subsequent research (Yong *et al.* 1986) are as follows:

- Good compressibility, ensuring ease in processing, handling and transport to the disposal facility.
- Low shrinkage in response to the drying that will probably occur in the area surrounding the canister, in order to prevent the formation of a network of fissures.
- Non-excessive swelling pressure, to avoid damage to the system.
- Suitable deformability, ensuring that the pressures generated by the rock massif and by the hydration of the expansive component of the barrier are absorbed and reduced by deformation of the barrier itself.
- Physical and chemical stability, ensuring the longevity of the system in relation to the conditions of the disposal facility, *i.e.* high temperatures, chemical gradients and the presence of vapour (Pusch & Gray 1989, Güven 1990).

Since the end of the 1980's, the agencies in charge of waste management in different countries have proposed other sealing materials, some based on the use of cement but most considering the use of bentonites, either non-sodic smectites (ANDRA, France; ENRESA, Spain) or mixtures of expansive clay and aggregates in different proportions. As regards the aggregates, tests have been performed using crushed granite (AECL, Canada), crushed basalt (DOE, United States), zeolytes and quartz (JNC, Japan), quartz and graphite (ANDRA, France; ONDRAF/NIRAS, Belgium). The main objective of adding inert aggregates is to increase the thermal conductivity of the barrier, improve the mechanical

resistance of the compacted blocks and reduce the cost of the material.

Although most of the studies have been carried out considering that the emplacement of the barrier will be made in the form of pre-compacted blocks, other systems have been proposed, among them the use of high density bentonite pellets combined with powdered bentonite that, once saturated and with the density of the overall assembly homogenised, give rise to a barrier density equivalent to that achieved with compacted blocks (Salo & Kukkola 1989; Volckaert *et al.* 1996). The advantage of this system is that it is easy simple to manufacture and install, especially in emplacements in the form of vertical shafts.

International activities in the field of geological disposal: clay barrier

The design of geological disposal facilities for long-lived, heat-emitting high level radioactive wastes poses complex problems, which are mainly addressed through international collaboration in inter-disciplinary research projects. This section looks at certain of the activities carried out by the international community in this area, with special reference to those relating to the engineered barrier, and more specifically to the sealing material.

Since 1982, the US Department of Energy (DOE) has been responsible for the construction and operation of a geological disposal facility for high level wastes. In this respect, nine possible sites were selected in 1983, and preliminary studies were carried out; these led in 1985 to the selection of three for intensive characterisation activities: Hanford (Washington), Deaf Smith County (Texas) and Yucca Mountain (Nevada). In 1987 the US Congress determined that the studies should be performed only at the last of these sites, this leading to the creation of the Yucca Mountain Project, the objective of which was to determine whether the site was suitable. With this aim in mind, studies were performed on the geology, hydrogeology, biology and climate of the area. In 1993, the excavation of an underground laboratory began, at a depth of 300 m, this being used to investigate the system of fractures, the response of the rock to stresses and heat, the movements of water and gas and radionuclide migration. The installation is excavated in a volcanic tuff, above the water table. The galleries are expected to be lined with concrete and the canisters to be placed on concrete platforms with specific protection against humidity.

The Japanese high level radioactive waste management programme, on the other hand, includes consideration of the multi-barrier concept for deep geological disposal. In view of the complex geology of the country –which is located in a tectonically active region– special emphasis is laid on the role of the near field. The disposal facility is expected to be excavated at a depth of 1000 m, in the case of hard rock, and 500 m if the rock is soft, with both the horizontal drift and vertical shaft options being possible. As regards the sealing material, the main studies performed refer to resaturation of the system of barriers, deformation due to expansion of the canister as it corrodes, settling of the canister, seismic stability, gas migration, extrusion of the sealing material through the fractures in the host rock and the possibility of manufacturing and installing this material. The material chosen for sealing is a mixture of quartz sand and bentonite in a proportion of 70/30, this being compacted to a dry density of 1.6 g/cm^3, with a thickness of between 0.4 and 0.7 m. Both the *in situ* compaction methods and the installation of the blocks have been tested at the Kamaishi mine. There is also an underground research facility at Gifu, known as Mizuname, and an installation for research into Geological Disposal is being built at the Tokai prototype nuclear power plant.

In Canada also, studies have been under way on the development of a permanent disposal method for nuclear waste since 1978. The disposal concept foresees the excavation of a network of tunnels, shafts and rooms in stable rock formations, at depths of between 500 and 1000 m. The canisters will be emplaced in the rooms or in shafts perforated in them, and all voids will be backfilled with an appropriate material. The research has included the construction of an underground laboratory excavated in the Canadian granite shield at a depth of 420 m, at the Whiteshell facilities (Manitoba). The underground migration of water and contaminants is monitored in this laboratory, and electrical heaters are used to simulate the heat generated by the wastes.

In Europe, a Swedish-American project (SAC, Swedish American Cooperation) was carried out between 1977 and 1980 in an iron mine excavated in granite at Stripa (Sweden). The Project comprised three main parts: heating experiments using simulated waste containers, assessment of fissure hydrology and geophysical measurements. Extensive informa-

tion was obtained on the mechanical reactions of rock in response to heat and on water flows in a fissured crystalline medium. These results attracted the attention of other countries, and around 1980 the Stripa international project got under way, an autonomous OECD activity for the development and testing of techniques for the isolation of high level radioactive wastes, with the participation of Canada, Finland, France, Great Britain, Japan, Sweden and the United States. The Project was led by SKB, the Swedish nuclear waste and fuel management agency, and included geophysical, geochemical and hydrogeological studies, as well as field tests on the sealing of radioactive wastes simulated using clay materials. The Project was undertaken in two consecutive phases, from 1980 to 1985 and from 1986 to 1991. Particularly significant among the larger scope tests performed at the Stripa mine, for its innovation and the repercussion that it has had on subsequent research, was the so-called Buffer Mass Test (BMT). The general aim of the BMT was to check the behaviour of certain sealing materials based on bentonite under real conditions, along with the techniques required for their preparation, handling and installation (Pusch *et al.* 1985). The test was located in a 30-metre long gallery, excavated at a depth of 340 m in the Stripa mine, and consisted of six shafts measuring some 3 m in depth and 0.76 m in diameter, housing electrical heaters surrounded by blocks of compacted, unsaturated sodium bentonite. The power of the heaters simulated the production of heat by the waste container (125 °C). A part of the gallery was backfilled with a mixture of sand/bentonite compacted *in situ*, and the shafts not located in this part of the gallery were plugged with a mixture of sand/bentonite covered by a slab of concrete measuring 1.6 m in thickness (Figure 2). During the test the temperatures, swelling pressures and water pressure in the granitic rock and sealing material were monitored, along with the water content of the clay, the relative displacement between the different components and variations in fracture opening.

After a year of testing, the physical properties (microstructure, swelling pressure, hydraulic conductivity) and chemical properties of the material that had been subjected to thermo-hydraulic gradients were determined in the laboratory, in order to compare the results with those obtained from untreated samples. No modifications of the hydro-mechanical properties were observed, and the chemical integrity of the bentonite following a year of heating at 125 °C was also corroborated.

Following closure of the Stripa mine, SKB initiated the construction of an underground laboratory to a depth of 450 m in the Äspö granite. The objective of this laboratory, which was completed in 1995,

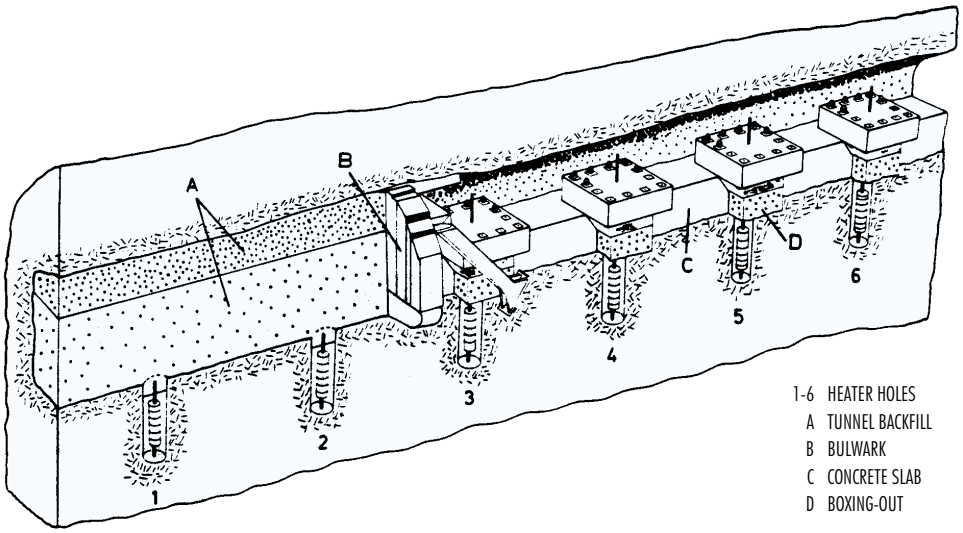

Figure 2. Schematic diagram of the Buffer Mass Test at Stripa (Pusch et al. 1985).

was to test rock research methods at the depth of a radioactive waste disposal facility (Figure 3). A joint research programme is being carried out at this laboratory, with the participation of Japan, France, Finland, Great Britain, Switzerland, Germany, Spain, Canada and the United States (Kärnbränslehantering 1999). Among the projects relating to the bentonite barrier performed at Äspö are tests on different backfill materials: the "Prototype" project, which will include the construction of a simulated disposal facility with backfill and sealing material and the "Long term tests of buffer material (LOT)". The latter is an *in situ* test based on the Swedish disposal concept but at a smaller scale, and is aimed at checking the long-term effectiveness of the barrier from the point of view of microbiology, radionuclide transport, corrosion and the transport of gas (Karnland 1996).

The HADES underground facility for research into nuclear waste disposal at Mol (Belgium) is the only one of its kind constructed in a clay formation (Figure 4). The facility is located at a depth of 200 m in the formation known as "Boom clay", and is part of the nuclear installation of the company SCK-CEN. HADES is also an interdisciplinary programme aimed at demonstrating the feasibility and long-term safety of radioactive waste disposal that, although adhering to the criteria of the Belgian agency ONDRAF/NIRAS, has received support from the European Community since 1975, as a result of which various of its projects include international participation.

The European Union has also taken into account the issue of radioactive waste management and disposal in its research activities. For the most part, the European Union's research activities are undertaken as part of the pluriannual research, technological development and demonstration (RTD) framework programmes. These research projects are performed by public and private organisations belonging to the member countries, by way of a shared cost system. From 1985 to 1994, the studies relating to radioactive waste management were encompassed in the "Management and Storage of Radioactive Waste" Programme. From 1995 onwards, all projects relating to nuclear energy were included in the Programme "Research and training in the nuclear energy sector. Safety of nuclear fission (NFS2)". For the scientific community, participation in these projects implies the possibility of exchanging information through both the periodic meetings held and

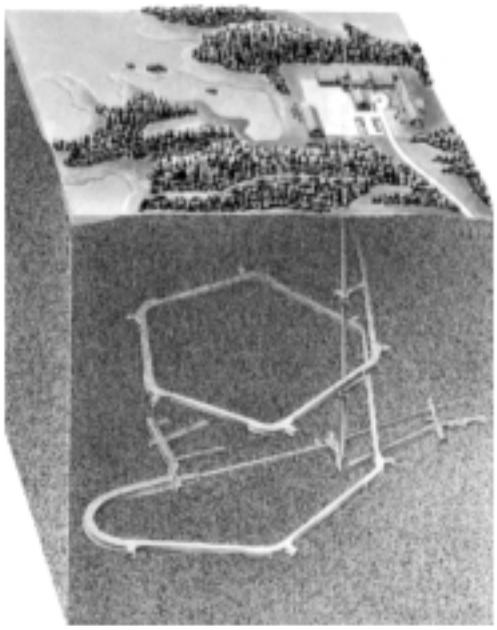

Figure 3. Schematic diagram of the Äspö underground laboratory (Kärnbränslehantering 1999).

Figure 4. The HADES underground facility (Mol).

the publication of progress reports and final EUR reports. The European Union also organises a Workshop on the sealing of radioactive wastes at the end of each Framework Programme, in collaboration with the OECD, these including the main results obtained from the different research projects (Braunschweig 1989, Luxembourg 1990 and 1996).

The programme covering the period 1985-1989 included the initiation of joint activities at the Asse salt mine (Germany) and the HADES facility at Mol (Belgium). In the latter, an experimental drift was excavated for the testing of different linings and work began on a heating/radiation test (the CERBERUS Project) and on the project known as the "Backfilling control experiment for high level wastes in underground storage" (BACCHUS-1). The latter consisted in using compacted blocks made of a mixture of the French FoCa bentonite, quartz and graphite to seal a shaft excavated in the Boom clay, in which a central heater was emplaced (Neerdael *et al*. 1992).

During the period 1990-1994, the 3rd Framework Programme included projects on both waste management and on the construction and operation of underground facilities (European Commission 1995). The main objective of the latter part of the programme was the development and demonstration of installation techniques and validation of the siting and design criteria for deep geological disposal facilities in both salt and clay formations. The projects referring to disposal in salt formations centred on the Asse mine (Germany), and to a lesser extent on the Amélie potash mine (France). Aspects relating to disposal in clay formations were mainly studied at the Mol underground facility (Belgium), although a research project was also undertaken in a tunnel excavated in argillites at Tournemire (France), on which the IPSN (Institut de Protection et de Sûreté Nucléaire) worked from 1988 onwards. In addition to the *in situ* tests, all the projects were complemented with laboratory testing programmes. Among the projects centering on the Mol underground laboratory, the BACCHUS-2 Project, "Demonstration of the *in situ* application of an industrial clay-based backfill material", focussed on the demonstration and improvement of a procedure for the installation of a clay-based sealing material and on the validation of a hydromechanical model. The material in question was made up of a mixture of high density pellets and of powder of the Boom clay itself. In parallel to the BACCHUS-2 Project, and in close collaboration with it, the "Modelling and validation

of the thermal-hydraulic-mechanical and geochemical behaviour of the clay barrier" project was performed, the objective of which was to analyse and model the behaviour of an engineered clay barrier during the hydration phase, under real disposal facility conditions. For this purpose, coupled thermo-hydro-mechanical and thermo-hydro-chemical models were developed simulating spatial distribution and the evolution of temperature, water content, suction, stresses, strain and the concentration of chemical species. The laboratory work, undertaken by various organisations (SCK-CEN, CIEMAT, CEA and UPC) in the context of this project, allowed the parameters required by the models to be acquired and the processes taking place during the transient to be identified (Volckaert *et al*. 1996).

In the area of "Radioactive waste management and disposal and dismantling" in the 4th Framework Programme (Sub-programme on "Safety of nuclear fission"), carried out during the period 1994-1998, the research relating to radioactive waste disposal was included under the headings "Underground laboratories for waste disposal" and "Supporting research". A review of the projects contained in these areas shows what issues were considered to be priorities by the European Union:

- Geomechanical behaviour of engineered barriers and host rocks.
- Testing and demonstration of disposal concepts.
- Study of natural analogues and systems.
- Gas generation and transport.
- Characterisation of waste forms and matrices.

The projects referring to study of the geomechanical behaviour of the barriers also include their study from the microstructural point of view and study of the chemical parameters (of both solids and groundwaters) related to their efficiency as sealing materials (Project on "Microstructural and chemical parameters of bentonite as determinants of waste isolation efficiency"). Another aspect considered is that of the modifications caused by interaction between the bentonite and the concrete used to plug part of the drifts in certain disposal concepts, and their repercussion on the behaviour of the sealing material (ECOCLAY Project). For their part the disposal concept demonstration projects are *in situ* tests in which a part of the disposal facility, with its different components, is simulated at full or near-full scale. With a view to promoting cooperation and information exchange, the European Commission has set up a coordination group known as CLUSTER (CLub of Underground Storage TEsting and Research facilities) for the activities and projects carried out in the different underground laboratories, which include the HADES installations at Mol (Belgium), the Asse salt mine (Germany), the mine excavated in granite at Grimsel (Switzerland), the tunnel in argillites at Tournemire (France) and the granite laboratory at Äspö (Sweden) (Haijtink & Davies 1998). Among the projects included are RESEAL and FEBEX. The RESEAL Project, led by the Belgian company SCK·CEN, with French and Spanish participation, is a large-scale demonstration of the possibility of sealing a vertical shaft in a clay formation by means of a mixture of pellets and powder of the French FoCa bentonite. The FEBEX Project, led by ENRESA, has been the first full-scale test of a disposal facility located in a gallery in granitic rock, constructed as described in detail in the following section. In addition to an *in situ* test of the Spanish concept, the FEBEX Project includes a test on an almost full-scale mock-up and a set of laboratory tests.

Furthermore, the PRACLAY Project is being carried out at the HADES underground facility at Mol, outside the European Union's framework of funding. This project consists in the full-scale simulation of a disposal drift in accordance with the Belgian concept. A central tube of stainless steel measuring 0.5 m in diameter, in which electrical heaters simulate the wastes, is emplaced in a concrete-lined drift measuring 2 m in diameter and 30 m in length, the tube being surrounded by blocks of compacted bentonite. Prior to this test, at the end of 1997, a mock-up test was initiated in a surface facility, in which the longitudinal dimensions of the system were reduced to 5 m (Figure 5).

As we have seen, much attention has been paid since the 1980's to the performance of tests at different scales, in both the laboratory and the field, in order to observe the thermo-hydro-mechanical processes taking place in the engineered barriers and the geological medium. The purpose of these experiments has been the direct observation of the phenomena occurring in the barrier and of the behaviour of the system, this providing the information required for the verification and validation of the mathematical models of the coupled processes and their numerical implementation. The result of these activities will allow trustworthy models to be developed, capable of predicting the thermo-hydro-mechanical and geochemical response of the engineered and natural barriers over the timescales

Figure 5. View of the PRACLAY Project mock-up before installation of the cover.

required for radioactive waste disposal. With this aim in mind, certain model validation or benchmarking exercises have been proposed, in which the predictions of different models are contrasted for a given case of increasing complexity, from the scale of simple laboratory tests up to that of complex *in situ* tests. Among these, the INTERCLAY II Project, undertaken within the framework of the European Community's RTD Programme for the period 1990-1994 and including the participation of ten organisations from Great Britain, Belgium, France and Spain, was dedicated to the rheological behaviour of clays as host formations. Between 1996 and 1998 the CATSIUS CLAY Project, "Calculation and testing of behaviour of unsaturated clay", coordinated by the Spanish Centro Internacional de Métodos Numéricos en Ingeniería (*International Centre for Numerical Engineering Methods*, CIMNE), analysed the predictions of various hydro-mechanical and thermo-mechanical codes regarding the behaviour of unsaturated clays subjected to conditions close to those of a disposal facility barrier. Among the cases studied were the BACCHUS-2 test, the FEBEX Project mock-up test and a test in thermohydraulic cell performed at CIEMAT using the Spanish reference clay (see section "THM behaviour studies on bentonite S-2 (1991-1995)").

The interest aroused by studies relating to the geological disposal of radioactive wastes has given rise not only to numerous articles in scientific journals, but also to international forums for the discussion of specific aspects of the behaviour of the system. Particularly interesting are a series of Workshops initiated at Lund (Sweden) in 1988, the objective of which is to bring together research workers having interests relating to the engineered clay barriers proposed for the geological disposal of nuclear wastes, during which updated reviews of each specific area are presented. A theme common to all these workshops has been the consideration of the thermo-hydro-mechanical processes taking place in these barriers (Selvadurai 1997), although each has focussed on a specific aspect:

- Lund (Sweden) 1988: "Longevity and rheology of smectites". The presentations referring to the geotechnical characterisation of remoulded smectites, and in particular to measurement of their hydraulic conductivity, were pioneer contributions in this area.
- Durham (United States) 1991: "Distribution of stresses in clays", including aspects of soil/water interaction, effective stress in expansive clays, the behaviour of unsaturated clays and water and contaminant flows. A conceptual model for the behaviour of unsaturated expansive clays was presented, and has since been widely referred to (Gens & Alonso 1992).
- Bergamo (Italy) 1993: "The thermo-mechanics of clays and clay barriers", exploring microstructural aspects and the influence of temperature and of the state of saturation, from the experimental and theoretical points of view.
- Montreal (Canada) 1995: "The hydro-thermo-mechanics of engineered clay and natural barriers", with special emphasis on modelling and on model verification and validation exercises.
- Barcelona (Spain) 1998: "Key aspects in waste disposal research". The number of areas of interest was even larger on this occasion: hydraulic, mechanical and chemical phenomena, large-scale *in situ* and mock-up testing, boundaries between fractures and interfaces, progress in laboratory techniques and gas generation and migration.

The papers presented at these workshops are reviewed and selected for inclusion in a Special Edi-

tion of certain international journals, such as the Canadian Geotechnical Journal (vol. 29), Engineering Geology (vol. 28 n. 3-4, vol. 41 n. 1-4, vol. 47 n. 4) and the International Journal for Numerical and Analytical Methods in Geomechanics (vol. 22 n. 1 y 7, vol. 23 n. 12).

The importance of microstructural aspects in the behaviour of clays used as barriers has recently received much attention, this having been reflected in an initial Workshop held in Lund in 1998: "Microstructural modelling with special emphasis on the use of clays for waste isolation", the contributions of which were also published in a Special Edition of the journal Engineering Geology (vol. 54 n. 1-2).

The study of clay barriers in Spain

The creation of ENRESA in 1984 marked the beginning of a new stage of research into the disposal of high level radioactive wastes in Spain. In 1990, a series of activities was initiated with a view to defining a disposal system adequate for the Spanish case, within the framework of the AGP (Almacenamiento Geológico Profundo) deep geological disposal Project, the basic objective of which is to "avoid any type of radiological damage to mankind and his environment, using the waste concentration and confinement strategy". The geological formations considered are granite, clay and salt. The definitive disposal of the HLW is planned to be accomplished in canisters placed in the centre of the drifts of a disposal facility excavated at depth and surrounded by a sealing material, as shown in Figure 6 for the granite case. The functions attributed to the sealing material surrounding the canister are those of reducing groundwater flows and the transport of corrosive substances, establishing a suitable physico-chemical environment around the canisters and providing mechanical protection against possible movements of the rock. Consequently, the properties to be provided by the sealing material are fundamentally low permeability and diffusivity, good thermal conductivity, a high sorption capacity and long-term stability (ENRESA 1994, 1995).

The research relating to deep geological disposal covers from the determination of areas suitable for the installation of disposal facilities to the study of the behaviour of the fuel and canister, including site characterisation (structural, hydrogeological, geo-

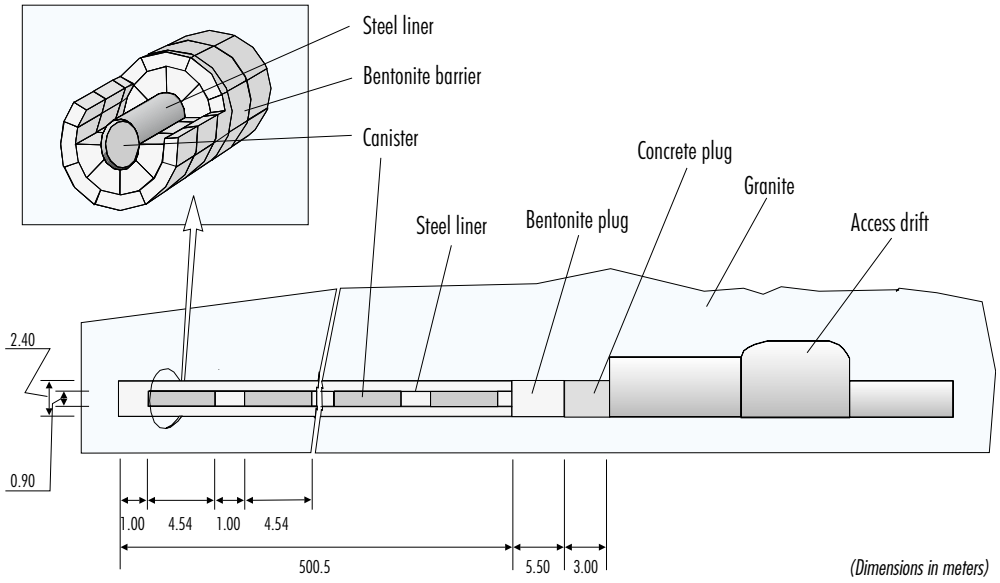

Figure 6. Longitudinal section of a disposal drift for the Spanish reference granite case (ENRESA 1997).

chemical and hydrogeochemical and radionuclide migration) and theoretical studies of engineered barriers. These research projects have often been carried out in collaboration with equivalent organisations in other European countries, and in accordance with their standards.

In the AGP Project, consideration has been given to compacted bentonite as the canister sealing material in the case of saturated formations (clay and granite) and to a mixture of sand and clay materials as the backfilling material for the galleries and cavities. The dry density considered for the bentonite receptacle surrounding the disposal capsule is 1.65 g/cm^3. The layer of bentonite will measure 0.75 m in thickness and its temperature will not exceed 100 °C. A series of suitability studies, in which CIEMAT participated actively from the very start, led to a bentonite exploited in the province of Almería being selected as the reference sealing material. The following sections recapitulate on the prospecting, selection and study of the behaviour of materials suitable for the construction of engineered clay barriers in Spain, with special emphasis on the work performed at CIEMAT and with a brief summary of the main results of each phase of the research.

Prospecting and initial selection (1987-1989)

The study of backfilling and sealing materials began in Spain in 1987, with a Project financed by the European Community (FI-IW-0191E), performed by CIEMAT with participation by ENRESA. This study had three objectives:

- To gain insight into the availability in Spain of clays suitable for use as backfilling and sealing materials.
- To study the possibility of using illitic clays as an alternative to smectitic clays, in order to minimise mineralogical unbalance with the granitic medium.
- To use ground granitic rock as an additive to the clay for backfilling material, this possibly reducing costs and contributing to the reconstitution of the environment of the disposal facility.

The prospecting of clay materials in Spain having been performed, study began on 30 samples from seven suppliers located in Gerona, Barcelona, Zaragoza, Segovia, Toledo, Jaén and Almería. An initial semi-quantitative determination of the mineralogy allowed 50 percent of the samples to be excluded because of their low content of philosilicates (lower than 65 percent). In accordance with the mineralogy of the fraction of less than 2 μm, seven of these samples were selected; two were mainly made up of illite and the rest were smectites from the Cabo de Gata region (Almería) and the Madrid Basin (Yuncos, Toledo) supplied by Minas de Gádor. Finally, two bentonites were selected that had not been subjected to treatment in the factory: one bentonite known as "Serrata natural" (M-26) from the Cortijo de Archidona deposit, in Almería, and an illite from Zaragoza (M-15), these being chosen for their low carbonate and colloidal mineral content and high degree of plasticity and compressibility. Analysis of the mechanical, hydraulic, thermal and physicochemical properties of both, and their behaviour when mixed with ground granite, allowed the following conclusions to be drawn (Mingarro *et al*. 1991):

- There are clays in Spain that might be used as backfilling and sealing materials.
- It is advisable to use smectitic clay and not illitic clay as a backfilling and sealing material, due to its greater swelling pressure, specific surface and cation exchange capacity.
- Ground granite may be used as an additive to the smectite in the backfilling material, as long as it does not exceed 25 percent of the mixture.

Parallel to the above, ENRESA promoted the study of two Spanish areas with important deposits of smectite clays that might be used as backfilling and sealing material for a future high level radioactive waste disposal facility. These areas were the volcanic region of Cabo de Gata, in Almería, and the Tertiary Basin of Madrid in the province of Toledo. Three deposits were selected from each, these being considered as potential points of supply of the material in the future, because of the characteristics already known and the estimated reserves, for joint study by CIEMAT and the Centro Superior de Investigaciones Científicas - Estación Experimental del Zaidín (CSIC-Zaidín), for the Cabo de Gata zone, and by the Universidad Autónoma de Madrid (UAM), for the area of the Madrid Basin, with advice from R. Pusch (Clay Technology, Sweden). CIEMAT was also aided by the collaboration of the Commisariat à l'Energie Atomique (CEA, France). The deposits selected for the Cabo de Gata area were Cortijo de Archidona, in the Serrata de Níjar, Morrón de Mateo, in the Rambla de los Escullos, and Los Trancos, in the northern area of the Sierra

de Gata. In the Madrid Basin the Cerro del Águila-Cerro del Monte, Santa Bárbara and Yuncos deposits were selected.

Two samples from each deposit, each weighing 200 kg, were received at CIEMAT. The granulometric distribution and specific gravity, mineralogy and geochemistry, Atterberg limits and total and external specific surface were determined for each of these samples. Dynamic and static compaction tests were also performed. The superficial thermal conductivity was determined at the CEA laboratories using compacted samples. The results obtained are to be found in (Rivas *et al*. 1991) and Pérez del Villar (1989a y b).

From the other part, CSIC-Zaidín and UAM performed a complete geochemical and mineralogical characterisation and alterability and stability studies on various samples collected from the Cabo de Gata and the Madrid Basin, respectively. The results obtained were included in reports published by ENRESA and by the European Community (Linares *et al*. 1993, Cuevas 1992, Astudillo *et al*. 1995).

On the basis of the results obtained by the laboratories, one deposit was selected from each zone, the Cortijo de Archidona at Cabo de Gata, made up mainly of montmorillonite type smectites, and the Cerro del Águila-Cerro del Monte deposit in the Tertiary Basin of Madrid, constituted fundamentally of saponite smectites, accompanied by varying proportions of illite and sepiolite. The criteria taken into account in making the selection were those indicative of the suitability of the material for use as a HLW disposal facility backfill and sealing material: mineralogical purity, a high specific surface, high liquid limit, a high proportion of fraction of less than 2 μm, high thermal conductivity and good compressibility, the latter being an additional requirement for the manufacturing of high density blocks (Rivas *et al*. 1991).

Selection of the Cortijo de Archidona deposit (Almería) (1989-1991)

Using the two selected reference clays, S-2 (Cortijo de Archidona in the Serrata de Níjar) and MCA-C (Cerro del Águila-Cerro del Monte, in the province of Toledo), CIEMAT continued the process of characterising their physicochemical properties and alterability. For this purpose, a 5000 kg sample from each deposit was used, dried at 60 °C to a water content of close to 10 percent and factory ground to a size of less than 5 mm. For use in the laboratory, the samples were ground to less than 2 mm (except in those cases in which the aim was to determine the effect of granulometry on a given property), and were stabilised at laboratory temperature and humidity conditions (18-25 °C, 50-60 % R.H.). A part of the prepared sample was sent to the CSIC-Zaidín (S-2), UAM (MCA-C) and CEA laboratories.

The characterisation performed at CIEMAT included tests for the determination of different parameters and of the influence on different properties of the dry density and water content of the sample, the temperature of the determination, the maximum grain size used, the addition of quartz sand in different proportions and the preheating of the clay used to different temperatures. The following studies were carried out on both clays:

- Dynamic compaction study by manual and semi-automatic beating in an axial press: determination of optimum water contents, necessary pressures and the influence on final density of granulometry and the addition of quartz sand in different proportions.
- Simple compressive strength: the influence of sample dry density and water content, of the granulometry used and of the addition of different proportions of quartz sand.
- Free swelling.
- Swelling pressure: analysis of the influence of dry density and of the proportion of quartz sand.
- Saturated hydraulic conductivity for different dry densities, proportions of quartz sand and measurement temperatures.
- Thermal conductivity: analysis of the influence of dry density, water content and the proportion of quartz sand.
- Oedometric tests: study of clay consolidation.
- Triaxial tests.
- Ion diffusion study: determination of coefficients of distribution.
- Determination of adsorption-desorption isotherms.
- Study of hydrothermal alterability: influence of treatment time and temperature and of the concentration of KCl.

The Atterberg limits, swelling pressure, simple compressive strength and hydraulic conductivity were also determined for a sample subjected previously

to heating to 100, 200 and 300°C. Also determined were the modifications caused by heating as regards mineralogy, specific gravity, specific external surface and texture observed through electron microscopy.

These studies and their results are included in Rivas *et al.* (1991), Pérez del Villar *et al.* (1991) and Villar & Dardaine (1990), and allowed the montmorillonite from the Cortijo de Archidona deposit, reference S-2, to be definitively selected, for its better densification and lower thermal repercussion, although both clays in fact fulfilled the requirements for use as a barrier material. The conclusions drawn during this phase were as follows:

- Both uniaxial and dynamic compression were adequate for the production of high density compacted blocks.
- The grain size distribution did not modify the final density of the blocks.
- The addition of quartz sand did not imply any major improvement in the properties of the material.
- Saturated hydraulic conductivity (k_w) and swelling pressure (P_s) depend on the dry density of the clay (ρ_d), in accordance with an exponential relation (Villar & Rivas, 1994). A dry density of 1.60 g/cm^3 meets the hydraulic requirements of the barrier.
- The hydraulic conductivity of the clay increases with temperature, this increase possibly being explained in terms of reduction of the kinetic viscosity of the water.
- The thermal conductivity of the material increases with dry density and water content.

Simultaneously, industrial type uniaxial compaction tests were performed on both clays under a contract with CEA, in collaboration with the company Constructions Thermiques Européenes (Montsemprom-Libos, France), the results of which may be found in Martín & Dardaine (1990) and Martín *et al.* (1990). Also carried out was a clay barrier validation tests in a vertical shaft, performed at Fanay-Silord using the S-2 clay (Astudillo *et al.* 1995).

THM behaviour studies on bentonite S-2 (1991-1995)

The second phase of characterisation of the S-2 clay from the Cortijo de Archidona deposit began in 1991, within the framework of Appendix V of the CIEMAT-ENRESA Association Agreement, "Research and technological development in the field of radionuclide migration and the behaviour of natural and artificial barriers in response to migration", in its Appendix C, "Basic studies of the thermal, hydraulic and mechanical behaviour of artificial barrier materials". For these studies, 24 t of bentonite were used, supplied by Minas de Gádor in October 1990 and prepared at its Almería plant by drying at 60 °C and grinding to a size of less than 5 mm. This material was further ground to less than 2 mm for use in the CIEMAT laboratories.

This phase included characterisation of the properties and behaviour of the material under the conditions to which it would be subjected once emplaced in the disposal facility, *i.e.* when subjected to simultaneous heating and hydration on opposing fronts over long periods of time. This included study of the effects caused by thermohydraulic flux in compacted blocks and study of the hydro-mechanical behaviour of the material in unsaturated conditions (Villar 1995a).

The first issue was addressed by means of tests consisting basically in subjecting cylindrical blocks of compacted clay, confined in hermetically sealed and non-deformable cells, to simultaneous heating and/or hydration on opposing fronts. The dimensions of the clay blocks used for these tests were between 8 and 14 cm in length and between 3 and 15 cm in diameter. Figure 7 shows the main components of a thermo-hydraulic test, with the cell in the central part.

The main conclusions of this work, which continues at the present time, may be summarised in the following points (Villar *et al.* 1997):

- The temperatures recorded within the clay subjected to heating and hydration in thermo-hydraulic cells depend on the geometry and power of the heater and, for the same boundary conditions, depend also on the water content of the clay, since any increase in water content leads to an increase in thermal conductivity.
- The speed of water intake for a constant injection pressure and clay density depends at each moment on the water content of the clay, in other words on suction, and no contribution by the thermal gradient has been identified in the process, even though this does not exist (Figure 8).

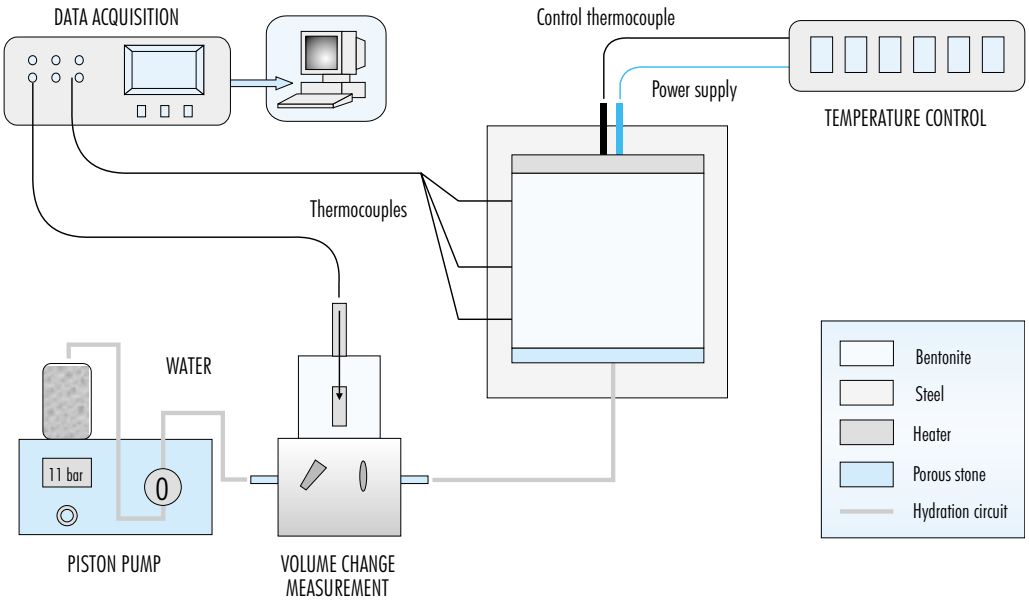

Figure 7. Schematic diagram of assembly for the performance of laboratory thermo-hydraulic test.

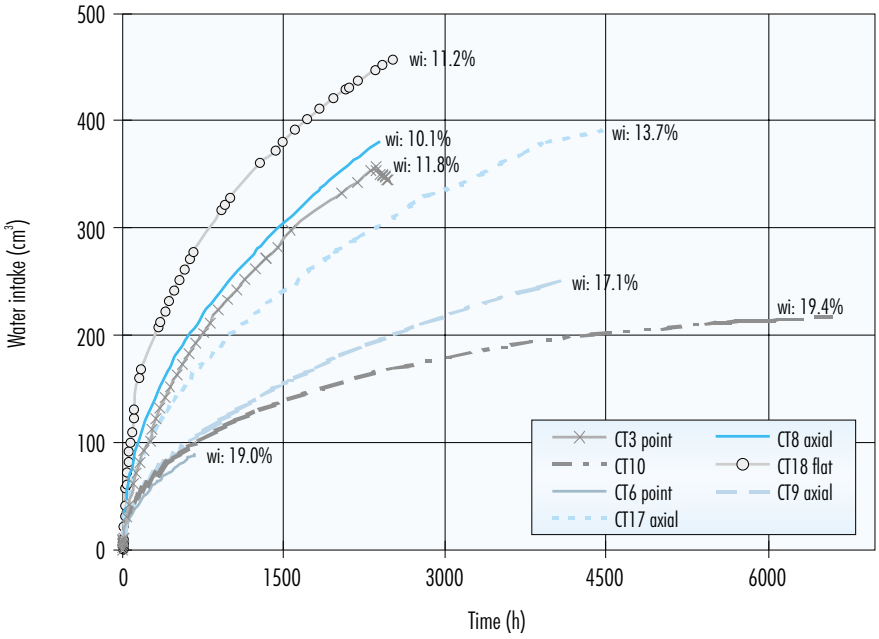

Figure 8. Velocity of hydration in the different thermo-hydraulic cell tests, with indication of initial water content (wi) and of type of heater (point, axial, flat). (Villar et al. 1997).

- In those tests in which only hydration is accomplished, the water content of the clay increases as the front progresses, and the dry density decreases due to swelling. This implies an increase in density in the areas furthest from the hydration surface, as a result of the compression exercised by the expanding clay, since the entire process occurs at a constant volume. When, in addition to hydration, the clay is heated by the opposing front, the distribution of water contents is initially affected by the thermal gradient, due to the desiccation that takes place close to the heater, but as saturation is approached, the profile of water contents and of densities becomes homogeneous. On heating, the increase in density of areas located at a distance from the hydration front is accentuated, since there is a contribution by the loss of water content caused by the temperature.
- As hydration progresses and saturation is reached, sealing of the bentonite blocks occurs, even when these are being heated.
- Three mechanisms involved in the transport of solutes, and acting jointly, have been identified:
  - Advection: with the hydration water, that causes the dissolution of salts that are entrained in ionic form towards more distant areas. This mechanism is particularly intense in the case of chlorides, which are rapidly dissolved and transported. Transport by advection operates regardless of the existence or not of a thermal gradient, although if one does exist the phenomenon is accentuated, probably due to an increase in suction, and consequently of avidity of water, in the heated and desiccated areas.
  - Advection-convection: in those not excessively short tests in which there has been heating, and regardless of whether or not there has been hydration, a concentration of salts may be observed in the areas surrounding the heater, this being attributed to a process of advection-convection. The spatial extent of this mechanism is particularly limited, and it would appear to affect sulphates with greater intensity.
  - Diffusion: this is a slow process that is not perceived until such time as a high degree of saturation has been reached and an important gradient of concentrations has been established by other mechanisms. It is difficult to identify because it is masked by other phenomena, and requires long experimentation periods. It may be clearly observed in long-term tests carried out in small cells. This process gives rise to a homogenisation of the concentration of soluble salts in the clay overall, since it acts contrary to the other two mechanisms described above.
- The saline fronts created cause the corrosion of the metallic elements of the system, leading to the formation of iron oxides and copper salts.
- The exchange complex is affected by the establishment of a thermal gradient. Particularly clear is the decrease in sodium and potassium towards the hotter areas, following the profile of the isotherms, this occurring even in the absence of hydration. Exchangeable magnesium also undergoes redistribution, conditioned by the thermal gradient, its content increasing towards the hotter areas. This last process was observed only in the presence of a hydration front.
- The reduction of the external specific surface towards hotter areas with lower degrees of water content may be attributed to a clustering of montmorillonite particles. This correlates well with the reduction of the percentage of small pores observed towards hotter areas. When montmorillonite clustering occurs, thus increasing particle size, the percentage of small pores decreases.
- No important and/or preferential concentrations of free silica were observed in any of the experiments, as a result of which it is assumed that no silica cementations have occurred.
- The swelling pressure of samples subjected to heating and hydration is related to dry density, and would appear to decrease with respect to the swelling pressure of untreated samples of the same density, this decrease being greater the higher the temperature to which the clay has been subjected, and the longer the heating period. Nevertheless, in another series of tests performed in smaller cells (diameter 5.0 cm and length 2.5 cm), a certain increase in swelling capacity was observed following thermo-hydraulic treatment with granitic water, this having been attributed to the dissolution of cementing agents (Cuevas *et al.* 1999). Consequently, the issue of modification of the swelling capacity by thermohydraulic treatment remains unevaluated.

- The hydraulic conductivity of samples subjected to heating and hydration is related to dry density, and undergoes a slight increase with respect to the hydraulic conductivity of samples of the same density not subjected to treatment. The same has been observed in the tests performed in small cells and mentioned in the previous point, especially when the treatment is carried out using saline water (Cuevas *et al*. 1999).

Furthermore, study of the material in the unsaturated state focussed on determination of the free volume suction/water content relation of the clay with different values of water content and density, and on the performance of oedometric tests with controlled suction. The oedometric tests followed two types of paths:

1) drying/wetting under constant load, followed by loading/unloading at the last value of suction reached, and
2) wetting/drying under constant vertical load, followed by loading/unloading at the last value of suction reached.

The maximum vertical pressure applied during these tests was 5 MPa, and the maximum suction 140 MPa, this implying that the water content of the clay in these tests was never below the hygroscopic water content. The results obtained show a hardening of the bentonite due to the effects of suction and the repercussion of the vertical load applied during hydration of the sample on the reversibility of the strain induced (Villar 1995b, Villar & Martín 1996).

Likewise, characterisation of the clay continued, with new aspects being addressed, such as determination of porosimetric distribution and of specific heat depending on temperature and new determinations of specific gravity, cation exchange capacity and exchangeable cations, thermal conductivity, etc. Other issues addressed for the first time were extraction and analysis of the interstitial water and bacteriological analysis (Villar *et al*. 1997).

From its part, during the period 1992-1995, CSIC-Zaidín carried out a study of the hydrothermal alterability of the bentonites from Almería, this being summarised in Linares *et al*. (1996).

The FEBEX Project

In the R&D plans performed prior to 1994, which have been partially summarised in previous sections, ENRESA studied sources of supply of the materials to be used in the clay barrier, along with its thermal, hydraulic, mechanical and geochemical behaviour. Likewise, integral characterisation studies were performed on granitic massifs. The next step in gaining insight into the feasibility of the AGP concept, and with a view to making progress regarding understanding and evaluation of near-field behaviour, was the performance of a large-scale experiment, the FEBEX Project (ENRESA 1997).

The purpose of the FEBEX Project is the study of the near-field components of a high level radioactive waste disposal facility in crystalline rock, in accordance with the Spanish concept (Figure 6), in which the waste canisters are placed horizontally in galleries, surrounded by a clay barrier made up of high density compacted bentonite blocks (ENRESA 1995). More specifically, three objectives were mapped out:

1) demonstration of the feasibility of handling and constructing a system of engineered barriers;
2) study of Thermo-Hydro-Mechanical (THM) processes in the near field; and
3) study of Thermo-Hydro-Geochemical (THG) processes in the near field.

The FEBEX Project is coordinated by ENRESA –assisted by NAGRA (Switzerland) in certain aspects–, and the initial phase included the participation of the following organisations: CIEMAT, AITEMIN, UPC, ULC, CSIC-Zaidín and UPM (Spain), ANDRA and G.3S (France) and GRS (Germany). The Project is co-funded by the European Commission.

The Project consists of three main parts: an *in situ* test under natural conditions and at full scale (Grimsel, Switzerland); a test on an almost full-scale mock-up (CIEMAT, Madrid); and a series of laboratory tests aimed at providing information complementary to the two large-scale tests. All these activities serve as a support for a far-reaching programme of modelling work (ENRESA 2000).

In the two large-scale tests, the thermal effect of the wastes is simulated by means of heaters, while hydration is natural in the *in situ* test and controlled in the one performed on the mock-up. Both tests are monitored, this allowing the evolution of the temperature, total pressure, water content, water pressure, displacements and other parameters to be obtained continuously in different parts of the barrier and the host rock, this information being used as a contrast to the predictions of the THM and THG models.

The *in situ* test is performed in a gallery excavated in the granite of the underground laboratory managed

by NAGRA at Grimsel (Switzerland). The basic components of the test (Figure 9) are: the gallery, measuring 70 m in length and 2.3 m in diameter; the heating system, made up of two heaters placed inside a liner installed concentrically with the gallery and separated one from the other by a distance of 1.0 m, with dimensions and weights analogous to those of the real canisters; the clay barrier, formed by blocks of compacted bentonite; the instrumentation and the monitoring and control system for data acquisition and supervision and control of the test both autonomously and remotely, from Madrid.

The mock-up test, performed at the CIEMAT installations (Madrid), consists of five basic components (Figure 10): the confinement structure with its hydration system, this being a cylindrical steel body measuring 6.0 m in length and 1.6 m in internal diameter, with nozzles for the supply of pressurised granitic water; the heating system, made up of two cylindrical heaters positioned concentrically with the confinement structure; the clay barrier, formed by blocks of compacted bentonite; the instrumentation and the data acquisition and heater control systems.

Figure 11 illustrates the process of assembling the bentonite blocks for the mock-up test.

The laboratory tests include characterisation tests and the acquisition of parameters, Thermo-Hydro-Mechanical (THM) tests and Thermo-Hydro-Geochemical (THG) tests, the objective of which is to measure the changes undergone by the bentonite in response to actions analogous to those taking place in the clay barrier and their repercussion on subsequent behaviour. In addition, these tests provide support for the THM and THG modelling, serving to check its predictive capacity. The work presented herein is part of the group of laboratory tests carried out on the bentonite for the FEBEX Project.

The clay used for all the Project experiments, both the large-scale and laboratory tests –the FEBEX clay–, comes from the Cortijo de Archidona deposit (Almería), and its basic characteristics are detailed in the section "MATERIAL".

Various types of blocks were manufactured from the bentonite for both the *in situ* and the mock-up tests, in the shape of a circular crown sector, with certain dimensional variations between the different types and with weights of between 20 and 25 kg. In the case of the mock-up test blocks, the approximate distance between the external radius (R) and the internal radius (r) is 31 cm, and the thickness 12.5 cm (Figure 12). The blocks were obtained through uni-

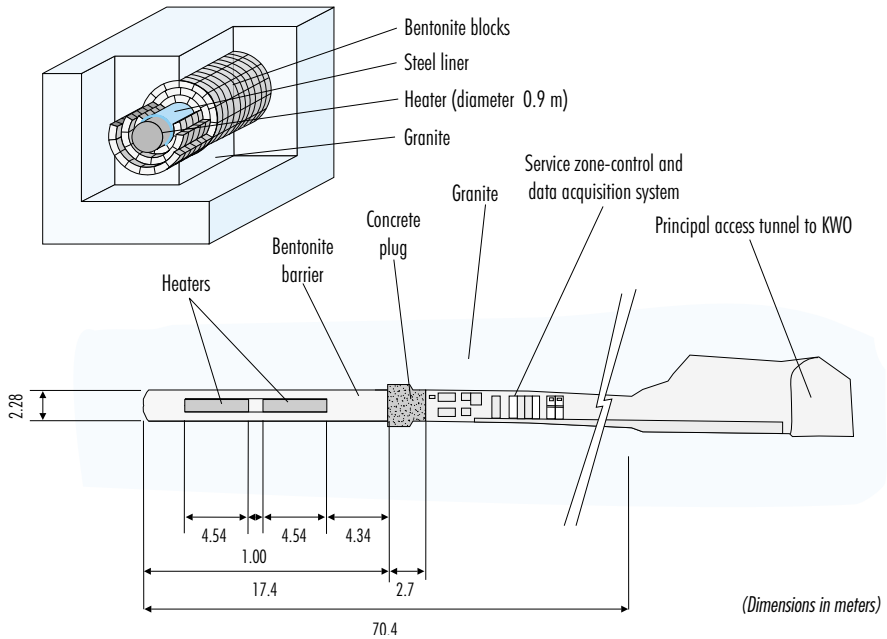

Figure 9. General view of the in situ test (ENRESA 2000).

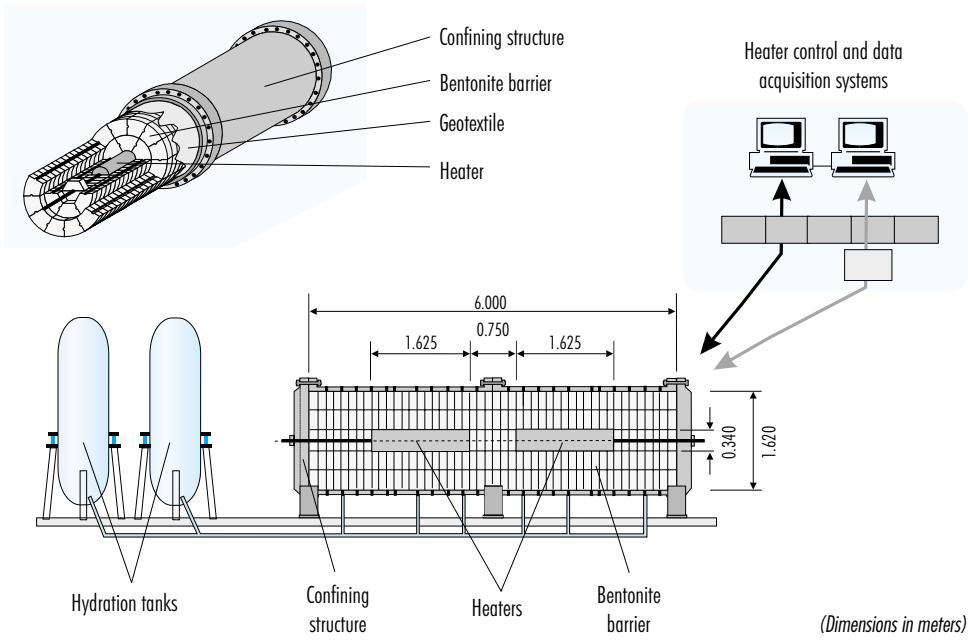

Figure 10. General diagram of the mock-up test (ENRESA 2000).

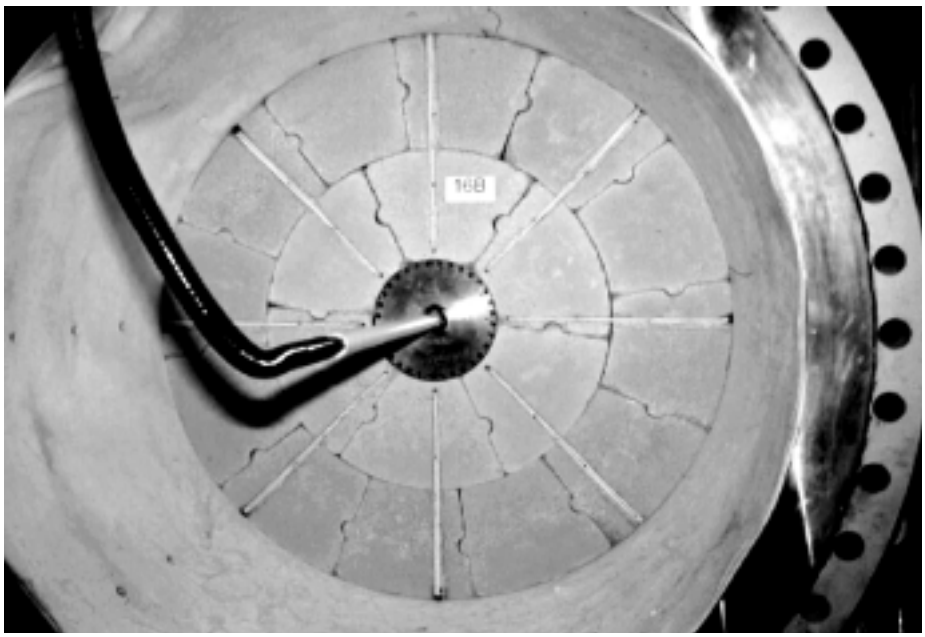

Figure 11. Appearance of one section of bentonite blocks with heater inserted in the mock-up test (Martín 1999).

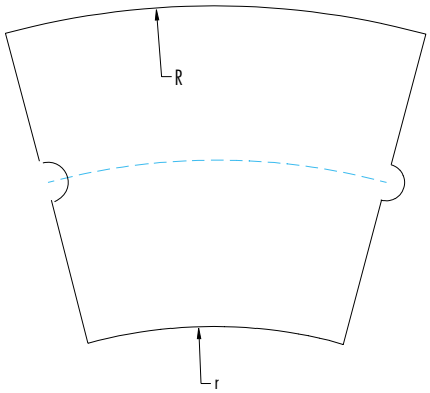

Figure 12. Top view of one of the blocks manufactured for the mock-up test.

axial compaction of the FEBEX clay with its hygroscopic water content at pressures of between 40 and 50 MPa.

Although FEBEX is basically an R&D project, ENRESA decided to apply a quality assurance programme to it, the basic aim of which is to reduce the probability of errors, this being done for the following reasons (ENRESA 1997):

- The results of FEBEX will be used for the design and behavioural assessment of the ENRESA Deep Geological Disposal Project (AGP).
- Given that it would be impossible to repair certain of the fundamental components of the large-scale tests during the operational phase, its manufacturing and assembly needed to be subject to quality control in order to reduce the probability of failures.
- The participation of numerous organisations requires the establishment of a set of regulations governing the activities of and relations between the working groups, facilitating Project management.
- The financial cost of FEBEX has been high.

The repercussions of establishing a Quality Assurance Programme for the work reflected in this study are detailed in the chapter on "METHODOLOGY".

3. Thermo-hydro-mechanical behaviour of expansive clays

3. Thermo-hydro-mechanical behaviour of expansive clays

In geotechnics, expansive soils are those constituted fundamentally by clay materials with a potentially unstable laminar structure, such as montmorillonite, vermiculite, chlorite or their corresponding interstratified materials. In general, they are soils with high liquid limits and a high degree of plasticity. They are characterised by a high degree of deformability on hydrating, since water is incorporated in the interlamina of the particles, thus increasing volume. Volume changes in these soils occur as a result both of variations in their external stress states and of internal changes in their microstructure, due to water content changes.

Expansive soils include bentonite, the subject of this study. The term bentonite is used to refer to clays arising as a result of the alteration of volcanic glasses. Like all clays, it is a fine grained material that becomes plastic when mixed with water, and is constituted by different minerals in variable proportions. Bentonite is made up fundamentally of minerals belonging to the smectites group (specifically by montmorillonite), this providing its extraordinary expansive properties, in addition to varying quantities of quartz, feldspar, micas and amphiboles, among others.

For this reason, the following section describes the constitution and characteristics of smectites, and their properties. This is followed by an analysis of the processes that are expected to occur in a disposal facility for high level radioactive wastes, and their repercussion on the bentonite in the barrier. The aim is to explain the type of characterisation to which the material has been subjected in the work described herein, which is conditioned by the highly specific use to which the bentonite is put as a barrier material, as regards preparation and operating conditions. Finally, in the last section of this chapter, the experimental techniques habitually used for the laboratory study of the behaviour of expansive materials and of unsaturated soils are reviewed.

Characteristics of smectites

Description

Smectites are clay minerals belonging to the philosilicates group and made up of structural units comprising two layers of polyhedra of tetrahedral coordination (T) between which there is a central octahedral layer (O), as a result of which they are known as 2:1 silicates. Inside each tetrahedron there is an atom of silicon coordinated with 4 oxygens or hydroxiles located at the tips. For their part, the octahedra contain atoms of aluminium, iron (II or III) or magnesium in their interior, in coordination with 6 oxygens or hydroxiles distributed on two surfaces parallel one to the other (Figure 13). All the vertices of the tetrahedra point in the same direction, towards the centre of the unit, while the bases of each of the layers of tetrahedra constitute the external planes of the unit. The tetrahedral and octahedral layers are combined in such a way that the vertices of the tetrahedra of each layer of silica and one of the surfaces of the octahedral layer are located on the same plane. The atoms common to the tetrahedral and octahedral layer are oxygens instead of hydroxiles.

When the cation of the octahedral layer is trivalent, as for example in the case of aluminium, one of every three cation positions is unoccupied, this causing the octahedral layer to have the structure of gibbsite, $Al(OH)_3$, and the smectite to be known as dioctahedral. This group includes montmorillonite, beidellite and nontronite. In trioctahedral smectites, the cation in the octahedral layer is divalent, as a result of which all the cation positions are occupied, this giving rise to an octahedral layer with the geometry of brucite, $Mg(OH)_2$. This is the case for the saponites and hectorites (Hurlbut & Klein 1982).

The T-O-T units are known as laminae and are continuous in directions *a* and *b*, in other words their extent is indefinite, while in direction *c* they are piled one on top of the other. When piling of the T-O-T units occurs, the oxygen planes of each unit are left adjacent to the oxygen planes of the neighbouring units. Depending on the isomorphic replacements that take place in the structure, the laminae will have a negative charge of a greater or lesser magnitude. For this reason, the positions between adjacent planes of oxygen are usually occupied by exchange cations. This means that water may enter between these units for solvation of the cations and other polar molecules, causing the crystalline network to expand in the direction of c-axis. For this reason, the dimension of smectite on c-axis is not fixed, but varies depending on the size of the molecule located between the units and on its hydration state. When there are no molecules between the laminae, the dimension of the *c*-axis will be between 9 and 10 Å (0.0009-0.001 μm), this possibly increasing to 16 Å when there are polar molecules or hydrated cations (Grim 1968). The number of cations required for electrical equilibrium to be reached is the cation exchange capacity (CEC) of the clay, which may be measured experimentally.

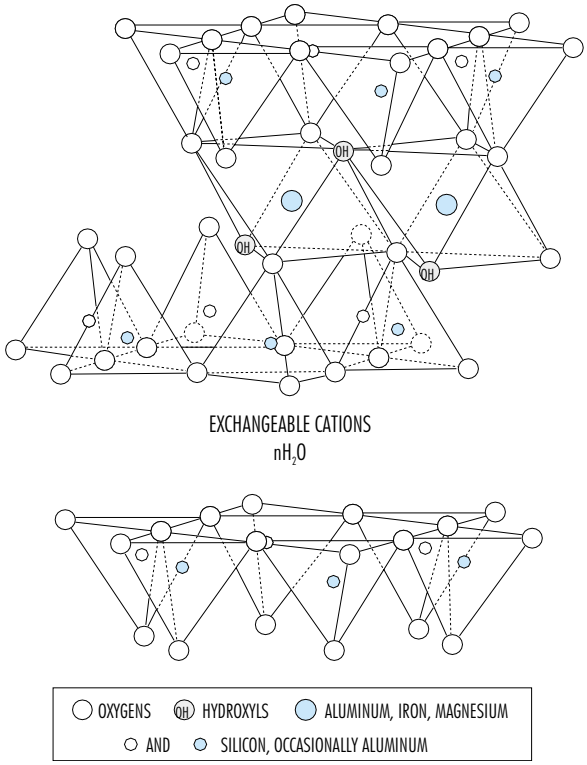

Figure 13. Schematic representation of the structure of montmorillonite (Grim 1968).

The piling of clay laminae forms primary particles with a thickness of between 0.0015 and 0.0150 μm, this possibly varying in the case of smectites depending on the hydration state and reaching up to 0.0600 μm (Ben Rhaiem *et al*. 1986). The piled laminae are separated by layers of water. When these layers are organised, the primary particles are known as quasi-crystals. These group together in turn, giving rise to aggregates.

As has been seen, the surface of the primary particles in 2:1 silicates is an interface with a negative electrical charge. Given that the water in the soil contains dissolved solutes, among which there are different cations, the interaction between the charged surface of the clay particle and the cations in the groundwater gives rise to an Electric Double Layer (EDL), that is to say, to ordering of the negative and positive charges around the electrical interface. However, given that the ions in a solution are endowed with mobility, the cations and anions will be mixed following the first layer of positive charges (that constitutes the EDL), with the former predominating close to the surface of the particle and with the charges equalling out as the distance from the particle increases. The area in which the electrical potential varies depending on the distance from the particle is known as the Diffuse Double Layer (DDL), or more accurately the Diffuse ion Layer (DL). Figure 14 is a schematic representation of the development of the EDL and the DL. When two particles are located close to each other, their DL's interact, giving rise to a repulsion between them whose magnitude is conditioned in part by the chemistry of the pore water. The thickness of the DL depends on a number of factors, among which are the concentration of salts, the valence of the exchange cations and temperature, which cause the thickness to decrease, and on the other hand the size of the hydrated ion and the dielectric constant and pH of the solution, that cause it to increase. These factors in turn influence the swelling capacity of the clay, since this increases with the thickness of the DL.

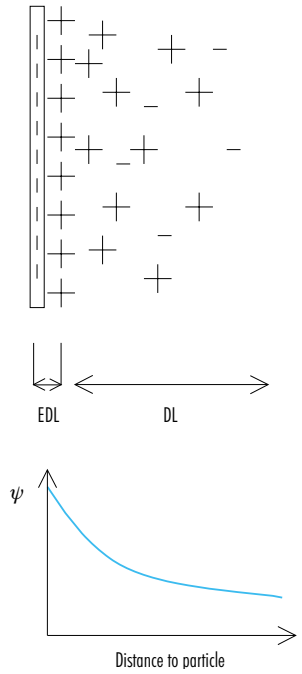

Figure 14. Schematic representation of a negatively charged clay particle interacting with the ions in the pore water. EDL: electric double layer, DL: diffuse ion layer, ψ electrical potential (Yong et al. 1992).

The organisation of the laminae, particles and aggregates in a clay material gives rise to different types of porosity. Insight into these types is necessary to understand the mechanisms and processes that take place at different structural levels inside the material, since each porosity is associated with a type of water having different properties (Stepkowska 1990). A distinction may be made between the following types of porosity, which are shown schematically in Figure 15:

- Interlaminar or interfoliar porosity, to which only polar molecules have access and whose spacing ranges from 2 to 10 Å (although this may be larger in the case of hydrated sodium smectites). This constitutes the cation solvation water. The water accessing this porosity is influenced by the electrical field and is strongly bound, as a result of which its properties are very different from those of free water, having less mobility. Some authors claim that this water may move freely across the surface of the lamina but not perpendicularly to it (Stepkowska 1990).
- Intra-aggregate porosity, inside the primary particles and between adjacent laminae piles. This is also known as lenticular porosity or microporosity, and includes pores having diameters of less than 0.0020 μm, although in high saturation states they may reach up to 0.0035 μm. The diffuse layers develop in these pores. The water that forms part of the diffuse layers is also adsorbed and cannot separate from the clay particle as a result of hydrodynamic action until the distance to the particle is sufficiently large.
- Inter-aggregate porosity (greater than 0.002 μm), which in turn may be classified as macroporosity or mesoporosity, depending on whether the diameter is above or below 0.05 μm. In these pores, the water is retained by capillary or gravitational forces, and is known as external water, in opposition to the water contained in the rest of the porosity, which is known as internal. The proportion of external water in smectites decreases with increasing material density and decreasing water content, and may be lower than 20 percent in the case of compacted calcium smectites with a dry density of 1.60 g/cm^3 (Pusch 1994). However, in the case of a calcium montmorillonite paste without confinement subjected to very low values of suction (0.032 bar), Ben Rhaiem *et al.* (1986) give a percentage of external water of 85 percent.

The retention of water in the soil occurs depending on different mechanisms, with one or another predominating depending on the water content of the soil (*i.e.* on the activity of the water): for low water contents the prevailing mechanism is adsorption, which depends on the specific surface and takes place in the micropores, while for higher water contents it is capillary condensation, which depends on the shape and arrangement of the particles and takes place in the mesopores and macropores (Everett & Haynes 1973). Adsorption creates pillars around the exchangeable cations and a film of water at the external surfaces of the particles or aggregates, both of these processes leading to an increase in the spacing between the laminae and the distance between particles, in other words to swelling. The adsorption forces that induce swelling are balanced by the capillary condensation forces (Prost *et al*. 1998).

The water contained in the different porosities is known overall as hydration water. The dehydration

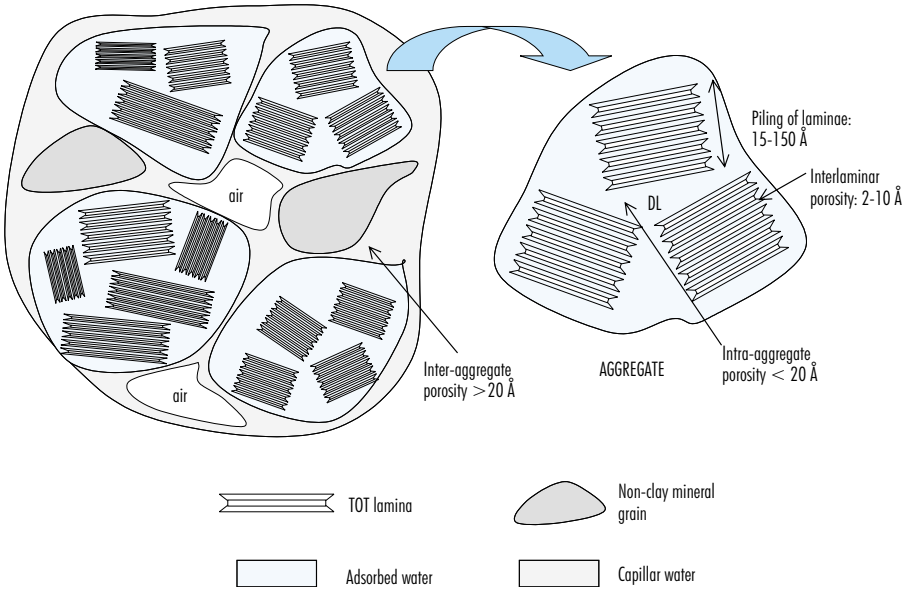

Figure 15. Schematic diagram of the organisation of a clay material: types of porosity and water.

of a mineral is a process that involves reactions having thermodynamic (temperature) and kinetic (time) conditioning factors (Cuadros *et al*. 1994). Thus, for example, hydration water is lost with heating to 110 °C if this is prolonged over 24 hours. In thermogravimetric studies, however, in which heating of the clay takes place at high speed (of the order of 10 °C/min), it is generally accepted that the hydration water exits the clay when it is heated to temperatures below approximately 300 °C, with the greater part being lost below 200 °C. Furthermore, thermogravimetric studies performed on smectites show a more or less continuous loss of mass at higher temperatures, with the hydration water loss temperatures overlapping those at which the loss of structural water occurs, *i.e*. the temperatures at which dehydroxilation (loss of OH groups) takes place, these being between 500 and 700 °C.

Hydro-mechanical properties

The constitution of smectites described in the previous section is responsible for the peculiar hydro-mechanical behaviour of the soils in which they are contained, the most outstanding characteristic of which is their capacity to change volume. This behaviour is common to other clay minerals (vermiculites, chlorites) having similar structural organisations. It is generally accepted that various mechanisms intervene in the expansion of a soil, that may be classified into three main interrelated groups (Mitchell 1976):

- Attraction of water by the clay particles. The negative charge of the surface of the clay particles is compensated by cations and dipolar molecules such as those of water. In turn, the attraction and fixing of the water molecules take place through two mechanisms:

  1) the binding of the hydrogen in the water molecules to the surface of the clay mineral, and

  2) dipole-dipole attraction between the different water molecules, allowing more than one layer of such molecules to be adsorbed. The orientation of these molecules of water with respect to the clay particles decreases with distance.

- Cation hydration. As the exchange cations bound to the surfaces of the laminae are hy-

drated, their ionic radius increases, causing the volume of the soil to increase.

- Osmotic repulsion. The concentration gradients that develop in the diffuse ion layers (DL's) associated with clays induce exchange with the free water, that attempts to pass towards the inside of these layers, the latter acting as a semipermeable membrane and causing an increase in volume to occur.

Furthermore, the Van der Walls forces and elastic relaxation in high density soils may contribute to a lesser extent to expansion phenomena.

The main factors that affect the expansion of a soil may be divided into three groups (Pousada 1984). The first group concerns the intrinsic properties of the particles and the conditions of the soil mass, and consequently includes the type of clay mineral and its proportion, dry density, water content, the orientation of the particles and the type and quantity of cations adsorbed (Pusch 1979). The second group refers to the composition and properties of the saturation water. Finally, external factors such as the soil stress history, temperature and the availability of water also influence swelling.

The increase in volume of an expansive soil in contact with water is greater the higher its dry density, and lower the higher its initial water content and the pressure applied to it. Furthermore, if an expansive material is saturated at a constant volume while its deformation is prevented, the particles will exercise a pressure on the confining structure. This is known as swelling pressure and reaches its equilibrium value when the sample is completely saturated. This swelling pressure is higher the greater the initial dry density of the material. Likewise, any saturated soil increases its volume when the effective pressure acting on it decreases, to an extent that depends on its initial dry density and the magnitude of the variation in pressure.

On the contrary, the volume of a saturated soil decreases as the water is expelled from the pores by the process known as consolidation (Atkinson & Bransby 1977). The movement of the water exiting from the internal pores of the soil to the exterior is controlled by Darcy's law, and causes a reduction in volume that depends on interaction between total and effective stresses, pore pressure, flow, hydraulic gradient and permeability. In an unsaturated soil, the application of a load causes an excess air and water pressure in the pores, that is also dissipated through consolidation, finally returning to the values existing prior to the load (Fredlund & Rahardjo 1993).

Jiménez & Serratosa (1953) studied the compressibility of a clay from the Serrata de Níjar (Almería) following modification of its exchange complex, observing that the hydration capacity of the exchange cation has an influence on the compressibility and permeability of the clay.

In general, the permeability of a soil is related to the size of its pores, being lower the smaller the average pore size. Given the small particle and pore size of clay materials, their permeability is very low, relating fundamentally to the water content and dry density of the material.

The permeability to water of any soil increases with its water content and decreases with dry density, while its permeability to gas (k_g) decreases with increasing water content and decreasing dry density. Permeability to water may increase by several orders of magnitude when the soil passes from the dry to the saturated state, the reverse being true for permeability to gas. As the degree of saturation increases, water pressure in the pores increases also, until the water cuts the interconnections between the pores occupied by air, the latter ceasing to be continuous. Under these conditions, the easiness of the air to move under the action of the pressure gradient decreases sharply. In fact, relative permeability (k_r), which is the ratio between the permeability to water of a soil at a given water content (k) and the permeability of the same soil when saturated (k_w), is related following a potential law to the degree of saturation. Nevertheless, the permeability to water may become zero even when this is not the case for the degree of saturation, because the water moving is that corresponding to the inter-aggregates, which are the first to become desaturated. The degree of saturation for which permeability becomes zero is known as the residual degree of saturation. Furthermore, under saturated conditions, *i.e.* when all the pores are occupied by water, hydraulic conductivity decreases exponentially with dry density.

The most peculiar aspect of the hydraulic behaviour of expansive soils is the modification of their intrinsic permeability depending on the degree of saturation. Intrinsic permeability (k_i) is a property that depends exclusively on the medium, and not on the properties of the fluid. The value of intrinsic permeability may be obtained from the measurement of air flow in totally dry soils or from the measurement of water flow in completely saturated soils. By definition, the value of the intrinsic permeability of a given soil

should always be the same for a given value of porosity, regardless of the fluid used for its determination. However, if there are interactions between the fluid and the medium, as occurs between expansive soils and water, the intrinsic permeability may undergo important variations depending on the degree of saturation, because the swelling of the clay lattice reduces the space available for flow (Tindall & Kunkel 1999).

The type of permeating fluid may also modify the values of hydraulic conductivity: an increase in the salinity of the fluid generates higher hydraulic conductivities, due to the osmotic contraction of the double layer and corresponding increase in pore size, which facilitates the passage of the fluid (Jiménez & Justo 1972).

Another fundamental characteristic of expansive soils, linked to the properties described above, is their high degree of suction, in other words their high water avidity and retention capacity. In unsaturated soils, three phases coexist: solid (mineral grains), liquid (interstitial water) and gaseous (the air and water vapour in the unsaturated pores). This modifies most of the physical phenomena occurring in the soil, with respect to saturated soils. The magnitude of the suction of smectites, when they are removed from the saturated state, is such that it cannot be measured directly by conventional methods, such as tensiometers, psychrometers, etc. This makes them highly hygroscopic materials with a high capacity to absorb water in the vapour phase.

The term suction (s) refers to the state of the free energy in the groundwater. This free energy may be measured by way of the partial pressure of the water vapour in the soil. The thermodynamic relation between both is expressed by means of the Kelvin equation:

$$s = -10^{-6}\frac{R \times T}{V_w}\ln\left(\frac{RH}{100}\right)$$

where R is the universal constant of the gases (8.3143 J/mol·K), T is the absolute temperature, V_w is the molar volume of the water ($1.80 \cdot 10^{-5}$ m^3/mol) and RH the relative humidity in percentage terms. The latter is given by the ratio between the partial pressure of water vapour in the pores and the saturation pressure of water vapour on a flat surface of pure water at the same temperature. The suction of the soil is zero when the relative humidity of the air in its pores is 100 percent, and increases as this relative humidity decreases.

According to the International Soil Science Society (ISSC 1965), total potential is the amount of work to be performed per unit quantity of weight of pure water to reversibly and isothermally transport an infinitesimal quantity of water from a recipient with a flat pure water surface at a specific elevation at atmospheric pressure to the soil water. Total potential is the result of adding up the following terms:

- Capillary or matric potential, which is associated with the phenomena of capillarity arising from the surface tension of the water.
- Osmotic potential, which corresponds to the osmotic attraction exercised by the soil water, containing salts, on pure water. The relative humidity of the soil decreases as the salts dissolved in the pore water increase, this giving rise to osmotic suction.
- Gravitational potential.
- Potential due to external gas or water pressures.

When gravitational and external pressures are insignificant, the total potential is equal to total suction, since the latter is the sum of the capillary and osmotic potentials.

In an unsaturated soil, and as a result of the menisci of the capillaries in which the air and water interact, the pressure of the water in the pores becomes lower than the pressure of the air, which is generally equal to atmospheric pressure. The difference between the pressure of the air (u_a) and that of the water (u_w) gives the value of capillary suction, and is a measure of the attraction exercised by the soil on water, in coarse-grained soils. The presence of these menisci modifies the relative humidity of the soil, and consequently its total suction, since as has been seen above, capillary suction is a component of total suction (Fredlund & Rahardjo 1993). In fine textured soils such as clays, the phenomena occurring at the mineral-water interface, *i.e.* adsorption, also contribute to the attraction of the water for the soil, especially for low degrees of saturation. Consequently, in an unsaturated clay soil, the water is linked to the solid phase not only by processes of capillarity but also by adsorption, giving rise to what some authors call matrix suction, although both terms –capillary and matrix– are frequently considered to be synonymous.

In a capillary pore, capillary suction varies with pore diameter in an inverse relation. If the pores are assumed to be cylindrical, capillary suction (h, in m) and the diameter of the affected pore (d, in μm) are related by the Jurin-Laplace law:

$$d = \frac{4 \times \sigma \times \cos\theta}{\rho_w \times g \times h} \times 10^6$$

where σ is the surface tension of the water ($72.75 \cdot 10^{-3}$ N/m), θ the angle of contact (0 °), ρ_w the density of the water (998.23 kg/m^3) and g the acceleration due to gravity (9.807 m/s^2).

From what is set out above it may be deduced that the water content of a soil depends on its suction. The relation between the water content and the suction of a soil may be expressed by graphically representing the volumetric water content in a given sample versus suction, this being known as the characteristic curve or soil retention curve. As will be seen below, one of the possible uses of the retention curve is as a basis for derivation of relative permeability.

When an expansive soil approaches saturation, collapse or swelling may occur, depending on its previous stress history. Nevertheless, high values of suction cause an increase in rigidity and in the degree of overconsolidation in soils (Alonso *et al*. 1987), and in clay soils there may be irrecoverable plastic deformation (Richards 1984). When the soil is expansive, the cyclic processes of hydration and drying may cause irrecoverable expansion during the first hydration, as from which the behaviour of the material becomes practically elastic (Pousada 1984). All these characteristics are indicative of the importance of the stress history as regards the behaviour of expansive soils, including changes in water content (suction).

In recent years, theoretical models have been developed capable of explaining this behaviour through consideration of the interaction between a macrostructure controlled by phenomena of capillarity and a microstructure in which physicochemical phenomena occur at particle level. Specifically, the model developed by Gens & Alonso (1992) for unsaturated expansive clays is capable of explaining that swelling depends on initial water content, dry density and the load applied; that swelling pressure depends to an enormous degree on void ratio; that the expansive deformations may be irreversible and conditioned by history; and that swelling pressure varies with the test method.

Finally, it should be pointed out that the capacity to adsorb cations and polar molecules and incorporate them into the exchange complex is the most highly valued property of smectites as regards their use as a barrier to radionuclide migration, since their capacity to retain them in their structure and minimise their movement makes these materials a particularly powerful geochemical barrier. Cation exchange, adsorption, precipitation, chemical reactions, molecular sieving and other mechanisms also contribute to the sorption by clays of radionuclides dissolved in aqueous solutions. All of these mechanisms are influenced by the type of clay material, the characteristics of the radionuclide, the composition of the interstitial solution and the physicochemical conditions (Meyer & Howard 1983).

Bentonite under disposal facility conditions

The performance of a disposal facility is influenced by the changes occurring in the mechanical, physicochemical and geochemical properties of the engineered barriers and the host rock. These changes are generated by the combined effects of the heat produced by disintegration of the wastes, water movements and the geochemical composition of the near field. The design criteria and construction procedures used for the engineered barriers also influence the performance of a disposal facility.

The Spanish concept for the disposal of high level radioactive wastes in stable geological formations at great depth (AGP) considers the excavation of galleries, in the centre of which the cylindrical waste containers would be emplaced and surrounded by sealing material (ENRESA 1995). The thermal load of the containers will be 1200 W, this meaning that, taking into account their spatial distribution in the facility, the maximum temperature in the bentonite closest to them will be 100 °C, ten years after their emplacement. The calculations performed foresee that the temperature of the barrier will be homogeneous and close to 60 °C within one thousand years (ENRESA 1997). During this time, hydration of the barrier will also take place, on account of which it is known as the transient disposal facility resaturation phase. The lifetime of the waste canisters is expected to exceed one thousand years, as a result of which, when the canister finally ruptures, with the corresponding release of radionuclides, the barrier will be completely saturated and in a position to exercise its retaining role.

During the disposal facility construction phase, the galleries and shafts and all other spaces will be filled with air at atmospheric pressure. The bentonite will be placed in the facility in the form of high density compacted blocks made from granulated clay. At such densities, the hydraulic conductivity of ben-

tonite is extraordinarily low, while its swelling capacity is very high. In order to facilitate the compaction and storage of the blocks, they will be manufactured with the clay at its hygroscopic water content, this meaning that for the intervals of density considered, the blocks will initially have degrees of saturation of between 50 and 60 percent. Consequently, the largest pores will contain air, while the intra-aggregate pores and interlaminar spaces will be hydrated. This confers upon the bentonite another characteristic that fundamentally conditions the performance of the barrier: a very high degree of suction. This high initial suction promotes and conditions the saturation of the blocks, which will take water from the surrounding geological medium via the largest pores, the latter acting as capillaries from which the water will be distributed to smaller pores, *i.e*. in accordance with a mechanism of double porosity flow.

Furthermore, the pressure of the water in the saturated pores of the host rock will be hydrostatic, and its magnitude will depend on the depth of the disposal facility, possibly being of the order of 5 MPa. The pressure gradient established in the disposal facility also forces water to enter the barrier, although this does not have any great influence until the suction of the bentonite becomes small, that is to say, towards the end of the process. The movement of water from the surrounding rock to the clay barrier may be facilitated to some extent by the increased permeability of the gallery walls, due to microfissures arising during excavation.

However, the low permeability of the bentonite, which is even lower when not saturated, will make the saturation process very gradual. The tests performed in the Stripa underground laboratory (Pusch & Börgesson 1985), and the *in situ* test carried out at the Grimsel underground laboratory for the FEBEX Project (AITEMIN 1999), have shown the transport of water from the rock to the bentonite to be highly uniform, and have also shown that the increase in the water content of the bentonite occurs in a spatially homogeneous fashion, without being affected by the existence of fractures or other hydraulically more active zones. This is due to the fact that the permeability of the rock is high compared to that of the bentonite, as a result of which water flow is determined by the hydraulic properties of the latter.

The air initially contained in the bentonite pores will become compressed as hydration advances, and the studies performed suggest that this air will be completely dissolved in the ingressing water, which will allow for the complete saturation of the barrier (Pusch & Börgesson 1985).

During the transient phase of the disposal facility, as the material in the clay barrier becomes hydrated, expansion occurs. In the areas closest to the surface of the gallery a gap will remain between the blocks and the host rock, due to the difficulties involved in ensuring a perfect fitting between both. This gap, and the joints between the different blocks, may partially absorb the increase in the volume of the bentonite, as a result of which its density will decrease in these areas, compared to the manufacturing density of the blocks. In fact, it has been shown that the high density compacted bentonite may penetrate the joints and the fractures in the rock. Also, the blocks become sealed after saturation. However, this reduction in the density of the bentonite will be local, since the overall barrier is confined, this meaning that when hydration occurs swelling pressures will be developed and, therefore, there will be an increase in the radial stresses in the barrier. During this transient state, these stresses cause the internal parts of the barrier, which have not yet been reached by the water, to compress, thus increasing their density. In this way a density gradient is established in the system, with lower densities in the areas affected by water, where the bentonite will have expanded, and higher in the innermost areas –not yet affected by water– which are "pushed" by neighbouring zones. These density modifications affect increasingly larger areas as hydration progresses.

The entry of water not only modifies the degree of saturation and the density of the bentonite but also causes the dissolution of certain mineral species (chlorides, sulphates, carbonates), which are transported by this advective flow, generating in turn geochemical concentration gradients, different for each mineral species depending on its mobility (Villar *et al*. 1997).

In the internal part of the barrier the heat generated by the waste canister causes an increase in temperature that is transmitted outwards by conduction, convection and radiation, generating a thermal gradient. The evaporation of the water, induced by the high temperatures close to the canister, causes desiccation of the bentonite and its shrinkage, this contributing to the decrease in the porosity of the blocks in the internal areas of the barrier. The thermal expansion of the bentonite is insufficient to compensate for this decrease in porosity (UPC 1998). The vapour generated spreads towards more external and colder regions of the system, where it condenses. This may give rise to local increases in the

degree of saturation (UPC 1998). The water that condenses in the colder areas may move once more towards the canister, due to a flow process caused by the suction gradients (Pusch & Börgesson 1985), but now charged with dissolved mineral species (those originally possessed by the clay and those provided by the advective flow from outwards), which precipitate close to the canister when the water evaporates. In this way the process of evaporation/condensation is repeated and small "convection cells" are established, the most evident effect of which is an increase in salinity in the hotter areas (Villar *et al*. 1997). This movement of vapour is, therefore, an important mechanism for the transfer of water content and heat. Some authors claim that the increase in temperature may cause the precipitation of silica in the pores of the bentonite –either that found in the bentonite as a labile phase or that released during the superficial degradation of the smectite–, causing a cementation that would reduce its swelling and ion exchange capacity and an increase in hydraulic conductivity (ENRESA 1997). However, this has not been experimentally confirmed in tests in which the compacted bentonite was subjected to conditions similar to those of a disposal facility (Pusch 1985, Cuevas *et al*. 1999).

Finally, once saturation is reached in the whole barrier, there is a recovery and a certain homogenisation of the void ratio, accompanied by closure of the joints between blocks and of whatever fissures might have been formed during desiccation. Long after the closure of the disposal facility, with the barrier now completely saturated and with the canister having degraded –these phenomena expected to occur after some thousand years– there might be an important generation of gases in the interior part of the barrier. The most important processes that would give rise to the generation of gas would be the corrosion of the steel of the canister, the bacterial degradation of organic matter and the radiolytic decomposition of water. Diffusion is the dominating gas transport mechanism during the initial stages of saturation of the barrier, when the only air available is that initially contained in the pores of the bentonite. In the event of very large volumes of generated gases, its evacuation through diffusion in the water might be made difficult. In this case, the gas might escape via instantaneous "fractures" in the barrier, a process known as break-through that consists basically in transport via preferential paths that dilate and propagate (Volckaert *et al*. 1995).

Consequently, the thermal, hydraulic and mechanical aspects of the system interact significantly. Thus, variations in the degree of saturation affect both temperatures, as a result of the dependence of thermal conductivity on water content, and the distribution of stresses, due to the changes in suction linked to changes in water content. Likewise, hydration leads to important changes in the volume and rigidity of the bentonite. In addition, the thermally induced strains lead to variations in stresses and to changes in hydraulic conductivity. The diffusion of vapour –favoured by the thermal gradients– and the dependence of water viscosity on temperature –with its consequences for hydraulic conductivity– also condition water transport phenomena. Finally, the changes in porosity caused by stress variations affect hydraulic conductivity and, therefore, the movement of water. The effects of the strains on temperature may also have some importance, although the variation of thermal conductivity with porosity is not large.

Experimental techniques for the study of expansive, unsaturated materials

We have seen that the material constituting the barrier is a high density compacted bentonite. Consequently, it is a highly expansive remoulded material. The emplacement of these blocks under the conditions of a disposal facility will subject them to thermal and hydraulic gradients. The fact that the blocks are not initially saturated, along with the low permeability of the bentonite, means that a relatively long transient period is foreseen, during which a part of the material will be unsaturated.

Consequently, the characterisation of the barrier material implies the use of experimental techniques adapted to the study of highly expansive soils, in both the saturated and unsaturated states. The following sections review the state of the art in these areas.

Expansive soils

Although many studies have been carried out on soils with a certain degree of expansibility, which abound especially in arid and semi-arid regions (Arnold 1984), there have been very few geotechnical studies of materials as expansive as bentonite, due fundamentally to the fact that their properties make them totally inadequate for civil works. These materials have been used especially as a result of properties such as adsorption capacity (bleaching of oils and fats, clarification and filtering of wines, cat litter,

in the petrochemical industry and petroleum refining, pharmaceutical excipient) or of rheological properties, especially viscosity, coating capacity and anti-static qualities (drilling muds, foundry moulding sands, carriers for agrochemicals, anti-caking compounds, paints, paper, fabric softeners). Geotechnical characterisation is not required for these uses. However, more recent applications, such as for impermeable layers in urban landfills, have promoted the analysis of other properties of bentonite, such as for example its permeability (Brandl 1992). As a result of its use for barrier material in radioactive waste disposal facilities being proposed (Pusch 1979), the study of different thermo-hydro-mechanical aspects of the behaviour of high density compacted bentonites has been undertaken.

In general, the conventional testing methods used for the identification and classification of expansive soils may be divided into three categories (Pousada 1984):

- *Indirect techniques*. These consist in measuring one or more intrinsic properties of the material of those having an influence on its expansibility. Among these properties are the composition of the soil (determined by X-rays, differential thermal analysis, infrared, etc.), its physicochemical characteristics (cation exchange capacity), physical characteristics (colloidal content, specific surface and microstructure), index properties (Atterberg limits and linear shrinkage) and geotechnical classification (performed on the basis of the aforementioned soil properties). Of all these properties, those having the greatest correlation with the degree of expansibility are mineralogy, cation exchange capacity and Atterberg limits. Given that determination of the two first requires complex techniques that are not normally available in geotechnical laboratories, much emphasis has been placed on the establishment of correlations between expansion potential and the different Atterberg limits, which are straightforward and rapid determination indices.
- *Direct techniques*. These include all those methods that quantitatively determine the characteristics of volume change in soils. These measures are carried out through oedometric type tests. Basically, three types of identification tests are performed using the oedometric equipment:
  1) the free swelling test, in which the sample is inundated under a minor load and allowed to expand to equilibrium or, in the swelling under load variation, soaking occurs under a load that is not necessarily small;
  2) the free swelling test with subsequent controlled load, in which after having reached maximum swelling, the sample is gradually loaded, with strain allowed to stabilise for each load increase; and
  3) the swelling pressure test, in which the sample is inundated and strain is prevented through the application of loads.
- *Combined techniques*. These correlate data from both direct and indirect techniques, such as the Atterberg limits, clay content, water content, free swelling or swelling pressure. On the basis of these correlations, which occasionally take the form of prediction equations, soils may be classified in groups of different magnitude of volume change, this allowing semi-quantitative estimates to be made. Furthermore, soil expansibility classifications have been performed on the basis of values obtained by means of indirect techniques. Table I shows a classification of free swelling potential, while the classification reflected in Table II is of ranges of swelling pressure in undisturbed soils, both depending on other parameters obtained by means of simpler determinations.

In addition to the techniques commented on above, aimed exclusively at identifying expansibility, the laboratory study of expansive soils also includes the quantification of expansibility and the determination of other properties, such as for example, permeability.

Quantification of expansion

The tests performed to quantify the expansion characteristics of soils may be divided into two major groups: soaking tests and controlled suction tests. The latter will be dealt with in the following section. Tests including inundation of the sample, *i.e.* those in which the sample remains saturated, may be carried out using conventional oedometers, oedometers modified for the measurement of lateral pressures, Rowe cells or triaxial equipment, as described below.

Conventional oedometer testing

These tests allow the percentage of swelling and the swelling pressure of the soil to be quantified. The combination of loading and unloading paths and of initial values of pressure and water content gives

Table I
Estimate of potential volume change (free swelling) in clays (Holtz & Gibbs 1956).

Fraction $<1\,\mu$m (%)	Plasticity index	Shrinkage limit	Probable expansion (% total volume change)	Potential for expansion
>28	>35	<11	>30	Very high
20-31	25-41	7-12	20-30	High
13-23	15-28	10-16	10-30	Medium
<15	<18	>15	<10	Low

Table II
Estimate of probable swelling pressure on the basis of data obtained in the field and laboratory (Chen 1988).

Fraction $<75\,\mu$m (%)	Liquid limit (%)	Standard penetration resistance (blows/300 mm)	Probable expansion (% total volume change)	Swelling pressure (MPa)	Degree of expansion
>35	>60	>30	>10	1	Very high
60-95	40-60	20-30	3-10	0.25-1	High
30-60	30-40	10-20	1-5	0.15-0.25	Medium
<30	<30	<10	<10	<0.05	Low

rise to multiple varieties of oedometer tests. The following are among the most useful oedometric testing methods for application in civil engineering (Pousada 1984):

- Direct oedometric test. The sample, with its natural water content, is subjected to a load corresponding to the overload of the terrain, is consolidated and subsequently inundated with water and is allowed to expand to a situation of stabilisation. The load is then increased step-wise and the new consolidation is observed. Finally, the load is removed.
- Multiple oedometric test. This consists in performing the direct oedometric test on various samples subjected to different initial overloads.
- Double oedometric test. This consists in simultaneously testing two samples of the same material, one that maintains its initial water content throughout the test and the other that is initially inundated under a minor load and allowed to expand. The two samples are then loaded step-wise to the same extent. Although this technique has been widely used for the study of collapsible soils, it has the disadvantage of not taking into account the fact that expansion depends on hydration and stress paths.
- Simple oedometric test. The sample is loaded to the pressure corresponding to the overload of the land. It is then unloaded to a low pressure, is inundated and is finally loaded gradually once more.
- Constant volume oedometric test. This consists in inundating the sample and preventing it from becoming deformed by the addition of loads, up to the maximum swelling pressure, following which the loads are removed step-wise.
- Oedometric test with inundated duplicate samples. One of the samples is tested in accordance with the previous procedure and the other is inundated under a minor load and, following the stabilisation of swelling, is incrementally loaded to the swelling pressure obtained with the other sample.

The choice of one type of test or another will depend on the objective of the determination (simple identification of expansibility or quantification) and on the loading conditions to which the soil is to be subjected (for example, on platforms with low load-

ing conditions free swelling will be preferable, while for applications in which the material is to be confined, such as a disposal facility, it is necessary to know swelling pressure). Krazynski (1973) underlined the importance, for volume change measurement, of considering the different factors relating to the state of the soil and environmental conditions, as well as simulation of the load to which the structure will be subjected.

Furthermore, for the application of these methods to highly expansive materials with very high swelling pressures, conventional oedometers have to be modified. In this respect, the lever arm ratio may be increased, load cells may be used instead of the mechanical system of levers, or the surface of the sample may be reduced, with which higher pressures are obtained for the same load applied.

Oedometric testing with measurement of lateral pressure

When performed using a conventional oedometer –the main advantage of which is its simplicity of use– the oedometric tests described in the previous section have the disadvantage that it is not possible to control or to gain insight into the stress states in the soil, since only the vertical stress applied is in fact known. For this reason, various researchers have developed methods for measurement of lateral stress in oedometric cells. Komornik & Zeitlen (1965) developed a device for the measurement of lateral swelling pressure that consists in using a thin oedometer ring with extensometric bands in its central part. Other methods have subsequently been used to measure lateral pressure in the oedometer, the majority based on the use of modified oedometric rings. Among these, Dineen (1997) underlines the oedometric ring with a water-filled chamber connected to a pressure transducer, the floating ring connected to a load cell and the split ring connected to LVDTs. Another solution is to use a load cell placed on the wall of the oedometer.

Triaxial test with control of vertical and lateral expansion

In certain cases, the single-dimension test devices described above do not fulfil the needs posed by the problem to be solved. Since the 1960's, various authors have developed apparatus to independently measure vertical and horizontal expansion, as well as swelling pressures, using triaxial cells modified in different ways. Tisot & Aboushook (1983) studied the swelling characteristics of a bentonite using different testing techniques on oedometric and triaxial equipment. They concluded that the direct method of measuring swelling pressure (*i.e.* the constant volume test) is the most effective, especially when performed using triaxial equipment, that allows the stress path to be monitored during swelling and insight to be gained into both axial and radial stress. The triaxial method also provides information on water flow with time. Triaxial methods are, however, hardly used for highly expansive materials, due to the long time periods required for the samples normally used with such equipment to become completely hydrated.

Measurement of permeability

Conventional permeameters are inadequate for the direct measurement of permeability in highly expansive materials, due to the deformation that the sample undergoes on saturation and to the very small flows generated, which imply very long stabilisation times. In order to overcome these limitations, use is normally made of triaxial cells with very high confinement pressures and gradients. Nevertheless, the most frequent way of determining the permeability of expansive soils is indirect, on the basis of analysis of the consolidation curves derived from oedometric testing. Although this last method provides approximate values, it is recognised as constituting an European Standard.

Khemissa (1998) presents a stainless steel cell that makes it possible to measure the permeability of cylindrical clay samples surrounded by a flexible sheath. The specimens are placed inside the cell, where they may be subjected to confinement pressures of up to 20 MPa and to temperatures of 200 °C. The coupled device allows water flows of as low as a few mm^3/h to be measured.

In the method used in this work, which is based on the constant load permeameter technique, the confinement pressure is replaced by a rigid cell in which injection pressure is applied by pumps and water flow is measured by means of precision volume change apparatus. This is described in detail in the section "HYDRAULIC CONDUCTIVITY".

Unsaturated soils

Given the complexity of the physicochemical phenomena that take place in unsaturated soils and that govern water-solid interactions, the experimental study of these soils requires more sophisticated

techniques than those normally used for saturated soils. The first experimental studies on unsaturated soils were carried out in the fields of edaphology and hydrology, and focussed fundamentally on the determination of retention curves and of relative permeability to water.

The first group to recognise the importance of fluid pressure in pores in relation to civil engineering was probably the Croney's group, at the London Road Research Laboratory, that took the terminology used by edaphologists and observed the effects of lack of humidity on soil behaviour (Croney 1952, Black & Croney 1957).

Furthermore, during the 1960's, various authors working in the field of geotechnical engineering began to criticise the conventional testing procedures used for expansive samples based on total inundation, since it is highly unlikely that the mass of soil *in situ* would have sufficient availability of water for complete saturation of the soil, and less so for this to occur immediately. For this reason the conventional techniques were considered to provide conservative measures and the need arose for variations in water content and the respective variations in interstitial pressure or suction to be reproduced in testing, in order to make the tests more representative. The geotechnical study of unsaturated soils in fact began with adaptation of the axis translation technique, described in the following section, to oedometric equipment.

At the beginning of the 1960's, methods were developed at the London University Imperial College for the measurement of air and water pressure in pores, along with equipment for the performance of consolidation tests with applied suction and theoretical studies on application of the principle of effective stress to partially saturated soils (Bishop & Donald 1961, Bishop & Blight 1963). This school continues to work to date (Ridley & Burland 1993, 1995, Dineen 1997).

At the University of Witwatersrand (South Africa) –partly in connection with Imperial College–, equipment was developed for the performance of oedometric and isotropic tests without material water content changes, in support of the theory of effective stress in unsaturated soils (Jennings & Burland 1962).

The application of the axis translation technique to oedometric, triaxial and shearing equipment at the Laboratorio de Geotecnia del Centro de Estudios y Experimentación de Obras Públicas (Geotechnical Laboratory of the CEDEX, Madrid) meant an important development of methodologies and led to the creation of a school of research (Escario 1967, 1969 and 1980, Escario & Sáez 1973).

At the University of Waterloo (Canada) studies were performed on volume changes in partially saturated soils, dealing with stress and suction as two independent variables, this allowing the history of soil states to be represented in a state surface (Matyas & Rhadakrishna 1968).

Since the 1960's, the theoretical aspects of the behaviour of unsaturated soils have been studied at the Australian CSIRO (Commonwealth Scientific and Industrial Research Organization), and various items of suction measurement and control equipment have been developed. The work carried out by Richards is particularly noteworthy. The contribution in the use of the psychometric technique for the measurement of suction is outstanding (Aitchison 1959, Aitchison & Martin 1973, Richards 1965, 1967, 1978, 1984, Richards *et al*. 1984, Woodburn *et al*. 1993).

Furthermore, Lytton (1967), at the University of Texas A & M, was a pioneer in the establishment of a solid theoretical basis for the study of unsaturated soils.

The University of Saskatchewan (Canada) has also stood out since the 1970's for its research in the field of unsaturated soils, and there is currently an Unsaturated Soils Group within the Department of Civil Engineering (Krahn & Fredlund 1972, Fredlund & Morgenstern 1977, Fredlund *et al*. 1978, Fredlund & Hasan 1979, Fredlund & Rahardjo 1993). Also in Canada, the McGill University has promoted study of flow mechanisms in unsaturated media (Wong & Yong 1975).

At the Faculty of Civil Engineering of the Israel Institute of Technology (Haifa), studies were performed on the relation between swelling pressure or shearing strength and suction (Kassiff & Ben Shalom 1970, 1971, Komornik & Zeitlen 1965, Komornik *et al*. 1980).

The Geotechnical Engineering Department of the Technical University of Catalonia (UPC) has been working since the beginning of the 1980's on the modelling of the behaviour of unsaturated soils and on the development of experimental techniques for its study (Gens *et al*. 1979, Lloret & Alonso 1980, Josa *et al*. 1987, Alonso *et al*. 1987 y 1990). This has led to an important number of doctorate theses relating to this subject, some of which are referred to in the following sections (Lloret 1982, Gili 1987, Josa 1988, Gehling 1994, Navarro 1996, Romero 1999).

The CERMES group, belonging to the Ecole Nationale des Ponts et Chaussées and to the Laboratoire Central des Ponts et Chaussées (Paris) is researching the behaviour of unsaturated soils, developing equipment for the performance of controlled suction tests, as described below (Delage 1987, Delage *et al*. 1987).

The main methods of measuring and controlling suction are described below since, as will be seen in the following section, the measurement of suction is a complicated issue, so most experimental studies are performed controlling suction instead of measuring it. Further on the evolution of the application of these techniques to studies of different aspects of unsaturated soil behaviour (volume change, permeability and strength) will be reviewed.

Measurement and control of suction

The measurement of suction in soils may be accomplished using direct and indirect methods.

Direct measurement is complex and is possible only for very low suction intervals. This measurement is performed through the exchange of water between the instrument and the soil, driven by the negative pressure of the water in the pores. This is relatively straightforward for values of less than 70 kPa, through the use of *tensiometers*. At Imperial College (London) an instrument has been developed, made up of a small pressure transducer capable of withstanding high negative absolute pressures and a high air entry value porous stone capable of measuring up to 1.5 MPa, although with certain problems of cavitation (Ridley & Burland 1993). Relative humidity may be measured using *psychrometers*, with subsequent transformation to suction through application of the Kelvin equation. In soils, Peltier effect psychrometers previously calibrated with saline solutions are used. These allow suctions of between 0.1 MPa and 6.0 MPa to be measured.

The indirect methods are based on the use of a calibrated porous medium placed in contact with the soil. Once the water content of the soil-porous medium assembly has reached equilibrium, the suction will be the same in both. If any of the properties of the porous medium sensitive to water content –such as electrical resistivity, dielectric constant, thermal conductivity or weight– has been calibrated for a given suction, the measurement of this property will give the value of suction according to the calibration curve (Delage 1993). These methods are limited by their high degree of sensitivity to hysteresis, as a result of which any soil water content cycling alters the measurement obtained.

Of these methods, the simplest is the filter paper method, in which a *filter paper* with a known retention curve is placed in contact with the soil sample until the water contents of both reach equilibrium. At this moment, the gravimetric water content of the paper and the corresponding suction are accurately determined from its retention curve. This method allows suctions of between 0.1 kPa and 150 MPa to be measured. The *gypsum cell* method measures the variation in electrical resistance of a porous plate (plaster or gypsum) placed in contact with the soil. The porous plate is previously calibrated to determine the electrical resistance/water content ratio and the ratio between suction and water content of the plaster. Suctions in the interval 40 kPa to 3 MPa may be measured. There are also sensors that measure the volumetric water content by measuring the thermal conductivity of the soil, such as the *thermal block*, which consists of a small heater placed inside a porous ceramic block, allowing suctions of between 0 and 0.3 MPa to be measured (Fredlund *et al*. 1992). Commercial *capacitative sensors* determine the relative humidity of the soil from variations in the dielectric constant of a previously calibrated porous medium. They may be applied across the entire range of suction, since they are capable of determining relative humidities of between 0 and 100 percent. The main limitation of these sensors is their size, which is too large for use in conventional laboratory tests.

As has been seen, suction measurement techniques cover only a limited range of values, insufficient for the high values of suction that may exist in unsaturated expansive materials. This, along with the experimental difficulties involved in the study of soil behaviour with the simultaneous measurement of suction, led to the development of techniques allowing the suction to which the soil is subjected to be controlled. Three methods are especially widely used: axis translation, control of relative humidity and the osmotic technique.

- *Axis translation*. This is the most widely used suction control technique, and has been adapted to the largest number of geotechnical testing systems. It is based on the fact that the liquid phase in a porous medium undergoes an increase in pressure equal to that of the gaseous phase (Hilf 1956). To apply this technique the pressure plate or the membrane cell are used (Coleman & Marsh 1961). The sam-

ple is placed in a hermetically sealed cell in contact with water at atmospheric pressure through a high air entry value porous plate or a semipermeable membrane (Figure 38). The cell is pressurised immediately, but this interface remains permanently saturated, since the air entry value of the porous plate is greater than the pressure inside the cell, and the membrane is permeable to water but not to gas. The pressure increase in the chamber causes the air pressure in the soil pores to increase by the same amount. There will be a transfer of water between the sample and the interface until equilibrium is reached, at which time the water pressure in the interface and in the soil will be atmospheric. Consequently, the air pressure applied is equal to the matric suction of the soil under the final test conditions ($s = u_a - u_w$). The method assumes the continuity of the gaseous phase, as a result of which its application under conditions close to saturation, when there may be important quantitities of occluded air, may lead to an overestimation of suction value (Bocking & Fredlund 1980). Furthermore, both the porous plate and the membrane are permeable to dissolved salts, as a result of which the method guarantees the control only of matric suction, but not osmotic. When the semipermeable membrane is used, suction values of up to 20 MPa may be reached, this value being defined by the mechanical limitations of the cell. Thomé (1993) proposes the use of springs on the sample to guarantee good contact between it and the membrane or porous stone. Another method of controlling suction in which the principle of axis translation is used is the suction plate, with which suctions of between 0 and 0.1 MPa may be applied, since with higher values the water cavitates (Croney & Coleman 1960).

- *Control of the relative humidity*. This technique is applied especially in the case of high suction values. It consists in placing the sample in a closed chamber in which the value of relative humidity is such that it generates the desired suction, as established by the Kelvin law. A vacuum desiccator is normally used, with the possibility of placing various samples on its porcelain plate (Figure 16). A sufficient quantity of an appropriate solution is placed in the bottom of the desiccator. Saturated salt solutions or solutions of a given product at a different concentration, frequently sulphuric acid, may be used. In this last case, the concentration of the product determines the activity of the water in the solution (partial vapour pressure), and consequently the relative humidity generated. The transfer of water between the environment and the sample takes place in the vapour phase, by a process of diffusion in accordance with the Fick law, as a result of which the process is slow. Vacuum is generated in the desiccator in order to speed up the process. In

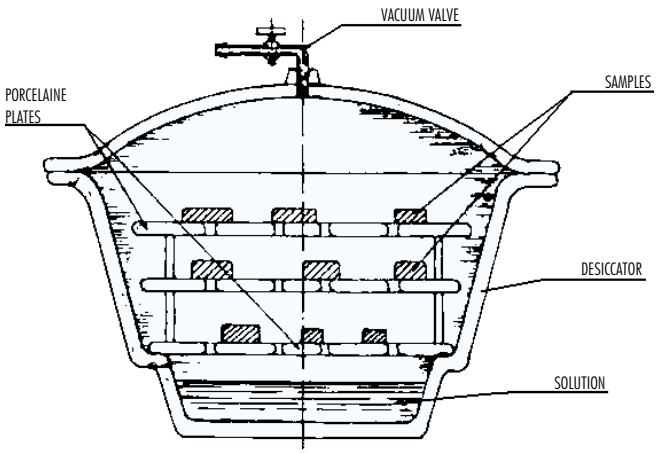

Figure 16. Desiccator with solution for the control of relative humidity (Esteban 1990).

view of the fact that the salts initially contained in the sample cannot leave it, this technique controls both matrix and osmotic suction. With saturated saline solutions, suctions of between 2 and 160 MPa may be applied, while with solutions of sulphuric acid of different concentration, the range of suction values is from 3 to 1000 MPa (Esteban 1990), although good control of suction is achieved only at values of below 600 MPa.

- Osmotic technique. The principle on which this method is based is that the potential of the water increases with hydrostatic pressure and decreases with solute concentration. Thus, a confined solution in contact with free water across a semipermeable membrane will be in equilibrium when the hydrostatic pressure applied to it is equal to osmotic suction, this constituting osmotic pressure. In applying this technique, a semipermeable membrane and a solution of large size organic molecules (polyethylenglycol, PEG) are used. The molecules of the solution cannot pass through the membrane, unlike the water. Consequently, when the solution is placed in contact with the water in the soil, the former will exercise an osmotic attraction over the latter, until the concentrations of both reach equilibrium. The suction applied depends on the concentration of the solution, and may reach up to 2 MPa in the absence of mechanical pressure. This method applies only matric suction, since the membranes are permeable to ions, which may move from the soil water to the solution. Recently, Delage *et al*. (1998) have increased the range of suction of the osmotic method for the determination of retention curves to 10 MPa.

The table III summarises the main characteristics and applications of the measurement and control techniques described above.

Volume change measurement

The first equipments used for the measurement of volume change in unsaturated soils were conventional oedometers with a device designed to keep the soil isolated from the exterior, in which suction was applied by means of a column of mercury. The maximum suction value achieved was 0.1 MPa (Escario 1965, 1967). Later, Escario (1969) developed a device that allowed swelling and swelling pressures to be measured, with control of suction up to 10 MPa. As in the case of the previous equipment, suction control is based on the principle of axis translation. The sample is confined laterally in a ring and is placed over a semipermeable membrane seated on a porous plate, inside a sufficiently robust pressure chamber. This chamber is pressurised with nitrogen gas. A second coarse-grained porous stone is placed over the sample, allowing the gas to act on the pores in the soil. Above this porous stone, a rigid metallic disk receives the vertical loads via a piston (Figure 17). Escario & Sáez (1973) made a subsequent modification to this cell. These

Table III
Suction measurement and control techniques (Ridley & Burland 1993).

Technique	Type of suction	Main use	Type of measurement	Range (MPa)	Equilibrium time
Vacuum desiccator	Total	Laboratory	Indirect	1-1000	Months
Psychrometer	Total	Field	Indirect	0.1-7	Months
Filter paper	Total Matric	Field Laboratory	Indirect	1-30 0.03-30	Weeks 1 week
Gypsum cell	Matric	Field	Indirect	0.03-3	Weeks
Thermal block	Matric	Field	Indirect	0-0.3	Days
Suction plate	Matric	Laboratory	Direct	0-0.1	Hours
Tensiometer	Matric	Field	Direct	0-1.5	Hours
Pressure plate	Matric	Laboratory	Direct	0-5	Hours

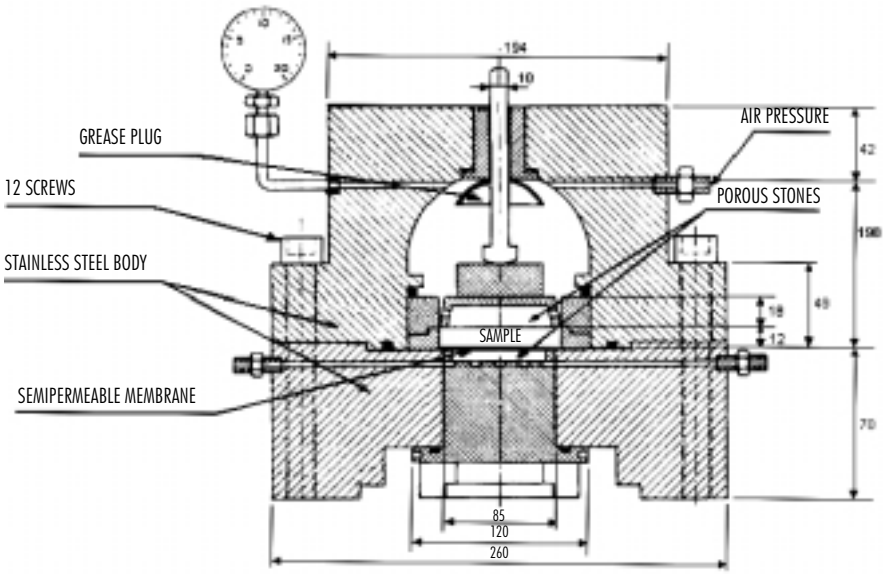

Figure 17. Oedometer with suction control by gas pressure (Escario 1969).

authors underlined the high compressibility of the cellulose membrane and the repercussion that it has on the total deformability of the equipment, this not being attributable to the sample and, therefore, implying the need for calibration. Another modification to this cell allows lateral pressure to be measured, through the incorporation of an extensometric band inside the ring (Cuéllar 1978).

Kassiff & Ben Shalom (1970) developed an item of equipment for the measurement of swelling potential (oedometer) in which water uptake by the sample is controlled by an osmotic system. A semipermeable cellulose membrane in contact with the upper and lower parts of the sample separates the latter from the osmotic solution of polyethylenglycol. Depending on the concentration of the solution, osmotic pressures of up to 2 MPa may be obtained. Vicol (1990) and Delage *et al.* (1992) improved the oedometer with suction control by the osmotic method, incorporating a closed circuit and a pump, in order to guarantee the circulation of the solution and allow for more accurate control of the exchanged volume of water.

Lloret (1982), using a modified Rowe cell, controlled air and water pressures and measured water intake through a porous stone having a high air entry value.

Pousada (1984) carried out a study of deformability mechanisms in expansive clays, with special attention to suction control and to the effects of compaction conditions, overload and hydration-desiccation cycles. For this purpose, he used the oedometer with suction control by nitrogen pressure developed by Escario & Sáez (1973), and simple cells for the consolidation of partially saturated soils. These cells allow the sample to be isolated from the external environment, thus preventing variation of the water content of the soil.

In his Doctorate Thesis on the experimental characterisation of the expansivity of an evaporitic rock, carried out at the CEDEX Geotechnical Laboratory, Esteban (1990) used different types of modified oedometers to work with unsaturated samples. The simplest of these, constructed entirely in stainless steel to avoid corrosion, included a perspex sheath hermetically covering the cell and preventing the exchange of water with the atmosphere. In this way, the sample was kept unsaturated, but there was no control over the suction value. For tests including suction control up to 12 MPa, he used a modification of the membrane cells designed by Escario &

Sáez (1973). For higher values of suction, he developed an oedometric cell in which suction control was achieved by imposing a given relative humidity by means of solutions of sulphuric acid of different concentrations, poured into a deposit located inside the cell (Esteban & Sáez 1988).

These controlled suction oedometric cells, both the pressure membrane and the solution types, are the ones used in the present study, therefore both the cells and the relation between the concentration of the sulphuric acid solution and the relative humidity generated are described in the section "Controlled suction oedometric tests". According to the author, suctions of between 0 and 1000 MPa may be applied by means of the solutions.

In relation to recent research focussing on experimental aspects, special mention may be made of the work carried out by Gehling (1994) on moderately expansive soils (Madrid clay, bentonite, sand and mixtures) –tested in conventional oedometers and in oedometers with suction control by gas pressure up to 5 MPa–, the most outstanding contribution of which is the verification of different aspects of the behaviour of unsaturated expansive soils included in the Gens & Alonso model (1992).

An oedometric system has been developed at Imperial College of London that simultaneously allows for the measurement of radial strain and the control and measurement of suction up to 1.5 MPa. The suction of the sample is controlled using the osmotic technique (Dineen & Burland 1995, Dineen 1997), through a semipermeable membrane in contact with the base of the sample. Suction is measured at the upper part of the sample using up to three suction probes developed at Imperial College, and described above (Ridley & Burland 1993). An oil compensation system is used to prevent lateral strain of the sample during testing (Figure 18).

In his Doctorate Thesis, Romero (1999) makes a study of the volumetric behaviour of unsaturated clays subjected to suction and temperature changes. For this purpose he uses fundamentally oedometric cells with suction and temperature control, although he also uses an isotropic "minicell" and modified triaxial equipment to analyse behaviour under isotropic conditions. In all these cells, suction is applied by means of the axis translation technique, to values of 1 MPa. The working temperatures were up to 80 °C. The oedometric cells are designed to allow for controlled loading, suction and temperature

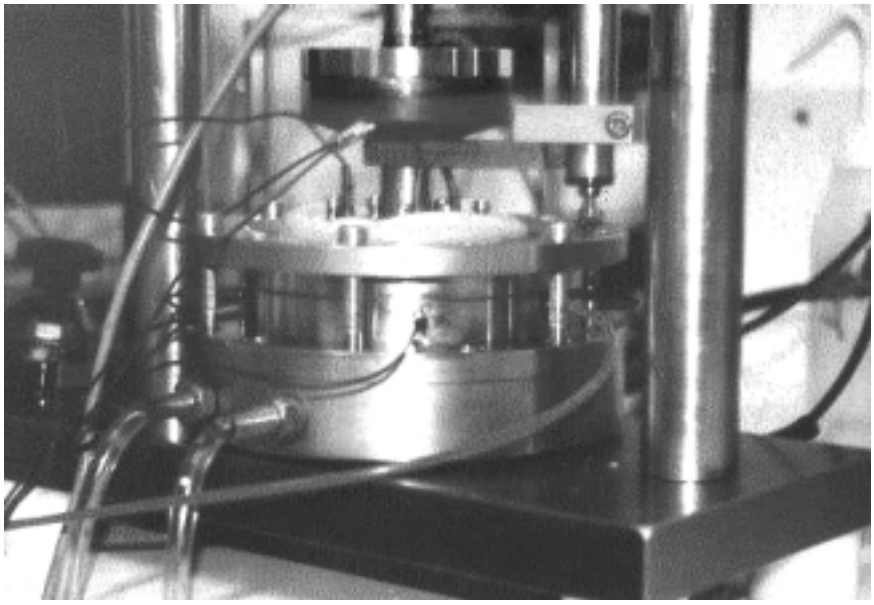

Figure 18. Oedometric cell developed at Imperial College (Dineen & Burland 1995).

paths. Furthermore, a lateral pressure measuring oedometer was adapted for the performance of tests with suction control and the measurement of swelling pressure without volume change. In the triaxial equipment used, suction control is accomplished at both ends of the sample, this reducing stabilisation times. Lateral strains are measured by means of an electro-optical laser system, and axial strains by internal LVDTs.

Permeability measurement

Despite the complications involved in the different physicochemical interactions between the three phases present in unsaturated soils, the laws governing the flow of the different constituents are not very different from the classical laws applied to saturated soils. In the case of water, the validity of Darcy's law has been experimentally verified, the coefficient of permeability depending on the degree of saturation. In any soil, permeability increases with the degree of saturation. Taking this into account, relative permeability (k_r) is defined for a given porosity and degree of saturation as the ratio between the unsaturated permeability (k) for this degree of saturation and the saturated permeability (k_w) for the same porosity, therefore it takes a value of between 0 and 1. It is generally accepted that relative permeability is related to the degree of saturation in accordance with a potential law.

Furthermore, air flow is governed by the Fick law which, when the air is considered to be a perfect gas, may be assimilated also to Darcy's law, with a coefficient of permeability to gas (k_g). Given that there are no important interactions between the air and the other constituents of the soil, air flow depends only on the air pressure gradient and on the volume of air in the soil, which in turn depends on the degree of saturation.

The methods used to determine permeability to water in the unsaturated state are based on the measurement or control of suction, this being necessary in order to determine the value of the gradient. Laboratory methods may be classified into two major groups: steady-state and transient (Klute & Dirksen 1986, Dirksen 1991), some being described below. The majority apply Darcy's law in a more or less rigorous manner or with some simplification.

The steady-state methods include the following:

- *Head-controlled*. This consists in performing steady-state measurements on a column of soil in which suction is controlled at both ends, normally by means of porous stones, such that it remains uniform along the entire length (Corey 1957). Measurement is accomplished using tensiometers. For suctions in excess of 30 kPa, the times required to reach the steady state may be very long.
- *Flux-controlled*. In this case, the measurements are performed on a column of soil in which a controlled flow is applied to one of the ends (Wooding 1968).

The most widely used transient methods include the instantaneous profile and pressure plate techniques:

- *Instantaneous profile*. Water contents and hydraulic potential are measured on the basis of time at different depths during the draining of an initially saturated column of soil. For certain times and depths, water content is deduced from the measured value of suction, with the help of the previously determined retention curve. If local suction and water content are known, it is possible to calculate permeability on the basis of the degree of saturation. Hydraulic potentials are measured directly using tensiometers, mercury pressure gauges or pressure transducers. Daniel (1982) used psychrometers to measure the potential of water, this making it possible to extend the range of degrees of saturation that may be tested to values of between 20 and 90 percent, depending on the type of soil. Capacitative humidity sensors have recently been used at CIEMAT to determine the value of suction at different points of a column of soil during evaporation/infiltration tests, this allowing the entire range of degrees of saturation to be covered (Villar & Martín 1999).
- *Evaporation method*. This is a modification of the instantaneous profile method that allows the retention curve and the hydraulic conductivity of a sample to be determined simultaneously. An initially saturated column of soil is allowed to evaporate from its upper end, while the total loss of weight and the pressure gradients are recorded at, at least, two different depths. These data allow the retention curve to be calculated by means of an iterative method. Once this is known, flow density may be determined at various points, this allowing hydraulic conductivity to be calculated through application of Darcy's law (Wind 1966).
- *Pressure plate* (Gardner 1956). This method uses the pressure plate equipment cited in the

section "Suction measurement and control", which is based on the principle of axis translation. The sample inside the cell is subjected to a stepwise higher suction while the water outflow is measured versus time. The increases in suction must be sufficiently small for the hydraulic conductivity to be considered constant, and the ratio between water content and suction linear. The results obtained are interpreted through application of the Richards equation, with numerous simplifications and assumptions. By means of this technique, Romero (1999) has recently measured the permeability of the Boom clay using data on inflow and ouflow from wetting/drying tests performed in oedometric cells with matric suction control. A variation of this method, which is quicker to perform but which entails more complex data analysis, is the so-called "one-step outflow" method.

None of these methods is directly applicable to expansive materials, due to the variations in volume that occur depending on the degree of saturation, the slowness of the evaporation and infiltration processes and the unsuitability of the procedures habitually used to measure water potential for the values of suction encountered in these materials. An alternative method for calculation of the permeability of these materials is the back-analysis of infiltration tests performed under transient conditions, through the application of a theoretical model for solution of the inverse problem (Kool *et al*. 1985; Pintado *et al*. 1998). This allows the exponent of the unsaturated permeability law to be identified and, if thermal flux is applied, the value of tortuosity.

There are also numerical methods that make it possible to calculate relative permeability from other known properties of the soil, such as the retention curve, porosimetric or granulometric distribution or saturated hydraulic conductivity. These theoretical methods are generally based on pore size statistical distribution models, which assume water flow to occur via cylindrical pores and incorporate the equations of Darcy and Pouseuille (Burdine 1953). The different methods use these parameters separately or in combination. For example, an habitual procedure for empirical prediction of the permeability function of an unsaturated soil consists in using the retention curve and the coefficient of saturated permeability, the latter being used as a fitting factor for the calculations to be more accurate (Marshall 1958, Mualem 1976, Fredlund & Rahardjo 1993). Other authors have developed models for the calculation of unsaturated conductivity from the measured retention curve (Millington & Quirk 1961). A very widespread technique consists in adjusting the retention curve data to a "closed" equation using the same parameters as the analytical expression of the relative permeability. One of the most widely used of these fittings is the van Genuchten fitting (1980). Recently, models have been developed that calculate the hydraulic conductivity of the soil depending on water content, on the basis of the density and particle size distribution of the soil (Arya *et al*. 1999). Pore size distribution is derived from granulometry, and conductivity from pore size distribution, since it is assumed that water flow depends on the size of the pores.

Even commercial programmes have been developed that perform the calculation of the coefficient of permeability on the basis of other parameters. For example, the RETC code (van Genuchten *et al*. 1991) calculates relative permeability, diffusivity and the five parameters for the fitting of the van Genuchten equation from retention curve data and the value of hydraulic conductivity for a single degree of saturation. The Rosetta code (Schaap 1999) calculates the retention parameters of van Genuchten (1980) and the saturated hydraulic conductivity using textural class, textural distribution, density and one or two points of the retention curve.

The fitting between the values obtained using theoretical models and experimental values is not always satisfactory, at least not for the entire range of suctions and especially in very fine textured soils. Nevertheless, its use is widespread because it facilitates and cheapens to an extraordinary extent the knowledge of a key property to understanding and predicting the transport processes in soils.

Measurement of strength

The first apparatus developed for the study of shear strength in unsaturated soils was presented by Bishop & Donald (1961). It consisted of a modified triaxial cell allowing for the measurement or control of water and air pressure, and the independent measurement of volumetric water and sample changes. Suction control is accomplished through application of the axis translation principle. The porous stone is placed at the base of the cell and air pressure is applied at the upper part of the sample. As the sample is desaturated, the water is expelled from the lower part. In order to avoid the leakage of gas through the membrane enclosing the specimen, it is surrounded by mercury. The level of mercury in the cell also indicates sample volume changes.

The principle of axis translation has also been applied to other triaxial systems, such as the one designed by Escario (1980), in which gas pressure is applied across a coarse-grained porous stone positioned at the upper part of the enclosed specimen. The lower porous stone, in contact with water at atmospheric pressure, has a high air entry value, in order to guarantee its permanent saturation. The volume changes occurring during the test are measured by means of an optical method.

A direct shear testing system was also developed at CEDEX, in which suction is controlled by the injection of nitrogen (Escario 1980, Escario & Sáez 1986). If high air entry value porous stones are used, suctions of up to 1.5 MPa may be applied, this increasing to 15 MPa when semipermeable membranes are used.

At the University of Oxford, Wheeler (1986, 1988) developed a twin-wall triaxial cell in which the water pressure in the pores of the sample is kept above atmospheric pressure by the principle of axis translation. The water pressure is applied at the base of the sample through a porous filter with an air entry value of 0.5 MPa, and air pressure is applied at the upper part of the sample through a filter with low air entry value. Specimen volume changes are measured by control of the water flow in the internal chamber of the cell.

A triaxial system was developed at the Geotechnical Engineering Department of the UPC, based on the equipment developed by Bishop & Wesley (1975), in which suction is controlled by air pressure applied across the upper porous stone. Vertical strain is measured by means of an inmersed LVDT, radial strain by a floating ring seated on the surface of the mercury and connected to an LVDT, and changes in the volume of the water in the sample by means of the level variation in a deposit of mercury included in the interstitial pressure control circuit (Josa 1988, Josa *et al*. 1987).

Komornik *et al*. (1980) developed a testing system for the swelling and shearing strength of partially saturated compacted samples, which was applied to clays having a relatively high swelling potential. The osmotic method was used to control humidity. The equipment consisted of a modified triaxial cell in which a cylindrical sample is inserted, with a central perforation covered by a cellulose membrane in contact with the osmotic solution. At the same time, the external part of the sample is subjected to the confining pressure of the cell chamber. Suctions ranging from 25 kPa to 0.3 MPa were applied. Delage *et al*. (1987) also developed a system in which two semipermeable membranes are placed at the base and upper part of the sample. The osmotic solution circulates behind the membranes. In this way, the suction is controlled at both ends of the sample, this allowing equilibrium times to be reduced. The typical stress/strain and volume variation curves obtained using this equipment show the increase in the strength, rigidity, brittleness and dilatant behaviour of the soil with suction (Cui 1993).

For the thermo-hydro-mechanical study of unsaturated soils on quasi-static paths, Saix & Jouanna (1990) presented a "thermal triaxial" system. The control of gas and water pressure is accomplished independently in the upper and lower parts of the specimen, respectively. The chamber of the cell in which the specimen is confined is filled with oil, through which radial pressure is applied. The temperature is regulated by means of electrical resistances inserted in the body of the cell (wall, cover and base), allowing temperatures of up to 80 °C to be reached. The entire assembly is surrounded by a thermal insulation system. The volume of water entering and exiting the sample is measured by displacement in a capillary tube of the meniscus formed by the water and a liquid not miscible with it and of slightly lower density. Capillary suction is measured or controlled via this same system, by means of a mercury pressure gauge. A perforated bronze disk located at the upper part of the sample allows for gaseous transfer between the sample and the exterior. The measurement of all temperature-dependent variables requires previous calibration of the equipment under the same conditions.

A triaxial system with suction control by means of the vapour equilibrium technique and simultaneous measurement of suction by psychrometers has recently been set up at the University of Manitoba (Canada) (Blatz & Graham 2000). The ionic solution that generates the desired suction is placed in a desiccator connected to the base of the sample. The upper part of the sample is also connected to this desiccator via a pump and an air flow meter, as a result of which the vapour passes across the specimen, aided by strips of geotextile positioned across the latter. The psychrometers are placed in two different positions inside the sample, and suctions of up to 8 MPa may be measured.

Finally, it should be pointed out that none of the items of equipment mentioned above is commercially available. They are prototypes, developed for specific research work, their handling is complex and their working suctions are too low for them to be of use with bentonite.

página en blanco

4. Material

4. Material

All of the experimental work described in this document has been carried out on bentonite from the Cortijo de Archidona deposit, selected by ENRESA during the preliminary phases of research as a reference material for the backfilling and sealing of a high level radioactive waste disposal facility in a deep geological formation (see section "THE STUDY OF CLAY BARRIERS IN SPAIN"). The S-2 clay, which was intensely studied during earlier research projects referred to in previous sections, was also extracted from this deposit.

The Cortijo de Archidona deposit is located in the SE end of the Serrata de Níjar, 12 km SE of the village of the same name (Almería). The Serrata de Níjar is made up of a succession of small hills running in the NE-SW direction and measuring some 11 km in length and 1.5 km in width on average. The area is located in quadrant III of the 1:25.000 scale IGN map "Fernán Pérez".

Geological context

Along with the Sierra de Cabo de Gata, the Serrata de Níjar constitutes the volcanic region of Cabo de Gata. The volcanic materials of this region form part of a more extensive assembly that to a large extent is submerged beneath the sea of Alborán, the main emerging deposits of which are found in the SE part of the provinces of Almería and Murcia, on the island of Alborán and in northern Africa. The origin of this volcanism is associated with the geotectonic dynamics of the Western Mediterranean during the Neogene. The radiometric dating of the volcanic episodes, which are calco-alkaline in type, indicates ages of between 15 and 17 million years (Fernández 1992). This volcanism frequently occurred under shallow submarine conditions. Episodes of both emersion and immersion of the volcanic complexes subsequently took place, as is shown by the interlayering of palaeosoils, bioclastic limestones and reef materials. For this reason, the volcanic rocks have been exposed to the action of both meteoric and marine waters, in both cases linked to hydrothermal systems caused by the volcanic activity itself. The action of these fluids at different temperatures contributed to the alteration of the volcanic rocks, giving rise to silica, alunite, jarosite, kaolinite or bentonites, depending on the composition of the solutions.

The Serrata de Níjar is a volcanic complex that forms part of an intensely fractured horst, bound by two fractures running parallel in the NE-SW direction that position it parallel to the Sierra de Cabo de Gata, located to the SE. Figure 19 shows the location of the zone within the context of the south-eastern Iberian Peninsula. Materials of the Bético substrate (Triassic-Jurassic limestones and dolomites), Tertiary limestones and Quaternary materials outcrop in this area, along with abundant volcanic rocks.

The Cortijo de Archidona bentonites deposit is located to the south of the Serrata de Níjar, an is reflected on sheet 1046 of the IGME 1:50.000 scale Geological Map, corresponding to Carboneras. Figure 20 shows a geological diagram of the deposit that illustrates the arrangement of the different materials. From the oldest to the most modern, these materials are as follows (Delgado 1993):

- Betic substrate, constituted fundamentally by a breccoid limestone of Jurassic age, in addition to Triassic dolomites and filites.
- Volcanic rocks, including polygenic and dacytic tuffs, amphibolic dacytes, riodacytic vitrophyres, pyroclastic breccia of dacyte and andesite and vitrophyres.
- Sedimentary covering, formed by Pliocenic and Quaternary materials and constituting the SE limit of the bentonitised zone, with which it enters in contact by means of a major fault.

The geometry of the quarry from which the mineral is extracted runs in two directions of maximum alteration, coinciding with areas of fracturing. The main mass of bentonite coincides with a fault running NW-SE, which is where the most important mining work has been carried out. A second zone, where the volume of altered material is smaller, coincides with a fault running NE-SW.

Origin

Volcanic rocks containing important quantities of volcanic glasses are easily altered, due to their disordered internal structure. If the circulation of fluids is favoured by the high permeability of the material –as is the case of volcanic tuffs– or by the existence of fractures, this process will be reinforced, its scope increasing with rising temperature.

The studies performed on the bentonites of the Cabo de Gata region have concluded that these materials have been formed by the hydrothermal alteration of acid volcanic rocks, dacytes and riolytes. The process involves the mobilisation of silica, iron,

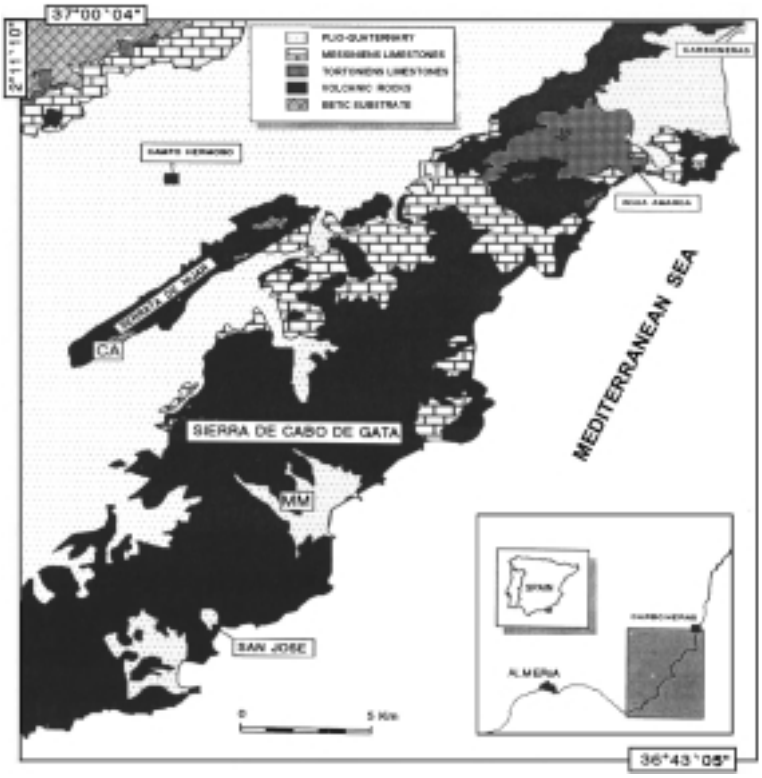

Figure 19. Location of the Cortijo de Archidona (CA) deposit in the context of SE Spain (from Delgado 1993).

alkali and alkaline earth elements. The newly formed materials present diverse characteristics, depending on the type of rock that has undergone alteration and on the chemical composition, origin and temperature of the altering solutions.

The bentonised materials of the Cortijo de Archidona deposit are darkly coloured vesicular riodacytic glasses and paler ignimbrites. The processes of alteration have been favoured by the intense brecciation of these materials in the fractured zones, which at the same time has allowed for the passage of altering solutions. The relation between the fractured zones and bentonisation is evident throughout the entire Serrata de Níjar. The bentonised zone disappears to the NW and SE, due to mechanical displacements caused by intense tectonic activity in the area during the Plioquaternary.

The first isotopic studies performed at Cabo de Gata suggested that bentonisation took place due to the effect of meteoric fluids at low temperatures, of around 40 °C in the case of the Serrata de Níjar deposit (Leone *et al.* 1983). Caballero *et al.* (1985) consider that the hydrothermal solutions that caused the alteration of the volcanic rocks of the Serrata de Níjar into bentonites were of chloride-sodium type, with a neutral or slightly acid pH.

Recent isotopic studies (Delgado 1993) consider that the bentonites of the Cortijo de Archidona deposit were produced as a result of the alteration of intensely brecciated volcanic glasses. The first hydration and devitrification states of the rock included the intervention of hydrothermal solutions, the temperature of which subsequently decreased to environment values, with which the smectites present in the deposit are in equilibrium.

Exploitation and processing

The bentonite deposits of the Cabo de Gata have been commercially exploited through open-pit quarries workings since the 1950's. There are more than 30 outcrops, the most important of which are those

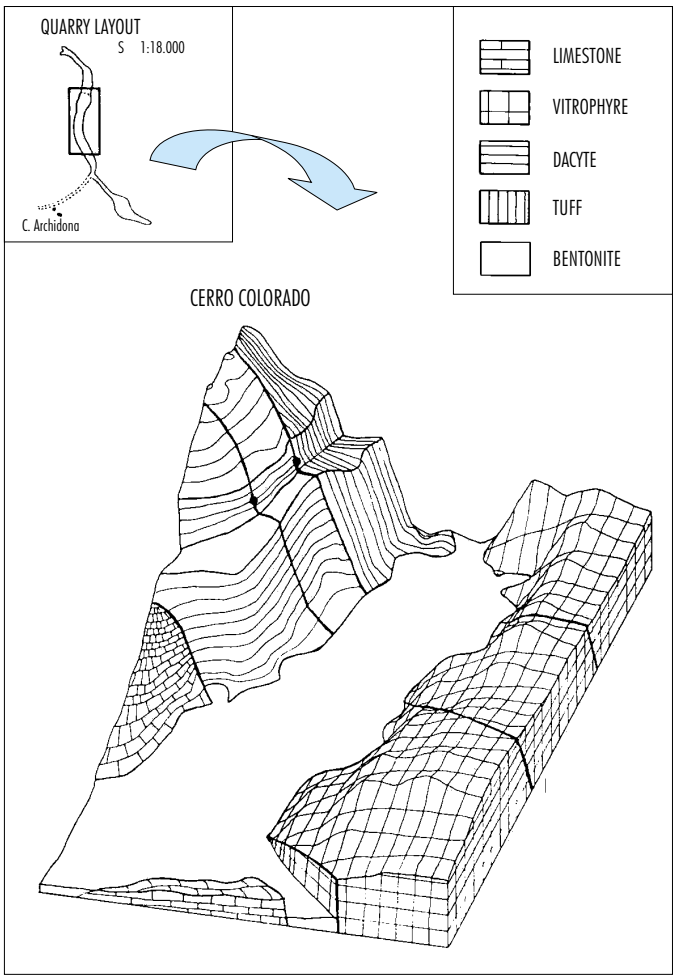

Figure 20. Diagram of the Cortijo de Archidona deposit and associated materials (from Delgado 1993).

found at Los Trancos and Cortijo de Archidona. There are also other bentonised areas in the Serrata de Níjar, among which Cerro Colorado, Collado del Aire, Pecho de los Cristos and Palma del Muerto are particularly significant.

The Cortijo de Archidona deposit is exploited by the company Minas de Gádor, which has supplied the material studied in two main phases. The first, around 1990, in which 20 t of clay ground to a size of less than 5 mm were supplied, this being given the reference S-2. Work was carried out using this material until 1995. The second delivery was made in 1995, for the FEBEX Project. Figure 21 shows a view of the cutting from which the FEBEX clay was extracted.

In this case, 660 t were extracted (from the area shown in Figure 21), which were homogenised and prepared at the quarry and in the factory in accordance with the following steps (ENRESA 1998):

- Homogenisation and drying at the quarry: the material gathered was spread over a platform to facilitate ploughing (Figure 22) and turning by chain machines; it was then crushed and homogenised by means of a rotary cultivator and the volcanic fragments were manually removed, after which it was left to dry for one day. Four homogenisation and drying cycles were performed.
- The following operations were carried out in the factory: fractioning and crushing of the

Figure 21. Workings zone seen from the NW. The FEBEX bentonite was taken from the central part.

Figure 22. Platform ploughing operation.

material by means of a bladed crusher, and subsequently a smooth roller and bladed roller disintegrator; drying in a rotary oven, without the temperature of the clay exceeding 60 °C, and sieving of the material by means of a 5 mm mesh.

As a result of this process, the final product has a granulometry of less than 5 mm and a water content in the factory of 14±1 percent. This material was packed in large impermeable bags of some 1300 kg. A 10-kg sample was taken from each of these bags. From each sample 6 kg were taken and they were all mixed by shovelling to obtain a homogeneous reference sample, 70-IMA-3-4-0 –from hereon FEBEX–, which was subsequently quartered. During the material characterisation stage, the main physical, mineralogical and geochemical characteristics of the different samples taken during factory processing of the clay were identified. This allowed the homogeneity of the material to be verified. The tests described in this document were performed using the FEBEX clay, although for several years work was performed in the laboratory using the S-2 clay. In addition to allowing for the detailed characterisation of this bentonite, this served to improve the equipment and methodology required to work with expansive materials. Certain of the basic thermo-hydro-mechanical characterisation tests described herein were performed on samples from the 10-kg bags, taken in the factory, although for the most part the homogenised 70-IMA-3-4-0 (FEBEX) sample was used. Given that the entire batch was seen to be particularly homogeneous, no distinction has been made between different samples, and the results were evaluated jointly.

Mineralogy and geochemistry

Characterisation of the material was carried out during the initial phases of the FEBEX Project, on samples from the 10-kg bags as well as samples from the mixed sample (FEBEX). The similarity of the results obtained from both led to the material's being considered homogeneous, with the possibility of giving a single average value with corresponding deviations. The preparation of the samples for mineralogical and chemical characterisation was performed by the Proyecto de Caracterización Hidrogeoquímica de Emplazamientos (Hydrogeochemical Site Characterisation Group), while analyses were carried out by the CIEMAT Analytical Chemistry Division. The methods and detailed results were collected by ENRESA (1998 and 2000) and are summarised below. These determinations were performed also in the laboratories of CSIC-Zaidín on aliquots of the homogeneous material. Although their results are not presented here, they are very similar to those obtained by CIEMAT (ENRESA 2000).

Mineralogical characterisation was performed by X-ray diffraction on samples dried at 60 °C and ground to grain sizes of less than 63 μm. The essential minerals were determined using the powder method in a Philips PW 1370 diffractometer. The fraction of less than 2 μm, obtained by suspension, sedimentation and filtering, was studied by oriented aggregates which were air-dried, solvated with ethylenglycol and heated to 550 °C. Furthermore, the accessory minerals were identified by means of stereoscopic microscopy, separated and analysed using a scanning electron microscope coupled to a dispersive X-ray energy analysis system (EDAX).

The analysis of 15 different samples allowed the semi-quantitative mineralogical composition of the FEBEX sample to be determined, the average values and standard deviations of which are shown in Table IV. The sample is made up fundamentally of smectite, with minor quantities of plagioclase, quartz and cristobalite. Potassium feldspar, tridimite and calcite appear in trace amounts (Tr).

Figure 23 shows a typical X-ray diffraction pattern of the samples analysed obtained using the powder method.

Other minerals present, identified by scanning electron microscopy, are micas (sericite, biotite, chloritised biotite), pyroxenes, amphiboles, pyrite, oxides (illmenite, magnetite) and phosphates (apatite, xenotime, monacite). All these come from the original volcanic rock and overall represent a proportion more of less than 1 percent. Sulphates, halite, or-

Table IV
Semi-quantitative mineralogical composition of the total sample (average values and standard deviations in percent).

Smectite	Quartz	Plagioclase	Cristobalite	K-Feldspar	Tridimite	Calcite
92±3	2±1	2±1	2±1	Tr	Tr	Tr

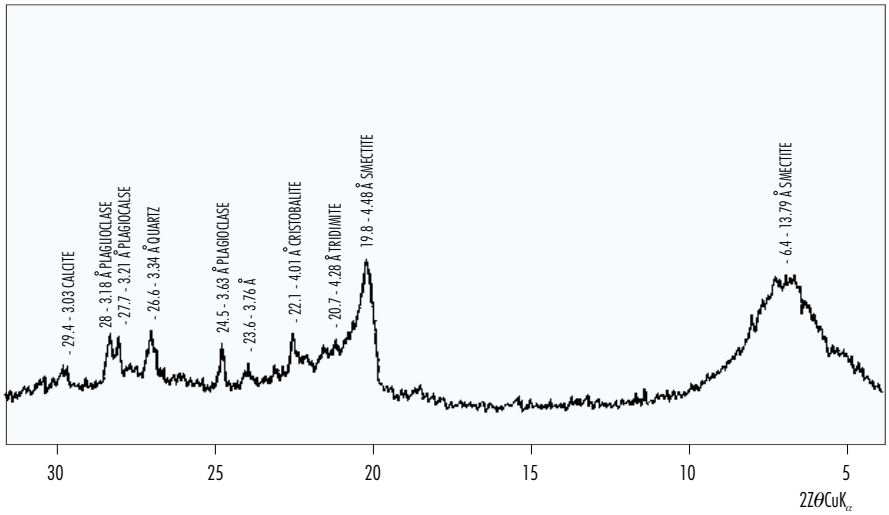

Figure 23. X-ray diffraction pattern of the total sample (ENRESA 1998).

ganic carbon and amorphous phases also appear, without their together exceeding 1 percent.

Analysis of the oriented aggregates of the fraction of less than 2 μm indicates that the latter is made up almost exclusively of smectite, since the peak at 14 Å of the untreated oriented aggregate changes to very strong reflection at 17 Å when the aggregate is treated with ethylenglycol, collapsing at bellow 10 Å when it is heated. The evolution of the position of the peaks on the X-ray diffractograms of the oriented aggregates, depending on the different treatments, is shown in Figure 24, which includes a set of patterns representative of the samples analysed. Analysis of the patterns for solvation with ethylenglycol, according to the method of Moore & Reynolds (1989), with consideration given to the distance between peaks for reflections 001/002 and 002/003, indicates that the smectite is dioctahedral, with a proportion of interstratified illite of between 10 and 15 percent.

The structural formula, determined by chemical analysis of the fraction of less than 2 μm of two samples homoionised in calcium, indicates that the smectite is aluminic dioctahedral and that the negative charge occurs as a result of magnesium replacement in octahedral positions, this indicating that the smectite is of the montmorillonite type (Newman & Brown 1987).

Analysis of the clay cation exchange complex, performed by successive displacements with ammonium acetate on 9 different samples, shows that the main exchangeable cations are calcium, magnesium and sodium, as indicated in Table V, which also shows the value of the cation exchange capacity (CEC) determined as the sum of cations.

Chemical composition was analysed on 6 samples dried previously at 60 °C and ground to a grain size of less than 63 μm. The analytical methodology used was as follows: coupled induction plasma spectrometry for Al_2O_3, Fe_2O_3 $_{total}$, Na_2O, MgO, MnO, TiO_2, CaO, As, Ba, Ce, Co, Cr, Cu, La, Ni, Sr, U, V, Y and Zn; X-ray fluorescence for SiO_2; atomic emission flame spectrometry for K_2O and Li; organic (CO_2org) and mineral (CO_2min) carbon and sulphur were determined using a Leco CS-244 elementary analyser; H_2O^- and H_2O^+ were determined by means of ATG, using a Seiko TG/DTA 6300 system. The average values and standard deviations obtained for each element analysed are shown in Table VI.

Of the trace elements found in the greatest proportion, Cl (592±10 ppm), Sr (220±21 ppm), Ba (164±234 ppm), Zn (65±4 ppm), Ce (74±5 ppm) and Li (54±3 ppm) were particularly significant.

The content of soluble salts was determined using aqueous extracts with a solid:liquid ratio of 1:4 on 10 different samples. In these extracts, chlorides were present in a concentration of 150±6 mg/L,

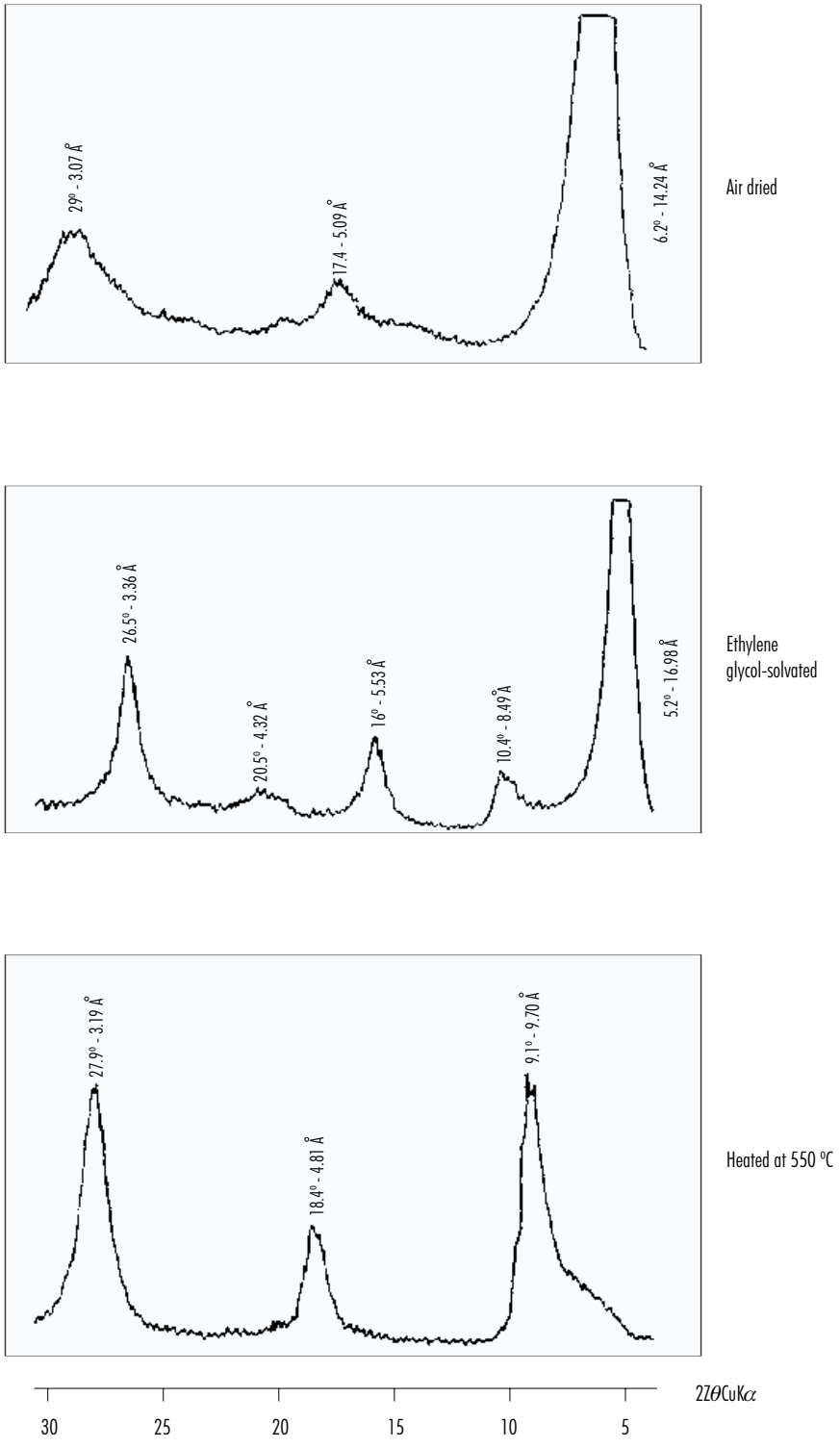

Figure 24. X-ray diffraction patterns of the oriented aggregates of the fraction of less than 2 μm (ENRESA 1998).

and sulphates in a concentration of 201±20 mg/L. Other extracts made at different solid:liquid ratios (Fernández *et al*. 1999) show that this concentration is inversely proportional to dilution of the extract, and that the cation maintaining the charge equilibrium is fundamentally Na (246±11 mg/L).

Finally, the total specific surface of this bentonite, determined by the hygroscopicity method developed by Keeling (1961), is 725±47 m^2/g.

Water used

In certain of the tests to be described in the following chapters, it is necessary to add water to the bentonite before testing or to saturate the material during test performance. Distilled water is normally used, except in those cases in which one of the aims is precisely to establish the influence of water type on the value of the determination performed, or when the conditions of the clay in the disposal facility are to be represented with greater fidelity.

In these cases, waters of two different compositions were used: granitic water or saline water. The granitic water represents the water that initially contacts the clay barrier in the disposal facility, coming from the surrounding geological medium. The saline water aims to simulate the water in equilibrium with the bentonite following saturation of the latter, which is in turn the water that will reach the internal parts of the barrier.

The granitic water used is a commercial product of well defined and verified composition (FONTVELLA). As saline water, a synthetic water was used, with a composition similar to that of the interstitial water in the bentonite compacted at a dry density of 1.65 g/cm^3 when saturated.

This interstitial water was obtained by compaction at high pressure (Fernández & Cuevas 1998), and the composition of the synthetic water for use in this work is simplified in order to reflect only the concentration of the major elements. The chemical composition of the two types of water is shown in Table VII.

Table V
Average values and standard deviations of the exchange complex (meq/100 g).

Ca^{2+}	Mg^{2+}	Na^{2+}	K^{+}	CEC
47±5	36±3	25±1	2.2±0.0	111±9

Table VI
Chemical composition of the total sample (average values and standard deviations in percent).

SiO_2	Al_2O_3	$Fe_2O_{3\ total}$	MgO	MnO	CaO	Na_2O	K_2O
58.7±1.9	18.0±0.7	3.1±0.1	4.2±0.1	0.04±0.00	1.8±0.1	1.3±0.1	1.1±0.1
TiO_2	P_2O_5	H_2O^-	H_2O^+	CO_2org	CO_2min	SO_2tot	F^-
0.2±0.0	0.02±0.00	6.6±2.5	6.4±0.3	0.4±0.0	0.3±0.1	0.2±0.1	0.2±0.0

Table VII
Chemical composition of the water used in the tests.

Element (mg/L)	Granitic	Saline
Cl^-	13.1	3550.0
SO_4^{2-}	14.4	1440.0
HCO_3^-	144.0	
Mg^{2+}	9,4	360.0
Ca^{2+}	44.9	400.8
Na^+	11.0	253.9
K^+	1.0	
pH	8.3	7

5. Methodology

5. Methodology

The experimental work included in this Thesis was carried out at the Soil Mechanics and Unsaturated Materials Laboratories of the Hydrogeochemical Characterisation Project (PCHE) of CIEMAT (formerly the Geological Techniques Division). The material used was the FEBEX clay, the basic mineralogical and chemical characteristics of which are described in the section "MATERIAL".

This chapter describes the methods used for the thermo-hydro-mechanical characterisation of the clay.

Quality control

The magnitude of the FEBEX Project led ENRESA to apply a quality assurance programme, with the objective of ensuring that the work were performed in a systematic, planned manner, thus reducing the probability of errors and malfunctions. The laboratory work was also conditioned by the application of this programme, since it was subject to test controls. The main requirements of this control are as follows (ENRESA 1997):

- Drawing up of specific procedures for each test type, when not performed in accordance with an official standard (UNE Standards). In view of the peculiarities of the material tested and of the techniques used, this was the case for most of the tests. It was necessary to draw up a large number of Procedures, either because no corresponding Standard existed or because that existing had to be modified to adapt it to the specific characteristics of the material.
- Conservation of test records. It was necessary to draw up records for each type of test in accordance with the quality control requirements, which consequently had to include both the test data and dates and a reference to the equipment used, the name of the operator and the signature of the person responsible for revision, along with the corresponding date.
- Control of inspection, measurement and testing equipment, included in an inventory detailing the data and dates of calibration of each item of equipment, a process that was required to be performed with an established frequency. In addition, all events, breakdowns, repairs and modifications were included. This control was undertaken in accordance with the requirements of the CIEMAT Procedure IMA/X8/BI-X5 for "Control of measuring and testing equipment".
- Each test and sample is referenced in accordance with previously established keys, ensuring traceability.

The above leads to achievement of the following objectives:

- Better knowledge of the process among the personnel, due to their having all their activities and functions in writing.
- Uniformity of criteria for the performance of tasks, leading to a lower degree of variability of the results due to the human factor.
- More rigorous and efficient control of the process, allowing non-conformities to be detected and their causes to be studied, for the implementation of whatever corrective and preventive actions might be required.

Basic characterisation

Specific gravity

The solid particles of the soil are characterised by their specific gravity (γ_s), which is defined as the relation between the weight of the solid and the volume occupied by it. It is necessary to gain insight into the specific gravity of the particles in order to calculate porosity and the void ratio, and therefore the degree of saturation of the soil. In minerals such as montmorillonite, specific gravity depends on isomorphic substitutions.

In the laboratory, the pycnometer allows the determination of the specific gravity of the grains (G_s), this parameter being defined as the relation between the weight of the solid and the weight of the same volume of water at 4 °C. In order to obtain specific gravity, the weight of the water displaced by a known mass of dry soil is determined.

For the work described herein, specific gravity has been determined using two aliquots of each sample, of between 1.5 and 2.5 g, taken from a 50 g portion of sample dried in the oven. Pycnometers of 50 cm^3 were used, and the procedure established in UNE Standard 103-302 "Determination of the relative density of soil particles" was adhered to. Distilled water was used for soil suspension and the ultrasonic and vacuum techniques were combined to remove the air from the suspension.

Gravimetric water content and density

The gravimetric water content (w) of the sample is defined as the relation between the weight of the water and the weight of the soil, in percentage terms. The weight of water is obtained by the difference between the initial weight of the sample and its weight after drying in the oven at 110 °C for 24 hours. In performing this determination, the UNE Standard 103-300-93 "Determination of soil water content by oven drying" was applied.

Dry density (ρ_d) is defined as the relation between the weight of the dry sample and the volume occupied by it prior to drying. In regularly shaped samples, volume is calculated from their dimensions, measured with a 0.01 mm precision gauge. The volume of irregularly shaped samples is determined by immersing them in a recipient containing mercury and by weighing the mercury displaced, as established in UNE Standard 7045 "Determination of soil porosity" (Figure 25). Prior to the test, the sample has to be trimmed in order to adapt it to the dimensions of the recipient, and its surface has to be scraped to remove any irregularity, superficial fissures or voids in which mercury might enter the sample. The density of the mercury being known, a value of 13.6 g/cm^3 having been taken, the volume of displaced mercury is calculated; this is equivalent to the volume of the sample, since mercury is not a wetting fluid and is not absorbed by the sample, which is covered perfectly.

Atterberg Limits

Plasticity is the property that allows a soil to deform without fracturing in response to the application of a pressure. Plastic soils may be remoulded when their water content is within a given range. When the water content of the soil is above this range, it behaves like a liquid, while for levels of water content below this range, the soil becomes a brittle solid that may break in response to applied pressure.

The liquid (w_L) and plastic (w_P) limits established by Atterberg define and quantify the transition between the liquid, plastic and brittle states of soil behaviour. Specifically, they are defined as the gravimetric water content at which a soil passes from the plastic to the liquid state (w_L), and the water content at which the soil passes from the plastic to the brittle state (w_P), both expressed in percentage terms. The nu-

Figure 25. Recipients for the determination of density by immersion in mercury.

merical difference between the liquid and plastic limits is defined as the plasticity index (I_P). Consequently, these limits are used as simple indicators to obtain the mechanical behaviour of the soil.

The limits are obtained in accordance with standard determinations, initially established by Casagrande and subsequently standardised.

The liquid limit has been determined in accordance with UNE Standard 103-103-94: "Determination of the liquid limit of a soil using the Casagrande apparatus method". Basically, this consists in determining the quantity of water that the soil must contain in order for it to fulfil the following: the soil having been placed in a standardised bowl pivoting on a horizontal axis, a groove opened in this soil with a standard channelling device closes along the bottom when the aforementioned bowl is allowed to drop 25 times from a given height onto a flat surface. The percentage of water content in the soil at this time is the liquid limit.

To obtain this, 150 g of air-dry soil passing through a 400 μm mesh is mixed with distilled water until a homogeneous paste is obtained, this then being left to settle for 48 hours. Although the Standard establishes a time of 2 hours, it has been verified that in expansive soils the result is more representative if the paste is allowed to homogenise over longer periods. The spoon is filled with part of the paste, the groove is opened and the number of impacts required for it to close is determined. If this number is between 10 and 15, a sample of the soil close to the groove is taken and its water content is determined by drying in the oven. The operation is repeated, adding distilled water to the paste or drying it with a dryer until the number of impacts is within this range. Four determinations are normally sufficient. The linear relation between the water content and the logarithm of the number of impacts is represented, and the percentage of water content that corresponds to 25 impacts gives the value of the liquid limit.

The plastic limit has been determined in accordance with the method described in UNE Standard 103-104-93 "Determination of plastic limit in soils", which consists in obtaining the lowest water content at which cylinders of soil measuring 3 mm in diameter may be obtained by rolling the soil with one's fingers over a flat surface, until the cylinders begin to shatter. In this work, the paste left over from determination of the liquid limit was used for this purpose.

The limits give an idea of the extent to which the soil particles are bound; the higher the inter-particulate forces, the greater the quantity of water content required to separate them and allow their behaviour to become liquid and, therefore, the higher their liquid limit. For this reason, the size of the particles, their specific surface and the nature of the clay minerals influence the plastic behaviour of a soil. In general, the liquid limit is directly correlated with the proportion of clay, the percentage of sodium in the exchange complex and the specific surface.

Granulometry

Given the range of sizes of the particles in the material analysed, two different techniques were used consecutively to quantify this parameter following dispersion of the sample. Particle sizes between 74 and 2 μm were analysed in accordance with UNE Standard 103-102 "Granulometric analysis of fine soils by sedimentation. Hydrometer method", while larger sizes were quantified in accordance with UNE Standard 103-101 "Granulometric analysis of soils by sieving", both with modifications to adapt them to clay soils difficult to disperse.

The first step in performing granulometry tests is dispersion of the sample, such that all particle sizes are represented in the analysis. This was accomplished by mixing 20 g of the sample with 0.5 L of distilled water and 5 g of sodium hexametaphosphate and agitating the mixture periodically for 48 hours. The quantity of sample used was selected in order to ensure that it were representative, on the one hand, and, on the other, that it were suited to the hydrometer method used for quantification, since an excessive quantity of the material increases the interactions between particles and the viscosity of the fluid, which would distort the measurement. Following the aforementioned period, the suspension is subjected to 5 sessions of ultrasonics lasting 5 minutes each, separated one from the other by a further 5 minutes mechanical agitation. Throughout the ultrasonics treatment the sample is also mechanically agitated.

Once the sample has been dispersed, the suspension is poured into a glass graduated cylinder, flushed with distilled water at 1 L and placed in a thermostatic bath at a fixed, known temperature of between 20 and 25 °C. The hydrometer is placed in the graduated cylinder containing the suspension and the hydrometer depth readings are taken at previously established times. For quantification of the different sample ranges the Stokes law is ap-

plied, which determines the drop speed of a sphere submerged in a fluid on the basis of the specific gravity of the sphere and the fluid, the diameter of the sphere and the viscosity of the fluid. The measurement performed using the hydrometer allows insight to be gained into the average specific gravity of the area occupied by the submerged part of the hydrometer, this in turn making it possible to determine the concentration of soil particles at the depth in question for each time period, which will be of a given size in accordance with the Stokes law. It should be pointed out that the particle sizes quantified using this method correspond to equivalent diameters; *i.e.* to the diameter of a sphere of the same specific gravity dropping at the same speed in a fluid of the same density and viscosity. In the case of laminar particles, such as those of clays, actual size may differ from equivalent size.

The sedimentation method allows granulometry to be performed for particles of between approximately 74 μm and 2 μm. Some authors claim that application of the Stokes law is incorrect for sizes in excess of 50-60 μm, since their sedimentation does not occur under the conditions of laminar flow for which such sedimentation is defined. Furthermore, particles having an equivalent spherical diameter of less than 1 μm may undergo Brownian movement in any direction, with a magnitude equal to or greater than the sedimentation induced by gravity, as a result of which this size constitutes the lower limit for which this method is applicable (Allen 1981).

The suspension is subsequently poured over the 74 μm mesh and the sample is washed. Following drying and weighing, the retained part is sieved using a battery of meshes, in order to obtain the granulometric distribution of the coarser particles, which are never larger than 5 mm, since this is the specification of the material as it leaves the factory. Meshes of the ASTM series with openings of 2.00, 1.19, 0.59, 0.297, 0.149 and 0.074 mm were used. Following weighing of the soil retained in each mesh, the percentages are calculated and the granulometric curve is plotted and adjusted using the data obtained by sedimentation.

Study of microstructure

The microstructure of a material is made up of the particles and voids that cannot be observed with the naked eye. The study of this microstructure consists in quantifying and characterising the shape, arrangement and interrelations between both. This requires special, and occasionally indirect, techniques. The importance of microstructural studies in expansive clays resides in the fact that the arrangement of the particles of smectite and the distances and forces acting between them determine swelling pressure, moving water, the movement of gas and diffusive transport capacity (Pusch *et al*. 1999). In this work, the study of microstructure has been addressed as a complement to the thermo-hydro-mechanical studies, and has included the determination of porosity distribution by means of mercury intrusion, the quantification of external specific surface by nitrogen adsorption and the study of the material by scanning electron microscopy.

Porosimetry

The porosimetric analysis of the compacted clay samples was carried out in a mercury intrusion porosimeter.

The mercury intrusion method is based on the physical principle that a non-wetting fluid, *i.e*. one whose angle of contact is greater than 90° on a given solid, does not spontaneously intrude the pores in the solid, although it will do this if the pressure applied is sufficient. The necessary pressure depends on the contact angle, the shape of the pore and the surface tension of the liquid. For cylindrical pores, the ratio between pressure and the minimum diameter of the pore that may be intruded is given by the Washburn equation:

$$P = \frac{-4\gamma\cos\theta}{d}$$

where P is the pressure required, γ is the surface tension of the liquid, θ is the contact angle and d is the pore diameter. Porous media contain irregularly shaped pores, but the pores intruded under a given pressure are considered to have a cylindrical diameter equivalent to that calculated by means of this equation.

This method has the following limitations (Diamond 1970):

- The pores must not contain any fluid prior to commencement of the test.
- Completely isolated pores inaccessible from the outside cannot be quantified.
- Pores which are accessible only through entry paths of a smaller diameter will be intruded only after sufficient pressure has been applied

for these "bottlenecks" to be penetrated, as a result of which the entire volume of such pores will inaccurately be assigned a more restricted size.

- It is not always possible to measure the entire volume of the pores, even in the absence of isolated pores, since this depends on the pressure capacity of the apparatus, and very small pores may remain unintruded.

In a work carried out for the IUPAC, Sing *et al*. (1985) classify pores into three groups on the basis of their size:

- Macropores, with a diameter of more than 0.05 μm.
- Mesopores, with diameters of between 0.002 and 0.05 μm.
- Micropores, with diameters of less than 0.002 μm.

According to this classification, and bearing in mind the injection pressures at which conventional porosimeters operate, the injection of mercury will access only the macroporosity and much of the mesoporosity.

The porosimeter used was the Poresizer 9320 by Micromeritics (Figure 26), with a mercury injection pressure range of 7 kPa to 210 MPa, this allowing pore diameters of between 200 and 0.006 μm to be measured, depending on the characteristics of the solid studied (fundamentally the contact angle). The equipment includes a sample preparation or low pressure unit and a high pressure unit (Micromeritics 1985).

Before performing the test, all the water in the pores of the sample must be removed by means of a method that does not cause any distortion to the fabric of the material. Depending on the characteristics of the material, the preparation method may vary from simple oven drying at 110 °C, for non-deformable materials, to freeze-drying for expansive clays. Following drying, the sample is placed in a penetrometer, formed by a glass stem inside which the mercury capillary tube is welded to the chamber containing the sample (Figure 27). The penetrometer must have appropriate characteristic; *i.e*. its chamber must be of a size as close as possible to that of the sample, and the diameter of the capillary tube must be related to the quantity of mercury that is expected to intrude, which will depend on the porosity of the material to be tested.

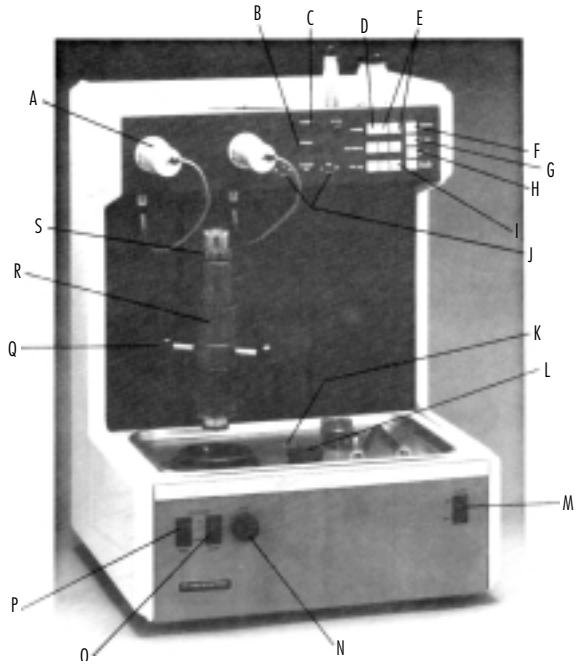

Figure 26. Poresizer 9320 by Micromeritics (A: low pressure unit, L: access to mercury container, M: ON switch, R: high pressure chamber).

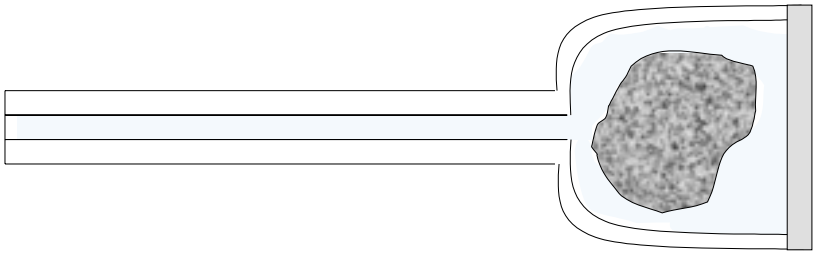

Figure 27. Schematic diagram of the penetrometer with the sample inside the chamber and the capillary tube and chamber full of mercury.

The penetrometer containing the sample is inserted in the low pressure unit, which allows the chamber to be filled with mercury by increasing pressure from the initial vacuum conditions to up to 0.21 MPa (30 psia), as a result of which the volume of pores having an equivalent diameter of more than 6 μm is determined. At the end of this stage the unit is depressurised and the penetrometer is extracted and weighed, full of mercury and the sample. The assembly then passes to the high pressure unit, where a pressure increase sufficient for the mercury to intrude the pores is applied, while the apparatus measures the intruded volume. Measurement of the volume is accomplished thanks to the variation in the electrical capacitance of a cylindrical coaxial condenser formed by an external metallic sheath around the stem of the penetrometer and by the internal mercury capillary tube. The level of mercury in this tube drops when the pores in the sample are filled, this causing a linear reduction in electrical capacitance as the pore volume increases. The changes in capacitance are converted to volume changes by multiplying by the calibration factor of the penetrometer. The process is repeated at stepwise higher pressures until the limit of the apparatus is reached. The pressure increases may be previously defined by the user depending on the characteristics of the material. In the specific case of the FEBEX bentonite, the pressure steps were established, after several check tests, with the criterion of having all significant pore sizes represented. The pressure steps (P) applied in this work are shown in Table VIII, along with equivalent pore diameter. This table also shows the steps in the mercury extrusion phase. Extrusion is accomplished, after reaching the highest pressure, by gradually reducing the injection pressure. This process is subject to hysteresis, on the one hand because the contact angle between the mercury and the walls of the pore differs depending on whether the fluid is advancing or retreating across the surface of the solid and, on the other, due to the existence of irregular pore geometries, with bottlenecks limiting the exit of the mercury. The stabilisation time established after each pressure step is reached is 15 s.

The volume of mercury intruded in each step is taken as the total volume of pores with equivalent diameters smaller than those corresponding to the preceding pressure and larger than those corresponding to the pressure causing the flow. By adding the results of all the steps, an accumulated distribution of volume depending on pore diameter is obtained. The equipment is connected to a personal computer containing a programme suitable for processing of the data with the necessary corrections and conversions. The value taken for the surface tension of the mercury is 0.484 N/m, and the contact angle has been established at 130°.

The data obtained through performance of the tests allow for the determination of both equivalent pore size distribution and the total porosity of the sample. For this, the following data are available:

- Dry sample weight, determined at the beginning of the test (W_s).
- Penetrometer volume (V_p), determined by previous calibration at a suitable temperature.
- Volume of mercury required to fill the penetrometer with the sample inside the low pressure unit (V_{Hg}). This is obtained from the weight of the mercury inserted and its density.
- Volume of the sample (V), obtained from the difference between the volume of the penetrometer (V_p) and the volume of mercury (V_{Hg}).

Table VIII
Pressure steps applied during the mercury injection test in the high pressure unit and equivalent pore diameters according to the Washburn equation.

Intrusion		Extrusion	
P (MPa)	Diameter (μm)	P (MPa)	Diameter (μm)
0.2	7.368	172.4	0.0074
0.5	2.456	137.9	0.0092
1.4	0.921	103.4	0.012
2.4	0.526	68.9	0.018
3.4	0.368	51.7	0.025
5.2	0.246	34.5	0.037
6.9	0.184	17.2	0.074
10.3	0.123	6.9	0.184
17.2	0.074	3.4	0.368
34.5	0.037	0.7	1.842
51.7	0.025	0.3	3.684
68.9	0.018	0.1	13.157
86.2	0.015		
103.4	0.012		
120.7	0.011		
137.9	0.0092		
155.1	0.0082		
172.4	0.0074		
189.6	0.0067		
206.8	0.0061		

- Pore volume (V_h^*), which is obtained from the mercury intruded during the high pressure test. This refers only to the volume of interconnected pores connected to the surface of the sample and having a diameter of more than 0.006 μm, as a result of which it is labelled with an asterisk, *, to differentiate it from total pore volume.
- Volume of the solid (V_h^*) obtained from the difference between the volume of the sample (V) and the volume of pores (V_h^*). Given that it is obtained from the data on mercury intrusion, this volume is larger than the actual volume of the solid (V_s), since the pore volume obtained may be minimised, as explained above.

The apparent specific gravity of the solid (γ_s^*) may be determined from these data; this would coincide with the specific gravity of the solid if there were no pores closed or inaccessible or smaller than 0.006 μm:

$$\gamma_s^* = \frac{W_s}{V_s^*} = \frac{W_s}{V - V_h^*}$$

It is also possible to determine the apparent void ratio of the sample (e^*) by means of the following expression:

$$e^* = \frac{V_h^*}{V_s^*}$$

Comparison between this apparent void ratio (e^*) and the void ratio calculated from the specific gravity obtained using the pycnometer and the density determined by immersion in mercury, in accordance with UNE Standard 7045 (e), gives the value of the percentage of the total pores that have been intruded by mercury and which are, therefore, larger than 0.006 μm and interconnected.

For this work compacted clay samples of between 8 and 15 g were used. It is generally accepted that when working with clay materials, the sample has to be freeze-dried in order to ensure that the pores are empty of water on test initiation, since oven drying implies shrinkage of the expansive materials and, therefore, considerable modification of their porosity (Diamond 1970, Tuncer 1988, Romero 1999). Freeze-drying, on the other hand, subjects the sample to pressure and temperature conditions that eliminate the surface tension between the air/water interface, preventing shrinkage of the solid. Preparation of the sample included rapid freezing in a cryogenic medium –liquid nitrogen, whose evaporation temperature is -196 °C–, which prevents the development of large ice crystals. Subsequently, the water is removed in a lyophilizer by vacuum sublimation at a sufficiently low temperature. The lyophilizer used was a Telstar, with a vacuum capacity of 10 Pa at a temperature of -40 °C. In order to ensure the effectiveness of the technique, the samples used must be of small size, with dimensions of less than 10 mm. Some authors claim that freeze-drying may cause modification of porosity distribution, giving rise to an increase in the proportion of larger sized pores with respect to the actual value (Lawrence *et al*. 1979).

External specific surface

It is normally considered that the external surfaces of a material are those surrounding the discrete particles or agglomerates, including all protuberances and the surface of cracks which are wider than they are deep. The internal surfaces are the walls of all fissures, pores and cavities that are deeper than they are wide (Sing *et al*. 1985). The external specific surface –unlike the total specific surface (internal and external)– is a property that depends not only on the type of material (its mineralogy) but that varies with the distribution of porosity and with the shape and size of the particles (degree of clustering). For this reason, the external specific surface may be indicative of variations in the microstructure and microfabric of the material, therefore in this work it has been determined after subjecting the clay to different treatments.

Likewise, the value of specific surface obtained depends on the type of adsorbent used for its determination and for preparation of the sample, especially in the case of expansive materials such as smectites. For example, the use of water vapour as an adsorbent will always give higher specific surface values than will gases of the nitrogen type, since the former penetrate the basal planes of the units of montmorillonite, while inert gases such as nitrogen do not. Consequently, when gases are used to determine the specific surface of expansive materials, only the external specific surface is quantified, while the use of polar molecules such as water will give the value of the total specific surface, both internal and external.

One of the most widespread methods used to determine the specific surface is the measurement of the adsorption of a given gas on the material (Sing *et al*. 1985). Adsorption (physisorption) is the enrichment in one or more components of an interface layer of a solid. This occurs when an adsorbable gas comes into contact with the surface of a solid (the adsorbent). In the case of single-layer adsorption, all the molecules of the gas are in contact with the surface layer of the solid. In this context, the specific surface (a_s) is defined as the surface of the solid that may be covered by a complete single layer of adsorbate per unit of mass. Calculation of this requires knowledge of the quantity of gas adsorbed and the area occupied by a molecule of adsorbate in the single layer.

Desorption is the reverse mechanism of adsorption, *i.e.* the mechanism by which the quantity of gas adsorbed in the solid decreases. The relation, at constant temperature, between the quantity of gas adsorbed and its equilibrium pressure is known as the adsorption isotherm. The analysis of vapour adsorption-desorption isotherms on solids allows the specific surface and the way in which it is distributed on the solid to be calculated, along with the shape, size and distribution of the porosity.

The most widely used method to calculate specific surface is the so-called BET method (Brunauer *et al.* 1938), whose equation describes the adsorption of a gas on a solid surface:

$$\frac{X}{V(1-X)} = \frac{1}{V_M C_{BET}} + \frac{C_{BET}-1}{V_M C_{BET}} X$$

Using a graphic representation of the volume adsorbed (V) versus relative pressure ($X=P/P_0$, where P is the pressure at the moment of measuring, and P_0 the gas saturation pressure, *i.e.* the vapour pressure of the liquefied gas at the temperature at which adsorption occurs), and taking the range of relative pressure in which this ratio is linear, the single layer volume V_M (the slope) is determined, along with a parameter C_{BET} (interception) related to the heat of adsorption of the adsorbate-adsorbent system, assuming that there is no limit to the number of layers adsorbed. The single layer capacity, V_M, is the quantity of gas, expressed as a volume under standard pressure and temperature conditions, required to cover the surface with a single layer.

Specific surface (a_s) is calculated on the basis of single layer capacity, V_M, in accordance with the following expression:

$$a_s = \frac{V_M \times a_m \times N}{V_0 \times W}$$

where a_m is the cross section of a molecule of adsorbate located in the single layer, N is Avogadro's number, V_0 is the volume of a mole of ideal gas under standard pressure and temperature conditions and W is the weight of the sample.

In a simplified manner, a single point on the adsorption isotherm, located within the linear range of the BET graph, may be determined. In this case, and with the necessary assumptions, the previous equation will be converted as follows:

$$a_s = \frac{V \times a_m \times N \times \left(1 - P/P_0\right)}{V_0 \times W}$$

where V is the volume of gas adsorbed under standard pressure and temperature conditions. This is the method used in this work.

The tests were performed using a Flowsorb II 2300 system by Micromeritics (Figure 28), through the adsorption of nitrogen from a mixture of nitrogen and helium with a ratio of 30/70 at the temperature of a

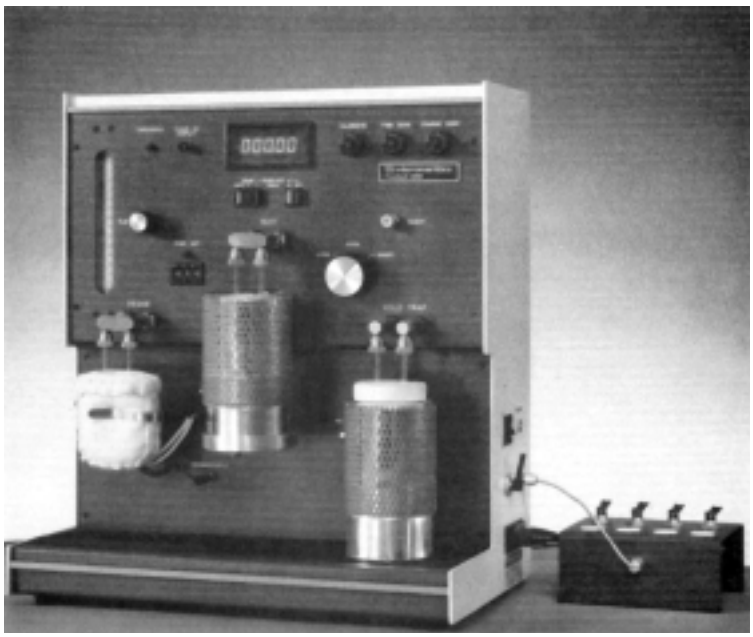

Figure 28. Equipment for the measurement of specific surface: Flowsorb II 2300 by Micromeritics.

bath of liquid nitrogen (-196 °C). The following values were used to calculate specific surface:

- Avogadro's number (N): $6.023 \cdot 10^{23}$ molecules/mol.
- Molar volume of a gas under standard pressure and temperature conditions (V_0): 22,414 cm^3/mol.
- Area of the solid surface occupied by an adsorbed molecule of nitrogen (a_m): $16.2 \cdot 10^{-20}$ m^2.
- P is atmospheric pressure multiplied by 0.30, since the mixture contains 30 percent nitrogen and adsorption occurs at atmospheric pressure. P_0 is the saturation pressure of liquid nitrogen, which is usually somewhat higher than atmospheric pressure.

For each determination 5 g of ground sample were used, dried in the oven at 110 °C for 24 hours in order to ensure that the pores did not contain any water preventing the entry of the gas. Once the sample had been placed in the apparatus, it was degassed at 60 °C for 15 minutes before measurement. The determination was accomplished on two aliquots, the value given for each sample being the average of the two determinations. In the event of important discrepancy between the two, a third measurement was performed.

Scanning electron microscopy

As a complement to the test performed, and with a view to gaining greater insight into the specific details of the behaviour of the FEBEX bentonite, the material was studied by scanning electron microscopy in the Electron Microscopy Laboratory of the Department of Materials Science and Metallurgical Engineering of the Technical University of Catalonia (UPC). Two systems having different technical characteristics were used, allowing the material to be analysed from different points of view. These were as follows:

- Scanning electron microscope JEOL JSM 6400, allowing images to be obtained with secondary and back-scattered electrons (Figure 29). This includes a coupled dispersive X-ray energy spectrometer, X LINK LZ_5, which allows for the qualitative and quantitative analysis of light elements from boron. Given that the samples studied are not conducting, it is necessary to cover them with gold in order to obtain good

Figure 29. JEOL JSM 6400 scanning electron microscope.

images from the microscope. The equipment used to accomplish this is a BALZERS SCD 004 metaliser that ionises the metal at a vacuum of $5 \cdot 10^{-2}$ Torr, depositing a layer of 300 to 400 Å on the sample. Apart from this vacuum metalisation, the samples do not undergo any type of drying or treatment prior to being inserted in the microscope.

- ELECTROSCAN 2020 environmental scanning electron microscope, allowing images to be obtained by means of secondary electrons with any degree of water content, since the water in the material itself acts as the conducting film (Figure 30). This allows work to be performed directly on the sample without manipulation. The equipment also incorporates a Peltier effect thermoelectric cooling sample-holder that allows the temperature to be varied by 20 °C above and below the laboratory temperature. This temperature variation is combined with variations in the pressure of the gas in the chamber, achieved by injecting water vapour and allowing up to 50 Torr to be reached. The joint variation of pressure and temperature, or the variation of either, allows work to be performed under different conditions of relative humidity, in accordance with the water phase diagram, maintaining the same sample in the microscope chamber. For this study, a pressure of between 5 and 10 Torr was used, with the temperature kept constant at 12 °C.

Hydraulic conductivity

The measurement of hydraulic conductivity in low permeability expansive clays cannot be carried out in conventional permeameters, since in these the sample is usually placed, enclosed in a latex membrane, in a perspex triaxial cell in which it is not possible to apply a confining pressure sufficient to counteract the swelling of the sample when it saturates, as a result of which its dimensions cannot be controlled. Furthermore, the high hydraulic gradients required to measure the water circulating inside a low permeability specimen cannot be achieved with conventional equipment, in which pressures are usually applied by means of columns of mercury.

For this reason, a method for the measurement of hydraulic conductivity in expansive soils through the determination of the coefficient of permeability (k_w)

Figure 30. ELECTROSCAN 2020 environmental scanning electron microscope.

which avoids these disadvantages, has been developed at CIEMAT (Villar & Rivas 1994). The novelty of the method with respect to the conventional measurement of permeability in a constant head permeameter with a triaxial cell is that it may be used with expansive materials which would modify their volume on saturation, and that different hydraulic gradients may be applied.

The theoretical principle on which the method is based is that of the constant head permeameter. Basically, it consists in measuring against time the volume of water that passes through a specimen, confined in a rigid cell preventing it from deforming, to which is applied a constant hydraulic gradient between the upper and lower parts. For this purpose a hydraulic head, that is to say, a difference in potential, is applied between the upper and lower parts of the previously saturated sample. The complete saturation of the sample and associated swelling guarantee perfect contact with the walls of the cell, preventing the flow of water between these and the sample. At the same time, the flow of water passing through the specimen is measured versus time.

The measuring system is made up of the following elements (Figure 31 and Figure 32):

- Stainless steel cell with water inlet and outlet, in which the sample is confined. The dimensions of the sample are 19.63 cm^2 in surface area and 2.50 cm in length, this implying a volume of 49.10 cm^3.
- Two pressure systems, for injection and downstream pressures. The system used for back pressure consists of a set of self-compensating mercury deposits equipped with an installation for deaerated water, while for injection pressure, Wykeham Farrance electrohydraulic constant pressure systems (for pressures of up to 3.5 MPa) or Gilson piston pumps (of the type used for high precision liquid chromatography – HPLC) are used. These pumps allow pressures of up to 42 MPa to be applied, although for the measurement of permeability the value of 7.2 MPa is never exceeded.
- Electronic volume change measurement system, with an accuracy of 0.001 cm^3.
- Data acquisition system.

The remoulded samples are prepared by compacting the clay directly inside the cell ring, through the application of a uniaxial pressure, to the desired

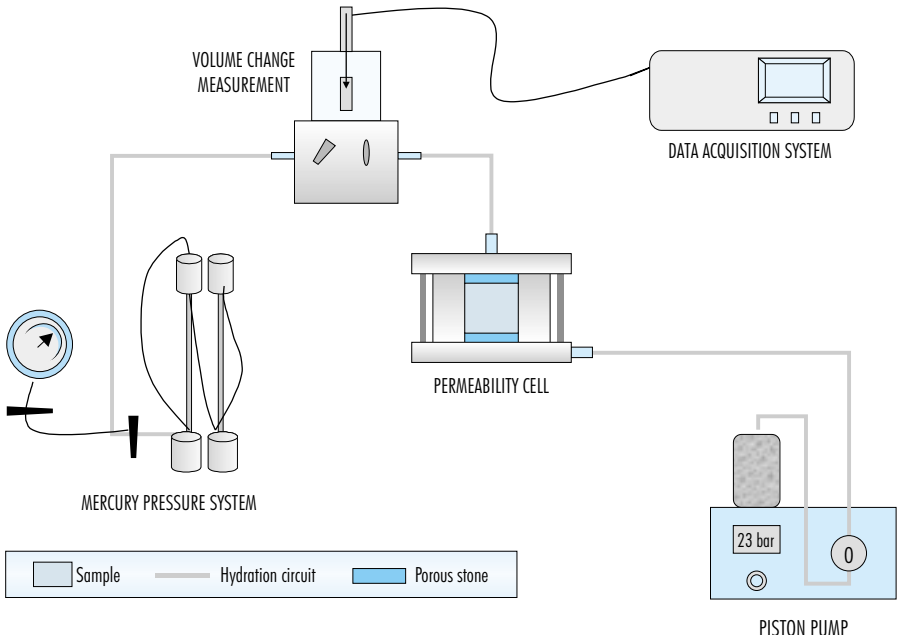

Figure 31. Schematic representation of permeability measuring assembly for expansive soils.

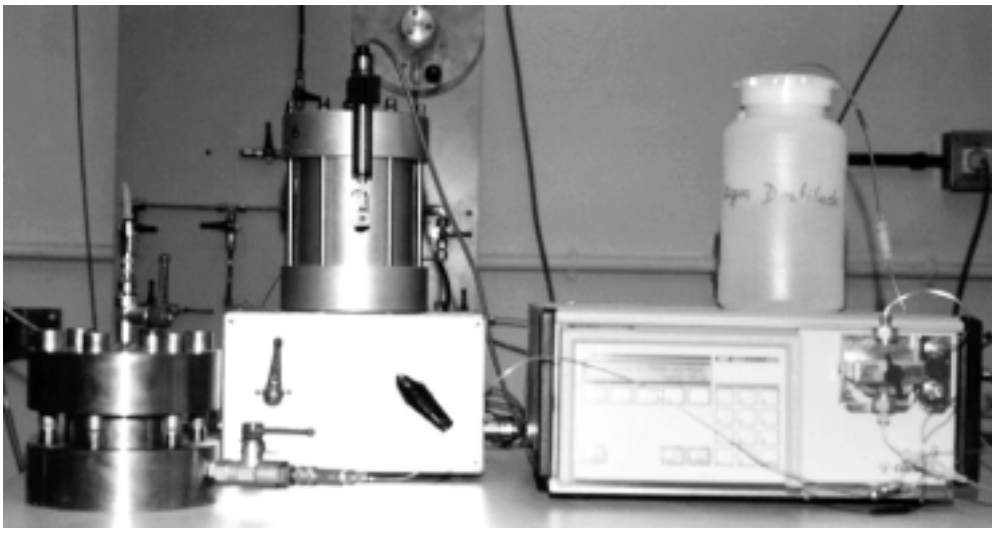

Figure 32. Permeability measuring assembly: cell, volume change apparatus and piston pump (from left to right).

density. In the case of undisturbed samples, it is necessary to adapt them to the diameter of the cell ring by working them with a cylindrical cutter, attempting not to modify either their moisture or density.

Filter papers are placed in contact with the upper and lower parts of the sample, followed by porous stones. Once the covers of the cell have been adjusted, the sample is saturated at 0.6 MPa from both faces. In this way the sample is hydrated to complete saturation over the necessary time period, which will depend on the type of sample and on its initial water content and density, this usually being established at a minimum of two weeks.

Once the sample is saturated, the hydraulic gradient is applied by increasing the injection pressure at the lower part of the cell (Pi), while the back pressure is maintained at 0.6 MPa (Pc), in order to favour the dissipation of air in the system. In this way a hydraulic head corresponding to the difference between the lower and upper pressures ($\Delta P = Pi - Pc$) is achieved. The supposedly linear hydraulic gradient is the ratio existing between the hydraulic head and the length of the specimen. An automatic volume change apparatus is installed between the upper inlet of the cell and the backpressure system. This device is connected to a data acquisition system and periodically records the volume of water passing through the sample. The test must run over a time period sufficient to determine that the volume of water passing through the specimen is linear and stable with time, this period normally being between 4 and 7 days. If no water flow is observed, it will be necessary to increase the hydraulic head by increasing the injection pressure.

Once constant flow is achieved, the volume of water passing through the sample (ΔV, cm^3) is determined over a given time period (Δt, s). Permeability k_w (cm/s) is calculated by applying Darcy's law for flow in porous media, this implying consideration only of the macroscopic movement of the water, assuming laminar flow and considering the porous solid to be macroscopically isotropic (Jiménez & Justo 1971):

$$k_w = \frac{\Delta V \times 1}{A \times \Delta t \times \Delta P}$$

where ΔP is the hydraulic head in cm of water, A is the surface area of the cell (19.63 cm^2) and l the length of the specimen (2.50 cm).

For each sample the determination of permeability has been performed with different hydraulic gradients, although in principle the value obtained should be independent from this factor if flow is ac-

tually Darcynian. Specifically, the values of hydraulic head applied in the tests ranged from 0.7 MPa, for dry densities of 1.30 g/cm^3, to 6.6 MPa for dry densities of 1.84 g/cm^3. Bearing in mind that the length of the specimen is 2.5 cm, the average hydraulic gradient was 15,200 m/m.

The final water content of the sample was determined on completion of the test.

Permeability depends on the density of the material and the type of water used. Temperature also influences permeability, so it must be kept constant throughout the test. The determinations recorded in this work were made at laboratory temperature (between 20 and 25 °C).

Permeability to gas

The mechanisms that give rise to the movement of gas in a soil are diffusion, that gives rise to a net movement of gas from areas of high concentration to others of lower concentration, and mass flow or advection, as a result of which the entire gaseous mass moves in response to a pressure gradient.

Under normal soil conditions, the main gas movement mechanism is diffusion, since the total gas pressure is the same in all the pores of the soil. The greater part of gas movement takes place in pores filled with air, since diffusion in the gaseous phase is almost four orders of magnitude higher than through water. Nevertheless, in the clay barrier of a disposal facility there are temperature gradients, gas generation and changes in the volume of accessible pores due to variations in water content, these giving rise to pressure gradients that cause advective flow of the gas.

The advective flows of water and gas (q_w, q_g) occur in accordance with Darcy's law, with relative permeabilities (k_{rw}, k_{rg}) that depend on the liquid degree of saturation:

$$q_w = -\frac{k_i k_{rw}}{\mu_w}(\nabla P_w - \rho_w g) = -k_w k_{rw}\left(\frac{\nabla P_w}{\rho_w g} + i_z\right)$$

$$q_g = -\frac{k_i k_{rg}}{\mu_g}(\nabla P_g - \rho_g g) = -k_{g0} k_{rg}\left(\frac{\nabla P_g}{\rho_g g} + i_z\right)$$

where k_i is the intrinsic permeability tensor, P_w, P_g, ρ_w, ρ_g, μ_w and μ_g are the pressure, density and dynamic viscosity of the water and gas phases ($_w$ and $_g$), g is gravity, i_z is the unit vector in the direction of the z axis, k_w is the hydraulic conductivity under saturated conditions and k_{g0} is the permeability to gas of the dry soil.

Ideally, intrinsic permeability (k_i) depends only on the structure of the soil, and has the same value for gas and water flow. This value is generally associated with pore diameter and with pore size distribution. Quantitatively, the effect on intrinsic permeability of pore size and total porosity may be assessed by means of the Poiseuille equation:

$$k_i = \frac{1}{2}\frac{n^3}{(1-n)^2}\left(\frac{D_h}{\alpha}\right)^2$$

where n is porosity, D_h is effective grain diameter and α is a coefficient of grain shape.

Consequently, and given that the air-filled porosity varies with water content and the degree of compaction of the soil, both factors have a decisive effect on the exchange of water and gas in the soil. Furthermore, gas flow requires the continuity of the gaseous phase. When the pores are full of water, the air is blocked, as a result of which the permeability to air decreases with increasing water content. Matyas (1967) considers that for degrees of saturation in excess of 90 percent, the gaseous phase is occluded, and consequently the movement of the gas is reduced to diffusion via the water in the pores. For degrees of saturation of below 85 percent, on the other hand, the gaseous phase is continuous, and gas flow commences (Corey 1957).

Gas permeability measuring methods are classified into steady-state and non-steady-state types. The method used for this work, the basic principle of which was developed by Kirkham (1946), is included in the latter variety. Basically, it consists in pressurising a tank and then releasing this pressure to the atmosphere across the column of soil whose permeability is to be measured. Permeability may be calculated by recording the decrease in the pressure in the tank with time. For this purpose it must be assumed that while the pressure is decreasing in the tank, the distribution of pressure in the soil sample is the same as would exist if this instantaneous pressure had been maintained in the tank for a long period of time.

The measurement of permeability to gas was performed on specimens of compacted clay, using the assembly shown in Figure 33 and Figure 34. The cylindrical sample of compacted clay is inserted in a triaxial cell confined between two porous stones and enclosed in two latex membranes, between which vacuum grease is applied in order to prevent the

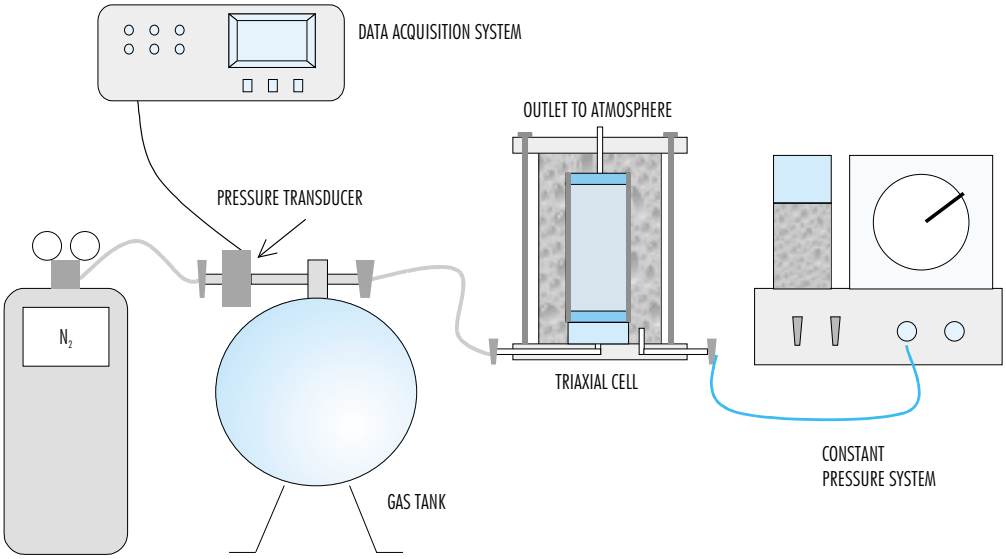

Figure 33. Schematic representation of the permeability to gas measuring system.

loss of gas. A pressure of 1.6 MPa is applied to the chamber of the triaxial cell, in order to ensure perfect adherence of the latex membranes to the walls of the sample. The inlet at the lower part of the sample is connected to an airtight tank of known volume, in which nitrogen gas is previously injected at a pressure slightly higher than atmospheric. The tank is instrumented with a pressure sensor, connected to a data acquisition system, which records the pressure of the fluid contained inside. The inlet at the upper part of the sample is left open to the atmosphere. The test consists in allowing the air in the tank to exit to the atmosphere across the specimen, while the decrease in pressure in the tank is measured versus time. The test must be performed at a constant temperature.

The permeability to gas is calculated in accordance with the following equation (Yoshimi & Osterberg 1963):

$$k_g = 2.3 \times \frac{V \times 1 \times \rho_g \times g}{A \times \left(P_{atm} + P_0/4\right)} \times \frac{-Log_{10}\left(P(t)/P_0\right)}{t - t_0}$$

where k_g is the permeability to gas (m/s), V the volume of the tank (m^3), l the length of the sample (m), A the surface area of this sample (m^2), ρ_g the density of the gas (kg/m^3), P_{atm} is atmospheric pressure (N/m^2), P_0 is the excess of pressure over atmospheric pressure in time t_0 (s) and P(t) is the excess over atmospheric pressure in the tank in time t. This equation was developed in a manner analogous to that used for the expression of permeability to water using a falling head permeameter, with the air continuity equation being applied through consideration of compressibility (Lloret 1982). In developing the equation, it has been assumed that the initial P_0 pressures are relatively small compared to atmospheric pressure.

The volume of the tank used is $2.21 \cdot 10^{-2}$ m^3, the nominal length of the sample is 8.00 cm and its surface area 11.40 cm^2. The gas used for all the tests was nitrogen, for which a density of 0.04 mol/L (Lide 1995) was taken. The pressure of the tank on test initiation is established at values close to 1.03 bar, since keeping the properties of the gas constant throughout the test requires that it not be subjected to high pressures, this also serving to prevent disturbance of the soil.

Taking into account the dynamic viscosity of nitrogen (μ_g, $1.79 \cdot 10^{-5}$ Pa·s), the following relation be-

Figure 34. Assembly for measurement of permeability to gas: triaxial cell with specimen, lateral pressure system, gas tank and nitrogen bottle.

tween permeability to gas (k_g, m/s) and the product of intrinsic permeability measured with nitrogen gas (k_{ig}, m^2) by the relative permeability to gas (k_{rg}) is obtained:

$$k_g = k_{g0} + k_{rg} = \frac{\rho \times g}{\mu_g} \times k_{ig} \times k_{rg} =$$

$$= 6.2 \cdot 10^5 \times k_{ig} \times k_{rg}$$

The specimens used for this measurement were manufactured by uniaxial compaction of the clay in an appropriate mould at different densities (Figure 35). The clay was used with its hygroscopic water content and with added water. In this last case, after mixing the clay with the quantity of water required to reach the desired water content, it was left to stabilise for several days in closed plastic bags, in order to facilitate a uniform distribution of moisture. For the manufacturing of specimens with water contents below hygroscopic, the clay was dried in the oven for different short periods of time (between 1 and 6 h) before compaction. On completion of the test, the dimensions of the specimen were measured using a gauge with an accuracy of 0.01 mm and its water content was determined (UNE Standard 103-300-93). These data were used to calculate the dry density of the clay for which the measurement was performed.

Oedometer tests

This chapter describes the methodology used to perform two tests: swelling pressure and saturation under load. These tests are carried out on the same equipment, the oedometer, as a result of which they share common assembly and disassembly phases. For this reason, the apparatus and certain operations are described only in the first section.

Swelling pressure

Soils containing clay minerals of laminar or expansive structure are characterised by their high deformability on hydration, since the particles incorporate the water in their structure, thus increasing the distance between interlaminae, in other words in the direction of c-axis (see section "CHARACTERISTICS OF SMECTITES").

If the material is saturated at constant volume and its deformation is prevented, the particles will exercise a pressure on the confining structure. This is known as swelling pressure, and reaches its equilibrium value when the sample is completely saturated and is at zero suction.

The swelling pressure test makes it possible to determine the equilibrium swelling pressure exercised by a sample on complete saturation at constant volume. For performance of this test, oedometer frames and conventional oedometric cells were used, in which the surface of the oedometer ring was reduced in order to counteract the high pressures expected. Figure 36 shows a schematic cross section of an oedometric cell. The sample is confined in a ring preventing it from deforming laterally, and between two porous stones at its upper and lower surfaces. The piston of the cell, which is adjoined to the upper porous stone, is in contact with the loading ram, whose displacement –or that of the piston itself– may be accurately measured by means of a dial gauge. The sample may be loaded via the ram by means of the system of levers of the oedometric frame on which the cell is located (Figure 37). The loading capacity of the equipment (140 kg), the lever arm (7.85 or 10) and the cross section of the

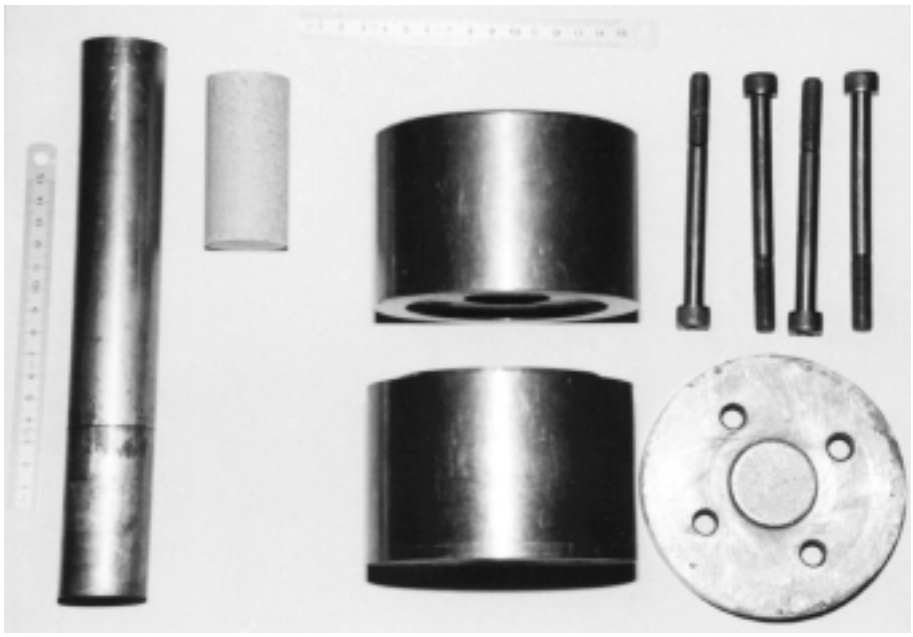

Figure 35. Mould for the manufacturing of specimens for measurement of permeability to gas.

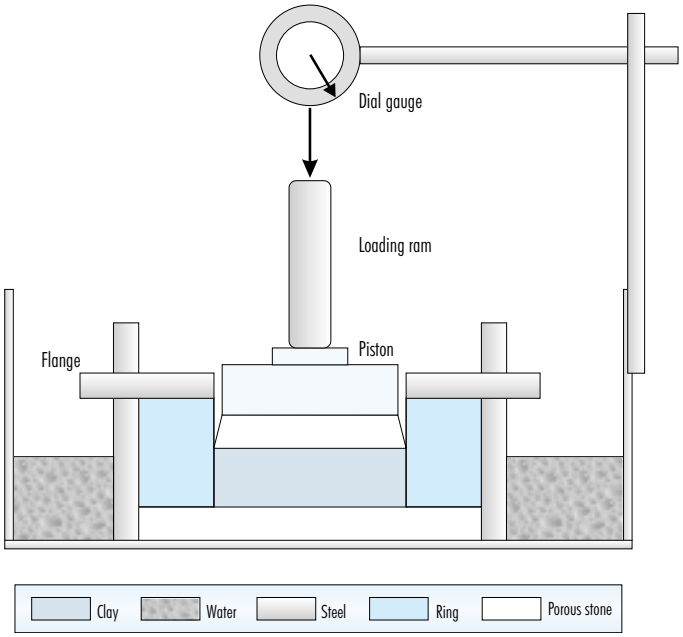

Figure 36. Schematic cross section of an oedometric cell.

Figure 37. Twin station oedometric frame with cells installed.

sample (9.98 or 11.40 cm^2) determine the maximum applicable pressure. These cells do not allow the pressure exercised by the sample to be measured directly, but rather determined indirectly from the load that has to be applied in order for the volume of the sample to be kept constant during saturation.

In most cases, the samples were prepared by means of uniaxial compaction of the clay directly in the oedometer rings. The weight of the sample required to manufacture the specimen was calculated taking into account the volume of the compaction mould and the desired density and water content.

The initial length of the specimen (1.20 cm) is always half the length of the oedometer ring (2.40 cm), in order to ensure that, in the event of major swelling, the sample does not ooze outside the ring and that the piston is always correctly guided. Rings measuring 3.81 and 4.95 cm in diameter were used. In certain clearly indicated cases, specimens trimmed from larger, previously compacted blocks were used instead of compacting the sample in the oedometer ring. For this purpose cylindrical cutters of appropriate dimensions were used, and the samples were placed in the oedometer ring once obtained.

The sample contained in the oedometer ring is placed inside the oedometer cell and the lower porous stone is covered with distilled water (unless some other type of water is indicated), such that the sample begins to saturate from the bottom upwards, allowing the air in the pores to escape from the upper part.

With the cell mounted in the oedometer frame, and the lower porous stone flooded, the displacement recorded by the dial gauge as the sample saturates is observed, and swelling of the sample is prevented by the application of loads. The reading of the dial gauge shall not drift excessively from the initial value (within a margin of ± 0.005 cm), thus preventing both the swelling and the consolidation of the sample. The test is considered to be completed when no strain is observed for at least 24 hours.

By applying the lever arm factor at the load required to stabilise strain and dividing it by the surface area of the specimen, the swelling pressure of the sample is obtained for the density and water content at which the test was performed.

The tests were performed at laboratory temperature, which ranged from 20 to 25 °C.

Swelling under load

The mechanisms described above, that cause the soil to exercise swelling pressure on hydrating at a constant volume, are also responsible for the deformability of the soil when it hydrates under a load of less than its swelling pressure (see section "CHARACTERISTICS OF SMECTITES").

In this case, and in addition to the factors already listed above (type of clay mineral, dry density, water content, particle orientation, type and quantity of adsorbed cations, composition of saturation water, soil stress history, temperature), the deformation capacity will depend on the specific load under which the test is performed, strain being larger the lower this load.

The deformation capacity of a soil, or swelling on saturating under load, is determined using the same oedometric equipment as described in the previous section and used for the performance of the swelling pressure test (Figure 36). Preparation of the sample is also undertaken in the same way, and samples of the same size have been used: length 1.20 cm and diameter 4.95 or 3.81 cm.

The assemblage of the sample in the oedometric cell is analogous to that undertaken for the swelling pressure test, the differences between the two determinations beginning at the moment of test initiation itself. In the case of swelling under load tests, the desired load is initially applied to the sample by means of the oedometric frame lever arm, the cell then being flooded such that saturation of the sample occur via the lower porous plate.

The sample begins to swell depending on its characteristics and on the pressure to which it is subjected. The strain indicated by the dial gauge is recorded at increasingly larger time intervals until this parameter stabilises for at least 24 hours, at which time the test is considered to have been completed.

The ratio between the final length increase undergone by the sample in equilibrium with the load applied and its initial length gives the strain value of the material on saturating under the load used for the test performance. The final result is, therefore, the percentage of strain of a sample of given initial dry density and water content on saturating under a given load.

The tests were performed at laboratory temperature, which ranged from 20 to 25 °C.

Controlled suction tests

It has been seen that measurement of the properties of saturated bentonite in the laboratory involves certain peculiarities that make it necessary to modify classical techniques and equipment when working with expansive materials, due fundamentally to their extraordinary swelling capacity, deformability and low permeability. Another characteristic, linked to those listed above, that conditions the behaviour of such materials, and consequently the techniques to be used for their study, is their great avidity for water and high water retention capacity, in other words, their high suction value. The magnitude of the suction of smectites when removed from the saturated state is such that it cannot be measured directly using conventional methods such as tensiometers or psychrometers, but only by means of capacitative sensors on very large samples (see section "Measurement and control of suction"). When the aim is to study their unsaturated behaviour without losing insight into their state variables, including suction, it is necessary to fall back on the alternative of imposing suction instead of measuring it, that is to say, of subjecting the sample to a given and known suction that conditions its water content, while the other variables (stresses, strains) are modified and measured in the traditional manner. The main experimental techniques and developments for the study of materials in unsaturated conditions have been described, along with the theoretical principles, in the section "Unsaturated soils". Two different techniques were used in the tests described in this work to impose suction: axis translation and the imposition of a relative humidity.

The principle of axis translation consists in modifying suction by increasing the pressure of the gaseous phase (Richards 1941, Hilf 1956). The sample is placed in a cell in contact with water at atmospheric pressure through a membrane permeable to water but not to gas (Visking type by Medicell Int. Ltd. or Spectra/Por Spectrum). These regenerated cellulose membranes are amorphous and gel type in nature and have a pore diameter of 2.4 nm, as a result of which they are flexible and suitable for filtration and osmosis work. The pressure in the cell is immediately increased by injecting gas at the desired pressure, this increasing the air pressure in the pores of the sample. This new situation forces the sample to exchange water through the membrane until equilibrium is reached once again. Given that the changes in capillary suction are caused by the difference between the pressure of the air in the pores

(u_a) and the pressure of the water (u_w), when air pressure is applied to the sample an increase in u_a is induced, while u_w remains the same as atmospheric pressure. In this way, capillary suction varies by the same amount as gas pressure. The membrane allows ions to pass through, as a result of which osmotic suction is not controlled by this method. Given the mechanical limitations of the cell, it is possible only to apply matric suctions of less than 14 MPa. Industrial nitrogen has been used as the gas.

The method of imposing a relative humidity (RH) is based on the fact that this conditions the pressure of the water and gas in the pores (u_w y u_a). This humidity may be imposed by means of solutions of sulphuric acid (although any other solution of known water activity may be used). The sample exchanges water with the atmosphere until thermodynamic equilibrium is reached with the vapour pressure of the solution, as a result of which total suction is modified. The suction in the pores of the sample (s, in MPa) is related to the activity of the water in the solution (a_w=RH/100) by means of Kelvin's law:

$$s = -10^{-6}\frac{R \times T}{V_w}\ln\left(\frac{HR}{100}\right)$$

where R is the universal constant of the gases (8.3143 J/mol·K), T is absolute temperature and V_w is the molar volume of the water ($1.80 \cdot 10^{-5}$ m^3/mol).

The relation between the activity of the solution (a_w) and the percentage in weight of sulphuric acid used to prepare it (p) is reflected in experimental tables (Gmitro & Vermeulen 1964). This relation depends on temperature, therefore the latter is required to remain constant throughout the tests. For 20 °C, the relation may be adjusted to a polynomial equation of the fourth order:

$$a_w = 7 \cdot 10^{-8}p^4 - 6 \cdot 10^{-6}p^3 -$$
$$- 0.0001p^2 - 0.0019p + 0.9927$$

The transfer of water between the clay and the atmosphere may cause the density of the solution to vary, as a result of which this should be checked prior to and following stabilisation, this being accomplished by means of pycnometers. There is an experimental relation between the specific gravity (or density) of the solution (d, g/cm^3) and the percentage in weight of the sulphuric acid in the solution (p, which in turn depends on activity, a_w), which is temperature-dependent (Lide 1995). For 20 °C, this relation may be adjusted to an exponential equation:

$$p = 145.8984 \times \ln(d) + 0.9807$$

Total suctions of between 3 and 500 MPa may be obtained using this method. In view of the influence of temperature on the activity of the solutions, this should be kept constant and known throughout the entire test.

Determination of the relation between suction and water content under free volume conditions

The relation between the suction and water content of a sample provides information on its water retention capacity. The procedure used to establish this relation basically consists in stabilising the sample at a given suction and determining its water content once equilibrium has been reached. The test is repeated for samples of the same material but using different values of suction, in order to establish the suction/water content relation over a wide range of suctions.

In addition to obtaining the suction/water content relation, subjecting different samples of the same material to different suctions, it is also possible to obtain the retention curve of this material, which is the evolution of the suction/water content relation that a material undergoes when subjected to suction increase or decrease paths (drying or wetting). Both tests are performed using a similar methodology.

The suction/water content relation may be conditioned by density and the initial water content of the sample, by the type of path followed in modifying suction –drying or wetting– and by the stress state. The test temperature also has an influence, as a result of which it should remain constant and known throughout the determination.

This section describes a procedure for determining the suction/water content relation in which the sample is not confined during the application of suction. This means that, as expansive materials are involved, the volume of the sample varies during the test, depending on whether water is taken up or given off. This implies a variation in the dry density of the sample that cannot be controlled, since the sample swells or shrinks due to water content changes: when water content increases, the sample swells, increasing its volume and thus reducing its dry density; when the water content of the sample decreases, it shrinks and consequently increases its density. However, the careful measuring of the dimensions of the sample once equilibrium is reached

allows insight to be gained into dry density at the end of the process of stabilisation and, therefore, into the degree of saturation.

The test begins with the manufacturing of specimens having the desired density and water content, through uniaxial compaction of the clay. The resulting diameter is 3.03 cm and the length 1.23 cm. When working with large compacted samples that are to remain undisturbed, these are trimmed with the help of a cylindrical cutter of suitable dimensions. The size of the specimen conditions stabilisation time, therefore the size selected is a compromise between test time and the representativeness of the sample.

Two different techniques have been used to control suction: membrane cells for matric suctions of between 0.1 and 2.0 MPa and desiccators with sulphuric acid solutions for total suctions of between 3.3 and 500.0 MPa. When the retention curve is being determined, the same sample –following stabilisation at a given suction– is placed in a cell or desiccator in which a higher or lower suction is applied, where it once more remains for the time required for its water content to stabilise. This process is repeated successively until a drying or wetting curve is obtained with all the intermediate points considered to be necessary.

Given that the test methodology is different for each technique –membrane cells or desiccators– these are described separately. The operations described below should be carried out in a room with a controlled and regulated temperature, which in our case has been established at 20°C.

Membrane cell testing

The membrane cells were manufactured by the company Mecánica Científica (Getafe) in accordance with an original design by Esteban (1990), developed at CEDEX. These are made up of a flat base and a cylindrical body leaving an internal space of 49 cm^3 (Figure 38). The base and the body, both of stainless steel, are adjusted by screws and the tightness of the overall assembly is ensured by means of an o-ring. The body is fitted with a gas inlet and a manometer indicating the pressure inside the cell. The lower part of the cell has an embedded porous stone, beneath which there are water intake lines connected to a water tank at atmospheric pressure. A semipermeable membrane

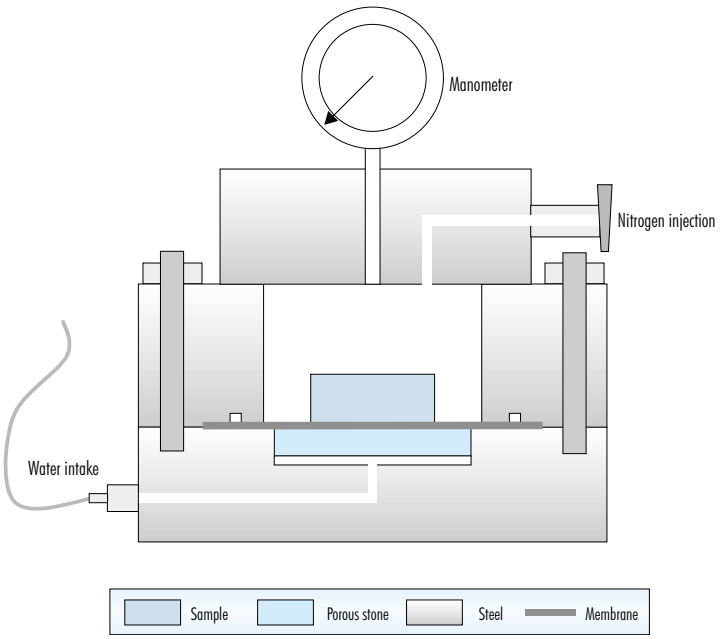

Figure 38. Schematic cross section of a membrane cell.

of regenerated cellulose, that allows water –but not gas– to circulate through it, is inserted between the sample and the porous stone. A peristaltic or centrifugal pump is located between the cell and the tank, this facilitating the removal of gas bubbles diffusing through the membrane, and consequently guaranteeing the continuity of the liquid phase.

The complete assembly is shown in Figure 39, which includes the pump and water tank. Although the cells may withstand gas pressures of up to 14 MPa, they have been used only for suctions equal to or lower than 2 MPa. Industrial nitrogen was used as the gas.

The specimen is placed on the membrane (one specimen per cell), the cell is closed, the pressure is increased and the water inlets are connected. A periodic check is made of the variation in water content of the sample, for which the cell is dismounted and the specimen is weighed and then placed again in the cell at the same pressure. Once stabilisation has been achieved, *i.e.* when no variations in water content of more than 0.1 percent are observed, the process is considered to be complete. For the specimens of the FEBEX bentonite used, the stabilisation time is between 20 and 30 days.

If a retention curve is being determined, the sample will be weighed and measured, to determine its dry density, before subjecting it to a further suction step. If, on the other hand, a single point of the suction/water content relation is being determined or the retention curve determination test is completed, the sample will be measured and dried in the oven at 110 °C for 24 hours to check its final density and water content.

Desiccator testing

In order to apply suctions in excess of 3 MPa, the control of the relative humidity of the atmosphere surrounding the sample has been used, the samples being placed in desiccators with a sulphuric acid solution of a weight percentage of between 6 and 72 percent.

Following manufacturing, the specimens are placed in the desiccator with an adequate solution, the assembly is closed and vacuum is generated to speed up the exchange of water between the sample and the desiccator atmosphere. Several specimens may be placed in each desiccator. In the desiccators measuring 20 cm in diameter used for this work,

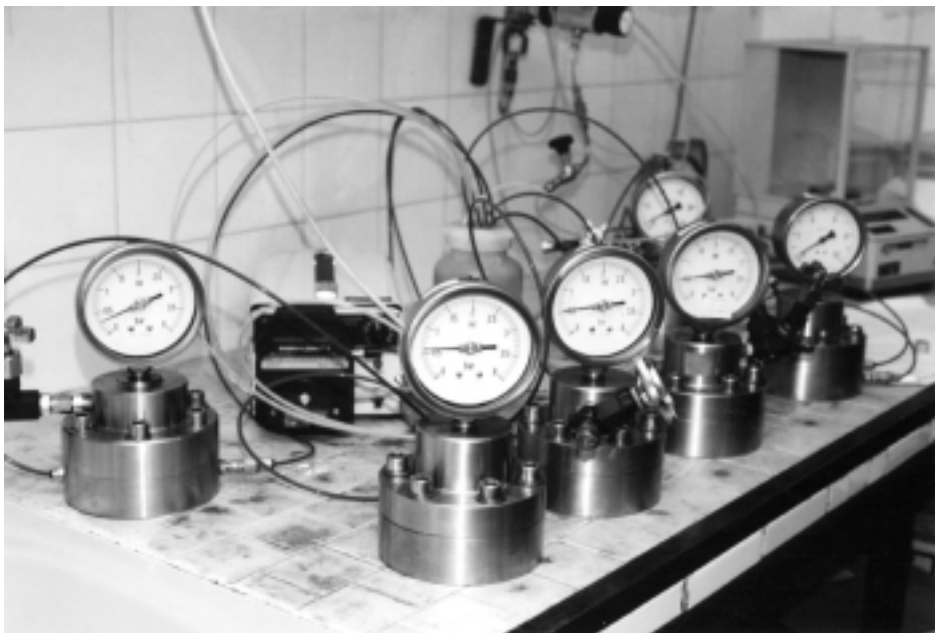

Figure 39. Membrane cells connected to the water tank via a peristaltic pump.

between 3 and 9 specimens are placed (Figure 40). A periodic check is made of the variation in water content undergone by the sample, for which the vacuum is removed, the desiccator is opened and the specimens are weighed and then replaced in the desiccator with the same solution (the frequency of the weighings may vary depending on the test requirements or the characteristics of the samples). Once stabilisation has been achieved, that is to say, when no variations in water content in excess of 0.1 percent are observed, the process is considered to be complete. For the bentonite studied in this work, the stabilisation time is around 30 days, in all cases somewhat longer than that required for stabilisation in membrane cells, since in this last case water content transfer occurs in the liquid phase, while in desiccators it occurs in the vapour phase.

If a retention curve is being determined, the sample will be subjected to a further suction step following the last weighing and measurement to determine its dry density. If, on the other hand, a single point of the suction/water content relation is being determined or the retention curve determination test is completed, the sample will be measured and dried in the oven at 110 °C for 24 hours to check its final density and water content.

Likewise, the final density of the sulphuric acid solution in the desiccator is checked, using a pycnometer. This will give the exact value of suction to which the samples have been subjected.

Retention curve at constant volume

The curves determined under free volume conditions, *i.e.* as described in the previous section, reflect the relation between suction and the degree of saturation of a material whose porosity varies constantly during testing. These variations in density will not occur in the case of the bentonite in the disposal facility barrier since, being confined, the volume variations will be minor.

Consequently, it was necessary to control the volume of the sample while suction was applied. In order to, on the one hand, reproduce the situation of the clay in the disposal facility as faithfully as possible and, on the other, maintain porosity –one of the fundamental characteristics of the material– constant throughout the determination, two experimental methods were set up, allowing the suction applied to be controlled and preventing sample volume variations during testing.

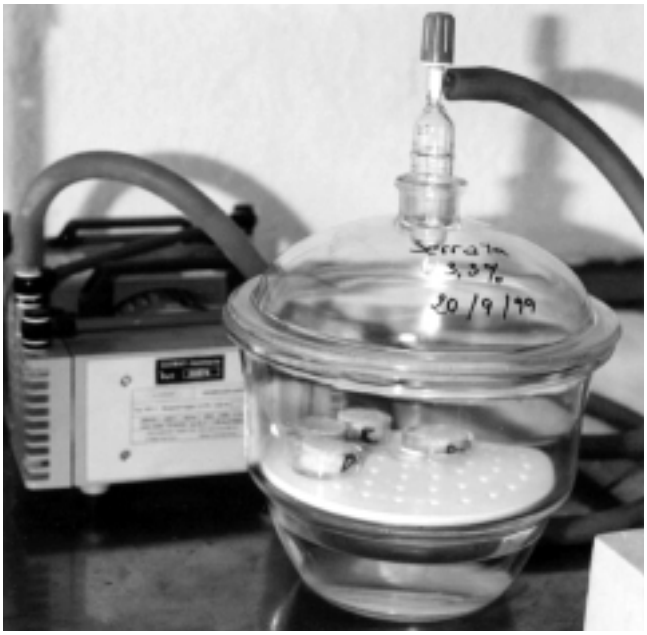

Figure 40. Desiccator with solution of sulphuric acid and specimens of bentonite at the moment of vacuum generation.

These methods are: determination of the retention curve in the oedometer with controlled suction and the use of perforated, non-deformable cells in an atmosphere with controlled relative humidity. The first of these was used to determine the curves at 20 °C, and the second, developed later, to determine the curve at 40 °C. The dimensional control of the sample, which is achieved only on wetting paths, is much better when the non-deformable cells, which were designed specifically for this type of test, are used.

Retention curve in the controlled suction oedometer

In order to maintain the density constant throughout the entire determination, this was carried out in controlled suction oedometers, in which it is possible not only to apply a given suction but also to keep the volume of the sample constant through the adpition of loads. This method allows the volume to be kept constant only during wetting paths, since swelling may be avoided by loading the sample, but not the shrinkage that occurs on drying. Furthermore, it is difficult to achieve perfect control of sample volume, and during the test minor variations in dry density occur, especially in the case of high dry densities, for which swelling cannot be completely counteracted with the capacity of the equipment used. In addition, the application of loads causes a deformation in the system that is occasionally difficult to distinguish from the deformation of the sample, despite previous calibration, this being especially true when membranes are used.

The oedometric equipment used includes modified oedometric cells in which suction may be applied. This equipment and its use are described in the following section, "Controlled suction oedometric testing".

The clay, with its equilibrium water content under laboratory conditions, was uniaxially compacted inside the cell rings to obtain cylindrical specimens measuring 1.20 cm in length and 11.40 or 19.24 cm^2 in cross section.

Once the oedometer ring with the sample has been placed in the oedometer, as described in the section "Controlled suction oedometric testing", the desired suction is applied and the strain recorded by the dial gauge is observed. When the clay begins to swell, loads are applied to counteract deformation, attempts being made to maintain this below 0.005 cm. Once equilibrium has been reached for a given suction, that is to say, when there is no longer any strain for a constant vertical stress, the cell is released, the ring and the sample are weighed (since the sample cannot be removed from the ring without undergoing disturbance) and the specimen is measured. The heigth of the sample (h_m) is determined indirectly, by the difference between the heigth of the ring (h_a) and that measured from the surface of the sample to the upper edge of the ring (h_d), as shown in Figure 41. Occasionally, when very high loads are applied, it is not possible to separate the load piston from the sample; in this case, indirect measurement of the specimen is accomplished as shown schematically in Figure 42. Afterwards, the oedometer ring is immediately assembled in the cell and vertical stress is applied, along with the suction existing prior to disassemblage, waiting for 24 hours until equilibrium is reached again before going on to the next suction step. The duration of each step has been established at a minimum 20 days, even if the strain for a given load has stabilised earlier.

In oedometers with suction control by solutions, the tests began at a suction similar to that existing under

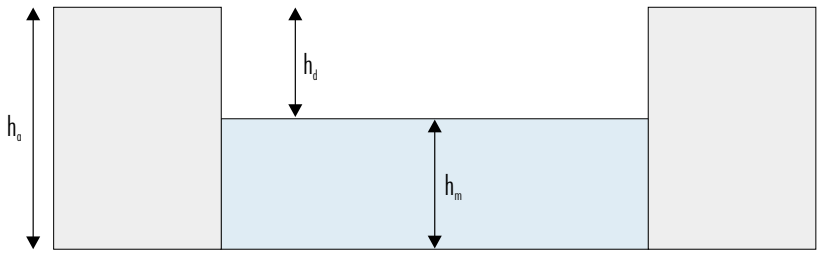

Figure 41. Indirect measurement of the sample in intermediate steps for the determination of the retention curve at constant volume.

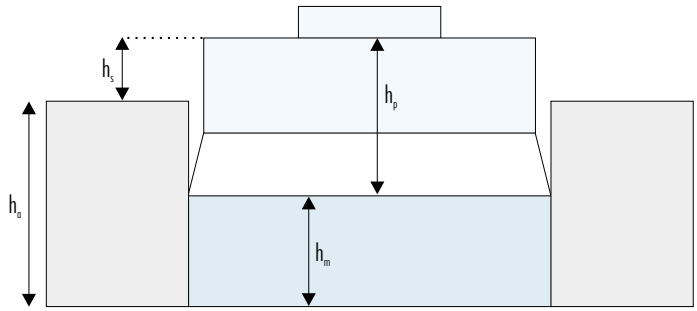

Figure 42. Indirect measurement of the sample in intermediate steps for determination of the retention curve at constant volume, when the piston cannot be separated.

laboratory conditions (RH 50 %, suction 130 MPa), this subsequently being reduced stepwise. In the tests performed using oedometers with suction control by nitrogen pressure, the maximum applicable suction, 14 MPa, is far from the initial equilibrium value in the laboratory environment, as a result of which there is always sudden hydration of the sample when it is placed in the oedometer. Subsequently, wetting (reduction of suction) or drying (increase in suction) paths were followed. All the tests were performed at 20 °C.

This technique is open to breakdowns that may invalidate the tests, especially in the case of oedometers with suction controlled by means of nitrogen pressure. Inaccuracies are also involved when determining the exact length of the specimen, and consequently its density. This is due to the fact that the equipment is disassembled for each change in suction, what could give place to some uncontrolled relaxation of the sample. While determining the suction/water content relation, this technique also allows insight to be gained into the swelling pressure for different suctions, corresponding to the load to be applied in each step to stabilise strain.

Retention curve in non-deformable cells

As has been pointed out above, the determination of the retention curve in oedometers with suction control does not make it possible to achieve perfect dimensional control of the sample throughout the entire process, especially in the case of high densities. Furthermore, the technique is difficult and is affected by breakdowns and inaccuracies. For these reasons, non-deformable cylindrical cells were designed during the final stage of this research, to prevent variations in the volume of the sample. These cells consist of a cylindrical body measuring 0.5 cm in thickness, with two perforated covers joined by bolts. All the elements were manufactured from high corrosion-resistant stainless steel by the company Mecánica Científica (Getafe) (Figure 43).

The sample is compacted directly inside the cell, from the granulated clay at hygroscopic water content. The length of the specimens is 1.20 cm and their cross section 3.80 cm^2. A porous stone and Whatmann 54 filter paper are placed between the covers of the cell and the sample. All the parts are weighed prior to initiating the test. Once the covers have been adjusted, the cell is placed in a desiccator with a sulphuric solution and vacuum is created. Three cells may be placed on the porous plate of the desiccator. The suction control method is, therefore, through the control of relative humidity, as explained above, so the test methodology is similar to that used to determine the retention curve under free volume conditions in the desiccator (see section "Desiccator testing").

The porous stone and the perforated covers allow for the exchange of water in the vapour phase between the clay and the atmosphere of the desiccator. This process is very slow –slower than when the retention curve under free volume conditions is determined in the desiccator– not only because not the entire surface of the sample acts as an exchange surface (but only the upper and lower parts) but also because the process is performed at constant volume. Periodically (every 3 or 4 weeks, in view of the slowness of the process), a check is made of the

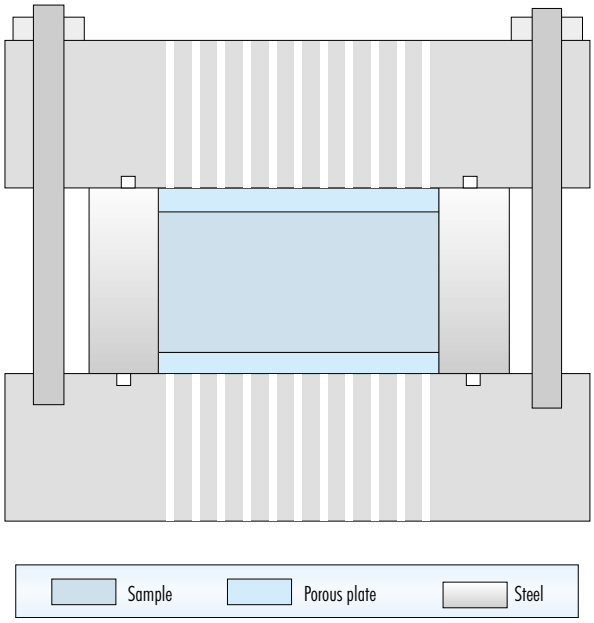

Figure 43. Non-deformable cell for the determination of the retention curve.

variation in weight of the sample. To accomplish this, the desiccator is opened, the cell covers are unbolted and the porous stone are removed. The cylindrical body is weighed along with the sample and the upper and lower filter papers, since these cannot be removed. For this reason, several filter papers of the same type and size must be introduced in the same desiccator, these being weighed at the same time as the cells in order to learn of their changes in water content and subtract these from those of the sample. On completion of the weighing process, the porous stones are replaced, the covers are retightened, the cells are placed in the desiccator and vacuum is created. The same sulphuric acid solution is maintained until the weight of the samples stabilises –this indicating that water transfer has finished– for which a period of between two and three months is required. Once equilibrium is reached, the solution in the desiccator is changed and its density checked, in order to calculate the suction applied at each step.

In this research, this method has been applied only for determination of the retention curves at 40 °C. For this purpose, the desiccator is placed inside an oven with regulated temperature, where it remains until weighing and changing of the solution (Figure 44). Measurement of the density of the solution removed from the desiccator is performed at 20 °C, that is to say, following cooling, as a result of which calculation of the correspondence between the density of the solution (d, g/cm^3) and the weight percentage of sulphuric (p) is carried out in accordance with the fitting for 20 °C, as shown in the section "CONTROLLED SUCTION TESTS". The relation between the weight percentage of the solution and its activity (a_w) is, however, established taking into account the temperature at which the determination was performed. For 40 °C this ratio is as follows (Gmitro & Vermeulen 1964):

$$a_w = 7 \cdot 10^{-8} p^4 - 7 \cdot 10^{-6} p^3 -$$

$$- 0.00001 p^2 - 0.0034 p + 0.9972$$

Likewise, the calculation of suction on the basis of relative humidity (RH = a_w/100) is accomplished by including the adequate temperature in the Kelvin equation.

As in the case of controlled suction oedometers, the cells only prevent variations in the volume of the sample when swelling occurs, that is to say, in the event of wetting, but not when there is shrinkage.

Figure 44. Desiccator with non-deformable cells inside the oven at the moment of vacuum generation.

Furthermore, these cells do not allow for the measurement of swelling pressure, something that can be accomplished in oedometers. Nevertheless, determination of the retention curve, although slow, is much simpler than with oedometers, and is free from errors.

Controlled suction oedometric testing

The oedometric test makes it possible to study the one-dimensional compressibility of soils. Thanks to this, it is possible to determine the speed and magnitude of the consolidation of a laterally confined soil when axially loaded and drained.

Conventional oedometric testing consists in laterally constraining a sample of soil and of loading it axially by steps, applying a constant force until the excess water pressure in the pores dissipates for each increase. During the compression process the variation in the height of the sample is measured, this allowing a relation to be established between effective stress and void ratio or strain (ASTM D 2435-80). The same equipment, with similar methodologies, allows the performance of tests to determine the magnitude of swelling under a given vertical pressure, as well as the pressure required to keep the volume of laterally confined and axially loaded samples constant (ASTM D 4546-85).

The oedometric cell consists basically of a rigid ring in which the soil is compressed between two porous plates, the relative displacement of which may be accurately measured. The load is applied axially to the sample via a system of levers.

When oedometric tests are performed with controlled suction, an additional state variable is introduced in the system of stresses, suction. This means that the sample, in addition to undergoing modifications in vertical stress, is subjected to different suctions during the test. Thus, the suction may be kept constant throughout the loading process, or drying or wetting paths may be experimented, by increasing or decreasing suction, while the vertical stress remains constant.

Two techniques described at the beginning of this chapter have been used to control suction: axis translation and the imposition of relative humidity. In both cases, suction is applied but is not measured, since there are no conventional techniques for the measurement in the laboratory of high

suctions in very expansive materials. Control of the suction (s) is accomplished by changing the values of air pressure (u_a) or water pressure (u_w) in the pores of the sample, since changes in matric suction are given by the difference between the two ($s=u_a-u_w$). Specifically, suction has been applied by nitrogen pressure for values of between 0.1 and 14 MPa, any by solutions of sulphuric acid for values of between 3 and 500 MPa.

In order to be able to apply suction during performance of the oedometric test, it is necessary to use modified oedometric cells. The cells used were similar to those developed at CEDEX and described by Esteban (1990) –the membrane cell– and by Esteban & Sáez (1988) and Esteban (1990) –the cell with a solution deposit–, both being manufactured by the company Mecánica Científica (Getafe).

Specifically, five cells for suction control by nitrogen pressure (Figure 45) and a further five for suction control by solutions of sulphuric acid (Figure 46) were used.

The membrane cell is manufactured in stainless steel and consists of a base, cover and central body (Figure 47). The oedometer ring is housed in the body of the cell. The upper part of the cell has a central orifice for passage of the loading ram. This rests on the load distributing piston, which has a porous stone attached to it at its lower end, which remains directly in contact with the sample. The cover of the cell also has a gas inlet with a manometer for values of up to 16 MPa. Externally, a strain dial gauge with a level of accuracy of thousands of a millimetre, coupled to the loading ram, rests on the cell cover. The base of the cell has an embedded porous stone, below which there are two inlet and outlet orifices, connected to a burette with water at atmospheric pressure. The semipermeable, regenerated cellulose membrane is placed over this stone, with the sample resting directly on it. This membrane allows water and ions to pass, but not gas. A peristaltic pump, installed between the burette and the cell inlets, facilitates the removal of the gas that could diffuse through the membrane. Industrial nitrogen was used as the gas.

The cell with a deposit for solutions consists of a base and cover of high corrosion-resistant stainless steel (AISI 316L) and a cylindrical body of transparent material (perspex) with an internal border on which rests a ring-shaped glass deposit (Figure 48).

Figure 45. Oedometric frame with five membrane cell stations.

Figure 46. Oedometric frame with five stations for cells with solution deposit.

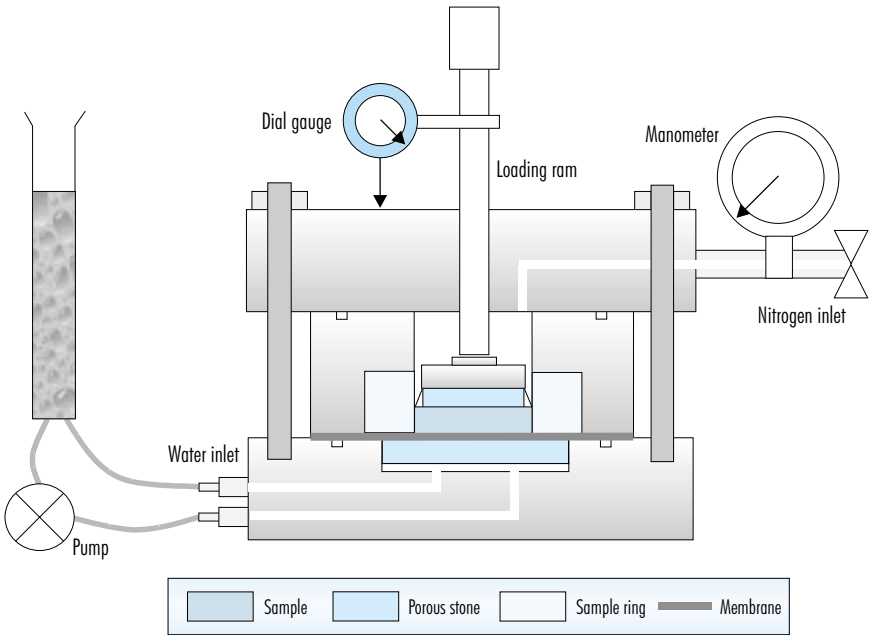

Figure 47. Schematic cross section of an oedometric membrane cell.

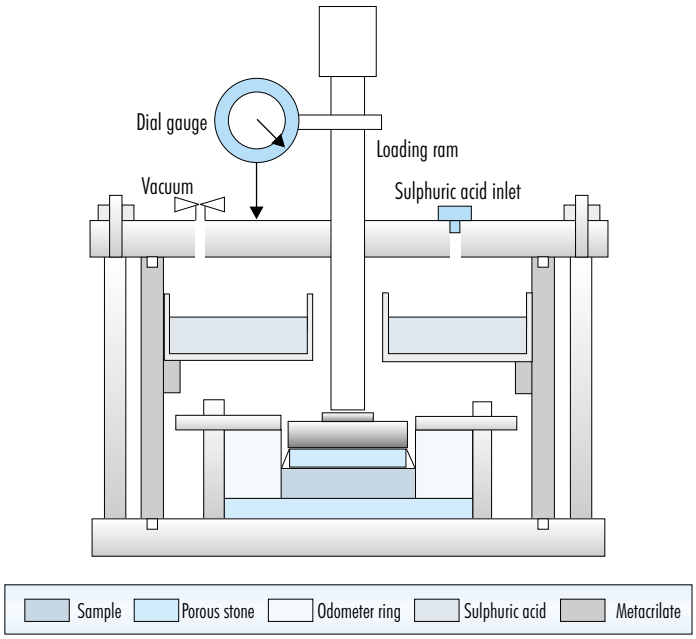

Figure 48. Schematic cross section of an oedometric cell with deposit for solutions.

A porous stone rests on the base of the cell, over which is the oedometer ring with the sample and finally, the upper porous stone attached to the piston. This assembly is attached to the base of the cell by means of a steel flange. The upper cover has an orifice for the loading ram, a perforation for insertion of the sulphuric acid and an inlet for the creation of the vacuum. Externally, a dial gauge accurate to thousands of a millimetre rests on the cell cover, coupled to the loading ram.

The test begins with manufacturing of the specimen by uniaxial compaction of the clay directly in the oedometer ring. All the tests were performed using compacted samples at a nominal dry density of 1.70 g/cm^3, with the clay at its hygroscopic water content. The pressure required to achieve this density is 20 MPa. The initial heigth of the specimen is 1.20 cm and its cross section 11.40 or 19.24 cm^2.

The values of suction and load to be applied (steps) are determined beforehand, the number of which will depend on the level of detail required for definition of the curve and on the characteristics of the sample. The initial values of vertical pressure and suction are defined and the loads to be applied calculated. The vertical load is obtained by applying lead weights to the hanger. The ratio between weights and pressure depends on the oedometer lever arm, which in the case of the oedometers used was 7.695, and on the surface area of the sample, as a result of which the maximum vertical pressure applicable in the oedometer is 9 MPa for the samples of smaller cross section and 5 MPa for the larger.

The oedometer ring is assembled in the cell and the latter is closed and placed in its housing. In the case of membrane cells, the first step consists in increasing the pressure in the cell by injecting nitrogen gas to the desired suction value. This pressure increase is applied gradually and is always preceded by application of the corresponding compensation load. The compensation load is necessary to avoid displacement of the loading ram due to the nitrogen pressure inside the cell. Its value depends on the section of the loading ram. Once the suction value has been reached, the desired vertical load is applied by placing weights on the hanger.

In the case of cells with deposits, once the oedometer ring has been mounted and the assembly has been placed in the oedometer housing, 150 cm^3 of sulphuric acid solution are poured in the deposit, at

a concentration adequate to generate the desired suction. Vacuum is then created in the cell and the vertical load is applied.

Once the foreseen values of suction and load have been achieved, recording of stress begins immediately, at gradually increasing time periods up to 24 hours.

Once the strain for the load and suction conditions corresponding to the initial step has stabilised, the step is changed. In highly expansive materials the time required for stabilisation may be very long, as a result of which the duration of each step may be established once the time required for most of the deformation to occur has been defined. In this work, a minimum value of 20 days has been established.

Unlike what occurs with vertical load, the effect of suction on the sample is not immediate, because the processes involved are slow, especially in clay materials. For this reason, when the step change implies modifying both suction and load, the suction should be changed first and the load subsequently.

In cells with nitrogen pressure the pressure change should be carried out gradually, and preceded by the corresponding modification of the compensation load. The strain recorded by the dial gauge during the nitrogen pressure change operation is considered to pertain to the apparatus itself and not to be attributable to the sample. This is because, as pointed out above, modification of the suction is not manifested immediately on the sample. Following the pressure change, the vertical load is modified and the readings sequence then begins immediately.

To perform the step change in cells fitted with deposits, the solution is extracted by means of a syringe via the inlet in the cell cover, and the new solution is introduced using a glass funnel. Once the cell has been closed, vacuum is created, the cover is tightened and the dial gauge reading is adjusted to the last reading of the previous step. If a change in vertical load has to be also carried out, the load modification will be performed at this time. The reading sequence then begins immediately. In order to gain insight into the exact value of suction to which the sample has been subjected, the density of the extracted and added solutions is checked using a pycnometer.

The oedometric equipment may undergo some instantaneous strain on loading and unloading. This deformation should be carefully measured in order to be able to distinguish at each moment which part of the measured strain actually corresponds to the sample and which should be subtracted due to its corresponding to the apparatus. This is accomplished by calibrating the equipment using a steel disc not subject to strain under the loads applied, of the same length as the sample habitually used and 1 mm less in diameter, which is included in place of the sample. Calibration should also be accomplished including the filter paper or membrane and saturating them with distilled water, as in the case of the test with the clay sample (ASTM D2435). The equipment is then loaded stepwise and subsequently the load is removed. The strain produced at each load step is recorded, with a view to obtaining a curve relating load to strain throughout the range of applicable loads. One curve has to be obtained for the loading cycle and another for unloading, since they are usually affected by hysteresis, especially when filter papers or membranes are used. The recorded readings should be corrected according to the deformation of the equipment as the loads are applied.

Figure 49 shows the calibration curves obtained for one of the oedometers with suction controlled by nitrogen.

Once equilibrium has been reached for the last step of the test, the equipment is disassembled. The sample is weighed and measured and its final water content is determined by drying in the oven at 110 °C for 24 hours. With these data it is possible to calculate and check dry weight, initial and final dry density and water content.

The following calculations are performed for each reading taken at different times:

1. The equivalence between the dial gauge reading and the heigth of the sample, taking into account the initial reading of the dial gauge, its appreciation and the initial heigth of the specimen. Once the heigth of the sample at each moment is known, the dry density may be calculated, and from this and the specific gravity of the material its void ratio may be calculated. The initial reading at each step is corrected in accordance with the equipment calibration data.
2. The strain at each moment in tieme (ε_t) is calculated as the ratio between the variation in heigth undergone by the sample (the difference between initial heigth and the heigth at each moment, Δh) and the initial heigth (h_i), expressed in percent, the increases in heigth considered to give rise to negative values.

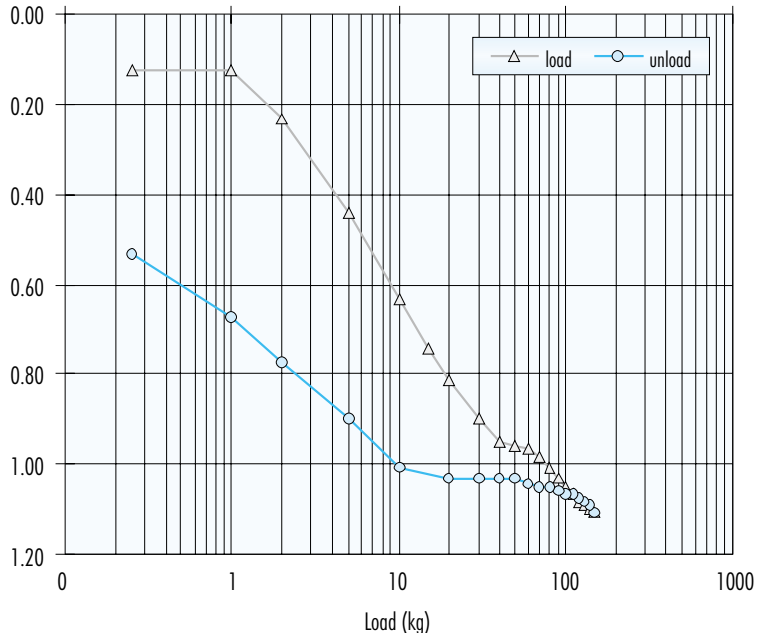

Figure 49. Calibration curves for an oedometer with suction controlled by nitrogen pressure, performed with the membrane saturated with distilled water.

$$\varepsilon_t = \frac{\Delta_h}{h_i} = \frac{h_i - h_f}{h_i}$$

The results for each step may be presented in the form of a semilogarithmic graph showing the evolution of the percent of strain or of void ratio versus time (consolidation or swelling curves).

The results for the test overall may be presented in the form of a semilogarithmic graph relating the final void ratio of each step to the corresponding vertical load or suction (oedometric curve).

Most of these tests were performed at a constant temperature of 20 °C. Certain of the tests were carried out in membrane cells in a thermostatic bath with fluid silicone (Figure 50). The temperature of this bath may be regulated, this having allowed tests to be performed at 40, 60 and 80 °C.

The cell inserted in the bath is similar in design to those described above, with the difference that the manometer controlling the applied pressure is not a part of the cell itself, but is connected to it by means of a stainless steel tube, this allowing it to be positioned at a distance from the thermostatic bath.

Thermal conductivity

Thermal conductivity is the capacity of a soil to conduct a quantity of heat in the presence of a temperature gradient. It is one of the properties that governs heat flux, and that must, therefore, be known in order to establish the distribution of temperatures in a soil and the influence of temperature on the movement of water, both key aspects as regards understanding of the behaviour of the clay barrier in a high level radioactive waste disposal facility.

Heat flux arises as a result of different transport mechanisms. In solid materials, heat flux is by conduction, while in pores the mechanisms of conduction, convection and radiation act in parallel. If, in addition there is water, the latent heat of vaporisation constitutes an additional factor (Jackson & Taylor 1965).

In homogeneous soils uniformly moist, heat flow may be assumed to be conductive and equal to a thermal conductivity times a temperature gradient (Fourier equation), where it is implicitly assumed that thermal conductivity includes the thermal vapour flux induced by the temperature gradient (Buchan 1991).

Figure 50. Oedometer with suction controlled by nitrogen pressure installed in a theromostatic bath (manometer to the right, peristaltic pump and water tank to the left).

Thermal conductivity is defined as the quantity of heat that flows through a unit of area in the unit of time under a unit thermal gradient. It may be expressed, therefore, in W/m·K.

Thermal properties in general, and thermal conductivity in particular, depend on the physical composition of the soil, especially on water content, and to a lesser extent on density, since both properties condition the quantitative relationship between the different phases of the soil (solid, water and air) and each of these phases contributes to macroscopic thermal conductivity. Likewise, there is a certain dependence on temperature, although this is insignificant in the range of temperatures typical of soils. Beziat *et al*. (1988) find that the increase in the thermal conductivity of a calcic smectite on increasing temperature from 50 to 188 °C is around 10 percent, much smaller than that observed when varying water content or density.

Superficial thermal conductivity was measured using a Kemtherm QTM-D3 system by Kyoto Electronics, which operates on the basis of the hot wire transient method (Figure 51). Transient methods have the advantage over steady-state methods that the movement of water in response to the thermal gradients applied for determination is minimised, especially if these gradients are small. Consequently, transient methods for the measurement of thermal conductivity are more to be recommended than steady-state methods for non-dry soils.

The hot wire transient method is based on the exponential increase in the temperature of a thin hot wire that occurs when a constant power is applied (heat flux), while the wire is stretched in the centre of a cylindrical sample or a rectangular parallelepiped of infinite length. This allows the thermal conductivity of the material to be calculated on the basis of heat flux (power and intensity), the characteristics of the heating wire (length, radius and resistance) and the increase in temperature of the wire over a given period of time.

The measuring equipment used is based on the probe method, a variation of the hot wire transient method in which the wire, instead of being inserted in the sample, is placed between the latter and an insulating material of known thermal conductivity (Kyoto Electronics 1987). This insulating material and the wire, along with a K-type thermocouple for the measurement of temperature variation, constitute the measuring probe. If this probe method is applied, thermal conductivity (λ, W/m·K) is calculated by means of the following equation:

$$\lambda = K \frac{I^2 \ln\left(t_2 / t_1\right)}{V_2 - V_1} - H$$

where V_1 and V_2 are the initial and final output voltage of the measuring equipment (V); I is current intensity (A); t_2 and t_1 are the end and beginning of the measuring time (s); and *K* and *H* are the constants of the probe, calculated on the basis of the resistance of the wire, the thermoelectric power of the thermocouple and the thermal conductivity of the insulating material. These constants must be verified and adjusted by comparison with the measurement obtained from three standard samples of known thermal conductivity.

The values of thermal conductivity obtained using this method or the conventional hot wire method coincide, since the relation between temperature variation and time is practically the same in both cases (Kyoto Electronics 1987). This was verified in measurements performed using both techniques on an-

Figure 51. Kemtherm QTM-D3 conductivity meter with probe and standard plates.

other bentonite from the Cortijo de Archidona deposit (Luis y Luis 1990, Rivas *et al*. 1991).

The measurement is performed at laboratory temperature, applying the probe to the sample to be tested. This supplies a known power via the wire for 60 s, causing a temperature increase of some 20 °C. Given that this is a short period of time, the sample is heated only in the area surrounding the heater wire, this implying that the value of the measurement corresponds to the thermal conductivity of the surface of the sample to which the probe is applied. For values of thermal conductivity of between 0.02 and 10 W/m·K, which are usual in geological materials, the flux generated by the heater wire is between 3 and 30 kcal/m·h.

In order for the calculation of thermal conductivity to be correct, the sample must have certain minimum dimensions preventing the heat generated from exiting it to the surrounding substance (for example, air), which would modify the measurement. These dimensions depend on the thermal conductivity of the sample. For this reason, and in accordance with the indications of the manufacturer, the thermal conductivity of the FEBEX clay was determined on specimens compacted in the form of parallelepiped measuring 10 cm in length, 4 cm in height and 3 cm in width, for which a specific compaction mould was designed (Figure 52).

After brushing the surface of the specimen to remove any loose material, the probe is placed on it, the temperature of both is allowed to stabilise to equilibrium and heat flux is applied for 60 s. A check must be made to ensure that the temperature increase caused is within the range 10 to 30 °C. If this is not the case, the measurement will not be valid, as a result of which the heater current intensity should be modified and the test repeated. Three valid measurements are performed on each sample, separated by a period of time guaranteeing cooling of the sample and the probe to laboratory temperature (15 minutes). The accuracy of the equipment measurement is 3 percent. The results are recorded by a printer connected to the equipment.

Measurements were performed on uniaxially compacted samples at different densities and water contents, with a view to checking the repercussion of both properties on the value of thermal conductivity. Following the measurement, the sample is weighed and measured and is dried in the oven at 110 °C for 24 hours (UNE Standard 103-300-93), this serving to check the water content and density corresponding to the measurement.

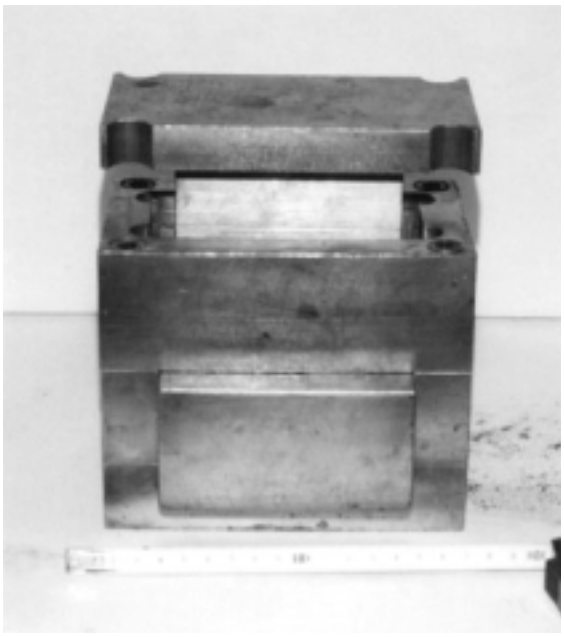

Figure 52. Mould for the compaction of parallelepiped specimens for the measurement of thermal conductivity.

página en blanco

6. Results

6. Results

Basic characterisation

The basic characterisation of a material includes the determination of properties that, being straightforward to obtain, bound its classification and condition its behaviour. It also includes the acquisition of basic parameters required to calculate other magnitudes.

Specific gravity

The relative specific gravity of the solid particles was determined by means of pycnometers, using distilled water as the suspension medium, in accordance with UNE Standard 103-302, as described in the section "Specific gravity". The variable was determined using 13 aliquots of the FEBEX sample during the basic characterisation stage and a further 7 aliquots during subsequent research. The average value obtained was 2.70 ± 0.04.

The theoretical specific gravity of a montmorillonite, calculated on the basis of the atomic weights of the elements of its crystalline network, is 2.74 g/cm^3 (Jiménez & Justo 1971, Lambe & Whitman 1979). Grim (1968) publishes values of between 2.20 and 2.74 g/cm^3, the latter corresponding to the specific gravity of a montmorillonite with an iron content of 3.6 percent. The FEBEX bentonite has an iron content of 3.1 percent, as a result of which the specific gravity value obtained appears to correspond closely to this parameter. Jiménez & Justo (1971) give values of between 2.65 and 2.84 for relative specific gravities determined in water, and Lambe & Whitman (1979) give values of between 2.75 and 2.78. The French FoCa reference calcium smectite has a grain density of 2.67 g/cm^3 (Lajudie 1986).

Atterberg limits, specific surface and granulometry

This chapter includes the results of various basic characterisation tests, all of which have in common the fact that the values obtained depend fundamentally on the percentage of clay sized particles and their mineralogy and textural peculiarities.

The liquid and plastic limits were determined on 19 different aliquots of the FEBEX clay, in accordance with the corresponding UNE Standards, with the specific characteristic that the sample maceration time was increased to 48 hours, as explained in the section "Atterberg limits". The average values and standard deviations encountered were as follows:

Liquid limit:	102±4 %
Plastic limit:	53±3 %
Plasticity index:	49±4

The average value obtained for external specific surface, determined as detailed in the section "Specific surface" on 20 aliquots using the single point BET method, was 32±3 m^2/g. Grim (1968) gives values for the external specific surface of different montmorillonites, determined with nitrogen and other gases, that range from 15 to 82 m^2/g, with values of between 30 and 38 m^2/g predominating, depending on the state of dehydration of the mineral. Olphen & Fripiat (1979) study the values obtained by different laboratories for the same montmorillonite, finding a variation of between 21 and 86 m^2/g, depending on the method used and the preparation of the sample. This variability confirms that the value of specific surface is not unique, and depends on factors such as the degassing conditions, the temperature of the measurement and the method used for calculation (single point BET or complete isotherm) (Sing *et al*. 1985). In fact, the determination of the specific surface of the FEBEX clay at other laboratories, by means of nitrogen adsorption at 77 K and applying the BET method in accordance with Standard ASTM D 3663-84, has given values of between 56 and 59 m^2/g (J. Cuevas, pers. com.).

Granulometric distribution was obtained by combining the sedimentation and sieving techniques, in accordance with the procedure described in the section "Granulometry". The difference between this and what is established in the UNE Standards is that the suspension is dispersed more intensely (including a longer hydration time and the use of ultrasonics) and that sieving is performed with the dispersed sample used for sedimentation. The results of the granulometry testing, performed on 11 different aliquots, are shown in Table IX and graphically represented in Figure 53.

As may be appreciated in Table IX, 67 percent of the material has a size of less than 2 μm, in other words, it belongs to the clay fraction, and 22 percent belongs to the silt fraction, since it has sizes ranging from 60 to 2 μm. Consequently, the material is included in the group of clays according to the USDA textural diagrams. On the basis of the Atterberg limits, however, and in accordance with the Casagrande classification, the material corresponds to an inorganic silt of extremely high plastic-

Table IX
Average granulometric distribution of the 11 samples analysed.

Size (mm)	Passing (average, %)	Passing (standard deviation, %)
2000	100	0
1.190	99	0
0.590	98	1
0.297	96	1
0.148	94	1
0.074	93	1
0.057	89	2
0.040	88	2
0.026	87	3
0.015	84	2
0.010	81	2
0.009	80	2
0.005	77	2
0.004	74	2
0.002	67	3

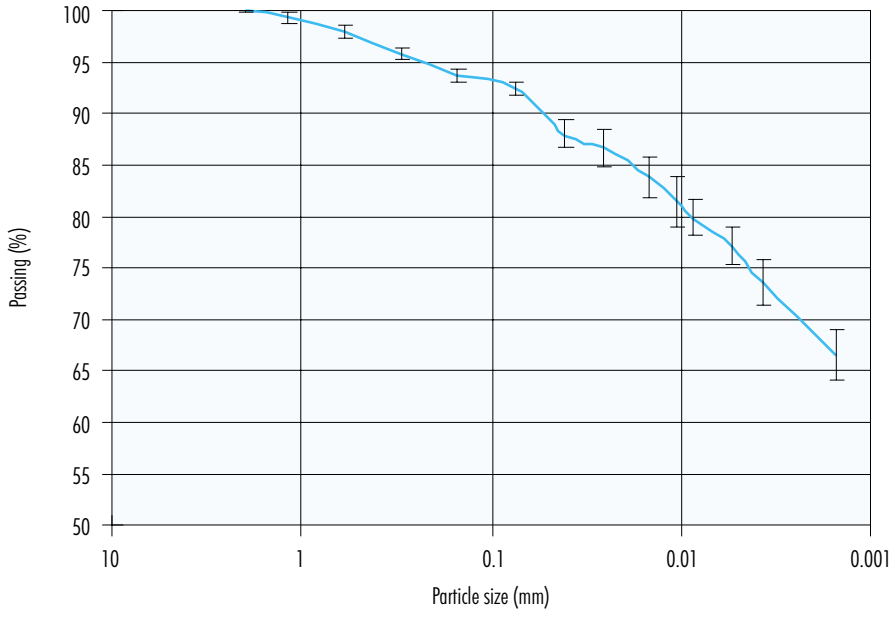

Figure 53. Average granulometry curve, with indication of standard deviations, for the samples analysed.

ity. Furthermore, the percentage of the clay sized fraction, *i*.e. smaller than 2 μm, is very low for a bentonite of this mineralogical purity, with more than 90 percent of smectite. This is so despite the fact that the sample was intensely dispersed prior to granulometry determination, including lengthy periods of hydration, agitation and ultrasonics.

This specific characteristic had been underlined during the first studies carried out on the bentonite from this deposit. Pérez del Villar (1989b) attributes the difficulty involved in dispersion of the clay to the agglutination of particles due to the existence of colloidal silica, originating during the transformation of the volcanic rock into smectite. White & Dixon (1997), in an electron microscope study performed on the same FEBEX clay, discover remains of silt-sized volcanic ashes pseudomorphised by smectite. These pseudomorphs, of silt size and smectitic composition, would be relatively stable and might explain the low plasticity of the clay and the low percentage of the clay fraction. The existence of pseudomorphs is not unusual in bentonites, as pointed out by Ross & Hendricks (1945), who stated that these might retain the structure of volcanic ashes with great perfection.

In order to confirm whether the low percentage of particles of less than 2 μm and the relatively low liquid limit are the result of a special clustering of the particles, gradually more intense treatments were performed on the clay, checking the evolution of the liquid limit, granulometric distribution and specific surface. The sample used for this was ground to a size of less than 0.4 mm and dried for several days at 150 °C. On removal from the oven, a part of this sample was taken for granulometry and another for the determination of specific surface, the remainder being mixed with distilled water and left to macerate for 48 hours. Following this time, the liquid limit was determined using the customary procedure. The remaining mixed sample was dried once more at 150 °C and disintegrated with a wooden roller on removal from the oven. The portions to be used for the determination of granulometric distribution and specific surface were separated and the remainder was mixed again with distilled water to determine liquid limit, the treatment being repeated to a total of 9 drying/wetting cycles.

Table X includes the values for liquid limit (w_L), percentage of particles smaller than 1.4 μm (corresponding to the smallest size identified by granulometry by sedimentation, and approximately equivalent to the percentage of clay sized particles) and external specific surface (a_s) for the different cycles.

Figure 54 shows the evolution of liquid limit, specific surface and percentage of particles of a size of less than 0.0014 mm during the different cycles, the values considered for cycle 0 being those of the clay without previous treatment.

Table X
Evolution of certain bentonite parameters following various drying/wetting cycles.

Cycle	w_L (%)	Fraction $< 1.4\,\mu$m (%)	a_s (m^2/g)
0	102	67	32
1	111		
2	123		
3	142	82	36
4	147	83	37
5	157	83	40
6	164	86	48
7	172	84	48
8	172	85	57
9	164		

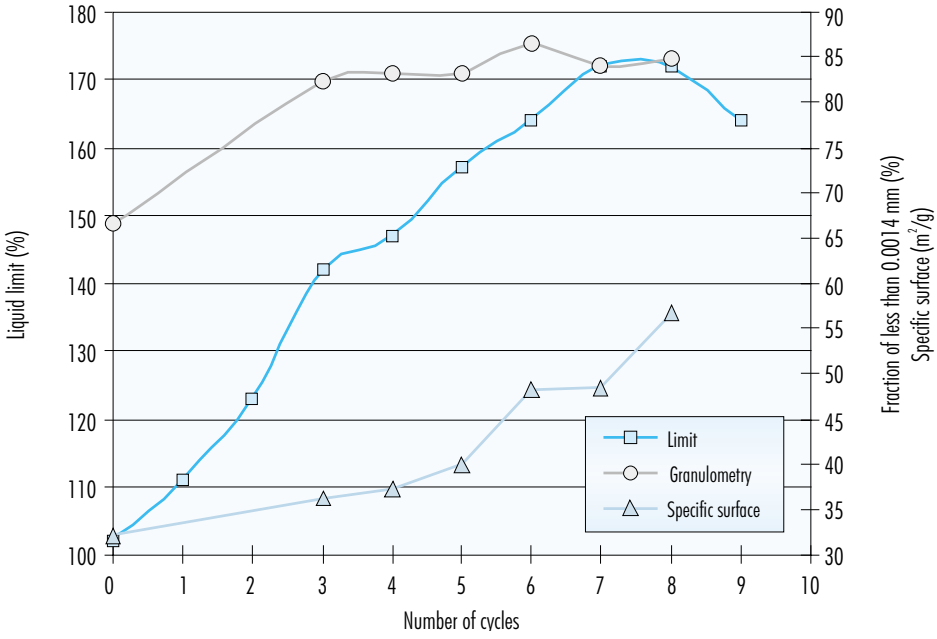

Figure 54. Evolution of values of liquid limit, specific surface and percent of particles of less than 0.0014 mm following various clay drying/wetting cycles.

The liquid limit increases following the first cycle of drying/wetting and mixing, reaching a maximum value of approximately 175 percent after the seventh cycle, the increase not continuing thereafter. As regards granulometry, the percent of particles of less than 1.4 μm is already higher than 80 percent after the third drying/wetting cycle, remaining at similar values or tending to increase following the subsequent cycles. The specific surface also increases considerably, especially from the fifth cycle onwards, reaching a value higher than that of the untreated sample by more than 50 percent after the eighth cycle.

In other words, it would appear to be confirmed that treatment of the clay by successive drying and mixing causes the clay particles to disintegrate, this translating into an increase in the number of accessible reactive surfaces and, therefore, in the plasticity of the material. Pusch (1994) points out that with heating of the montmorillonite the grains break and the number of individual low thickness pilings, and therefore the quantity of diffuse double layers, increases, causing a homogenisation of the microstructure. In her Doctorate Thesis, Tsige (1999) concludes that the wetting/drying cycles that occur in excavated clay terrains as a result of percolation of rainwater and evaporation lead to an increase in crumbling and to the separation of aggregates, due to variation in internal pressures and to weakening of electrochemical binding.

The electron microscope study of this bentonite –performed in collaboration with the Department of Materials Science and Metallurgical Engineering of the Technical University of Catalonia (UPC, Barcelona)– reveals that the most frequent microstructure is made up of pilings of smectite laminae that appear to pseudomorphise original mineral grains of the volcanic rock, as shown in Figure 55 and in greater detail in Figure 56. The smectite laminae develop perpendicularly to what appear to be alignments of the precursor mineral, appearing in a much more orderly manner than is habitual in clay materials. These pilings, which are purely smectitic in composition, might be responsible for the "rigidity" of the untreated material.

Another aspect of these structures in the material is shown in Figure 57, in which the alignments are seen to be curved.

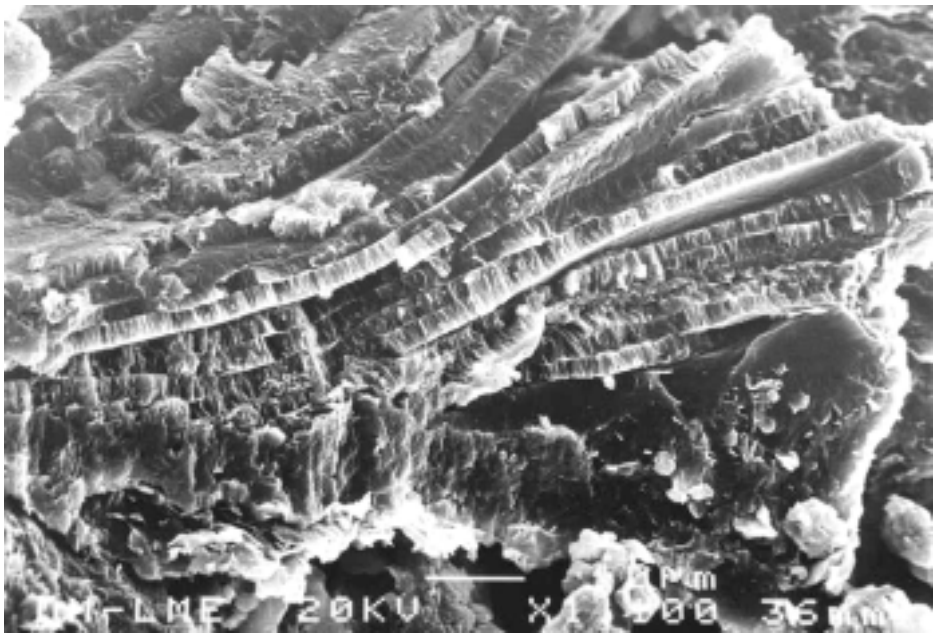

Figure 55. Photograph magnified by 1,100 of the bentonite, taken with the scanning electron microscope.

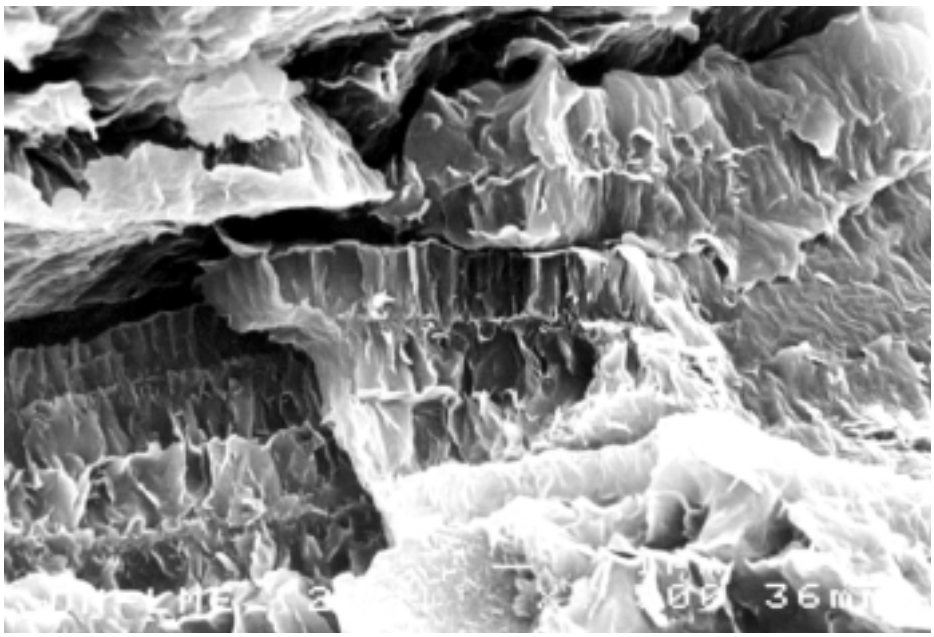

Figure 56. Photograph magnified by 4,500 of the bentonite, taken with the scanning electron microscope.

Figure 57. Photograph magnified by 2,000 of the bentonite, taken with the scanning electron microscope.

Silica is also present in the bentonite, with "balls" of cristobalite/tridimite and botroidal coverings frequently appearing. The latter may act as cementing agents, making dispersion of the clay more difficult (Figure 58).

Porosity

The study of the microstructure of the compacted bentonite samples, in an interval of dry densities of 1.67 to 1.78 g/cm^3, was performed by mercury intrusion porosimetry. This technique allows the determination of pore size distribution by injecting mercury into the sample at different pressures while controlling the volume intruded. The pressure applied may be related to the minimum pore diameter intruded, taking into account the characteristics of the fluid.

The ratio of the volume of mercury intruded (pore volume) to applied pressure (which conditions the minimum pore diameter) allows accumulated curves to be obtained determining the volume of pores greater than a given size, along with distribution curves establishing the percentage of pores of a size included within a given range.

For this work a Poresizer 9320 porosimeter by Micromeritics was used, with a mercury injection pressure range of 7 kPa to 210 MPa, this allowing pore diameters of between approximately 200 and 0.006 μm to be measured. Consequently, the mercury does not intrude the microporosity (pores of a size of less than 0.002 μm, according to the classification of Sing *et al*. 1985). Before the samples are inserted in the porosimeter, the water is removed from the pores by freeze-drying. The data obtained are given in accordance with the following key (Tuncer 1988):

- e_1: void ratio calculated from the experimental measurement of specific gravity (with pycnometers) and dry density (by immersion in mercury, UNE Standard 7045).
- e_2: void ratio calculated by mercury intrusion in the porosimeter (or apparent void ratio, e*).
- % total: total percent of pores intruded by mercury.
- ϕ avg. (μm): average pore diameter.
- % large, medium or small: percent of large pores (diameter greater than 6 μm), medium-sized pores (diameter between 6 and 0.2 μm)

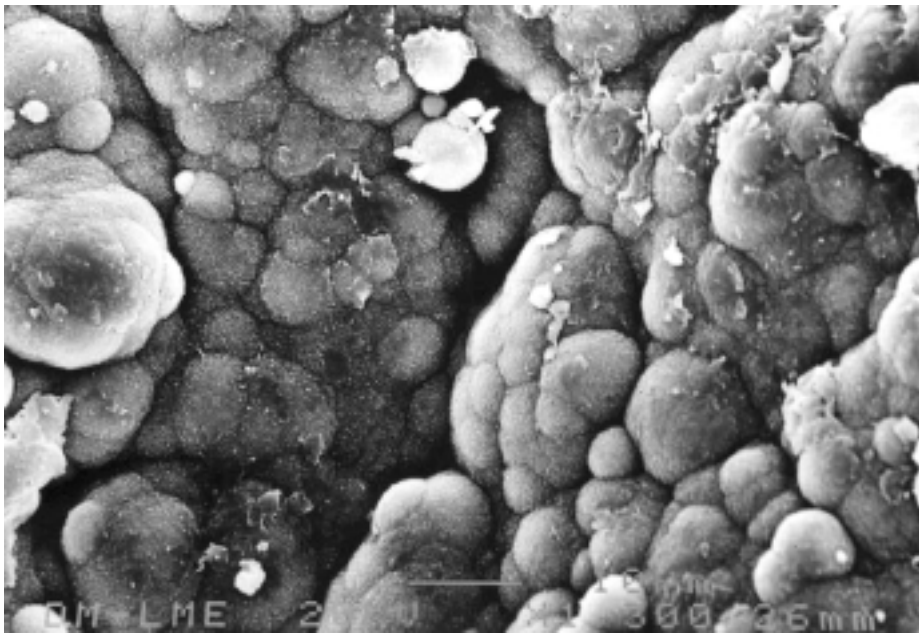

Figure 58. Botroidal covering in the bentonite. Photograph magnified by 1,300 taken with the scanning electron microscope.

or small pores (diameter between 0.2 and 0.006 μm) with respect to the total volume of intruded pores. This size classification was developed on the basis of porosimetry results obtained from a large number of FEBEX clay samples analysed, and includes only macro and mesoporosity. The limits between families may vary slightly between different samples.

- Large, medium or small pore mode (μm).
- unif.coef.: uniformity coefficient of pores ϕ_{40}/ϕ_{80}.

The porosimetry study was performed on the compacted blocks used for the FEBEX Project mock-up test, obtained by uniaxial compaction of the granulated clay at pressures of between 40 and 50 MPa (see section "The FEBEX Project"). These blocks were sampled in order to determine their density, water content and porosimetric distribution at 15 different positions in the block (the 5 positions marked on the surface of the block in Figure 59, repeated for the upper, intermediate and central parts).

Once it had been determined that there were no important differences between the different positions in the same section, the decision was taken to perform the porosimetry determination on only three samples from each block, located in the upper, intermediate and lower central parts (position 2 in Figure 59). These three levels show certain differences in dry density, which is higher in the upper part of the block due to friction against the walls of the mould during compaction. The data on this study may be found in Villar (1997) and are summarised in Table XI.

Figure 60 shows a typical porosimetric curve for three compacted samples of the FEBEX bentonite, belonging to each of the three sections (upper, intermediate and lower), in which the three main families of pores (large, medium and small) may be appreciated. It may also be seen that the mercury intrusion method allows access to be gained only to the macroporosity and to part of the mesopores. Given that the curve reflects the percent increase in pore volume between two consecutive injection pressure steps, the diameters referred to are calculated as the average of the diameters corresponding to the two steps. The large pores are analysed in the low pressure unit of the porosimeter and those of a diameter of less than 6 μm in the high pressure unit.

The porosimetry study does not show any significant variations between the different positions in a block. It may be observed that the percent of the porosity

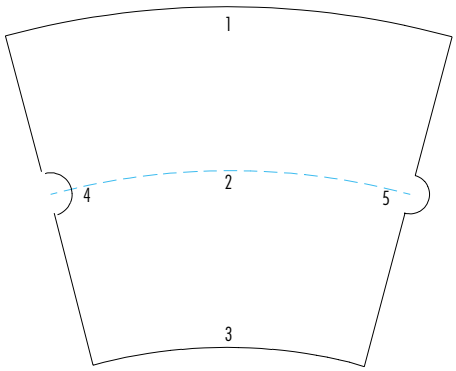

Figure 59. Distribution of sampling positions (from 1 to 5) on the block surface.

intruded by the mercury is fairly low (33 percent on average), this meaning that there is an important volume of pores (67 percent) with a size of less than 0.006 μm (equipment access limit), or that are not intercommunicated. Taking this into account, the percentage of pores in each size range may be recalculated, the merely orientative average values shown in Table XII being obtained. This distribution corresponds to the sample with its hygroscopic water content, and may not coincide with the distribution of the saturated sample, since given that it is a reactive material, the diameter of the pores varies with water content. Table XI also shows a low uniformity coefficient, since there is a clear predominance of the smaller pores.

Figure 61 shows the distribution of pore sizes obtained for the upper, intermediate and lower parts of the sampled blocks.

Figure 62 shows the same curves presented in Figure 60 expressed in terms of the accumulated percent of pore volume versus their diameter. This figure also includes the mercury extrusion curves, that is to say, those reflecting the expulsion of the mercury contained in the sample on gradual release of the injection pressure applied. During intrusion, the entire accessible and interconnected space is filled with mercury, as a result of which the intrusion curve

Table XI
Data on porosimetry by mercury intrusion in the upper, intermediate and lower parts of the sampled blocks.

	Upper	Interm.	Lower	Total
No. of samples	15	15	15	45
ρ_d (g/cm^3)	1.73±0.01	1.72±0.03	1.68±0.19	1.71±0.11
e_1	0.593±0.110	0.570±0.033	0.640±0.281	0.599±0.168
e_2	0.201±0.058	0.183±0.045	0.193±0.088	0.192±0.065
% total	35±11	32±7	34±17	33±12
Avg. diameter (μm)	0.06±0.06	0.04±0.04	0.04±0.04	0.04±0.04
% large	24±7	23±7	23±5	23±6
Mode large (μm)	17±5	18±8	20±12	18±4
% medium	23±7	22±7	22±5	26±6
Mode medium (μm)	0.76±0.58	0.90±0.78	0.60±0.06	0.76±0.56
% small	53±12	55±12	55±6	54±10
Mode small (μm)	0.018±0.010	0.019±0.040	0.014±0.004	0.016±0.006
Unif. coef.	36±26	42±34	44±33	41±31

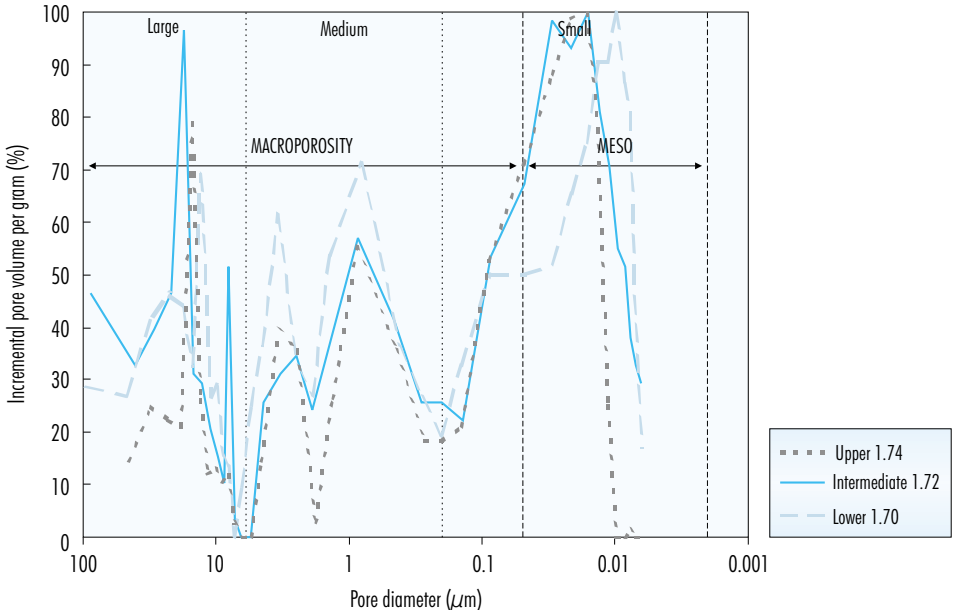

Figure 60. Incremental porosimetric curve for samples from different sections (upper, intermediate and lower) of the blocks of FEBEX bentonite, with indication of dry density in g/cm³.

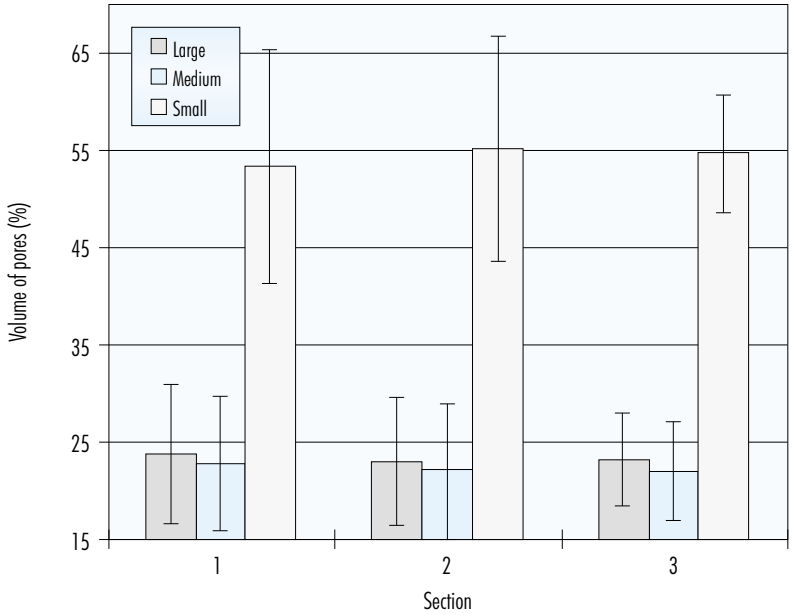

Figure 61. Distribution of large (> 6 μm), medium (between 6 and 0.15 μm) and small (between 0.15 and 0.006 μm) pore sizes in the upper (1), intermediate (2) and lower (3) parts of the sampled blocks, obtained by mercury intrusion.

Table XII
Orientative distribution of total porosity for the FEBEX bentonite compacted with hygroscopic water content.

Size range (μm)	Volume (percentage)
> 6	7
6 – 0.2	8
0.2 – 0.006	18
< 0.006	67

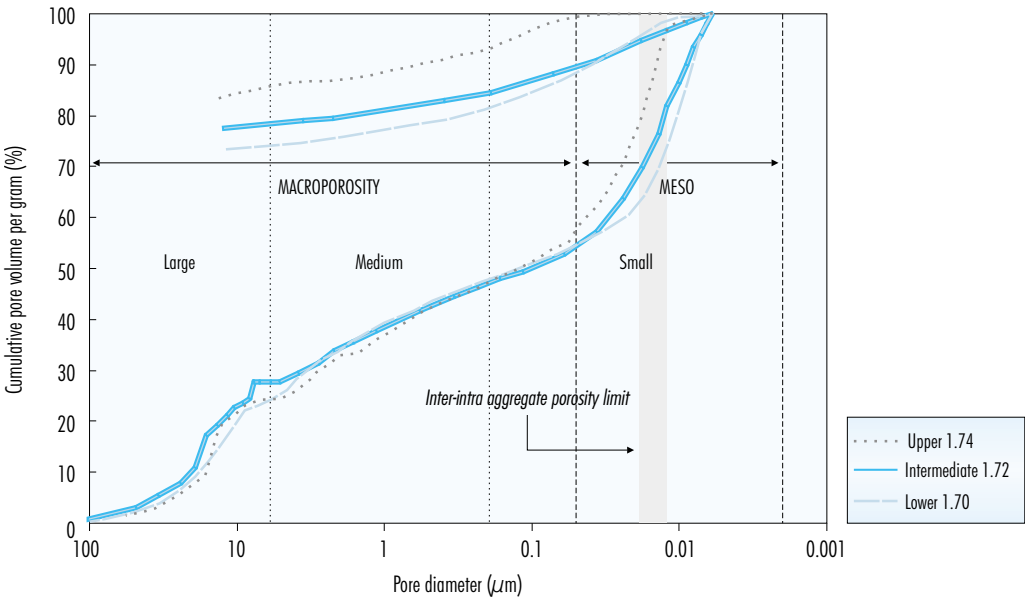

Figure 62. Porosimetric curve (intrusion and extrusion) for samples from different sections (upper, intermediate and lower) of the FEBEX bentonite blocks, with indication of dry density in g/cm^3.

gives the distribution of the total porosity accessible to the mercury. However, when the injection pressure is relaxed, only the mercury contained in the non-constrained pores emerges, the remainder being retained by the clay bridges that form due to the irregular conformation of the aggregates, which act as bottlenecks (Romero 1999). Between 73 and 83 percent of the intruded mercury is retained within the FEBEX bentonite. Some authors suggest that this difference between the intruded and extruded volumes is equivalent to the inter-aggregate porosity, and that the pore inlet size corresponding to this percent on the intrusion curve marks the limit between inter-aggregate and intra-aggregate porosity (Romero 1999, Romero *et al*. 1999). On the basis of the intrusion-extrusion curves shown in Figure 62, this pore diameter value would be between 0.01 and 0.02 μm, which is of the same order of magnitude as the limit between macro and mesoporosity established by Sing *et al*. (1985), 0.05 μm. This pore size would appear to be too large to define the intra-aggregate porosity limit, since the intra-aggregate pores of a clay material are considered to have sizes of less than 0.002 μm (section

"CHARACTERISTICS OF SMECTITES"). This lack of correlation between the theoretical value and that obtained by mercury intrusion may be due to the small percentage of total porosity that is actually intruded, and to the fact that in the FEBEX bentonite the mineral grain pseudomorphs may act as aggregates, their internal porosity being greater than that which may appear in aggregates made up of originally clay particles. Bearing in mind that only 33 percent of the total porosity is accessed on average by the mercury (*cf.* "% total" in Table XI), the inter-aggregate porosity (greater than 0.01-0.02 μm) would imply between 22 and 27 percent of the total porosity, the remainder corresponding to intra-aggregate pores.

Density of water

In the following sections we shall see that the degree of saturation of the clay at the end of the tests in which the sample is saturated at constant volume –calculated from its density and water content and the specific gravity of the solid particles– is frequently greater than 100 percent. These are specifically the tests on permeability, swelling pressure, saturation under load and retention curves at constant volume. Of these, the last three types are performed in an oedometer. In general, the difference with respect to the value of 100 percent increases with dry density, becoming particularly significant for dry densities in excess of 1.60 g/cm^3. Various causes that might explain this anomaly have been analysed, and it has been found that the following factors may make some contribution:

- Deficient determination of specific gravity which, if greater than that considered (2.70 g/cm^3), would give rise to lower degrees of saturation. In order for the degrees of saturation to approximate to an average value of 105 percent, the specific gravity would have to exceed the improbable value of 2.90 g/cm^3. Even so, the tests performed at higher dry densities would continue to end with calculated degrees of saturation of between 110 and 120 percent.
- Error in determining final water content. Specifically, in the oedometer tests, and if the cell were not emptied of water before unloading, the sample might take up water during decompression, giving rise to a higher value of final water content than it actually had on test completion. Given the speed at which the process of disassembly is carried out, and the low permeability of the clay, it is not considered that any such modification might be significant.
- Inaccuracy in measuring the length of the sample placed in the cells, which might lead to the calculation of dry densities higher than those actually existing, and therefore to exaggerated degrees of saturation. In the case of the permeability tests, the swelling of the clay might cause stretching of the cell covers, allowing for a certain, undetected expansion of the sample. In the case of the oedometer tests, this might occur due to failure of the dial gauge, faulty calibration of the equipment or exceeding the load limit for which the equipment was designed. Although attempts have been made to prevent this –through verification of the dial gauges and application to the measurements of the correction factor for the calibration carried out under the same test conditions– it might contribute to some degree to the acquisition of inaccurate degrees of saturation, but never as large as those observed. For example, for the final degree of saturation in the swelling pressure tests to be 100 percent, fixing final water content, the dry density of the sample determined from the dial gauge reading would have to be reduced by an average 5.6 percent, reaching 10 percent for higher dry densities. Nevertheless, it has been seen that even when final dry density is calculated from the length of the sample when extracted from the cell on completion of the test –which will always be lower than the dry density of the sample in the oedometer, because of the elastic relaxation that occurs due to decompression when the equipment is unloaded for disassembly– degrees of saturation averaging 105 percent, and reaching 110 percent, are also obtained. Consequently, if the issue were to be resolved by correcting the dry densities until the degree of saturation adjusted to 100 percent, it would be necessary to reach values of density lower than those obtained experimentally, *i.e.* unacceptable values.

From what has been established above it may be concluded that, although various factors might lead to the acquisition of fictitious degrees of saturation somewhat higher than 100 percent, the high values obtained are not justified.

Furthermore, the calculation of degrees of saturation is accomplished by systematically attributing a value of 1.0 g/cm^3 to water density. Nevertheless,

various authors have pointed out that in the vicinity of clay laminae, the structure of water molecules is disturbed, their properties differing from those of free water (Sposito & Prost 1982). This modification of the properties of the adsorbed water becomes more noteworthy with low contents of water.

Specifically, for the density of water adsorbed in montmorillonite, Martin (1962) includes data from other authors obtained by means of pycnometers and X-ray diffraction, among which there are values of 1.32 g/cm^3 for 28 percent clay water content, 1.37 g/cm^3 for 17 percent water content and 1.41 g/cm^3 for 12 percent water content. In their studies, Pusch *et al*. (1990) find that the density of water in sodium montmorillonite at different densities has a maximum value of 1.05 g/cm^3, depending on the degree of ordering and the presence of molecules of interstitial water. The variation of water density with water content has also been checked for other materials, with values of 1.48 g/cm^3 having been measured in wheat flour (Multon *et al*. 1981).

Bearing this in mind, a calculation was made of the density that the water should have in order for the degree of saturation to adjust to 100 percent in each of the tests performed. Figure 63 shows the hypothetical values of water density versus the water content of the clay for the different types of tests included in this work. It may be observed that as the water content of the clay decreases, water density increases, up to values of close to 1.36 g/cm^3.

Although this increase may not in fact be so high, if it is taken into account that the degrees of saturation calculated might be exaggerated due to the factors indicated above, the values obtained are in the order of those reported by Martin (1962), as is shown in the same figure.

The dispersion observed in Figure 63 implies that samples of different density have reached saturation with the same water content. This may be due to various factors, among which the test temperature, its duration and experimental errors in determining the dry density and water content of the clay may be singled out. Furthermore, the pressure of the interstitial water may have an influence on the quantity of water that may enter the interlaminar space (Pusch *et al*. 1990), which might have a repercussion on final water content in the permeability tests, in which the water is injected at different pressures.

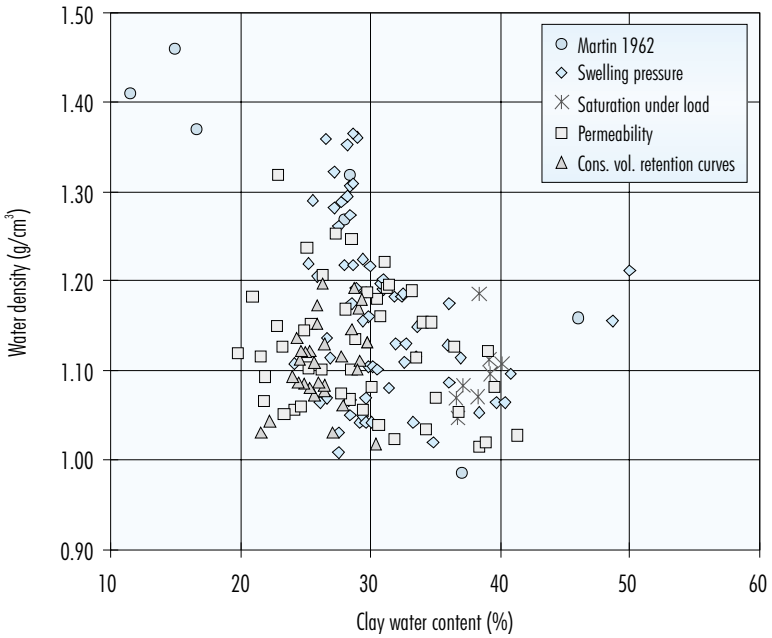

Figure 63. Water density calculated to maintain the degree of saturation of the clay at 100 percent for different types of tests and experimental values reported by Martin (1962).

In order to reduce the effect of this dispersion, all the data for samples saturated at constant volume have been grouped on the basis of dry density, in ranges of 0.05 g/cm^3, the average values of water content and density of the water adsorbed corresponding to each density range having been found. The data from 150 permeability, swelling pressure, saturation under load and constant volume retention curve tests were used, the sample having been saturated with distilled water at constant volume in all these tests. The average values obtained are shown in Table XIII and represented in Figure 64.

A determination was made of the coefficients of correlation between the average values of dry density of the clay, its water content and the water density calculated for the degree of saturation to adjust to 100 percent (Table XIII). This showed that the dry density of the sample has the greatest repercussion on water density (although logically the water content for saturation will be lower the higher the dry density), both being directly related. Consequently, the modification of water density might be determined not only by the water content of the clay but also by its porosity, since the reduction in pore size with increasing dry density might make the development of diffuse double layers more difficult. Obviously, this refers to the case in which the clay is saturated at constant volume, preventing the expansion that would otherwise occur.

What has been shown in this section is only an explanation on how degrees of saturation in excess of 100 percent can be obtained when these are calculated considering the density of the water to be that of the free water (1.00 g/cm^3). As has been seen, this is not correct, and in order to underline the fact, the symbol S_r^* is used from hereon to refer to the degree of saturation calculated in this way.

However, the experiments dealt with in this work were not aimed specifically at determining the density of the water adsorbed; this, added to the dispersion of the data and to the fact that only saturated samples are referred to, makes it impossible to give specific values for the variation of water density with the density and water content of the clay. For this reason, the degrees of saturation have been calculated, as is habitual practice on geotechnics, assuming the density of the water adsorbed to be the same as that of free water (S_r^*).

Table XIII
Values of density of ad sorbed water calculated for samples of clay of different dry density (ρ_d) saturated with distilled water at constant volume.

ρ_d (g/cm^3)	Water content (%)	Water density (g/cm^3)
1.28	44.3	1.094
1.34	39.7	1.053
1.37	39.1	1.085
1.42	36.0	1.093
1.47	33.6	1.088
1.52	31.0	1.087
1.58	29.7	1.128
1.62	28.0	1.141
1.67	26.1	1.152
1.71	26.1	1.225
1.76	23.7	1.201
1.83	21.2	1.207

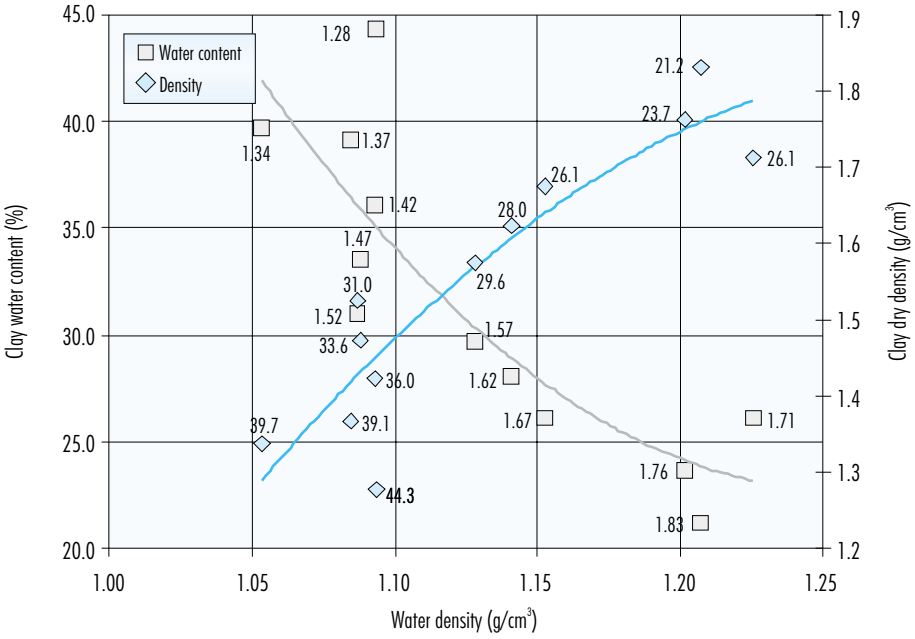

Figure 64. Values of density of water adsorbed calculated for samples of clay of different dry density saturated with distilled water at constant volume.

Hydraulic characterisation

Hydraulic conductivity

The determinations of hydraulic conductivity were carried out in accordance with the method described in the section "HYDRAULIC CONDUCTIVITY". During determination, the sample remains in a cylindrical stainless steel cell measuring 5.0 cm in diameter and 2.5 cm in length. Prior to measurement, the samples are saturated by injecting water at a pressure of 0.6 MPa at their upper and lower parts, this lasting between a week and a month depending on the density of the specimen. A hydraulic gradient is then applied by increasing the injection pressure at the lower part, and the volume of water passing through the specimen is measured versus time. The coefficient of permeability is calculated by applying Darcy's law.

The determination is performed for various hydraulic heads, which are always lower than the swelling pressure of the sample, without the use of one or another implying any significant variation in the coefficient of permeability obtained. This aspect is discussed in greater detail in the section "Influence of hydraulic head applied". All the tests were carried out at the temperature of the laboratory, between 20 and 25 °C.

Measurements were performed for a wide range of densities. Likewise, a check was made on the influence of the direction in which the measurement was made with respect to the direction of compaction of the sample. A study was also made of the repercussion of the type of water used as permeating fluid. Each of these aspects is dealt with separately in the following sections.

Variation depending on dry density

Hydraulic conductivity was determined using cylindrical specimens of different density uniaxially compacted inside the permeability cell from the clay with its hygroscopic water content. The range of dry densities studied was from 1.30 to 1.84 g/cm3. Distilled water was used as permeating fluid.

The average values obtained in the different determinations are shown in Table XIV, including dry density, initial and final water content and final de-

gree of saturation. The final degree of saturation for each test is calculated with consideration given to a water density equal to 1.00 g/cm^3, as is customary in geotechnics. For this reason values in excess of 100 percent appear, since the density of the water adsorbed in the smectite varies depending on the dry density and water content of the clay, as discussed in the section "DENSITY OF WATER".

These values of the permeability to water of the saturated sample (k_w) may be used to calculate the intrinsic permeability (k_{iw}) corresponding to each determination, by means of the following expression:

$$k_{iw} = \frac{k_w \times \mu}{\rho \times g}$$

where μ and ρ are the viscosity and density of the water and g is gravitational acceleration. For these parameters, values of 10^{-3} Pa·s, 10^3 kg/m^3 and 9.81 m/s^2 were taken respectively, since the determinations were performed at an average temperature of 20 °C. It has been seen that not including the variation of water density and viscosity with the water content and density of the clay in the calculation does not imply any important repercussion on the value of intrinsic permeability obtained, since the range of variation of these properties is small. The values of intrinsic permeability deduced are also shown in Table XIV.

Figure 65 shows all the values obtained versus dry density. There are significant variations in permeability depending on the dry density of the sample, the former decreasing clearly as the latter increases. The greater dispersion observed among the values corresponding to high densities is probably due to the difficulty involved in determination, since in view of the low permeability of bentonite, highly accentuated by the increase in density, water flows are very small and their measurement difficult, the hydraulic gradients needing to be increased to make the measurement possible with the available techniques.

The values of hydraulic conductivity (k_w, m/s) are exponentially related to dry density (ρ_d, g/cm^3) and a distinction may be made between two different fittings –also shown in the figure– depending on the density interval:

- for dry densities of less than 1.47 g/cm^3:

$$\log k_w = -6.00\ \rho_d - 4.09 \quad (r^2 = 0.97,\ 8\ points)$$

- for dry densities in excess of 1.47 g/cm^3:

$$\log k_w = -2.96\ \rho_d - 8.57 \quad (r^2 = 0.70,\ 26\ points)$$

For each test the theoretical value of permeability was calculated according to these fittings (k_{wt}), along with the percentage deviation of this theoretical value with respect to the experimental value (k_w in Table XIV): $((k_w-k_{wt})/k_{wt})x100$. The variation in the experimental values with respect to these fittings is smaller for low densities than it is for higher values, with an average –in absolute values– of 30 percent. This should be evaluated taking into account that the values of permeability are of the order 10^{-13} m/s. This percentage of deviation is indicated also in Figure 65.

This "threshold" value of around 1.47 g/cm^3 separates two intervals of density for which the hydraulic behaviour of the clay is somewhat different, since for densities below this value the increase in permeability that occurs with decreasing dry density is more evident.

The values of intrinsic permeability obtained from the hydraulic conductivity tests (k_{iw}, m^2) are represented versus porosity (n) in Figure 66. The correlation between the two variables develops exponentially for porosities of between 0.32 and 0.52, in accordance with the following equations:

$$\log k_{iw} = 7.99\ n - 23.55 \qquad for\ 0.32<n<0.46$$

$$\log k_{iw} = 16.21\ n - 27.29 \qquad for\ 0.46<n<0.52$$

and it is possible to distinguish a porosity threshold that marks a sharper increase in intrinsic permeability with increasing porosity. This threshold value coincides with the one underlined for hydraulic conductivity.

Pusch (1979) explains the extremely low permeability of the bentonite compacted at high density in terms of the low water contents required to saturate the highly compacted clay, since under these conditions, the thickness of the film of interlaminar water is very small (3-5 Å) due to its high specific surface, this meaning that the molecules of water are strongly adsorbed to the surfaces of the clay minerals, leaving only a very tortous interparticle channels for the transport of water. Besides, in the calcium montmorillonite compacted at dry densities in excess of 1.60 g/cm^3, more than 90 percent of the total volume of the pores is occupied by this interlaminar water of restricted mobility (Pusch *et al.* 1990).

Furthermore, the relation between hydraulic conductivity and porosity (or dry density) is exponential for a wide variety of geological materials. Wilkinson & Shipley (1972) adjust this type of equations to the

Table XIV
Results of hydraulic conductivity tests with distilled water.

ρ_d (g/cm^3)	e	Initial w (%)	Final w (%)	Final S_r^* (%)	k_w (m/s)	k_{iw} (m^2)
1.3	1.084	14.3	41.3	103	$1.1\cdot10^{-12}$	$1.2\cdot10^{-19}$
1.34	1.019	13.6	38.3	102	$7.6\cdot10^{-13}$	$7.7\cdot10^{-20}$
1.36	0.988	14.4	39.6	108	$7.2\cdot10^{-13}$	$7.3\cdot10^{-20}$
1.39	0.938	13.8	39.0	112	$3.5\cdot10^{-13}$	$3.6\cdot10^{-20}$
1.43	0.894	14.0	34.2	103	$2.2\cdot10^{-13}$	$2.3\cdot10^{-20}$
1.43	0.886	12.4	35.1	107	$2.2\cdot10^{-13}$	$2.2\cdot10^{-20}$
1.44	0.874	14.7	36.5	113	$2.0\cdot10^{-13}$	$2.0\cdot10^{-20}$
1.47	0.841	13.7	31.9	102	$1.0\cdot10^{-13}$	$1.0\cdot10^{-20}$
1.50	0.797	14.4	34.1	116	$1.1\cdot10^{-13}$	$1.1\cdot10^{-20}$
1.50	0.795	13.9	30.6	104	$8.2\cdot10^{-14}$	$8.3\cdot10^{-21}$
1.54	0.752	14.7	29.4	106	$4.1\cdot10^{-14}$	$4.2\cdot10^{-21}$
1.58	0.709	14.0	31.3	119	$8.3\cdot10^{-14}$	$8.5\cdot10^{-21}$
1.59	0.698	14.8	30.5	118	$3.1\cdot10^{-14}$	$3.2\cdot10^{-21}$
1.59	0.698	12.5	28.5	110	$6.4\cdot10^{-14}$	$6.5\cdot10^{-21}$
1.60	0.688	15.0	31.1	122	$5.9\cdot10^{-14}$	$6.0\cdot10^{-21}$
1.60	0.688	13.3	28.9	113	$6.0\cdot10^{-14}$	$6.1\cdot10^{-21}$
1.61	0.677	11.7	29.8	119	$5.9\cdot10^{-14}$	$6.0\cdot10^{-21}$
1.64	0.644	14.7	26.2	110	$2.8\cdot10^{-14}$	$2.8\cdot10^{-21}$
1.67	0.617	14.5	28.5	125	$3.7\cdot10^{-14}$	$3.8\cdot10^{-21}$
1.69	0.598	11.7	25.5	115	$3.2\cdot10^{-14}$	$3.3\cdot10^{-21}$
1.70	0.587	14.3	24.9	114	$2.2\cdot10^{-14}$	$2.2\cdot10^{-21}$
1.70	0.588	14.8	21.3	98	$3.8\cdot10^{-14}$	$3.9\cdot10^{-21}$
1.70	0.588	15.1	20.7	95	$2.9\cdot10^{-14}$	$3.0\cdot10^{-21}$
1.70	0.588	13.4	26.3	121	$3.8\cdot10^{-14}$	$3.9\cdot10^{-21}$
1.70	0.588	11.9	27.3	125	$4.1\cdot10^{-14}$	$4.2\cdot10^{-21}$
1.73	0.558	14.3	23.3	113	$1.8\cdot10^{-14}$	$1.8\cdot10^{-21}$
1.74	0.547	13.8	25.1	124	$3.0\cdot10^{-14}$	$3.0\cdot10^{-21}$
1.75	0.540	15.5	21.9	109	$5.8\cdot10^{-15}$	$5.9\cdot10^{-22}$
1.76	0.536	15.2	22.8	115	$1.2\cdot10^{-14}$	$1.2\cdot10^{-21}$
1.77	0.524	15.8	21.6	112	$9.6\cdot10^{-15}$	$9.8\cdot10^{-22}$
1.83	0.477	13.0	20.9	118	$1.1\cdot10^{-14}$	$1.1\cdot10^{-21}$
1.83	0.478	14.4	19.8	112	$4.2\cdot10^{-15}$	$4.3\cdot10^{-22}$
1.84	0.470	14.2	23.0	132	$2.6\cdot10^{-14}$	$2.6\cdot10^{-21}$

**Degree of saturation calculated considering the density of free water.*

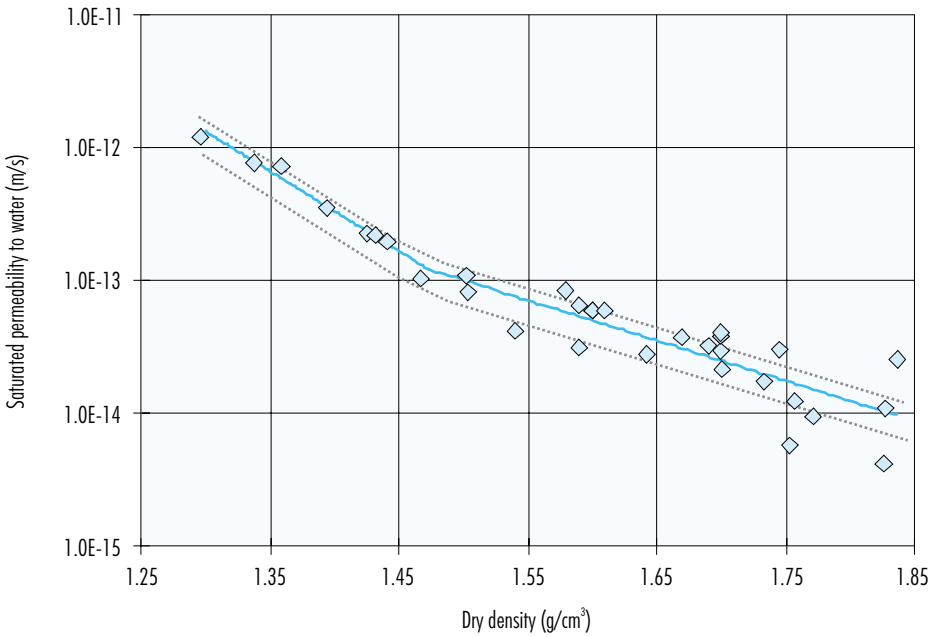

Figure 65. Permeability to distilled water versus dry density of the clay and fittings obtained, along with the average range of deviation of experimental values with respect to theoretical values.

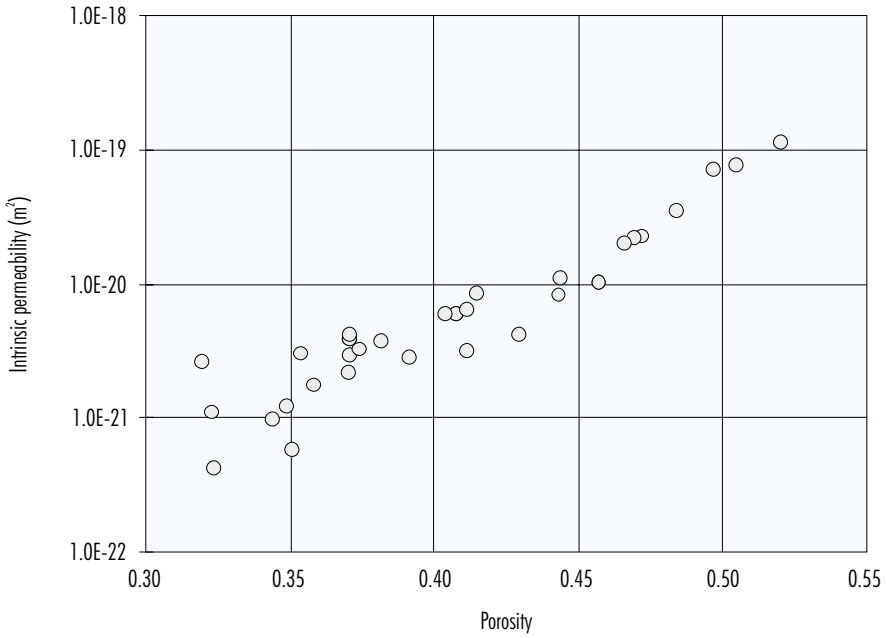

Figure 66. Variation in intrinsic permeability with porosity from saturated hydraulic conductivity tests.

results obtained from the testing of silty, laminate and organic clays and kaolins. Geneste *et al*. (1990) find a relation between dry density and hydraulic conductivity for the French calcium smectite known as "FoCa" similar to those included herein. Consequently, the relation established in this work between hydraulic conductivity and density follows the patterns indicated by several other authors, and is closer to that reported by Pusch (1979) for the case of sodium bentonite, where a distinction is made between two intervals of density for which the increase in hydraulic conductivity with decreasing density is different. Villar & Rivas (1994) find this threshold for the S-2 bentonite (from the same deposit than the FEBEX clay) and interpret it as being caused by the sharp decrease in swelling pressure for densities below this value, this leading to a more significant increase in the size of the flow paths. Given that intrinsic permeability, and consequently hydraulic conductivity, is related to pore diameter by the Poiseuille equation, the increase in the average diameter of the pores due to lower swelling, from a given density threshold value down, leads to a sharper increase in permeability. The noteworthy decrease in the swelling pressure of the FEBEX bentonite for dry densities of less than 1.47 g/cm^3 is clearly reflected in Figure 99.

Studds *et al*. (1998) find that the permeability to distilled water of the Wyoming bentonite compacted to much lower densities than those tested in this work (between 1.35 and 0.25 g/cm^3) is potentially related to the void ratio, which would confirm the sharp increase in permeability below a certain density threshold.

Variation depending on water type

It is an accepted fact that the type of water used as a permeating agent, and especially its salinity, may have an impact on the coefficient of permeability of a soil (Klute 1965, Olsen 1962). With a view to verifying this issue, the saturated permeability of specimens of different density compacted with the hygroscopic water content of clay was determined, using granitic or saline water as permeating agent instead of distilled water.

The results obtained are shown in Table XV for granitic water and in Table XVI for saline water, in both cases with the value of permeability that would correspond to the dry density of each sample according to the fittings obtained for distilled water presented in the previous section. The "Deviation" column indicates the percentage of deviation with respect to the value expected for distilled water, such that negative deviations imply that the permeability obtained is lower than the theoretical value, and *vice versa*.

Figure 67 shows the values for granitic and saline water along with the fittings obtained for distilled

Table XV
Results of hydraulic conductivity tests performed with granitic water.

ρ_d (g/cm^3)	Initial w (%)	Final w (%)	Final S_r^* (%)	k_w (m/s)	k_w distilled (m/s)	Deviation %
1.36	13.9	39.0	107	$5.6 \cdot 10^{-13}$	$5.5 \cdot 10^{-12}$	2
1.38	15.8	37.7	106	$6.1 \cdot 10^{-13}$	$4.3 \cdot 10^{-13}$	41
1.41	13.8	36.8	109	$2.1 \cdot 10^{-13}$	$2.7 \cdot 10^{-13}$	-20
1.48	15.3	32.6	107	$1.2 \cdot 10^{-13}$	$1.1 \cdot 10^{-13}$	9
1.52	16.0	31.0	107	$5.9 \cdot 10^{-14}$	$8.7 \cdot 10^{-14}$	-32
1.60	13.7	26.6	104	$2.3 \cdot 10^{-14}$	$5.1 \cdot 10^{-14}$	-55
1.65	14.3	30.2	127	$6.4 \cdot 10^{-14}$	$3.6 \cdot 10^{-14}$	78
1.69	14.8	24.3	111	$1.4 \cdot 10^{-14}$	$2.6 \cdot 10^{-14}$	-47
1.74	13.8	23.6	116	$1.5 \cdot 10^{-14}$	$1.9 \cdot 10^{-14}$	-18
1.80	15.3	21.2	114	$8.0 \cdot 10^{-15}$	$1.3 \cdot 10^{-14}$	-39

**Degree of saturation calculated considering the density of free water.*

Table XVI
Results of hydraulic conductivity tests performed with saline water.

ρ_d (g/cm^3)	Initial w (%)	Final w (%)	Final S_r^*	k_w (m/s)	k_w distilled (m/s)	Deviation (%)
1.31	15.7	39.4	101	$3.6 \cdot 10^{-12}$	$1.1 \cdot 10^{-12}$	233
1.33	15.0	41.2	108	$9.7 \cdot 10^{-12}$	$8.4 \cdot 10^{-13}$	1062
1.39	12.9	35.0	100	$1.5 \cdot 10^{-12}$	$3.9 \cdot 10^{-13}$	280
1.39	14.8	36.4	104	$3.5 \cdot 10^{-13}$	$3.7 \cdot 10^{-13}$	-5
1.45	13.5	33.3	104	$7.8 \cdot 10^{-13}$	$1.7 \cdot 10^{-13}$	370
1.50	14.7	31.6	106	$1.7 \cdot 10^{-13}$	$1.0 \cdot 10^{-13}$	67
1.58	13.2	28.2	107	$1.1 \cdot 10^{-13}$	$5.8 \cdot 10^{-14}$	91
1.59	14.0	28.5	111	$1.8 \cdot 10^{-14}$	$5.1 \cdot 10^{-14}$	-64
1.62	13.7	27.1	110	$4.7 \cdot 10^{-14}$	$4.3 \cdot 10^{-14}$	9
1.65	13.6	26.3	112	$3.1 \cdot 10^{-14}$	$3.4 \cdot 10^{-14}$	-10
1.66	14.4	26.8	115	$8.4 \cdot 10^{-14}$	$3.2 \cdot 10^{-14}$	160
1.68	14.2	25.7	115	$1.8 \cdot 10^{-14}$	$2.8 \cdot 10^{-14}$	-36
1.72	13.3	24.1	115	$5.4 \cdot 10^{-14}$	$2.1 \cdot 10^{-14}$	154
1.74	14.1	23.9	116	$7.1 \cdot 10^{-14}$	$1.9 \cdot 10^{-14}$	270

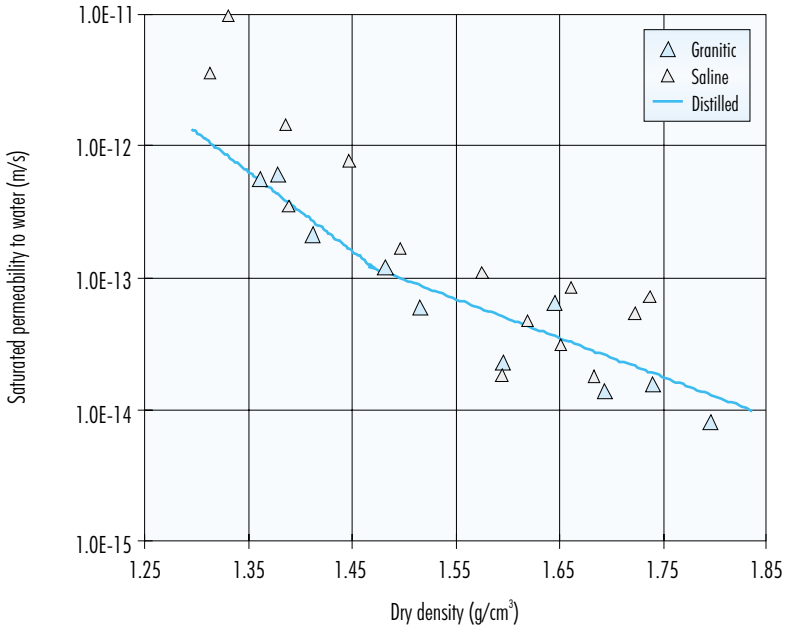

Figure 67. Hydraulic conductivity for granitic or saline water versus the dry density of the clay and fitting obtained for distilled water.

water and included in the previous section. No clear trend is observed concerning the variation of the values obtained with granitic water with respect to those obtained with distilled water. The values obtained with saline water are, however, 184 percent higher on average than those expected for a sample of the same density tested with distilled water, and in addition, they show greater dispersion. This higher permeability to saline water with respect to that expected for distilled water is more significant for low densities.

The increase in permeability with the salinity of the permeating fluid has been underlined by various authors. In particular, it has been seen that the permeability of clays and clayey sandstones increases with the concentration of NaCl in the water (Jiménez & Justo 1972). Rolfe & Aylmore (1977) attribute the changes in permeability observed in their tests with montmorillonite and illite to changes in ion distribution associated with variations in the cation exchange complex and to the concentration of the electrolyte used as a permeating agent. There are various mechanisms that contribute to these changes, among them the following:

1) alterations in pore dimension distribution as a result of variations in swelling pressure in the clay matrix,
2) variations in the mobility of the molecules of water associated with the exchangeable cations adsorbed on the surfaces or forming diffuse double layers (DDL),
3) alterations in the viscous behaviour of the structure of the water.

As a result of these mechanisms, as the concentration of the electrolyte increases there is a reduction in the swelling pressure of the clay particles, the size of the flow channels increasing to the detriment of the number of small channels, this causing flow –and therefore, permeability– to increase enormously. On the contrary, the increasing development of diffuse double layers on reduction of the concentration of the electrolyte causes a decrease in permeability. In expansive materials, it is the intrinsic permeability of the material itself that is altered by interactions between the fluid and the solid, and the largest variations in permeability with the composition of the fluid are found in soils with a high content of montmorillonite (McNeal & Coleman 1966). In their studies with sodium montmorillonite, Studds *et al*. (1998) observe a clear increase in hydraulic conductivity as the saline concentration of the permeating agent increases, which they attribute to the modifications induced by the latter in the effective porosity of the clay. The reduction of effective porosity with the decreasing salinity of the permeating agent would be due to the fact that the pore space is occupied by the bound water (DDL), the viscosity of which is higher than that of free water. According to the diffuse double layer theories, the thickness of it decreases as the concentration of water in the pores increases, as a result of which, for a given porosity, the effective porosity of the clay would increase with increasing concentration of the solution, with the corresponding increase in permeability.

Variation depending on the direction of measurement

The determination of hydraulic conductivity, as described in the previous sections, is always performed using specimens compacted directly in the ring of the cell and with flow running parallel to the compaction force. In order to check the influence of the direction of measurement on the value of the coefficient of permeability, in other words, the anisotropy of this property in the compacted sample, various determinations were performed using specimens obtained by trimming from larger blocks. Specifically, the blocks manufactured for the FEBEX Project mock-up test were used (Figure 68). The trimming was carried out using a cylindrical cutter of appropriate dimensions in two different directions: parallel to the block compaction force, *i.e*. vertically as the block is placed in its manufacturing position, and perpendicular to this force, *i.e*. in the horizontal direction. The specimen obtained is placed in the ring of the permeability cell and is saturated with distilled water, the conventional method then being used to determine permeability. Given that the fit between the trimmed specimen and the walls of the cell is not perfect, some swelling occurs during saturation, and therefore a certain reduction in density.

Table XVII and Table XVIII show the results obtained depending on the direction of determination, along with the theoretical value that would have been obtained for a specimen of the same density compacted directly in the cell ring, with flow in the parallel direction ("Theoretical k_w" column, deduced from the fittings dealt with in previous sections). The percentage of deviation of a value with respect to another is shown in the "Deviation" column, in which negative values indicate that the hydraulic conductivity obtained is lower than the theoretical

Figure 68. Appearance of a block placed in the manufacturing position prior to trimming.

Table XVII
Values of hydraulic conductivity obtained from samples trimmed in a direction perpendicular to the compaction force.

ρ_d (g/cm^3)	Initial w (%)	Final w (%)	Final S_r^* (%)	k_w (m/s)	Theoretical k_w (m/s)	Deviation (%)
1.39	14.3	36.8	105	$2.3 \cdot 10^{-13}$	$3.7 \cdot 10^{-13}$	-38
1.54	15.9	33.2	119	$6.0 \cdot 10^{-14}$	$7.4 \cdot 10^{-14}$	-19
1.58		30.7	116	$6.4 \cdot 10^{-14}$	$5.8 \cdot 10^{-14}$	10
1.58	14.9	31.4	120	$5.8 \cdot 10^{-14}$	$5.6 \cdot 10^{-14}$	3
1.59	13.5	27.8	108	$3.9 \cdot 10^{-14}$	$5.3 \cdot 10^{-14}$	-26
1.64	15.3	28.1	117	$5.0 \cdot 10^{-14}$	$3.8 \cdot 10^{-14}$	30
1.66	13.9	24.7	106	$2.7 \cdot 10^{-14}$	$3.3 \cdot 10^{-14}$	-19
1.69	16.3	23.4	105	$9.2 \cdot 10^{-15}$	$2.7 \cdot 10^{-14}$	-66

**Degree of saturation calculated considering the density of free water.*

value, and *vice versa*. The dry density indicated corresponds to that of the sample once saturated when, due to swelling, its dimensions correspond to the volume of the cell.

Figure 69 shows the values obtained from trimmed specimens for two different directions, along with the fitting obtained for specimens compacted in the ring of the cell shown in the section "Variation de-

Table XVIII
Values of hydraulic conductivity obtained from samples trimmed in a direction parallel to the compaction force.

ρ_d (g/cm³)	Initial w (%)	Final w (%)	Final S_r^* (%)	k_w (m/s)	Theoretical k_w (m/s)	Deviation %
1.33	15.2	38.9	102	$5.9 \cdot 10^{-13}$	$8.4 \cdot 10^{-13}$	-30
1.49	14.7	33.5	111	$1.3 \cdot 10^{-13}$	$1.0 \cdot 10^{-13}$	25
1.49	14.2	34.7	115	$1.3 \cdot 10^{-13}$	$1.0 \cdot 10^{-13}$	28
1.54		30.1	108	$6.4 \cdot 10^{-14}$	$7.3 \cdot 10^{-14}$	-12
1.57	16.2	28.4	107	$4.3 \cdot 10^{-14}$	$6.0 \cdot 10^{-14}$	-27
1.67	17.3	25.2	110	$1.8 \cdot 10^{-14}$	$3.1 \cdot 10^{-14}$	-41
1.67	13.7	24.1	106	$1.5 \cdot 10^{-14}$	$3.0 \cdot 10^{-14}$	-52
1.74	12.4	21.8	107	$1.2 \cdot 10^{-14}$	$1.9 \cdot 10^{-14}$	-37

* *Degree of saturation calculated considering the density of free water.*

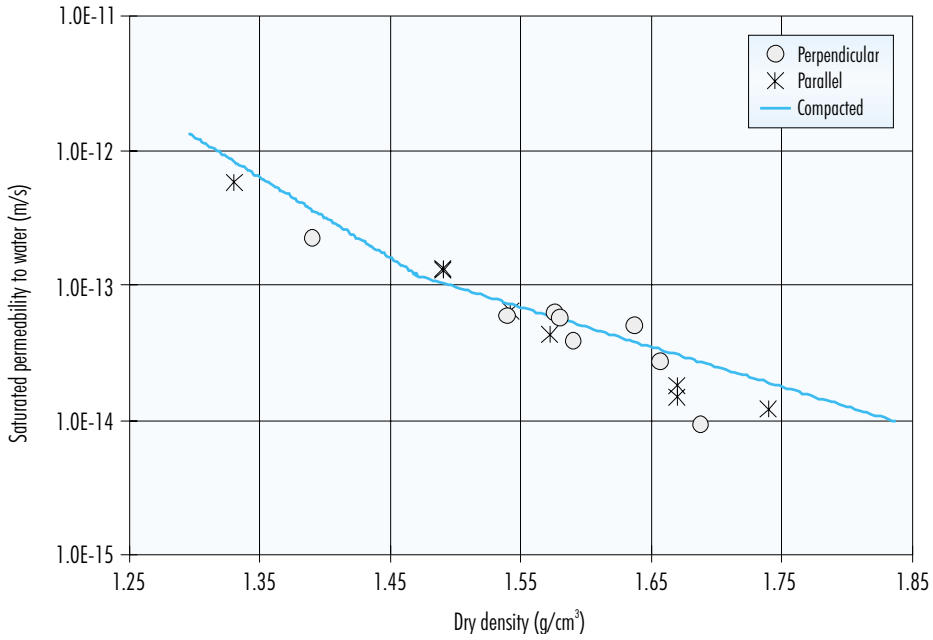

Figure 69. Hydraulic conductivity obtained from trimmed specimens with flow perpendicular and parallel to the compaction force (the fitting obtained for compacted samples with flow parallel to the compaction force is also included).

pending on dry density". The values obtained from trimmed samples are, overall, somewhat lower than the theoretical values for compacted specimens, but no difference has been found between the hydraulic behaviour of the specimens trimmed in one direction or another, since the percentage of deviation is 18 percent in the case of specimens trimmed in the direction parallel to the compaction force and 16

percent for the perpendicular. However, in undisturbed clayey soils, horizontal permeability is in principle expected to be higher than vertical permeability, since such soils are constituted by laminar or acicular particles subjected to anisotropic load. In the case of the material studied in this work, this difference has not been observed, due probably to the effect of remoulding and compaction, which was performed very rapidly with the clay in the dry state, as a result of which the particles did not reorganise. Pousada (1984) reports on the contributions made by various authors, underlining the fact that static compaction –of the type performed in this work– produces a flocculated structure analogous to that of compacted soils in the dry side of the Proctor curve. Furthermore, the anisotropy of permeability decreases with the presence of montmorillonite in the soil (Jiménez & Justo 1971), due to the irregular shape of the crystals of smectite, which prevents orientation. Another factor that might have an influence on the lack of orientation of the particles, is the rather non-uniform granulometric distribution (Tsige 1998), since bentonite contains 22 percent of silt-size particles.

Furthermore, the reduction in the permeability of trimmed specimens with respect to the value expected in compacted samples might be due to the fact that the dry density considered for the trimmed specimens is that resulting from assuming a volume of sample equal to the internal capacity of the cell. However, this density is probably not homogeneous, and although it might be very low at the edges, where the clay has expanded to backfill the initial gap, the central part of the sample has a higher density. It is the latter that has most influence on the volume of water passing through the sample with time, and consequently on the value of permeability determined, which for this reason will be lower than expected.

Influence of hydraulic head applied

The application of Darcy's law for the calculation of the coefficient of permeability requires that the velocity of the flow be proportional to the hydraulic gradient, that is to say, that the value of the coefficient obtained be independent of the hydraulic gradient applied during determination. This means that the relation between flow and hydraulic gradient is linear, and that this linear relation passes through the origin. For different reasons, this condition may not be fulfilled, thus invalidating the use of the Darcy's expression. These deviations have been attributed to causes as diverse as the existence of experimental artefacts, the development of a modified water structure in the vicinity of the clay surfaces, the reorganisation of particles during the flow process and, in certain reactive systems, electrokinetic phenomena associated with ion distribution in the porous medium (Rolfe & Aylmore 1977).

The measurements performed by Wilkinson & Shipley (1972) in various clay soils point to the validity of Darcy's law, except in specific cases that might be explained in terms of the use of fluids not in chemical equilibrium with the clay, which under conditions of low effective stress might cause the particles to migrate, with the corresponding plugging of the flow channels.

Pusch (1994) considers hydraulic conductivity to be independent of the hydraulic gradient applied to measure it, but recognises that, in bentonites, the high gradients that need to be applied for performance of the measurement may lead to compression of the material.

For this reason, in all the tests performed in this work the injection pressure has been kept below the swelling pressure expected for the dry density of the sample (see section "Swelling pressure"). Specifically, the values of hydraulic head applied in the tests are between 7000 cm, for dry densities of 1.30 g/cm^3, and 66000 cm, for dry densities of 1.84 g/cm^3. Taking into account that the length of the specimen is 2.5 cm, the average hydraulic gradient was 15200 m/m. All the samples were tested with at least two different hydraulic gradients suitable for their dry density, in other words, sufficiently high so as to provide a measurable flow but below swelling pressure, in order not to cause compression of the material (Pusch 1994).

The values of hydraulic conductivity obtained for the two hydraulic gradients applied in each test (from those shown in the tables in previous sections) are represented in Figure 70. The points joined by lines correspond to the same test; *i.e.* to the measurements performed on a specific sample of a given dry density. It may be observed that, although there may be a certain difference between the value of conductivity obtained with the different gradients for the same sample, such variations are probably the result of the experimental method, since there is no trend for one variable with respect to the other. This would confirm the independence of the flow observed from the hydraulic gradient applied, and therefore the validity of Darcy's law for calculation of the coefficient of permeability.

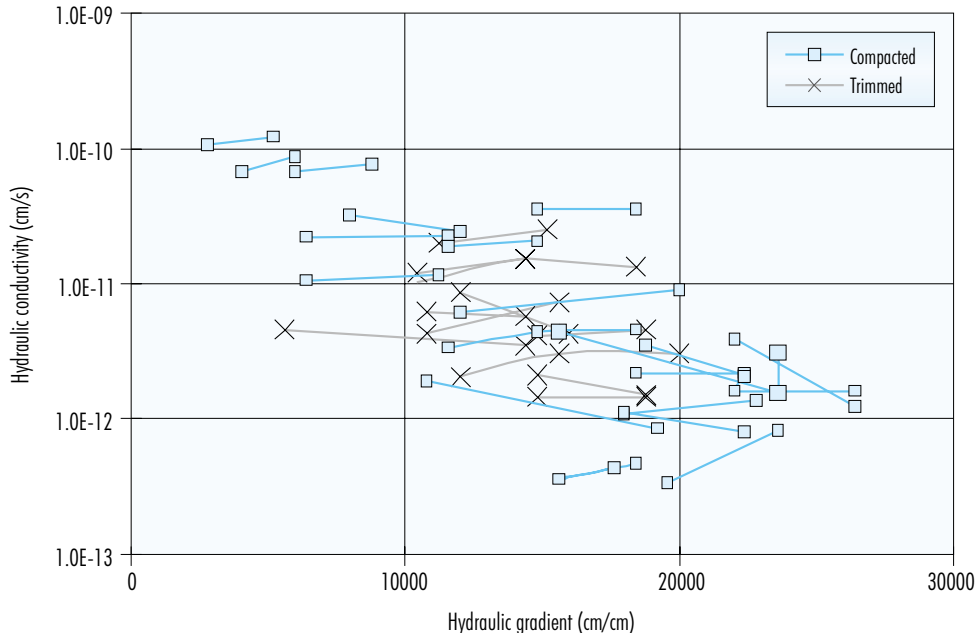

Figure 70. Variation in hydraulic conductivity obtained for different samples versus the hydraulic gradient as a function of the kind of sample preparation (points joined by lines correspond to the same sample).

It may also be appreciated in the figure that, as the permeability of the sample decreases, in other words, as its dry density increases, the value of the hydraulic gradients applied for performance of the measurement increases, this being necessary in order to be able to measure very low flows. However, it is not possible to determine whether no flow occurs in the case of lower hydraulic gradients or whether it is simply not possible to measure it with the available technique. Consequently, it has not been established whether or not the threshold hydraulic gradient pointed to by several authors exists, below which the relation between flow and gradient in clays deviates from linearity (Olsen 1962). For sodium or lithium montmorillonite soils, no flow apparently exists below this threshold, possibly due to the non-Newtonian behaviour of the water in the small pores in such soils, since this water is adsorbed and quasi-solid and may require high shearing stresses in order to move (Jiménez & Justo 1971). In any case, the importance of this adsorbed water decreases as the water content of the soil increases, as a result of which the threshold would be lower for samples of lower dry density, the saturation of which is reached at higher water contents. This would appear to be confirmed by the fact that lower hydraulic gradients need to be applied in samples with lower dry densities, although as has been explained above, this might be due simply to the fact that for these densities flows are larger and easier to measure. Yong *et al*. (1986) find this threshold in their tests performed with mixtures of expansive clay and crushed granite, and explain it in terms of the existence of active surfaces that, in the presence of water, would cause interaction between particles, with which the flow would be restricted for hydraulic gradients below the apparent threshold. For larger hydraulic gradients, they observe a linear relation between flow and hydraulic gradient.

Permeability to gas

Permeability to gas tests have been carried out on the FEBEX clay at different water contents and compacted to various nominal dry densities. The procedure used, which has been described in the methodology section "PERMEABILITY TO GAS", consists basically in letting the gas contained in a tank of known volume pass through a clay specimen while

measuring the pressure decrease in the tank versus time, calculating the intrinsic permeability of the sample from the data obtained, the dimensions of the specimen and the characteristics of the fluid. Nitrogen was used as the gas in these tests.

To work with water contents higher than hygroscopic, the clay is mixed with an appropriate quantity of water and is left to stabilise for a time before manufacturing the specimen. For water contents lower than that of the clay in equilibrium with laboratory conditions, the clay was slightly dried in the oven before compaction of the specimen was performed. This procedure does not allow to test the clay with degrees of saturation of less than 30 percent, since below this value, the specimens have no cohesion and crumble. For this reason, certain tests were performed with specimens made from the clay with its hygroscopic water content and subsequently dried in the oven at 110 °C, prior to the permeability measurement. When the sample is dried in the oven it shrinks, and the dry density of the specimen increases with respect to the nominal density at which it was compacted.

The results obtained are shown in Table XIX to Table XXII, which in addition to the dry density (ρ_d), water content (w) and degree of saturation (S_r) of the specimens, include the values of permeability to gas (k_g) and the result of multiplying intrinsic permeability by relative permeability ($k_{ig}{\cdot}k_{rg}$), obtained as described in the methodology section "PERMEABILITY TO GAS".

For each density there is a water content above which it will not be possible to measure air flow, and from which, in fact, the latter may not even occur, due to the degree of saturation increasing to such a point that the air in the specimen is occluded. This value of water content is higher as the dry density is lower. For a dry density of 1.70 g/cm^3 it is not possible to perform measurements with water contents higher than 14 percent, which corresponds to a degree of saturation of 60 percent. Likewise, for each water content there is a value of dry density above which it is not possible to measure air flow, if it ever exists. For the hygroscopic water content of the clay, the maximum dry density at which the measurement could be performed was 1.90 g/cm^3, corresponding to a degree of saturation of 80 percent. When interpreting these values it should be remembered that the gas injection pressure is just 0.1 MPa.

Figure 71 shows the evolution of pressure in some of the tests performed with clay compacted at a nominal dry density of 1.70 g/cm^3 with different water contents. It may be observed that the air flow is slower in samples with higher degrees of saturation (greater water content), this translating into a lower value of permeability.

Likewise, Figure 72 shows the evolution of pressure in some tests performed using clay with its hygroscopic water content and compacted at different densities. This figure shows that the time required for a pressure reduction to be noticeable in the tank increases with dry density, and how the subsequent pressure decrease is also slower.

When representing the values of permeability to gas obtained for a given clay water content versus dry density, it may be observed that permeability decreases exponentially as density increases, as it is shown in Figure 73. The relation between the permeability obtained with gas flow (k_g, m/s) and the dry density (ρ_d, g/cm^3) for a given value of water content (w, %) may be adjusted to the following expressions, which should not be extrapolated beyond the degrees of saturation tested:

Table XIX
Values of permeability obtained with gas flow for clay compacted at a nominal dry density of 1.50 g/cm^3.

ρ_d (g/cm^3)	w (%)	S_r (%)	k_g (m/s)	$k_{ig}{\cdot}k_{rg}$ (m^2)
1.53	11.2	40	$6.3{\cdot}10^{-8}$	$1.0{\cdot}10^{-13}$
1.50	13.9	47	$9.5{\cdot}10^{-8}$	$1.5{\cdot}10^{-13}$
1.50	15.0	51	$1.0{\cdot}10^{-7}$	$1.7{\cdot}10^{-13}$
1.49	15.9	53	$1.6{\cdot}10^{-7}$	$2.6{\cdot}10^{-13}$
1.54	23.9	86	$3.1{\cdot}10^{-10}$	$5.1{\cdot}10^{-16}$

Table XX
Values of permeability obtained with gas flow for clay compacted at a nominal dry density of 1.60 g/cm^3.

ρ_d (g/cm^3)	w (%)	S_r (%)	k_g (m/s)	$k_{ig} \cdot k_{rg}$ (m^2)
1.57	7.3	27	$2.8 \cdot 10^{-7}$	$4.6 \cdot 10^{-13}$
1.55	11.3	41	$4.9 \cdot 10^{-8}$	$8.0 \cdot 10^{-14}$
1.56	11.6	43	$4.3 \cdot 10^{-9}$	$7.0 \cdot 10^{-15}$
1.60	11.9	47	$7.2 \cdot 10^{-8}$	$1.2 \cdot 10^{-13}$
1.61	12.1	48	$5.6 \cdot 10^{-8}$	$9.2 \cdot 10^{-14}$
1.60	12.4	49	$9.6 \cdot 10^{-8}$	$1.6 \cdot 10^{-13}$
1.58	13.6	52	$1.5 \cdot 10^{-7}$	$2.4 \cdot 10^{-13}$
1.58	14.2	54	$6.5 \cdot 10^{-8}$	$1.1 \cdot 10^{-13}$
1.61	14.3	57	$7.3 \cdot 10^{-8}$	$1.2 \cdot 10^{-13}$
1.59	14.7	57	$1.6 \cdot 10^{-8}$	$2.6 \cdot 10^{-14}$
1.63	16.1	66	$1.4 \cdot 10^{-9}$	$2.3 \cdot 10^{-15}$
1.60	16.2	64	$1.7 \cdot 10^{-8}$	$2.8 \cdot 10^{-14}$
1.60	18.2	71	$8.8 \cdot 10^{-10}$	$1.4 \cdot 10^{-15}$
1.61	18.4	73	$5.5 \cdot 10^{-9}$	$8.9 \cdot 10^{-15}$
1.63	22.4	92	$2.9 \cdot 10^{-12}$	$4.7 \cdot 10^{-18}$

- For w = 6.7 %
  $\log k_g = 8.00 - 9.19\,\rho_d$ $(r^2=0.94)$
- For w = 13.6 %
  $\log k_g = 5.47 - 8.02\,\rho_d$ $(r^2=0.90)$
- For w = 15.6 %
  $\log k_g = 11.29 - 12.12\,\rho_d$ $(r^2=0.88)$

Figure 74 shows the permeability to gas versus the volume of accessible pores, that is to say those pores that are available for the passage of gas, represented as the product of void ratio times the unit minus the degree of saturation.

This factor is in fact the one that shows the highest correlation with the values of permeability obtained, greater than the dry density or the water content considered separately. The following potential relation between permeability to gas (k_g, m/s), degree of saturation (S_r) and void ratio (e) may be deduced from this figure:

$k_g = 2.29 \cdot 10^{-6} (e\,(1-S_r))^{4.17}$ $(r^2=0.77,\ 41\ points)$

Figure 75 shows all the values of intrinsic permeability times relative permeability, obtained with gas flow versus the degree of saturation for each dry density. Also included are the values of intrinsic permeability obtained from the measurement of hydraulic conductivity (fittings included in the section "Hydraulic conductivity"), which consequently correspond to the saturated sample (relative permeability to water equal to 1).

It may be observed that the intrinsic permeability for a given degree of saturation depends on the dry density of the sample. It is also clear that the reduction in permeability to gas for degrees of saturation in excess of a given threshold value (between 65 and 80 percent, depending on dry density) is particularly sharp, this marking the discontinuity of the gaseous phase.

Table XXI
Values of permeability obtained with gas flow for clay compacted at a nominal dry density of 1.70 g/cm^3.

ρ_d (g/cm^3)	w (%)	S_r (%)	k_g (m/s)	$k_{ig} \cdot k_{rg}$ (m^2)
1.75*	5.0	25	$5.9 \cdot 10^{-9}$	$9.5 \cdot 10^{-15}$
1.68	6.1	27	$5.3 \cdot 10^{-8}$	$8.5 \cdot 10^{-14}$
1.66	6.4	28	$8.3 \cdot 10^{-8}$	$1.4 \cdot 10^{-13}$
1.67	7.2	32	$3.9 \cdot 10^{-8}$	$6.3 \cdot 10^{-14}$
1.70	8.4	39	$2.4 \cdot 10^{-8}$	$3.8 \cdot 10^{-14}$
1.70	10.2	47	$1.5 \cdot 10^{-8}$	$2.4 \cdot 10^{-14}$
1.70	10.7	49	$1.7 \cdot 10^{-9}$	$2.8 \cdot 10^{-15}$
1.68	11.0	49	$1.0 \cdot 10^{-8}$	$1.6 \cdot 10^{-14}$
1.67	12.0	53	$1.8 \cdot 10^{-8}$	$2.9 \cdot 10^{-14}$
1.69	12.0	54	$1.5 \cdot 10^{-8}$	$2.5 \cdot 10^{-14}$
1.68	12.4	55	$7.1 \cdot 10^{-9}$	$1.1 \cdot 10^{-14}$
1.70	12.4	57	$1.9 \cdot 10^{-8}$	$3.1 \cdot 10^{-14}$
1.69	12.8	58	$1.6 \cdot 10^{-8}$	$2.6 \cdot 10^{-14}$
1.70	13.8	63	$2.2 \cdot 10^{-9}$	$3.5 \cdot 10^{-15}$
1.70	14.0	61	$5.3 \cdot 10^{-9}$	$8.7 \cdot 10^{-15}$
1.70	14.0	64	$1.0 \cdot 10^{-8}$	$1.7 \cdot 10^{-14}$
1.64	14.4	60	$4.4 \cdot 10^{-10}$	$7.2 \cdot 10^{-16}$

**Compacted at a dry density of 1.70 g/cm^3 and dried in oven.*

Table XXII
Values of permeability obtained with gas flow for clay compacted at a nominal dry density of 1.80 and 1.90 g/cm^3.

ρ_d (g/cm^3)	w (%)	S_r (%)	k_g (m/s)	$k_{ig} \cdot k_{rg}$ (m^2)
1.81*	1.3	7	$2.8 \cdot 10^{-8}$	$4.5 \cdot 10^{-14}$
1.80	12.7	69	$1.8 \cdot 10^{-9}$	$2.8 \cdot 10^{-15}$
1.80	12.4	67	$1.3 \cdot 10^{-9}$	$2.2 \cdot 10^{-15}$
1.86*	0.9	5	$1.4 \cdot 10^{-8}$	$2.3 \cdot 10^{-14}$
1.90	12.4	80	$1.1 \cdot 10^{-10}$	$1.8 \cdot 10^{-16}$

**Compacted at a dry density of 1.70 g/cm^3 and dried in oven.*

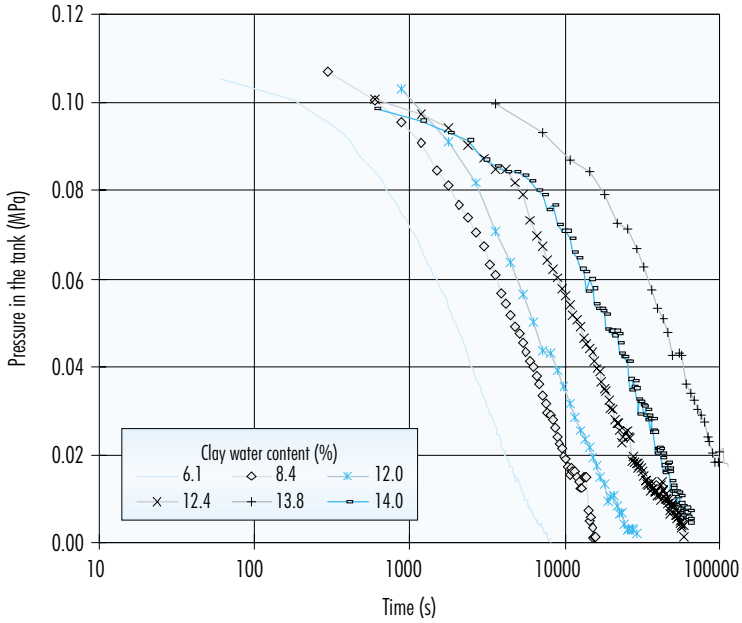

Figure 71. Evolution of gas pressure in the test performed with clay compac ted at a dry density of 1.70 g/cm³ with different water contents.

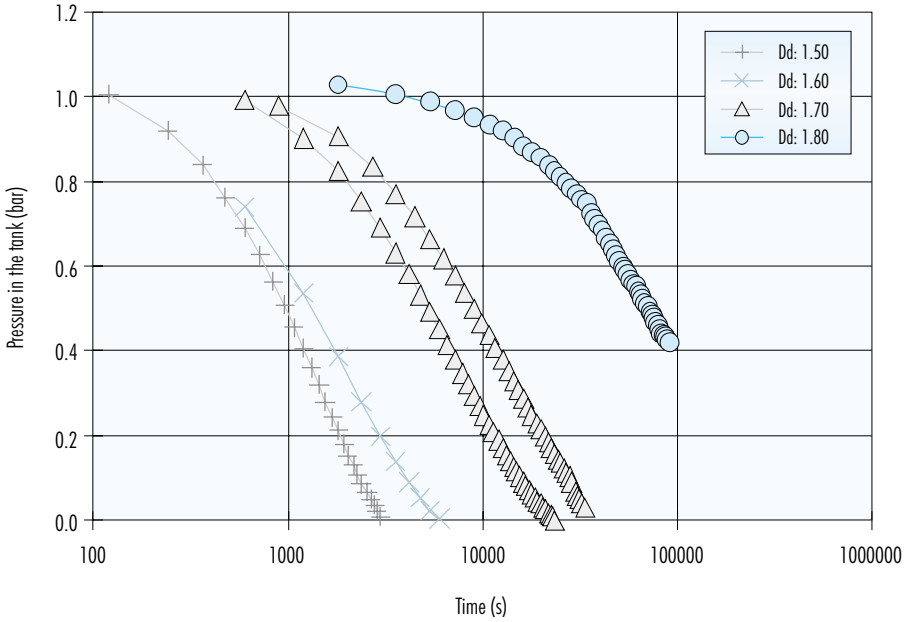

Figure 72. Evolution of gas pressure in tests performed using clay with hygroscopic water content compacted at different dry densities (Dd, g/cm³).

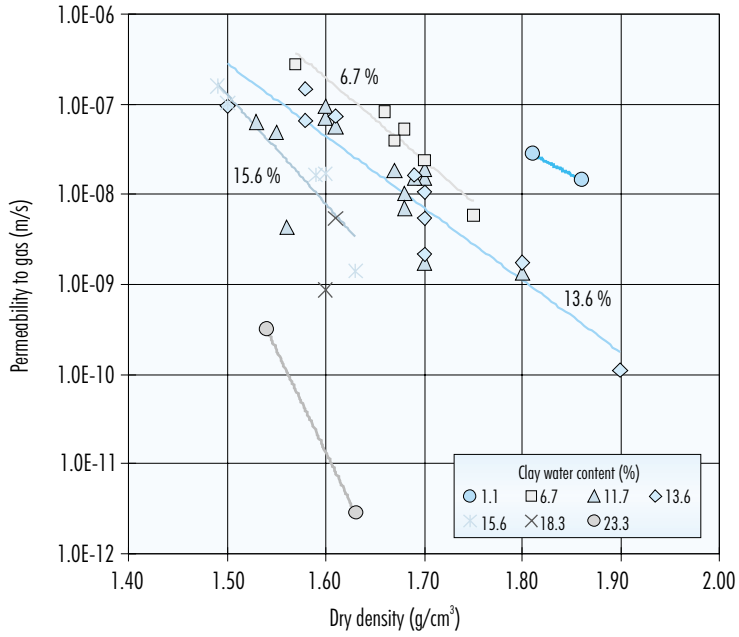

Figure 73. Permeability to gas versus clay density for samples compacted at different water contents.

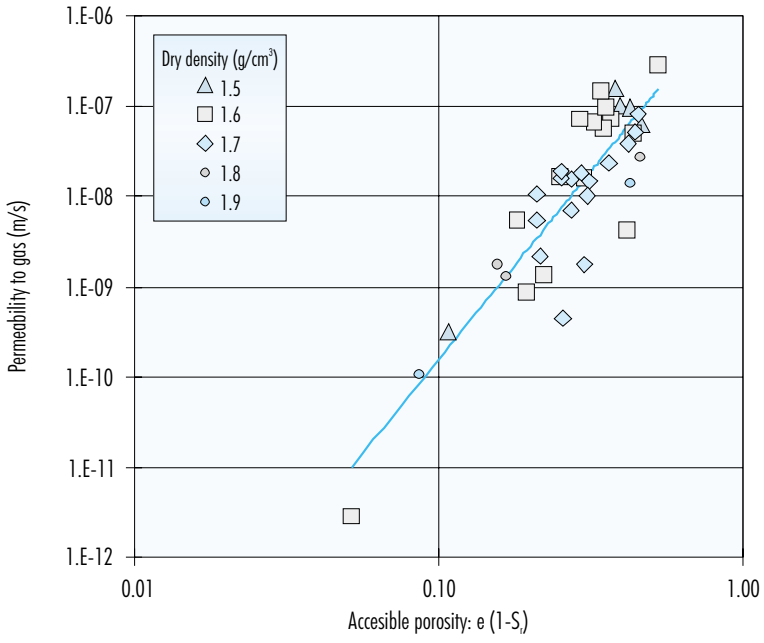

Figure 74. Relation between permeability to gas and the volume of pores accessible to the gas.

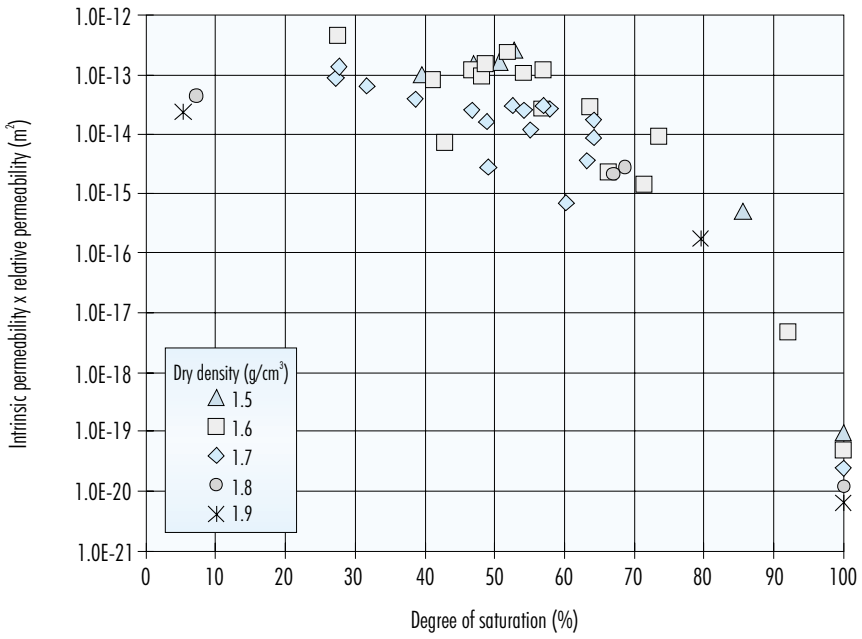

Figure 75. Product of relative permeability times intrinsic permeability measured with gas flow on samples compacted at different density and water content (the values corresponding to S_r=100 % come from the measurement of hydraulic conductivity).

If in the previous equation the degree of saturation is made equal to 0, the permeability to gas in dry bentonite compacted at different densities (k_{g0}, m/s) is obtained. Once this value has been obtained, it is possible to estimate the intrinsic permeability of the bentonite, measured with gas flow, from the following expression (see section on methodology "PERMEABILITY TO GAS"):

$$k_{ig} = \frac{k_{g0} \times \mu_g}{\rho_g \times g \times k_{rg}} = \frac{k_{g0}}{1.6\ 10^{-6} \times k_{rg}}$$

where ρ_g and μ_g are the density and dynamic viscosity of the nitrogen, k_{ig} is the intrinsic permeability measured with nitrogen gas (m^2) and k_{rg} is relative permeability to gas (which, given that the degree of saturation is 0, will be equal to 1). The values obtained by means of this calculation are shown in Figure 76. This figure also shows the variation in intrinsic permeability with void ratio obtained from the tests performed with water flow included in the section "Hydraulic conductivity". For a given void ratio, differences of up to eight orders of magnitude may be observed between the values of intrinsic permeability of dry and saturated clay.

These observations suggest that there is a fundamental difference in the microstructural arrangement of saturated and unsaturated samples, caused by the swelling of the clay upon hydration, a difference that would not be encountered in non-expansive materials. Intrinsic permeability is a property that depends exclusively on the medium. Consequently, if the fluid does not interact with the soil changing the properties of one or the other, the same value of intrinsic permeability would be obtained with any fluid.

However, if interactions between the fluid and the soil alter the structure of the medium, intrinsic permeability may also be modified. This is the case of expansive clays when water is used as the fluid, which causes an expansion of the clay laminae that gives rise to a reduction in the space available for flow (Tindall & Kunkel 1999).

The hydration of clay particles at a constant volume causes a reduction in the size of pores between clay aggregates. Under dry conditions, the diameter of the macropores accessible to gas flow may even exceed 10 μm. Under conditions of confinement, the hydrated clay shows the same overall volume of

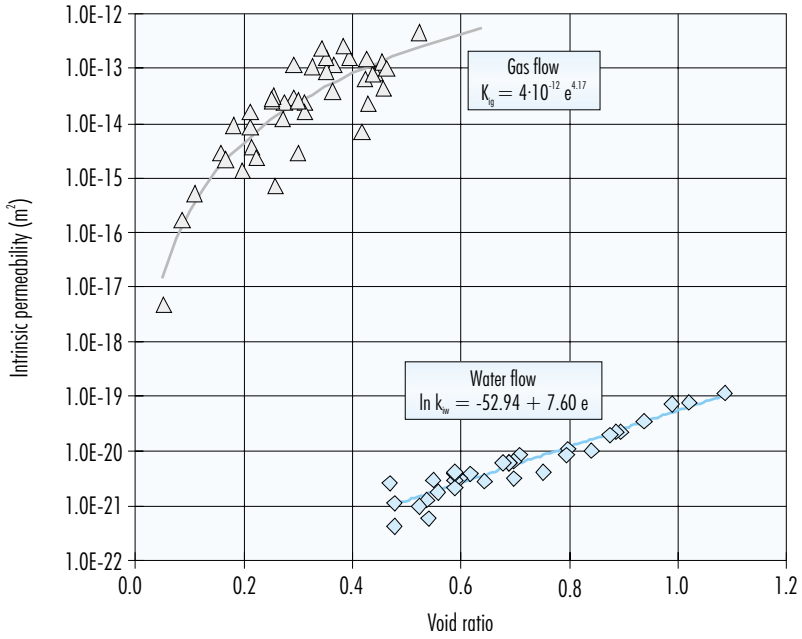

Figure 76. Intrinsic permeability of compacted bentonite obtained from tests performed with water flow on saturated samples and with gas flow on dry samples.

pores as a dry sample having the same dry density, but the spaces between aggregates are reduced or eliminated, due to the swelling of the clay particles. In other words, during hydration of the clay at constant volume, the volume occupied by small mesopores and micropores increases, while that occupied by macropores decreases. Under saturated conditions, the average diameter of the accessible pores corresponds to the range of the meso and micropores, that is to say, it is smaller than the diameter of the large inter-aggregate pores by more than three orders of magnitude. This variation in the average diameter of the pores available for flow explains the great difference in the values of intrinsic permeability measured in dry and saturated samples.

A verification of the above was found in the environmental scanning electron microscope (ESEM) study performed on the FEBEX clay. This equipment makes it possible to observe the microstructure of the clay under different conditions of relative humidity, and therefore of saturation. Figure 77 shows the appearance of the aggregates of clay compacted at a dry density of 1.70 g/cm3 under conditions of hygroscopic water content. The photograph was obtained in the ESEM chamber with a relative humidity of 50 percent, which is approximately that with which the clay was in equilibrium when compacted. This sample was gradually hydrated through the application of increasing relative humidity in the chamber of the microscope. Figure 78 is a photograph taken with a relative humidity of 100 percent after saturation of the sample through a gradually increase of relative humidity over 5 hours. The volume of the sample tested is very small, as a result of which hydration occurs very quickly. Despite the absence of confinement, a reduction in the size of certain inter-aggregate pores may be observed.

It should be pointed out that the values of intrinsic permeability for different degrees of saturation obtained using this method do not necessarily represent exactly the evolution of intrinsic permeability that would occur in a specimen saturated at constant volume. The values presented in this section correspond to samples obtained from the compaction of the clay at a given water content, and their microstructure is not necessarily the same than that of a sample gradually saturated under conditions of confinement.

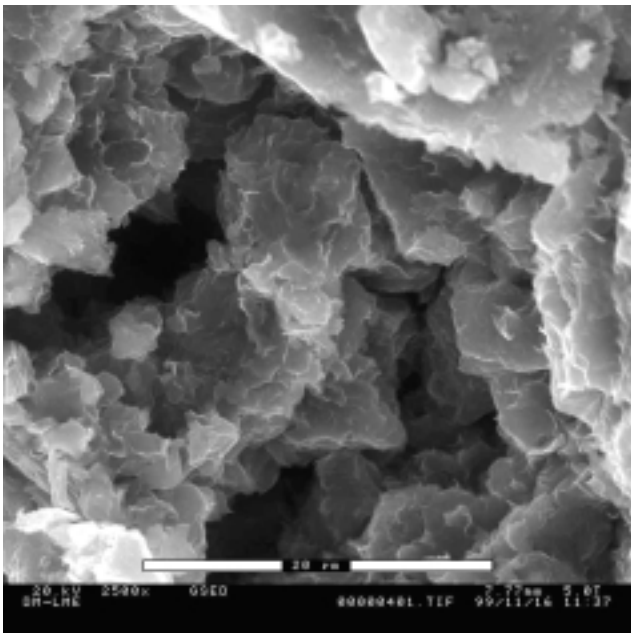

Figure 77. Photograph of the FEBEX clay compacted at a dry density of 1.70 g/cm^3 with hygroscopic water content, taken in the ESEM at a relative humidity of 50 percent.

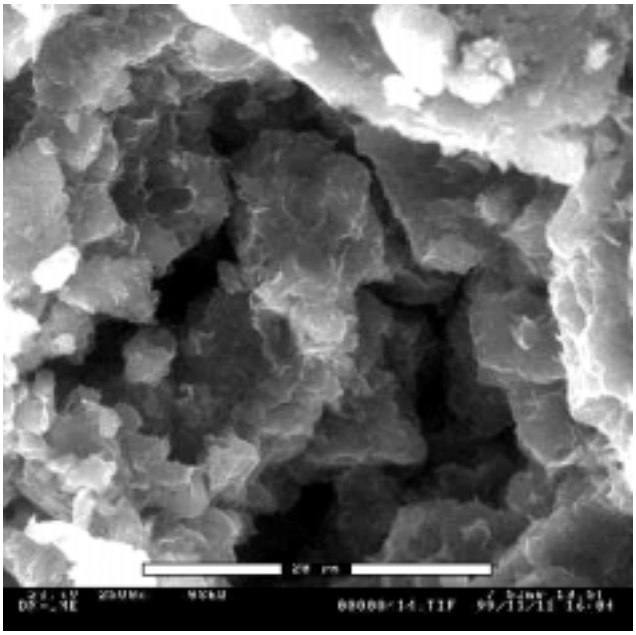

Figure 78. Photograph of the same area in Figure 77, taken in the ESEM at a relative humidity of 100 percent.

Retention curve

The retention curve describes the evolution of water content undergone by a sample when subjected to gradually increasing or decreasing suctions, that is to say, to drying or hydration paths.

The work was performed on samples obtained from the compaction of clay granulate with hygroscopic water content at different densities. In standard determinations of the retention curve the sample is not confined, this meaning that, in the case of expansive soils, the volume of the specimen is modified during the determination, due to the loss or uptake of water. This implies that the variations in the degree of saturation are not of the same order as those of water content, as was verified in the case of the free volume determinations included in the next section. Bearing this in mind, and taking into account that in the barrier the bentonite will be confined, experimental techniques that allow the determination of the suction/water content relation at constant volume have been implemented, the results of which will be shown below.

Free volume retention curve

The retention curve for the unconfined sample was determined by using two different techniques for the application of suction: control of the relative humidity by means of sulphuric acid solutions, and the axis translation technique in membrane cells. For suctions higher than 3 MPa, the first technique has been used, placing the samples in dessicators with solutions of a weight percentage of sulphuric acid between 6 and 67 percent. From 3 to 9 specimens were put in each desiccator. To apply suctions of between 2.0 and 0.1 MPa, the membrane cells have been used, injecting nitrogen into them to the desired pressure. A single specimen was placed in each cell. In both cases the nominal diameter of the specimens was 3.00 cm and their length 1.20 cm. Each specimen remains in the corresponding desiccator or cell for a time ranging from 20 to 30 days, after which it is weighed and measured to determine its water content and density. It then passes to the next suction step (desiccator or cell, as the case may be). The aforementioned period was established after verifying that it represents the time required for the clay to reach the stabilisation water content for a given value of suction.

As the test is performed at free volume, the sample swells or shrinks depending on whether it takes up water or loses it. By measuring the dimensions of the sample after each suction step, it is possible to determine its density, which, although not controlled, is known at each moment in time. This free variation in density prevents a clear relation being established between suction and degree of saturation, but not so between suction and water content.

The retention curve was determined for samples prepared in two ways: specimens compacted from the granulated sample and specimens trimmed from the blocks manufactured for the mock-up test of the FEBEX Project. The following two sub-sections present the results obtained in these two cases, followed by a combined analysis of the different retention curves obtained under free volume conditions.

All the determinations were performed at 20 °C.

Compacted specimens

Initially, the suction/water content relation was determined for three different values of suction, these being the equilibrium value at laboratory conditions (140 MPa), a higher value (260 MPa) and another lower (14 MPa). The determinations were performed using specimens uniaxially compacted at a nominal dry density of 1.60 g/cm^3 with hygroscopic water content (14±1 %). Seven samples were used for the determination carried out at the higher value of suction, 13 for the intermediate value and 10 for the lower suction. The average values obtained for each suction are shown in Table XXIII.

Table XXIII
Final average values of water content and density corresponding to different suction for specimens compacted at an initial dry density of 1.60 g/cm^3 and a water content of 14 percent.

No of samples	Suction (MPa)	ρ_d (g/cm^3)	Water content (%)	S_r (%)
7	257.7±2.7	1.64±0.02	8.7±0.4	36±2
13	138.2±7.0	1.61±0.02	12.1±0.8	48±3
10	14.5±0.4	1.36±0.03	22.3±0.3	62±3

Subsequently, other samples were used to determine two retention curves on different paths: a wetting path (from 148 to 0 MPa) and a drying/wetting path (from 140 to 313 MPa and to 0.1 MPa). In both cases, the initial suction was that corresponding to the sample with its hygroscopic water content, and three specimens were used for each determination, these being uniaxially compacted at an initial nominal dry density of 1.75 g/cm^3 and a water content of 14.2 percent, both these being similar to those of the blocks manufactured for the mock-up test. Furthermore, an additional drying/wetting path was performed using specimens compacted at a dry density of 1.70 g/cm^3 with a water content of 13.6 percent. In this last case the drying was more intense, with suctions of up to 517 MPa being reached.

The average values of the three determinations for the wetting path are shown in Table XXIV, which shows the significant increase in water content that occurs with decreasing suction, which is associated with a reduction in the dry density of the sample, this implying that the degree of saturation is not overly modified. The standard deviation of the three measurements performed for water content is between 0.0 and 3.4 percent and for dry density is between 0.00 and 0.03 g/cm^3, both increasing with decreasing suction. A graphic representation of these values may be found in Figure 80 and Figure 81.

For suctions of between 148 and 0.1 MPa, it is possible to fit the following equations for an initial dry density of 1.75 g/cm^3, relating suction to water content and dry density:

$$w = -5.04 \ln s + 38.35 \qquad (r^2 = 0.98,\ 30\ points)$$

$$\rho_d = 1.14\ s^{0.08} \qquad (r^2 = 0.99,\ 30\ points)$$

where w is water content in percent, s is suction in MPa and ρ_d is dry density in g/cm^3.

The average values for each suction on the drying/wetting curves obtained for two different initial dry densities are shown in Table XXV. The graphic representation of these values may be found below, in Figure 82 to Figure 85. During the drying process, the reduction in water content is associated with an increase in dry density, that subsequently decreases during wetting, while water content increases. The standard deviation of the three measurements performed for water content is between 0.0 and 1.7 percent (although for the majority of the suction values it is between 0.3 and 0.4 percent). The standard deviation for dry density ranges from 0.01 to 0.06 g/cm^3, the disparity increasing for lower values of suction, due to experimental difficulties associated with crumbling of the specimens.

For the tests performed with specimens with an initial dry density of 1.75 g/cm^3, the following fittings

Table XXIV
Values of water content and density obtained at the end of each step on a wetting path for specimens compacted at an initial dry density of 1.75 g/cm^3 (average of 3 determinations).

Suction (MPa)	ρ_d (g/cm^3)	Water content (%)	S_r (%)
148.2	1.76	13.6	69
79.2	1.66	16.0	69
34.3	1.52	21.3	74
13.3	1.42	24.6	74
6.6	1.35	27.7	74
3.8	1.29	29.9	74
2.0	1.17	35.7	74
1.0	1.13	39.7	77
0.5	1.09	43.5	80
0.1	0.98	50.4	77

Table XXV
Values of water content and density obtained at the end of each step on the drying/wetting path for compacted specimens (average of 3 determinations).

Initial dry density 1.75 g/cm³				Initial dry density 1.70 g/cm³			
Suction (MPa)	ρ_d (g/cm³)	w (%)	S_r (%)	Suction (MPa)	ρ_d (g/cm³)	w (%)	S_r (%)
140.0	1.76	13.8	70	139.2	1.66	13.3	57
217.0	1.77	12.3	63	196.1	1.67	11.2	49
313.0	1.81	8.9	49	259.8	1.69	9.3	42
223.0	1.77	11.5	59	356.3	1.71	6.4	30
135.0	1.73	13.5	65	516.9	1.72	4.4	21
29.0	1.49	21.1	70	264.2	1.69	7.8	35
13.3	1.42	24.1	72	187.3		10.9	
6.7	1.34	26.6	71	126.4		12.6	
3.9	1.24	28.5	65	74.9	1.56	15.7	59
2.0	1.19	36.1	77	32.9	1.45	20.0	63
1.0	1.12	40.0	77	12.4	1.36	23.5	65
0.5	1.06	43.8	77				
0.1	1.04	56.8	95				

were obtained for the drying path, from 140 to 313 MPa:

$$w = -6.07 \ln s + 44.15 \quad (r^2 = 0.93, 9 \text{ points})$$

$$\rho_d = 1.48\, s^{0.03} \quad (r^2 = 0.66, 9 \text{ points})$$

and for wetting after drying, from 313 to 0.1 MPa:

$$w = -5.54 \ln s + 39.77 \quad (r^2 = 0.98, 33 \text{ points})$$

$$\rho_d = 1.15\, s^{0.08} \quad (r^2 = 0.98, 32 \text{ points})$$

In turn, for the tests performed using specimens with an initial dry density of 1.70 g/cm³, the following fittings were obtained for the drying path, from 139 to 517 MPa:

$$w = -7.06 \ln s + 48.29 \quad (r^2 = 0.98, 15 \text{ points})$$

$$\rho_d = 1.42\, s^{0.03} \quad (r^2 = 0.73, 15 \text{ points})$$

and for wetting after drying, from 517 to 12 MPa:

$$w = -5.21 \ln s + 37.55 \quad (r^2 = 0.98, 21 \text{ points})$$

$$\rho_d = 1.16\, s^{0.06} \quad (r^2 = 0.98, 15 \text{ points})$$

in all cases, w is water content in percent, s is suction in MPa and ρ_d is dry density in g/cm³.

Specimens trimmed from blocks

In order to check whether the suction/water content relation is modified on varying the method used to initially prepare the specimens, various determinations were carried out in accordance with the procedure described, using specimens obtained by trimming certain of the blocks manufactured for the mock-up test (see section "The FEBEX Project").

The trimming was performed using a cylindrical cutter in two different directions: parallel to the block compaction force, *i.e.* vertical with the block in its manufacturing position, and perpendicular to the compaction force, *i.e.* in the horizontal direction (Figure 68). The dimensions of the cylindrical cutter make it possible to obtain specimens of the same size as those compacted, that is to say, 3.00 cm in diameter and 1.20 cm in length.

Two curves were determined, beginning in all cases from the suction value corresponding to the clay at its equilibrium water content at laboratory conditions, but following two different paths: a wetting path, through the reduction of suction to 0.1 MPa, and a drying process to 394 MPa, followed by wetting to 0.1 MPa. For determination of each of the curves 3 specimens trimmed in the horizontal direction and 3 trimmed vertically were used. Although the process began using blocks with a dry density in excess of 1.75 g/cm^3, this density decreased on trimming, and not in the same way in all the samples, as a result of which the average initial dry density of the trimmed specimens is 1.67 g/cm^3, varying between 1.59 and 1.73 g/cm^3. The initial water content is 14.2 percent.

The average values obtained for the wetting curve are shown in Table XXVI, and their graphic representation in Figure 79. This figure also includes the evolution of dry density on decreasing suction. It should be pointed out that the determination of dry density for the lower values of suction is difficult, since the specimen loses its consistency and crumbles easily.

There are no significant differences between the values obtained for specimens trimmed in one direction or the other, as a result of which common fittings may be obtained for the entire wetting path, from 117 to 0.1 MPa, relating suction to water content and dry density:

$$w = -5.19 \ln s + 38.13 \quad (r^2 = 0.95, 54 \text{ points})$$

$$\rho_d = 1.12\, s^{0.08} \quad (r^2 = 0.96, 47 \text{ points})$$

where w is water content in percent, s is suction in MPa and ρ_d is dry density in g/cm^3.

The values obtained for the drying/wetting path are shown in Table XXVII and are represented in Figure 82 to Figure 85.

On the initial drying path to 394 MPa, the water contents reached are independent from the type of specimen, and correlate with suction by means of the following expression (s, suction in MPa and w, water content in percent):

$$w = -6.42 \ln s + 44.97 \quad (r^2 = 0.88, 24 \text{ points})$$

However, although no significant differences were identified in this case between specimens trimmed in one direction or another, it is not possible to obtain a good fitting between dry density and suction during drying, since the initial dry densities are different and barely vary during this initial path.

Once again, there are no significant differences between the values obtained for specimens trimmed in one direction or another on the wetting path performed after drying to 394 MPa. Even the dry density of the different specimens evolves in a similar

Table XXVI
Values of water content and density obtained at the end of each step on a wetting path for specimens trimmed perpendicular and parallel to the block compaction force (average of 3 determinations).

Suction (MPa)	Perpendicular trimming			Parallel trimming		
	ρ_d (g/cm^3)	Water content (%)	S_r (%)	ρ_d (g/cm^3)	Water content (%)	S_r (%)
116.7	1.67	14.1	61	1.67	14.2	62
79.2	1.61	16.0	64	1.62	16.1	65
31.2	1.48	20.7	67	1.47	20.7	67
13.5	1.40	23.4	69	1.39	23.6	68
3.9	1.30	28.5	71	1.25	29.2	68
2.0	1.14	34.1	68	1.21	33.8	74
1.0	1.08	36.5	66	1.06	37.0	65
0.5	1.05	40.3	69	1.06	40.4	71
0.1	0.97	53.9	82	0.97	51.2	78

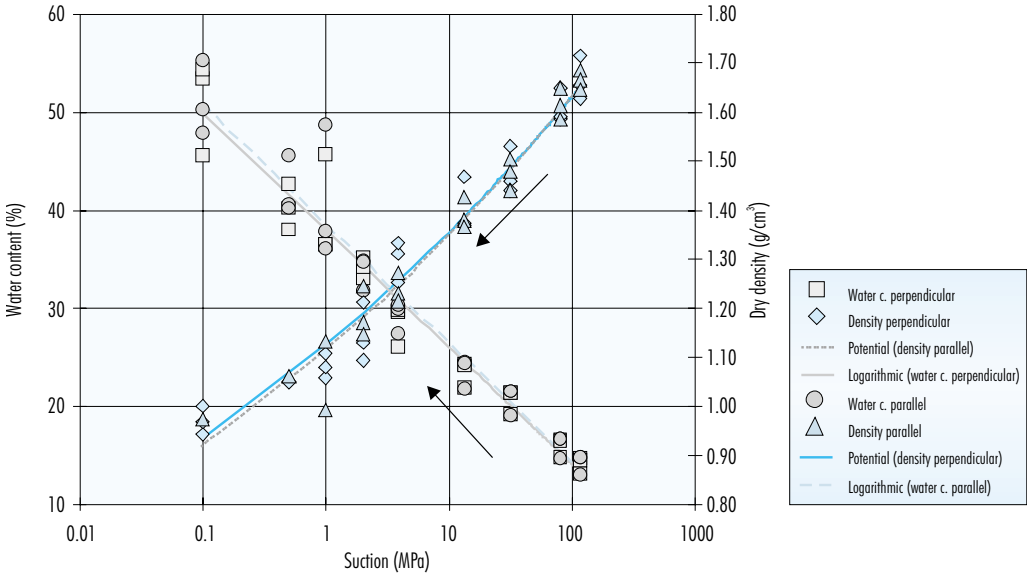

Figure 79. Density and water content obtained in successive steps on a wetting path for specimens trimmed perpendicular and parallel to the block compaction force.

manner, since the initial differences are attenuated during wetting, as a result of which the following common fittings may be obtained for both types of specimens:

$$w = -5.20 \ln s + 37.48 \quad (r^2 = 0.98, 69 \text{ points})$$

$$\rho_d = 1.13\, s^{0.07} \quad (r^2 = 0.94, 69 \text{ points})$$

where w is water content in percent, s is suction in MPa and ρ_d is dry density in g/cm^3.

Analysis of the curves obtained

As has been seen in the previous sections, the suction/water content relation determined under free volume conditions for this bentonite may be expressed by means of a logarithmic relation between the two variables: the water content of the sample decreases on drying paths (increasing suction) and increases during the process of wetting (decrease of suction). In its side, the modification of dry density with suction on these paths follows a potential law. The behaviour of the trimmed and compacted specimens follows the same patterns. The influence of the type of path and initial dry density on the values of water content and dry density reached at each step is minor, but it has been possible to establish certain differences, as may be appreciated from the fittings and figures presented below.

Taking into account the fittings presented in previous sections for the different paths studied –wetting, drying and wetting after drying– and for the different initial dry densities with which the work has been carried out –1.60, 1.70 and 1.75 g/cm3 for compacted specimens and an average value of 1.67 g/cm3 for specimens trimmed in both directions– relations between suction and water content and between suction and dry density depending on initial dry density have been established, these matching the following expressions:

$$w = (a\,\rho_{d0} + b)\ln s + (c\,\rho_{d0} + d)$$

$$\rho_d = (e\rho_{d_0} + f)\, s^{(g\rho_{d_0}+h)}$$

where s is suction in MPa, w is water content in percent, ρ_d is dry density in g/cm3, ρ_{d0} is initial dry density in g/cm3, and the rest of the symbols are the coefficients of the fittings.

The coefficients obtained between suction and water content for each path are shown in Table XXVIII, and those between suction and dry density are included in Table XXIX.

Table XXVII
Values of water content and density obtained at the end of each step on a drying/wetting path for specimens trimmed perpendicular and parallel to the block compaction force (average of 3 determinations).

Suction (MPa)	Perpendicular trimming			Parallel trimming		
	ρ_d (g/cm^3)	Water content	S_r (%)	ρ_d (g/cm^3)	Water content	S_r (%)
116.7	1.64	14.1	59	1.67	14.3	63
199.4	1.67	11.1	49	1.70	11.3	52
265.7	1.69	9.3	42	1.72	9.4	45
394.4	1.71	6.2	29	1.75	6.4	32
265.7	1.69	8.1	36	1.73	8.2	39
182.2	1.66	10.6	46	1.69	10.8	49
116.7	1.61	13.2	53	1.64	13.2	55
69.7	1.56	16.1	59	1.57	16.2	61
31.2	1.46	20.0	63	1.49	20.2	67
12.9	1.38	22.8	64	1.41	23.1	68
4.0	1.27	28.7	69	1.28	29.2	71
2.0	1.17	33.1	68	1.20	32.0	69
1.0	1.11	37.1	70	1.13	35.7	69
0.5	1.06	39.9	69	1.08	39.2	70
0.1	0.97	49.0	75	0.99	47.4	74

Table XXVIII
Coefficients of logarithmic fittings between suction and water content depending on the type of path.

Type of path	Suction range (MPa)	a	b	c	d
Wetting	148 – 0.1	-3.28	0.57	25.40	-5.52
Drying	117 – 517	5.98	-16.73	-17.67	75.96
Wetting after drying	517 – 0.1	-4.47	2.32	30.17	-13.22

Table XXIX
Coefficients of potential fittings between suction and dry density depending on the type of path.

Type of path	Suction range (MPa)	e	f	g	h
Wetting	148 – 0.1	0.18	0.83	0.06	-0.02
Drying	117 – 517	1.37	-0.92	0.05	-0.05
Wetting after drying	517 – 0.1	0.16	0.87	0.09	-0.08

The following figures show jointly the experimental values included in the tables of previous sections and the curves obtained using the fittings presented above, logarithmic for the suction/water content relation and potential for the suction/dry density relation, with the coefficients included in Table XXXVIII and Table XXIX.

Figure 80 and Figure 81 show the experimental values and fittings for the wetting paths, the first in terms of water content and the second in terms of dry density. It may be appreciated that for a given value of suction, the water content reached is higher for the samples of higher initial dry density, and that even though the dry density of these samples remains higher along the entire path, its reduction is greater, as a result of which the influence of initial dry density on the dry density values attained becomes insignificant for suctions of less than 0.5 MPa.

Figure 82 shows the evolution of water content with suction for the drying paths. For greater clarity, suction is expressed on a linear scale. As occurs in the case of the wetting paths, the water content for a given value of suction is greater the higher the initial dry density. Figure 83 shows the evolution of dry density in samples subjected to drying. Dry density increases slightly during drying above 130 MPa. Due to the dispersion of the results, especially for the trimmed specimens (whose average initial dry density is 1.67 g/cm^3), the fittings are not good, although they do make it possible to appreciate that the difference in initial dry density remains approximately constant throughout the drying process.

Following the process of drying described above, the sample was hydrated. The values of water content and dry density reached during this process of wetting after drying are shown in Figure 84 and Figure 85, respectively, along with the theoretical fittings. The trends observed are similar to those already dealt with above: greater increase in water content and greater reduction of dry density for samples with higher values of initial dry density, as a result of which the differences in dry density become increasingly smaller. In any case, the degree of saturation is higher throughout the entire process for samples with higher values of initial dry density (Table XXV and Table XXVII).

All the curves presented were obtained by combining two different suction control techniques: the imposition of a relative humidity, for high values of suction, and axis translation for suction values be-

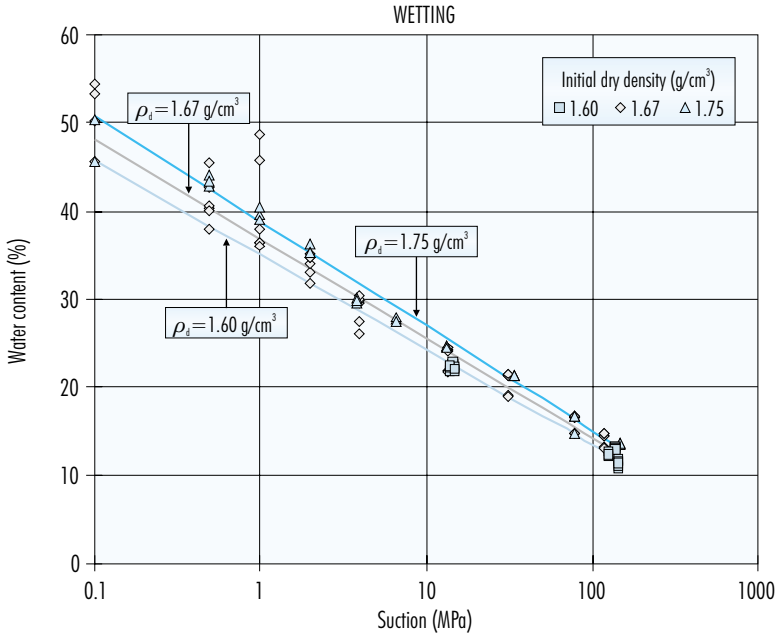

Figure 80. Values of water content obtained on wetting paths for different initial dry densities and fittings as a function of initial dry density.

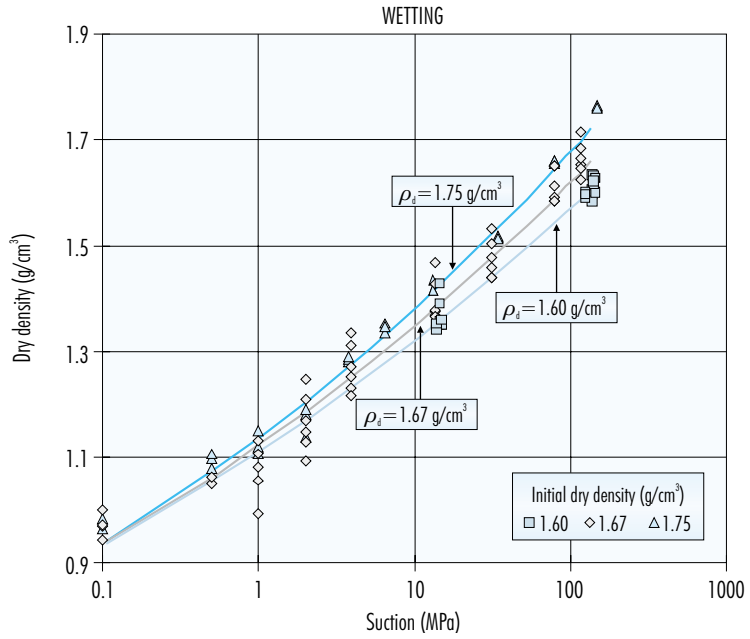

Figure 81. Values of dry density obtained on wetting paths for different initial dry densities and fittings as a function of initial dry density.

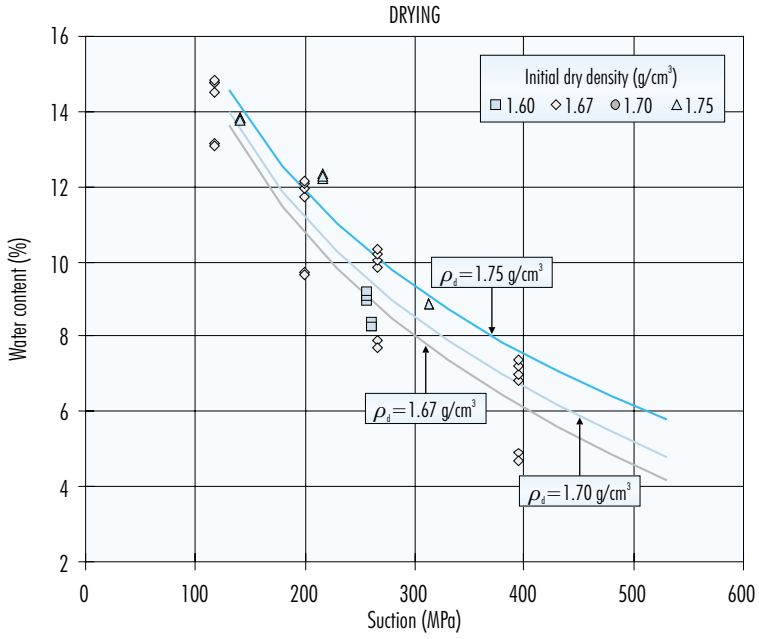

Figure 82. Values of water content obtained on drying paths for different initial dry densities and fittings as a function of initial dry density.

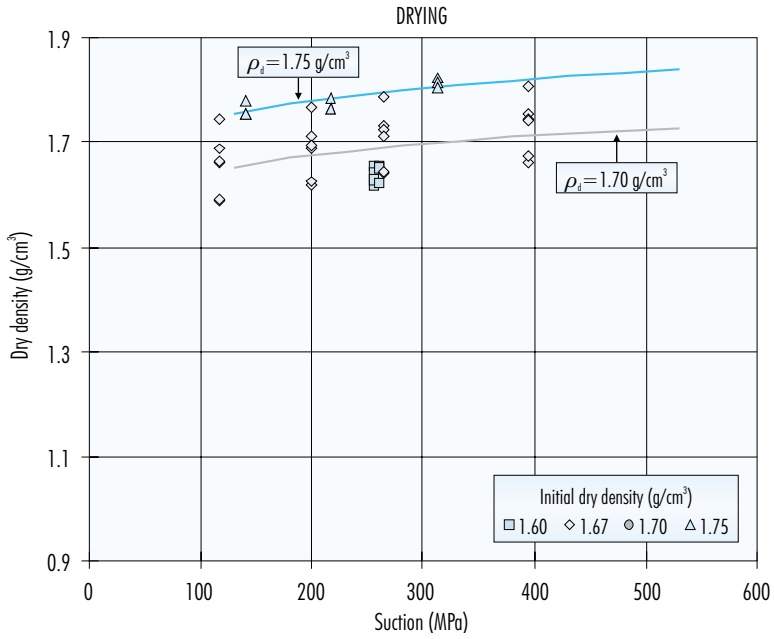

Figure 83. Values of dry density obtained on drying paths for different initial dry densities and fittings as a function of initial dry density.

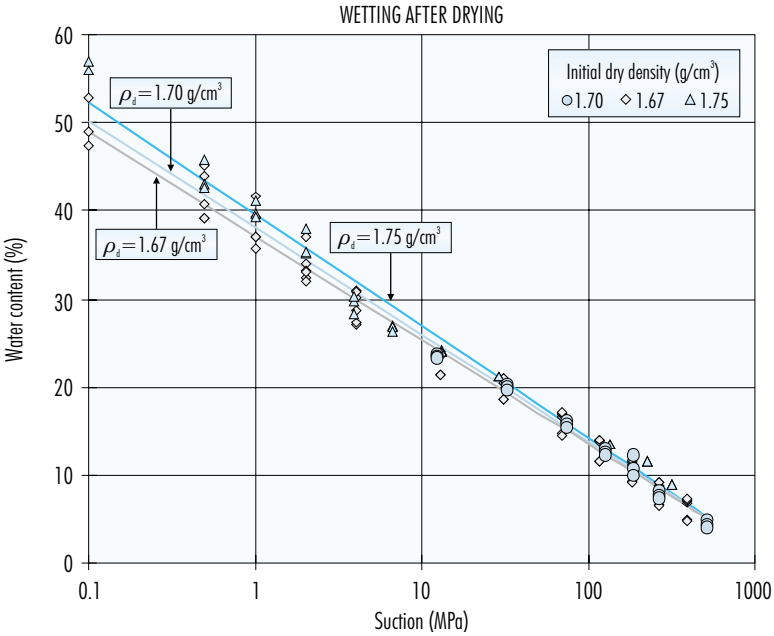

Figure 84. Values of water content obtained on wetting after drying paths for different initial dry densities and fittings as a function of initial dry density.

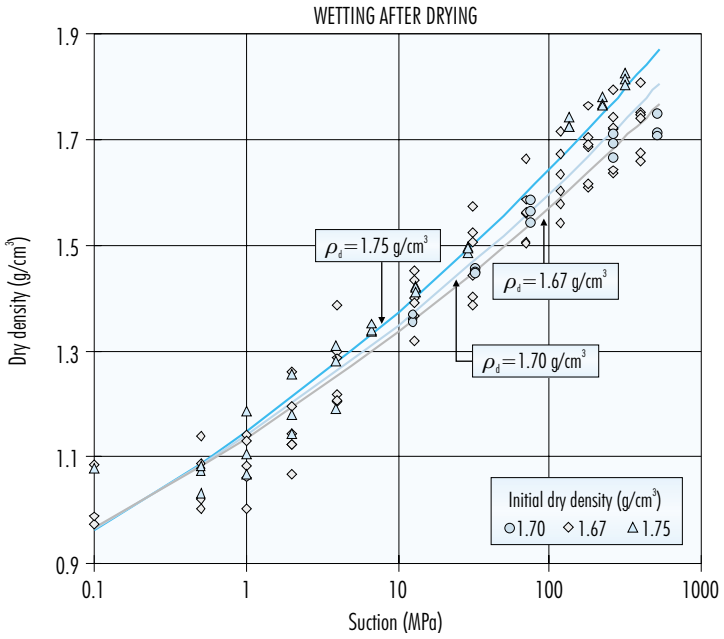

Figure 85. Values of dry density obtained on wetting after drying paths for different initial dry densities and fittings as a function of initial dry density.

low 2 MPa. As indicated in the section "EXPERIMENTAL TECHNIQUES FOR THE STUDY OF EXPANSIVE, UNSATURATED MATERIALS", one of the differences between both techniques is that in the second one there may be ion exchange between the sample and the water on the other side of the membrane, since the latter allows solutes to pass through it, this preventing any control over osmotic suction. This does not occur with the suction control technique consisting in the application of relative humidity, since in this case the exchange of water occurs in the vapour phase, and consequently, it is not accompanied by the transfer of solutes. As a result, the participation of osmotic suction is also allowed. In view of the fact that the curves that have been plotted show a perfect correlation between the values obtained using both of these techniques, it may be assumed that the contribution made to the total value of suction by osmotic suction is insignificant and that, in this bentonite, suction is fundamentally of the matric type (Thomé 1993, Villar & Martín 1996, Romero 1999). Wan *et al*. (1995) conclude that the variations in water content in a sand/bentonite mixture are also conditioned fundamentally by matric suction.

As it has been seen in the previous pages, the detailed analysis of the retention curves determined under free volume conditions makes it possible to identify the influence of initial dry density in them. For the range of dry density analysed –which is strongly limited, between 1.67 and 1.75 g/cm^3– the repercussion of initial dry density is small. Retention curves have been determined for this bentonite for different initial dry densities of between 1.64 and 1.75 g/cm^3, similar to those presented herein (ENRESA 2000). However, in studies performed on a bentonite from the same deposit (reference S-2), it was not possible to determine the influence of initial dry density on the suction/water content relation under free volume conditions for initial dry densities in the range 1.40 to 1.95 g/cm^3 (Villar 1995a). The same is true for the work carried out by Wan *et al*. (1995), who were unable to identify the influence of initial dry density on retention curves determined for mixtures of sand and bentonite and sand and illite. The retention curves plotted for samples of Boom clay compacted at dry densities of between 1.1 and 1.8 g/cm^3 are very similar one to the other, this being explained by Bernier *et al*. (1997) as a consequence of intra-aggregate porosity and smectite

content –parameters that both condition matric suction– not being modified by compaction. Therefore, in unconfined materials with a degree of expansibility, a single suction/water content relation independent from the value of initial dry density is frequently considered.

The fact that, for a given value of suction, the equilibrium water content is somewhat greater for samples having higher values of initial dry density may be explained in terms of the increase in the relation between the volume of small and large pores that occurs during compaction as dry density increases. During wetting processes, the smaller pores saturate earlier and take longer to desaturate during drying. This allows the samples with higher values of initial dry density, which have a large volume of small pores, to take up more water at the beginning of hydration, when suction is high. Furthermore, the greater expansion of samples having higher initial dry densities contributes to the increase in porosity during hydration, and therefore in the volume of pores accessible to water. In this way, when lower values of suction are reached, the dry densities of all the samples equal out at a value of around 1 g/cm^3, as a result of which the degrees of saturation of samples having higher values of initial dry density –which have higher water contents– are also greater.

By the other hand, the comparison of the curves corresponding to wetting paths and those for wetting after drying shows that the water contents reached for a given value of suction are somewhat higher if there has been no previous drying, as a result of which in the case of wetting after drying, the initial water content value is not reached again until a suction value lower than the initial one is reached. However, this water content difference between the processes of wetting and wetting after drying becomes smaller as suction decreases, and, from a given value of suction, the water contents obtained are even higher in previously dried samples. This value is approximately 7 MPa for an initial dry density of 1.75 g/cm^3 and 3 MPa for an initial dry density of 1.67 g/cm^3. However, when drying is accomplished by heating at 100 °C, until water content is reduced to 0 percent, there may be irreversible modifications in the rehydration capacity. In fact, Rivas *et al*. (1991) found that the rehydration capacity following heating to 100 °C of the S-2 bentonite, from the same deposit as the FEBEX clay, is only 82 percent, decreasing as the pre-treatment temperature increases. It should be remembered that the minimum water content reached on the retention curves determined for this work is between 4 and 6 percent, this suggesting that the interlaminar water solvating the exchange cations has probably not been lost.

However, for a given initial dry density, the dry densities found on the path of wetting after drying are similar to those corresponding to the wetting path (Figure 86), although the increase in dry density during initial drying is smaller than the reduction in dry density that occurs during the first part of the subsequent process of wetting (Table XXV and Table XXVII).

The data obtained show that the degree of saturation cannot be related to a single value of total suction. This may be appreciated in Figure 87, which shows the values of degree of saturation versus suction for different dry densities on wetting paths. However, the degree of saturation is higher for samples with higher initial dry densities throughout the entire process. Both observations have been made also on paths for wetting after drying (Figure 88).

When there is a constant change in the porosity of the sample during wetting, the increase in the degree of saturation that would occur as a result of increasing water content is counteracted by the decrease in dry density, and consequently, there is a range of suction in which the variation in suction hardly modifies the degree of saturation. This range of suction values is between 100 and 0.5 MPa, approximately.

Several authors who have worked under free volume conditions with compacted clays, such as Wan *et al*. (1995) with sand/bentonite mixtures and Romero (1999) with the Boom clay, have pointed out that for certain ranges of suction it is advisable to use water content rather than degree of saturation as a state variable.

It is observed, on paths of wetting after drying, that for values of suction in excess of 100 MPa, the entry of water in the sample causes the structure to expand, and consequently gives rise to an increase in porosity (Figure 85), but this is accompanied by a loss of air, that is to say, the water replaces the air, as a result of which there is an increase in the degree of saturation with decreasing suction. Below this value of suction, the intake of water is not accompanied by a loss of air, but only by an increase in porosity due to expansion of the clay, as a result of which the degree of saturation does not increase, although water content does (Figure 84). The value

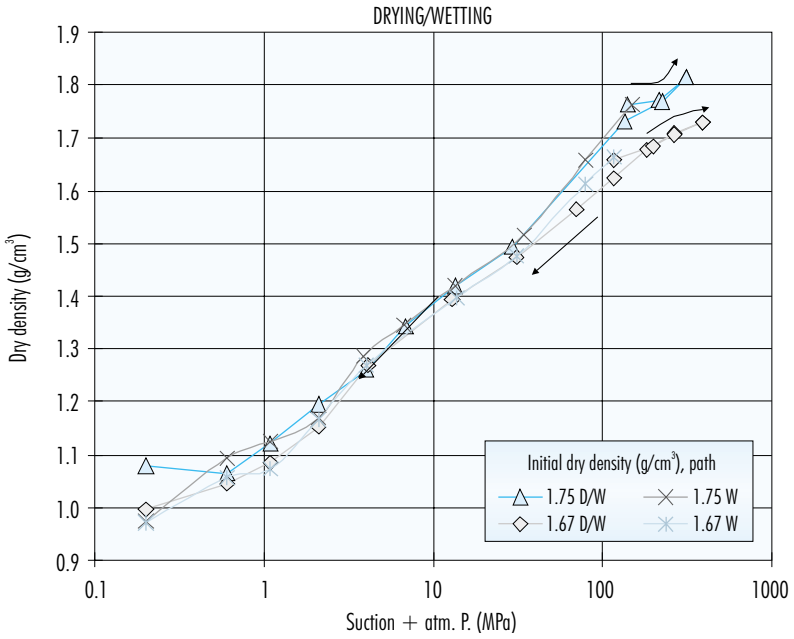

Figure 86. Evolution of dry density on paths of drying/wetting (D/W) and wetting (W) (average values for 3 or 6 determinations).

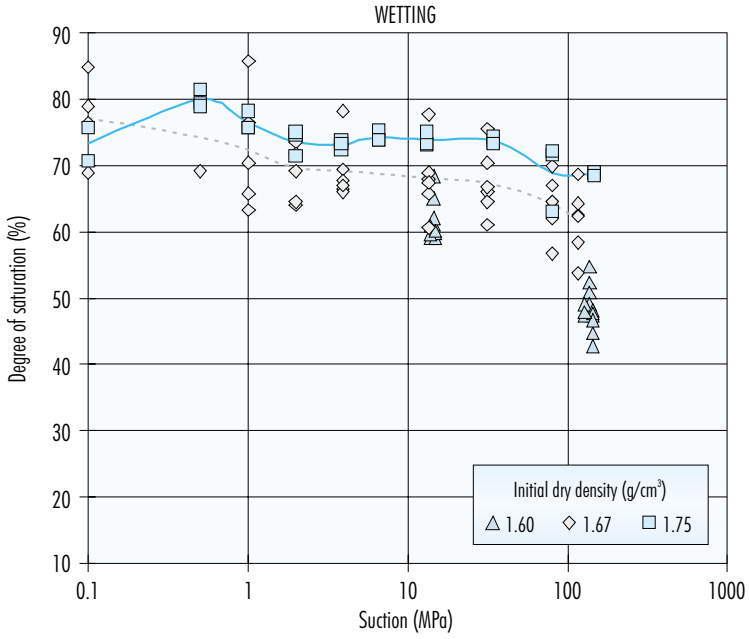

Figure 87. Values of degree of saturation versus suction for different initial dry densities on wetting paths.

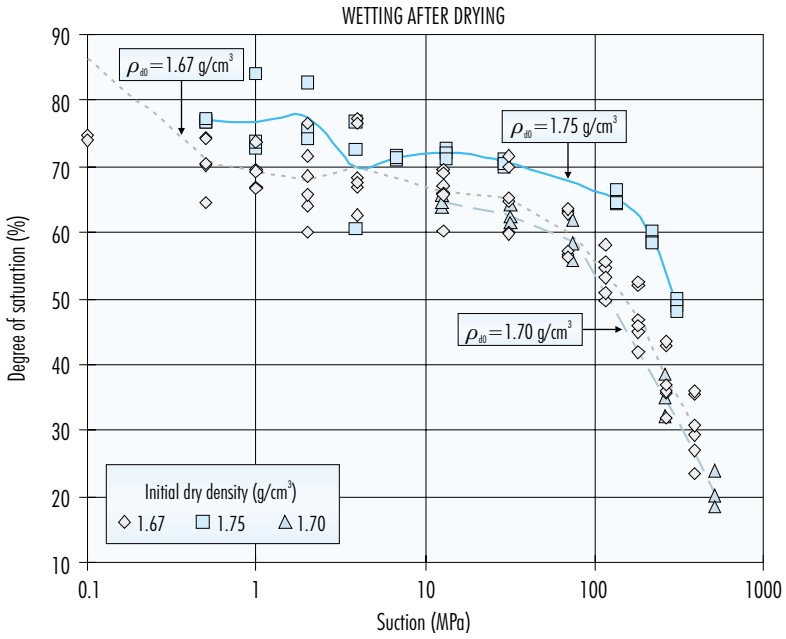

Figure 88. Values of degree of saturation versus suction for different initial dry densities on paths of wetting after drying.

of around 100 MPa must, therefore, be the point at which the air exits the microstructure on wetting paths. Delage *et al*. (1998) find, for the French FoCa smectite, that the initial value of suction used in their tests (113 MPa) separates two zones with completely different behaviour patterns: below this value there is only exchange of water, with the volume of air remaining constant.

The value of 0.5 MPa, below which there is an increase in the degree of saturation, corresponds to the beginning of saturation of pores larger than 0.59 μm (applying the Jurin-Laplace law for capillary suction in cylindrical pores), which belong to the macroporosity domain (intermediate pores), and must therefore be the point at which the air exits the macrostructure on wetting paths. The entrance of water in the macropores is accompanied by a loss of air, as a result of which the degree of saturation of the material increases. Wan *et al*. (1995) suggest that, for high saturations, it is probably possible to use relations between degree of saturation and total suction to analyse the soil behaviour.

If the results presented are expressed in terms of effective volumetric water content versus suction, they may be fitted to the following expression (van Genuchten 1980):

$$\theta_e = \left[\frac{1}{1+(\alpha h)^{1/1-m}}\right]$$

where θ_e is the effective volumetric water content, h is potential expressed in MPa and α and m are fitting parameters. The effective volumetric water content is determined in accordance with the following expression:

$$\theta_e = \frac{\theta - \theta_r}{\theta_s - \theta_r}$$

where θ is the volumetric water content, θ_s is the saturated volumetric content and θ_r is the residual volumetric water content, which indicates the quantity of water that cannot be extracted without subjecting the sample to a very high increase in suction.

A θ_r of 0.07 has been taken to calculate the effective volumetric water content. Given the difficulty involved in measuring or graphically deducing the value of θ_r in expansive materials (Vanapalli *et al*. 1999), this has been taken on the basis of the experimental results, which show decreases in water content versus suction ($\Delta\theta/\Delta s$) of the same order

across the entire range of suctions investigated, these decreases becoming smaller only for suctions in excess of 400 MPa, for which a volumetric water content of close to 0.07 was measured. For θ_s values of between 0.71 and 0.74 were taken, depending on dry density. These values are based on the volumetric water contents measured experimentally in samples of different initial dry density saturated to equilibrium under free volume conditions in an atmosphere having a relative humidity of 100 percent, which have shown that, for the range of dry densities analysed, the samples do not reach full saturation under free volume conditions.

The following figures show the average of the experimental values obtained for each suction, along with the fittings obtained using the van Genuchten expression. Figure 89 refers to the wetting path and Figure 90 to the wetting after drying path. Both curves show that the values of volumetric water content for a given value of suction are higher for higher dry densities, as it was observed for the degrees of saturation. The coefficients of the fittings, calculated using a non-linear least squares technique, are shown in Table XXX. The results obtained on the drying paths do not fit well with this expression.

The fittings obtained for wetting after drying deviate significantly from the experimental values for values of suction in excess of 100 MPa, which, as has been seen, corresponds to the point at which the air starts to leave the microstructure. In assessing the goodness of these fittings, it should be remembered that the van Genuchten model was developed for non-expansive materials whose volume does not change when suction is modified. The retention curve data may also be fitted to the van Genuchten expression using the RETC code (van Genuchten *et al*. 1991), which allows for the simultaneous determination of the parameters α, m, θ_s and θ_r, considering all of them to be simple fitting parameters without any physical meaning. Values of 0 have been obtained for θ_r and of between 0.7 and 0.8 for θ_s on the wetting paths. In the case of wetting after drying, much higher values are obtained for θ_s.

Retention curves at constant volume

When retention curves are determined under free volume conditions, *i.e*. as described in the previous section, the structure and dry density of the bentonite undergo important changes throughout the pro-

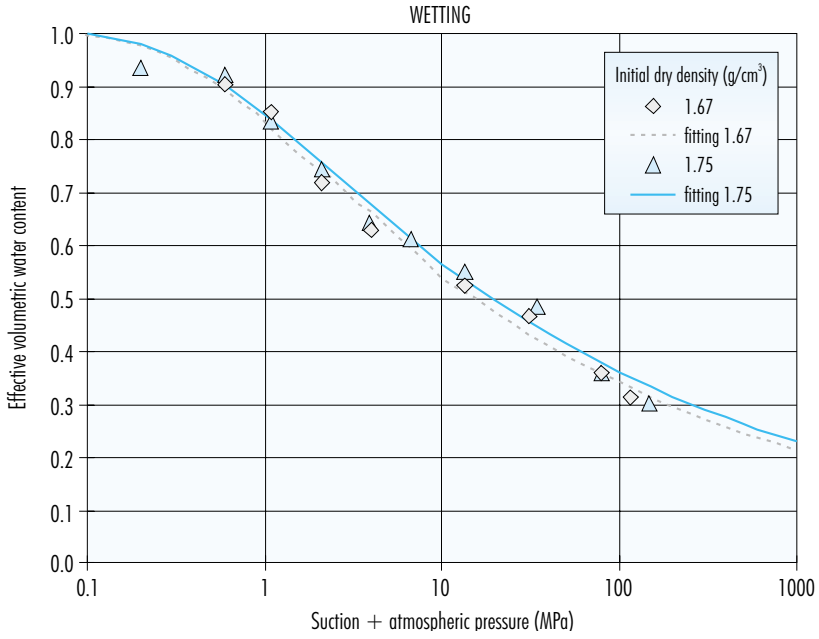

Figure 89. Experimental values obtained on wetting paths (average of 3 or 6 determinations) and fittings of the van Genuchten expression for different initial dry densities.

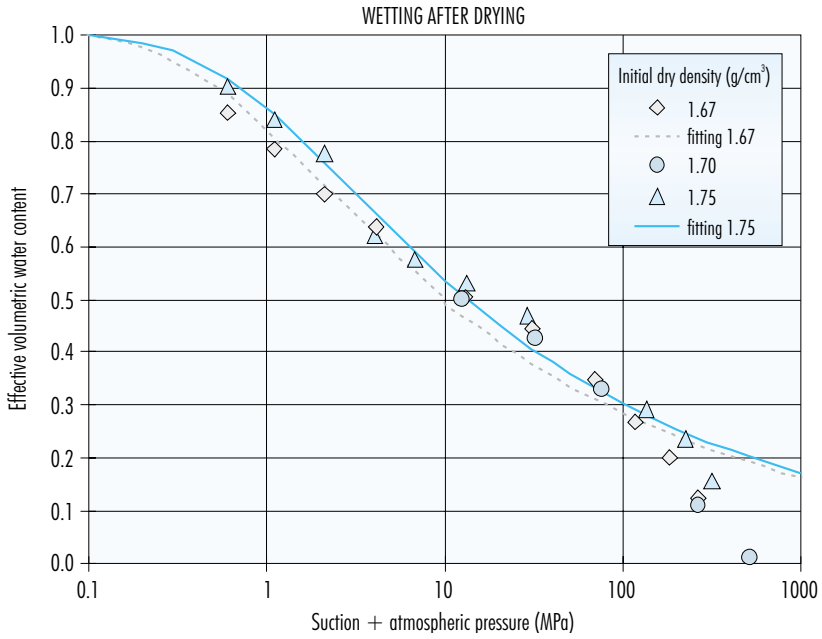

Figure 90. Experimental values obtained in wetting after drying paths (average of 3 or 6 determinations) and fittings of the van Genuchten expression for different initial dry densities.

Table XXX
Coefficients of the van Genuchten expression between suction and effective volumetric water content depending on the type of path.

Type of path	Initial ρ_d (g/cm^3)	α (MPa^{-1})	m	θ_s	θ_r	r^2
Wetting (148-0.1 MPa)	1.67	1.86±0,34	0.17±0.01	0.710	0.07	0.989
	1.75	1.74±0,37	0.16±0.01	0.735	0.07	0.988
Wetting after drying (394-0.1 MPa)	1.67	1.76±0.55	0.19±0.02	0.710	0.07	0.962
	1.75	1.21±0.27	0.20±0.01	0.735	0.07	0.98

cess. However, the actual situation of the clay in an engineered barrier will not allow important variations in volume to occur. In order, on the one hand, to reproduce as faithfully as possible the situation of the clay in the disposal facility and, on the other, maintain a fundamental characteristic of the material, as it is porosity, constant throughout the determination, two experimental methods have been set up, allowing the suction applied to be controlled and preventing variations in the volume of the sample during the test.

These methods are: determination of the retention curve in oedometers with suction controlled and the use of perforated, non-deformable cells in an atmosphere of controlled relative humidity. The experimental procedures are described in the section "Retention curve at constant volume". The first has been used to determine the curves at 20 °C, and the second, which was developed later on, to determine the curve at 40 °C. The dimensional control of the sample, which is achieved only on wetting paths, is much better when the non-deformable cells are

used, these having been designed specifically for this type of test.

Retention curve at 20 °C

In order to determine the retention curve at 20 °C, oedometers with controlled suction were used, as described in the section "Controlled suction oedometric testing", these allowing suction to be controlled by means of two different techniques. For suctions in excess of 3 MPa, the technique used consists in controlling the relative humidity of the atmosphere surrounding the sample, introducing sulphuric acid solutions with a weight percentage of between 6 and 67 percent in the deposit placed inside the oedometer cell (Figure 48). For suctions of between 14 and 0.1 MPa the axis translation technique was used, applying the desired nitrogen pressure inside the oedometer cell (Figure 47).

In oedometers it is possible to maintain the volume of the sample constant only during hydration processes, since swelling may be avoided by loading the sample, but not the shrinkage that occurs on desiccation. Furthermore, it is difficult to achieve perfect control of the sample volume, and a certain variation of dry density occurs during the test, especially in the case of high dry densities specimens, whose swelling cannot be completely counteracted given the capacity of the equipment.

The specimens used were obtained by uniaxial compaction of the clay directly in the oedometer ring, with its hygroscopic water content. These specimens have initial dry densities of 1.60, 1.65 and 1.70 g/cm^3, and measure 1.20 cm in length, with a cross section of 11.40 or 19.24 cm^2.

The table XXXI shows the characteristics of the tests performed. Given that all the samples initially have their hygroscopic water content, which is equivalent to a suction of approximately 130 MPa, in the tests performed using oedometers with suction control by nitrogen pressure, in which the maximum applicable suction is 14 MPa, the sample initially undergoes a sudden reduction in suction, with the corresponding hydration. Wetting paths were applied, beginning at 14 MPa in the case of the oedometers with suction control by nitrogen pressure, and at 130 MPa in the oedometers in which suction is controlled by solutions. This last value was chosen because it is the suction of the compacted clay with its hygroscopic water content, and therefore, the initial one of the blocks manufactured for the *in situ* and mock-up tests of the FEBEX Project. In certain cases, a drying path was applied following saturation.

The following tables summarise the characteristics of the sample at the end of each step in the different tests performed. In the test carried out with nitrogen pressure, the tables indicate as the first step the conditions of the compacted sample prior to initiation of the test. Also included is the pressure that needs to be applied to maintain volume constant at each step, this indicating the swelling pressure of the clay for different suctions. The degree of saturation reflected in the tables has been calculated considering the density of the water to be 1.00 g/cm^3, that is to say, that of free water. As explained in the section "DENSITY OF WATER", this might not be the case when the sample is saturated at constant volume, and consequently "fictitious" degrees of saturation of more than unit value have been obtained. Furthermore, it may be appreciated that, as hydration progresses, there is a reduction in dry density, which, especially in the case of oedometers with suction controlled by nitrogen pressure, may be important.

Table XXXI
Tests performed to determine the retention curve at constant volume at 20 °C.

Reference	Dry density (g/cm^3)	Suction control	Path* (MPa)
EDN1_6	1.59	Nitrogen	14-0
EDN4_8	1.60	Nitrogen	0-14-0
EDN5_7	1.75	Nitrogen	0-14-0
EDS1_11	1.75	Solutions	114-2-476
EDS5_6	1.64	Solutions	118-1-130

**The initial value of suction is in all cases approximately 130 MPa (laboratory RH).*

Table XXXII
Results of the retention curve for the wetting path at a nominal dry density of 1.60 g/cm^3 (EDN1_6).

Suction (MPa)	ρ_d (g/cm^3)	w (%)	S_r^*
130	1.59	12.8	0.49
14.0	1.58	23.8	0.90
8.0	1.58		
5.0	1.58	27.1	1.03
3.0	1.58	27.9	1.06
1.5	1.58	29.0	1.10
0.5	1.58	29.8	1.13
0.1	1.58	29.2	1.11
0.0	1.58	29.8	1.13

**Degree of saturation calculated considering the density of free water.*

Table XXXIII
Results of the retention curve for the wetting/drying/wetting path at a nominal dry density of 1.60 g/cm^3 (EDN4_8).

Suction (MPa)	ρ_d (g/cm^3)	w (%)	S_r^*	P_s (MPa)
130	1.60	14.4	0.57	0.0
0.0	1.53	27.9	0.99	5.7
0.1	1.53	28.1	1.00	5.7
0.5	1.53	27.6	0.98	5.7
1.5	1.54	26.3	0.94	5.6
3.0	1.54	27.1	0.98	5.6
5.0	1.56	26.0	0.96	5.5
8.0	1.58	24.9	0.95	5.4
14.0	1.62	23.0	0.93	5.1
8.0	1.61	23.3	0.93	5.4
3.0	1.60	23.8	0.94	5.5
1.5	1.59	25.7	0.99	5.5
0.5	1.58	25.6	0.98	5.5
0.1	1.49	32.2	1.08	5.6
0.0	1.49	30.4	1.02	5.6

Table XXXIV
Results of the retention curve for the wetting/drying/wetting path at a nominal dry density of 1.75 g/cm^3 (EDN5_7).

Suction (MPa)	ρ_d (g/cm^3)	w (%)	S_r^*	P_s (MPa)
130	1.75	13.4	0.67	0.0
0.0	1.65	26.5	1.13	9.4
0.1	1.64	26.1	1.09	9.4
0.5	1.62	26.5	1.08	9.4
1.5	1.63	26.5	1.08	9.3
3.0	1.64	25.6	1.07	9.2
5.0	1.66	25.6	1.11	9.1
8.0	1.67	24.9	1.08	8.9
14.0	1.71	24.3	1.14	8.2
8.0	1.70	24.0	1.09	8.2
5.0	1.68	24.4	1.09	8.4
3.0			1.25	8.5
1.5	1.68	25.1	1.12	8.6
0.5	1.65	25.4	1.08	8.7
0.1	1.68	25.3	1.12	8.7
0.0	1.68	25.9	1.15	8.7

*Degree of saturation calculated considering the density of free water.

The water contents reached during the hydration processes are shown in Figure 91. The figure also includes the fittings between suction and water content for the same type of path obtained in free volume tests. The dry density intervals indicated in the figure correspond to the values at the beginning and the end of the path. The difference between the values of water content reached on the free volume and constant volume paths is particularly noteworthy. In the case of the free volume paths, the water content reached for a given value of suction is greater than in the case of constant volume, the difference between the two increasing with decreasing suction. The value of suction from which the difference between the two paths becomes clearer is higher for the higher densities. Thus, for a dry density of 1.75 g/cm^3, this value is around 30 MPa, and for a dry density of 1.60 g/cm^3 it is around 8 MPa. In both cases, it is necessary to apply the maximum vertical load to counteract swelling when the sample is close to saturation. Furthermore, it may be seen that, unlike what occurred on the free volume paths, the water content reached for a given value of suction is higher the lower the initial dry density, although this difference is appreciated only for suctions of less than 14-30 MPa.

Romero (1999) points out that for the Boom clay there is a range of suctions, between 200 and 2 MPa, in which dry density has very little influence on the value of water content reached for a given suction, due to the fact that transfers of water occur at intra-aggregate level and depend on the specific surface of the clay; *i.e.* its mineralogical composition. Nevertheless, this author warns of the error that may occur if these suction/water content relations, determined without taking initial dry density into account, are extrapolated for suctions below

Table XXXV
Results of the retention curve for the wetting/drying path at a nominal dry density of 1.75 g/cm^3 (EDS1_11).

Suction (MPa)	ρ_d (g/cm^3)	w (%)	S_r^*	P_s (MPa)
114	1.75	13.4	0.67	0.4
75	1.74	16.3	0.80	2.4
31	1.74	19.3	0.94	9.6
14	1.72	22.2	1.04	9.6
4	1.69	24.7	1.12	9.6
2	1.69	26.4	1.20	9.6
4	1.69	25.9	1.17	9.6
13	1.69	24.5	1.11	9.6
34	1.72	21.6	1.03	9.6
72	1.75	19.4	0.97	6.4
132	1.77	14.6	0.74	0.1
179	1.77	12.0	0.62	0.1
251	1.77	8.2	0.42	0.1
476	1.79	6.0	0.32	0.1

**Degree of saturation calculated considering the density of free water.*

Table XXXVI
Results of the retention curve for the wetting/drying path at a nominal dry density of 1.67 g/cm^3 (EDS5_6).

Suction (MPa)	ρ_d (g/cm^3)	w (%)	S_r^*	P_s (MPa)
118	1.67	13.0	0.56	0.0
73				0.3
33				3.5
14	1.61	19.3	0.78	4.5
4	1.61	27.7	1.12	5.4
1	1.58	28.5	1.15	5.6
4	1.59	29.3	1.18	5.6
13	1.58	29.0	1.17	5.4
22	1.63	28.8	1.19	5.6
60	1.68	19.6	0.87	1.6
130	1.69	16.3	0.75	1.6

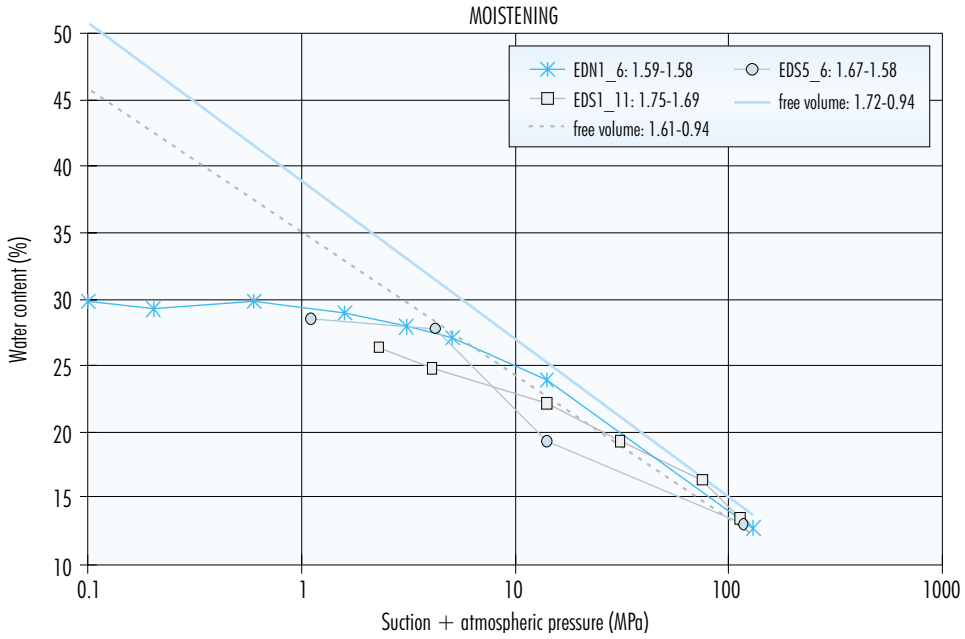

Figura 91. Values of water content reached on wetting paths at constant volume compared to those obtained at free volume for different dry densities (expressed in g/cm³).

the lower limit of the range. In fact, as may be appreciated on the different curves adjusted in this work, the repercussion of initial dry density on the value of water content reached is more obvious as suction decreases. In the case of the FEBEX bentonite, however, the lower limit of suction above which the influence of initial dry density is not noticeable is between 8 and 30 MPa, depending on dry density (Figura 91). In other words, while in a weakly expansive clay, such as the Boom clay, the lower limit of intra-aggregate suction is at 2 MPa, in a highly expansive clay, such as the FEBEX clay, it is located at higher values, this also reflecting the differences in reactive porosity between the two.

Furthermore, unlike what occurred for the curves determined at free volume, the confined samples reach total saturation, for a value of suction that becomes higher with increasing dry density. Thus, the samples with a dry density of 1.75 g/cm³ are saturated below a suction of 14 MPa, while for those having a dry density of 1.60 g/cm³ this value is at around 4-5 MPa, this probably being due to the smaller average diameter of the pores in samples compacted at higher density. Figure 92 shows the variation of the degree of saturation with suction on these wetting paths. It may be observed that the degrees of saturation calculated using the value of 1.00 g/cm³ for water density are greater than the unit. On these curves no value is distinguished for the exit of air from the macroporosity, as was the case for the curves determined at free volume. This is due to the fact that, being in confined conditions, the intra-aggregate pores invade the space occupied by the inter-aggregate pores, because saturation at constant volume causes macropores to disappear in favour of smaller pores, thus reducing the average pore size.

Two of the tests represented in Figura 91, EDS1_11 and EDS5_6, continued with drying of the sample. The water content reached at each step, on both the wetting path already dealt with and on drying, is shown in Figure 93. The effect of hysteresis –which is higher in the sample of lower density– may be appreciated, this resulting in a value of water content being reached during the process of drying higher than that obtained for the same suction during previous wetting. Thus, for example, when a specimen with a dry density of 1.75 g/cm³ is hydrated from initial equilibrium conditions, the degree of saturation reaches 1,0 below suctions of 14 MPa. When

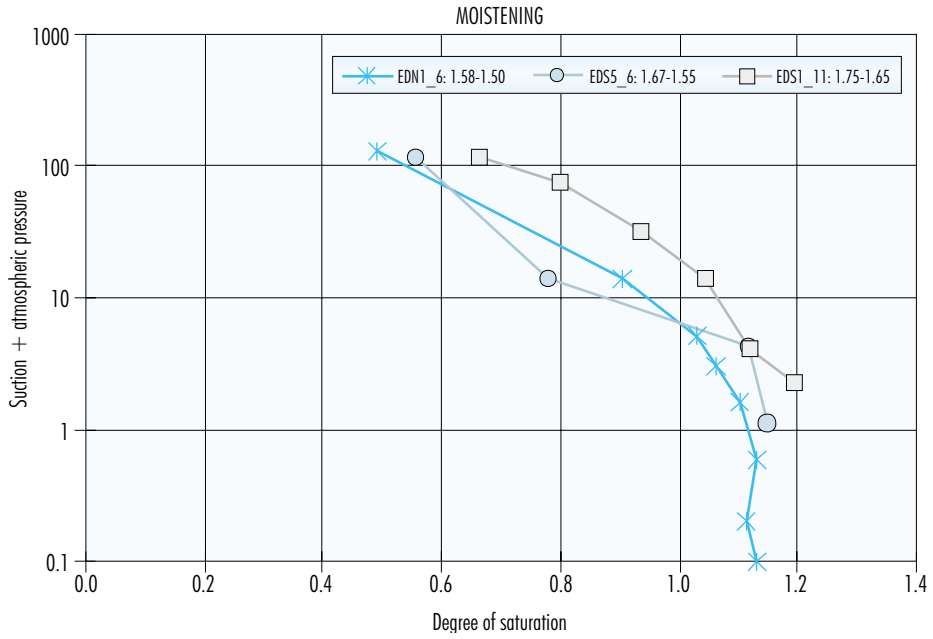

Figure 92. Retention curves at constant volume for different dry densities (expressed in g/cm³).

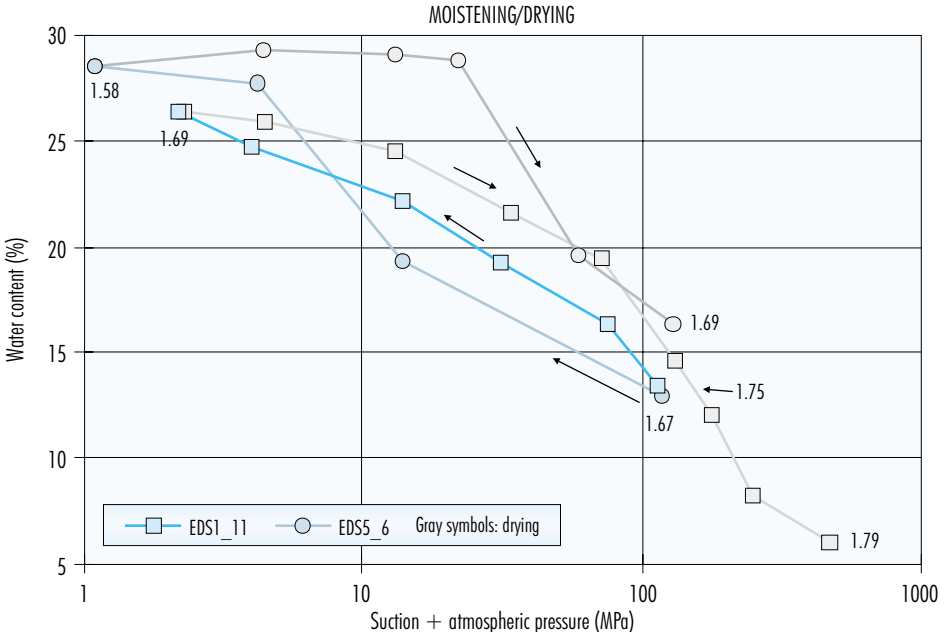

Figure 93. Values of water content reached on wetting/drying paths at constant volume (the dry densities corresponding to the ends of each path are indicated in g/cm³).

the suction applied is later increased, the specimen does not begin to desaturate until values of more than 40 MPa are reached (test EDS1_11). A contributing factor to this is probably the reduction in volume that the sample undergoes during drying, which cannot be avoided and which causes an increase in the degree of saturation. In the EDS1_11 test the sample dried to a water content of 6 percent for a value of suction of 476 MPa, with a degree of saturation of 0.32, which is not too low since dry density undergoes an important increase during drying.

Figure 94 once again shows the values corresponding to the process of drying after wetting for the two previous tests, along with those corresponding to tests EDN4_8 and EDN5_7. In the latter, the initial wetting path consists in a single step, in which the sample changes, when placed in the oedometer at the beginning of the test, from 130 MPa –the value corresponding to the hygroscopic water content– to 0 MPa, after which the drying of the sample commences. The figure also includes the fitting between suction and water content for the drying path obtained during free volume testing. This last curve was obtained for values of suction in excess of 139 MPa in samples that had not previously been hydrated, and consequently it does not correspond exactly to the path followed at constant volume. The intervals of dry density indicated in the figure correspond to the values at the beginning and the end of the path. During drying, there is not a significant reduction in water content until values of suction of above 14 MPa, this becoming clearer from a slightly higher value. This value is probably different for each dry density, although there are insufficient experimental data for this to be corroborated. For suctions in excess of this limit value, the curves obtained under free and constant volume conditions overlap, since in neither case is it possible to avoid shrinkage of the sample, the difference between the two methods disappearing.

The results of the complete wetting/drying/wetting cycle for the EDN4_8 and EDN5_7 tests, which have been partially presented above, are shown in Figure 95. The effect of hysteresis may once more be appreciated, this leading to higher values of water content for a given degree of suction on the drying after wetting path than during subsequent wetting. However, this difference becomes smaller at lower values of suction, as happened on the curves determined under free volume conditions.

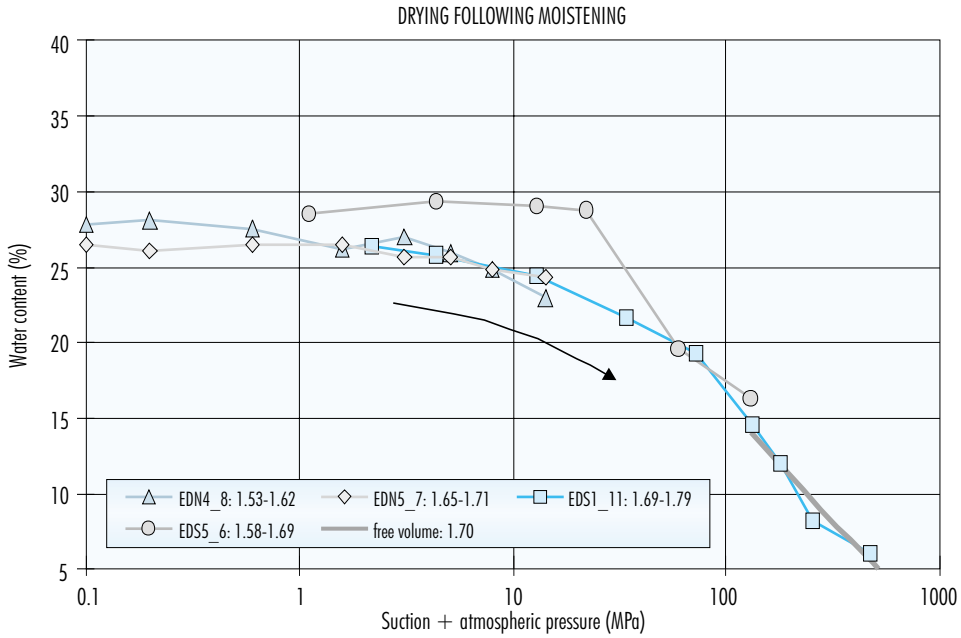

Figure 94. Values of water content reached on drying after wetting paths at constant volume compared to those obtained at free volume (drying) for different dry densities (expressed in g/cm³).

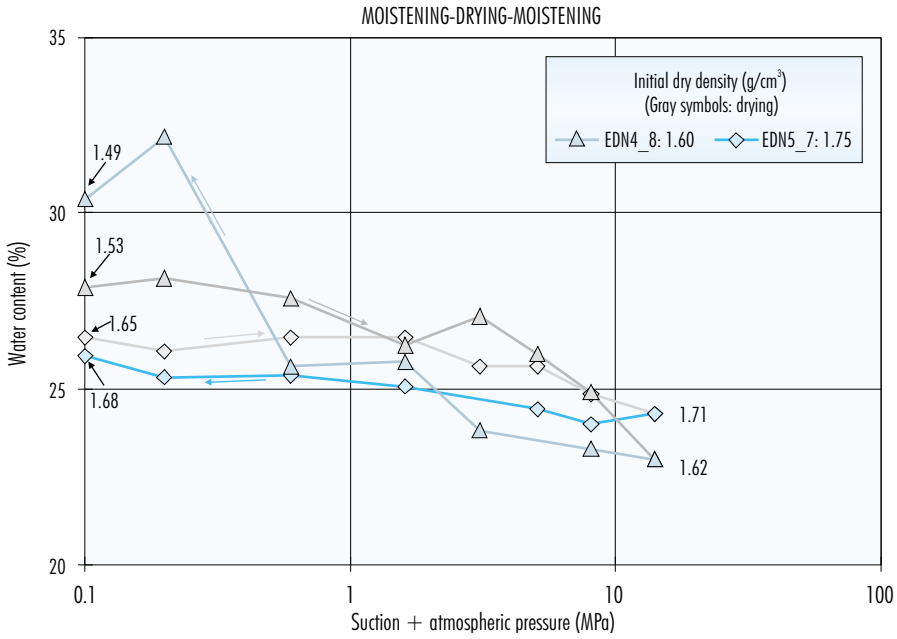

Figure 95. Values of water content reached on wetting/drying/wetting paths at constant volume. The initial wetting consists of a single step. The dry densities corresponding to the ends of each path are indicated in g/cm³.

Retention curve at 40 °C

In view of the fact that the clay in the barrier of a disposal facility will be subject to different temperatures, depending on its exact position with respect to the waste container and on the time elapsing after its emplacement, it is necessary to check whether the retention curves determined at 20 °C are valid for higher temperatures. This issue has been addressed in a preliminary manner in this work through the determination of two retention curves at 40 °C. For this purpose we have designed cylindrical cells in which the sample is compacted directly and in which volume variation is prevented, while the exchange of water content between the sample and the atmosphere of controlled relative humidity in which the cell is placed (desiccator with sulphuric acid solution) is allowed. The desiccator is in turn placed in an oven with regulated temperature. The same value of suction is maintained until the weight of the samples stabilises –this indicating the completion of water transfer– for which a period of between two and three months is required. Once equilibrium has been attained, the process moves on to the next suction step, with the solution in the desiccator being changed. The determination is accomplished following the procedure described in the section "Retention curve in non-deformable cells".

As was the case with the oedometers, the cells prevent variations in the volume of the sample only when swelling occurs, *i.e.* on wetting paths, this not being the case when there is shrinkage. With this method, the restriction of deformation imposed on the sample during hydration is complete, as a result of which there is no interval of densities for the same curve, as is the case when controlled suction oedometers are used. However, these cells do not allow for the measurement of swelling pressure that is possible in the oedometers.

Two curves were determined for a wetting path for suction values of 150 to 2 MPa. One of the curves corresponds to samples with a dry density of 1.65 g/cm^3, and the other with a dry density of 1.70 g/cm^3. The determination of each of the curves was performed using three samples having the same initial characteristics, each in its own cell. The length of the specimens was 1.20 cm and their cross section 3.80 cm^2. The pressure applied for compaction was between 19 and 35 MPa.

The results obtained are shown in Table XXXVII.

Table XXXVII
Results for the retention curve at 40 °C on the wetting path at constant volume (average of 3 determinations).

Dry density: 1.65 g/cm^3			Dry density: 1.70 g/cm^3		
Suction (MPa)	w (%)	S_r^*	Suction (MPa)	w (%)	S_r^*
149.4	13.6	0.58	151.3	13.9	0.64
71.0	16.8	0.71	58.1	17.9	0.82
31.6	20.2	0.86	32.2	20.4	0.94
12.0	22.9	0.97	12.3	22.8	1.05
3.2	24.9	1.06	5.2	24.1	1.11
2.3	26.1	1.11	2.3	25.6	1.17

*Degree of saturation calculated considering the density of free water.

For all values of suction, the samples having a dry density of 1.70 g/cm^3 reach higher degrees of saturation than those having a dry density of 1.65 g/cm^3, due to their smaller pore size (Figure 96). Furthermore, the samples with a dry density of 1.70 g/cm^3 reach saturation for a higher value of suction than those with a density of 1.65 g/cm^3. This value is between 30 and 12 MPa for the first of these densities and between 12 and 3 MPa for the second. Below this value of suction, degrees of saturation even higher than unit value are recorded, this being due to the fact that the calculation was performed considering the density of the water to be equal to 1.00 g/cm^3 (see section "DENSITY OF WATER"). This value of suction, below which the sample is saturated, is of the same order as that found for samples of similar dry density at 20 °C (test EDS1_11).

The values of water content versus suction are shown in Figure 97, along with the results obtained at 20 °C on the constant volume retention curves belonging to the ranges of dry density closest to those studied at 40 °C (tests EDS5_6 and EDS1_11). The figure also includes the fitting obtained for the free volume wetting path for an initial dry density of 1.75 g/cm^3 at 20 °C (which remains at lower values of dry density along the entire path). Although there are no major differences between the water content curves for dry densities of 1.65 and 1.70 g/cm^3 at 40 °C –probably due to the fact that these are very close values–, at the beginning of hydration the water content of the samples with a higher dry density is greater for the same values of suction. However, when lower values of suction are reached, the water content of the denser samples is lower. This is because the volume of small pores is higher in samples with a higher dry density, due to the fact that the volume of large pores is reduced during compaction, as a result of which the sample takes up more water at the beginning of hydration. As suction decreases and the degree of saturation increases, however, the lower total porosity of the samples of greater density limits their possibility for water uptake.

The curves obtained at 40 °C are very similar to those plotted for the interval of dry densities of 1.75-1.69 g/cm^3 at 20 °C (test EDS1_11); although for the same suction certain slightly higher values of water content are recorded at 40 °C than at 20 °C.

Consequently, it has not been possible to clearly identify the influence of temperature in the range 20-40 °C on the retention curve values in terms of water content, which, in any case, would not appear to be important. On retention curves determined under free volume conditions for compacted Boom clay, the behaviour trend observed is that the water content of the sample decreases with temperature for a given value of suction (Bernier *et al*. 1997, Romero 1999).

Fittings to the van Genuchten expression

A fitting was performed using the experimental values obtained during the different tests with common paths taking an expression of the van Genuchten equation (1980), which relates the effective degree of saturation (S_{re}) and the suction (s) by means of

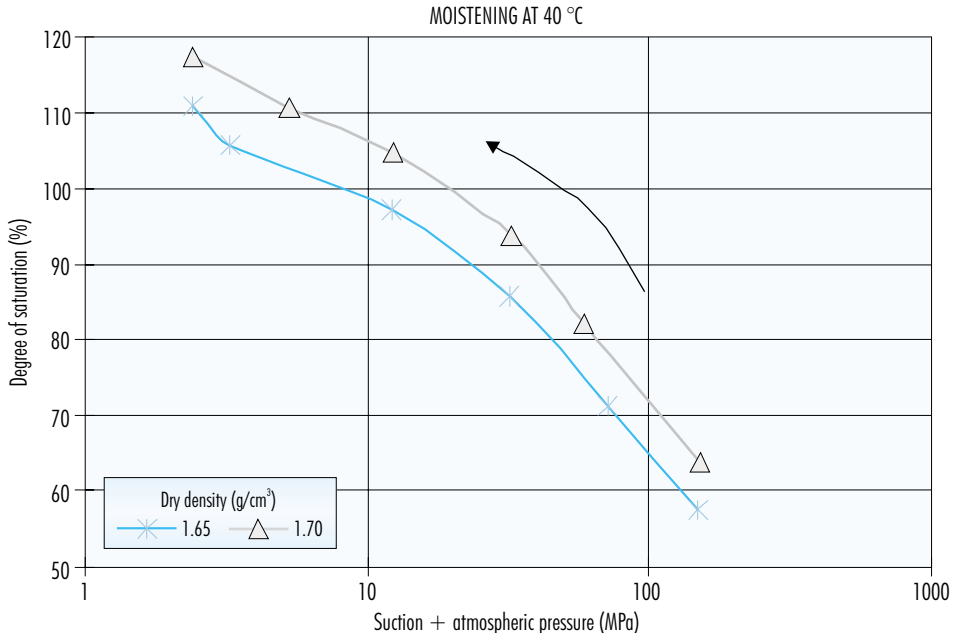

Figure 96. Average values of degree of saturation reached on wetting paths at constant volume at 40 ° C.

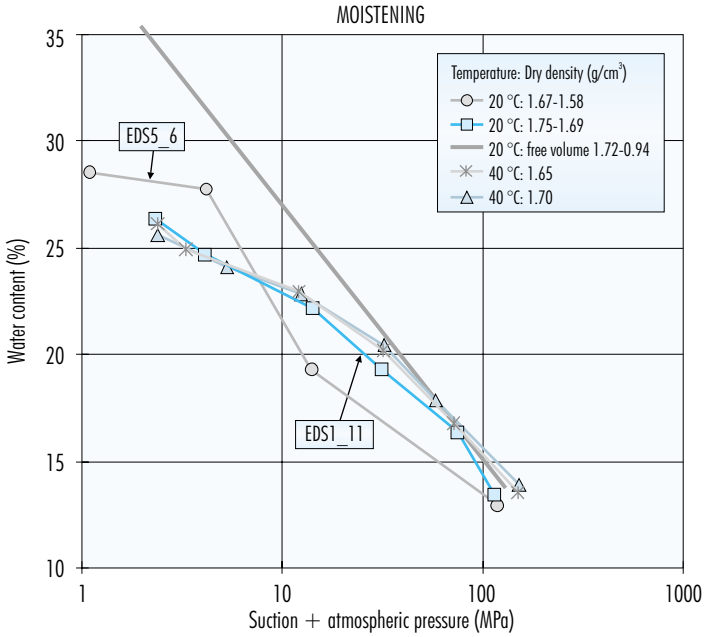

Figure 97. Values of water content reached on wetting paths at constant volume and fitting obtained at free volume for different temperatures.

the following expression, corresponding to the wetting path:

$$S_{re} = \frac{1}{\left(1+\left(s/P_w\right)^{\frac{1}{1-\lambda_w}}\right)^{\lambda_w}}$$

and its equivalent for the drying path:

$$S_{re} = \frac{1}{\left(1+\left(s/P_d\right)^{\frac{1}{1-\lambda_d}}\right)^{\lambda_d}}$$

where P_w and λ_w are parameters of the material for wetting and P_d and λ_d are for drying. The effective degree of saturation is determined in accordance with the following expression:

$$S_{re} = \frac{S_r - S_{r\,res}}{S_{r\,max} - S_{r\,res}}$$

where S_r is the degree of saturation, $S_{r\,max}$ is the maximum degree of saturation and $S_{r\,res}$ is the degree of residual saturation, which indicates the quantity of water that cannot be extracted without subjecting the sample to a very high increase in suction.

An $S_{r\,res}$ of 0.16 or 0.18 has been taken to calculate the effective degree of saturation, depending on the dry density of the test. This was taken in view of the experimental results from the retention curves determined at free volume, which show decreases in water content depending on suction of the same order for the entire range of suctions investigated, these becoming smaller only for suctions in excess of 400 MPa, for which a degree of saturation close to these values was measured (Table XXV). The use of these data deduced from the free volume curves is justified since, for high values of suction, both methods –free volume and confined– are equivalent, this being the case because there is no swelling to be counteracted and the changes in density are not over large. The maximum degree of saturation ($S_{r\,max}$) is considered to be 1.00, since, on being confined, the sample saturates completely in all the tests.

Table XXXVIII reflects the tests from which data were taken for the different fittings and the values obtained for each parameter depending on the path involved. The coefficients of the fittings are calculated using a non-linear least squares technique. In carrying out these fittings, all those points at which the degree of saturation was higher than 1.00 due to the density of free water having been used for calculation, were taken to this value. No fitting was made for wetting after drying (tests EDN4_8 and EDN5_7) because the data were inadequate, since the sample remained saturated along the entire path.

Table XXXVIII
Coefficients of fittings according to the van Genuchten expression between suction and effective S_r versus type of path, dry density and temperature.

Tests	Dry density (g/cm³)	Path (MPa)	P_w or P_d (MPa)	λ_w or λ_d	Max. S_r	Residual S_r	r^2
EDN1_6 EDS5_6	1.60	Wetting 130 to 0	15.94±4.19	0.29±0.03	1.00	0.16	0.962
EDN4_8 EDS5_6	1.60	Drying / wetting 130 / 0 / 130	66.78±29.42	0.28±0.10	1.00	0.16	0.815
EDS1_11 EDN5_7	1.75	Wetting 130 to 0	80.76±6.37	0.46±0.03	1.00	0.18	0.994
EDN5_7 EDS1_11	1.75	Drying / wetting 130 / 0 / 476	146.86±4.71	0.65±0.02	1.00	0.18	0.995
40 °C	1.65	Wetting 150 to 2	40.24±3.35	0.34±0.02	1.00	0.17	
40 °C	1.70	Wetting 150 to 2	70.31±8.25	0.39±0.04	1.00	0.18	

A graphic representation of the experimental values and fittings is shown in Figure 98, which includes the curves at 20 and at 40 °C. It may be appreciated, on the one hand, that the effective degree of saturation for the same suction is higher in the samples of greater dry density and, on the other, that the effect of hysteresis is clearer for lower densities. Likewise, the retention curve at 20 °C for a dry density of 1.75 g/cm^3 practically coincides with the curve for a dry density of 1.70 g/cm^3 at 40 °C. This suggests an increase in retention capacity with increasing temperature or deficient control of the volume of the sample during determination for the dry density of 1.75 g/cm^3, which was accomplished in controlled suction oedometers, the dry density possibly having decreased to values close to 1.70 g/cm^3.

The first hypothesis would coincide with the fact that the water contents for a given suction are slightly higher at 40 °C than they are at 20 °C. This tendency is contrary to that found with other materials, where the free volume retention capacity decreases with temperature (Romero 1999). Once again, this difference might be the result of the method used for determination, since the behaviour of the sample might differ depending on the possibility for volume variation.

Conclusions

From what has been dealt with in previous sections, the following conclusions may be reached as regards the retention curves:

- The contribution made by osmotic suction to the total value of suction is insignificant, this meaning that in this bentonite the suction is fundamentally of the matric type.
- In this bentonite, the relation between suction and water content does not depend on the method used to manufacture the sample, trimming or compaction.
- On the curves determined under free volume conditions, the porosity of the bentonite varies with varying suction, with dry density decreasing with increasing water content and *vice versa*. On these curves, the relation between suction and water content is logarithmic on any type of path, while the relation between

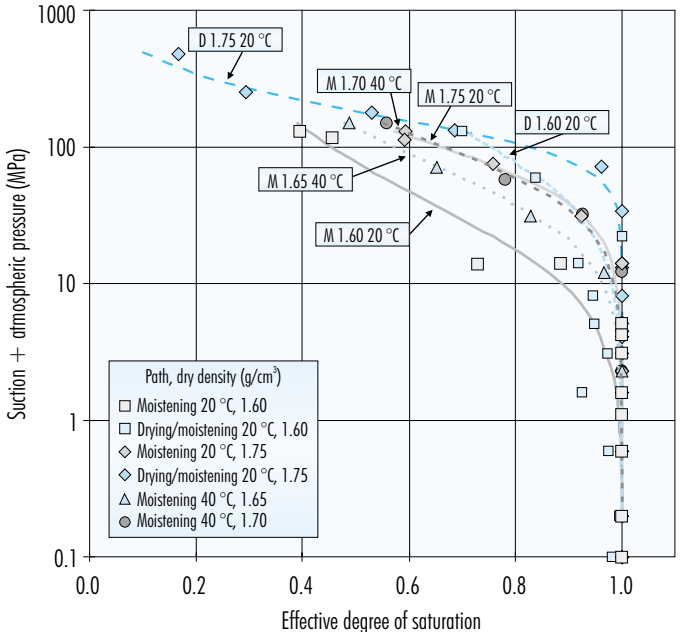

Figure 98. Experimental values of the retention curve for different densities (in g/cm^3), temperatures and paths, and fittings according to the van Genuchten expression.

suction and density fits better with a potential type equation.

- For free volume paths, a certain influence of the path and the value of initial dry density is appreciated on the retention curves, equations relating suction with water content and suction with dry density, depending on initial dry density, having been obtained for wetting, drying and wetting after drying. The samples with higher initial dry density reach higher values of water content for the same suction, this being attributed to the larger number of small pores, susceptible to being affected by a given value of suction during wetting.
- The water contents reached for a given value of suction are somewhat lower if there has been previous drying, although this difference in water content between the wetting and wetting after drying paths tends to become smaller as suction decreases. In fact, from a certain value of suction, the values of water content obtained are even higher in previously dried samples.
- On free volume paths, with a constant change in the porosity of the sample during wetting, the increase in the degree of saturation that would be caused by the water content increase is counteracted by the reduction in dry density, as a result of which there is an interval of suction in which variations in this parameter do not modify the degree of saturation. This suction interval spans approximately 0.5 to 100 MPa, the lower value being the point at which air exits the macropores and the higher value the point at which this same occurs from the microstructure on wetting paths. Furthermore, on free volume retention curves the maximum degree of saturation is between 60 and 80 percent, depending on initial dry density.
- On retention curves at constant volume, on the contrary, the water content reached for a given value of suction is greater the lower the initial dry density, but the degree of saturation for a given suction is always higher in samples with higher dry density. For all the dry densities tested, the samples saturate completely below a given value of suction, this being lower the lower the dry density of the sample.
- On drying after wetting paths at constant volume, the water content reached during drying is greater than that obtained for the same value of suction during previous wetting.
- On paths under free volume conditions, the water content reached for a given value of suction is higher than that attained at constant volume, the difference between the two increasing as suction decreases. The value of suction as from which the difference between the two paths becomes more accentuated is higher for higher densities, and is located approximately between 30 and 8 MPa. Above these values, the suction/water content relation would be controlled by the microstructure and would be independent from dry density (intra-aggregate suction), while below them it would be controlled by the macrostructure (inter-aggregate suction).
- The difference between the curves obtained at constant volume at 20 and 40 °C is very small, and cannot be further evaluated.

Mechanical characterisation

The mechanical characterisation of the material has been addressed only from the point of view of volume changes under different saturation and load conditions, without including the study of strength.

Swelling pressure

For this study, swelling pressure has been determined using samples with different values of dry density, compacted directly in the oedometer ring and saturated with distilled water. A check has been made also on the influence of the type of water used to saturate the samples, with tests performed using granitic and saline waters (see section "WATER USED"). Likewise, and with a view to checking the anisotropy of this property, the test was carried out on specimens trimmed in two directions from larger blocks, placed in the oedometer parallel and perpendicular to the direction of compaction of these blocks. In all cases the clay was used at its hygroscopic water content and with the granulometry it had on leaving the factory (maximum grain size 5 mm). The specimens measured 19.63, 11.40 or 9.98 cm^2 in cross section and 1.20 cm in length.

Variation depending on void ratio

Swelling pressure was determined using specimens compacted uniaxially inside the ring of the oedometer to different densities. The sample is saturated with distilled water from the lower porous stone and

loads are applied to prevent deformation. Occasionally, and especially for dry densities in excess of 1.60 g/cm^3, the loading capacity of the equipment does not make it possible to completely counteract the deformation of the specimen, as a result of which the final swelling pressure value obtained does not correspond to nominal (initial) dry density but to final dry density, which is lower. For this reason, Table XXXIX includes the swelling pressure obtained in each test and the initial and final values of dry density and water content, as well as the final degree of saturation. It may be appreciated that the degrees of saturation obtained exceed 100 percent, especially for higher dry densities. As was discussed in the section "DENSITY OF WATER", these values for the degree of saturation are the result of using the density of free water for calculation, what might not be correct, especially in the case of higher dry densities. The greater experimental difficulty encountered in determining very high values of swelling pressure –arising from the limitation of the equipment, which is not designed for the application of such high loads– translates into a wider dispersion of the values obtained for dry densities in excess of 1.65 g/cm^3.

Table XXXIX
Swelling pressure of specimens compacted at different dry densities and saturated with distilled water.

Initial ρ_d (g/cm^3)	Final ρ_d (g/cm^3)	Initial w (%)	P_s (MPa)	Final w (%)	Duration (days)	Final S_r^* (%)
1.29	1.26	15.0	0.5	48.6	3	116
1.29	1.28	14.9	0.3	49.9	3	121
1.34	1.34	13.2	0.8	40.3	3	107
1.35	1.35	12.5	0.5	40.8	3	110
1.36	1.35	14.0	1.0	39.7	3	106
1.37	1.36	12.6	1.4	38.4	3	105
1.41	1.40	14.5	2.0	34.8	4	102
1.45	1.43	13.0	1.5	36.9	6	111
1.47	1.45	11.7	1.6	35.9	2	113
1.48	1.45	11.6	2.9	33.2	6	104
1.50	1.49	14.1	3.4	33.5	3	112
1.52	1.50	12.5	3.6	32.7	3	111
1.54	1.51	12.0	3.3	33.6	3	115
1.54	1.53	13.1	4.3	32.0	3	113
1.57	1.53	13.9	5.2	29.6	3	104
1.58	1.54	16.3	5.0	29.4	5	105
1.58	1.55	14.8	4.2	32.4	4	118
1.58	1.52	13.4	6.0	30.1	2	104
1.59	1.56	15.6	6.2	27.5	4	101
1.59	1.54	12.3	5.2	29.2	4	104
1.59	1.55	13.0	4.1	32.5	4	119

**Degree of saturation calculated considering the density of free water.*

Table XXXIX
Swelling pressure of specimens compacted at different dry densities and saturated with distilled water. (Continuation)

Initial ρ_d (g/cm³)	Final ρ_d (g/cm³)	Initial w (%)	P_s (MPa)	Final w (%)	Duration (days)	Final S_r^* (%)
1.59	1.56	13.8	3.6	29.9	3	111
1.59	1.54	14.0	5.6	29.7	4	107
1.60	1.54	12.9	4.9	30.5	7	110
1.60	1.56	14.1	5.6	28.5	4	105
1.60	1.57	12.5	5.2	28.4	3	107
1.60	1.56	14.2	3.4	31.9	3	118
1.61	1.57	13.5	6.8	28.3	5	107
1.62	1.59	12.9	3.2	29.9	5	116
1.62	1.59	13.0	5.4	31.0	7	119
1.62	1.55	13.0	5.6	30.2	7	110
1.63	1.57	12.7	4.8	27.5	3	103
1.64	1.61	12.0	5.2	26.7	3	107
1.66	1.63	14.2	13.6	26.1	4	107
1.67	1.63	12.0	9.9	26.9	6	111
1.68	1.65	12.5	8.9	26.7	5	114
1.69	1.67	11.6	9.2	28.0	7	122
1.69	1.67	16.6	8.4		3	
1.71	1.70	11.7	7.8	28.4	3	131
1.71	1.69	14.4	8.3	28.4	2	127
1.72	1.70	14.3	10.9	28.6	2	131
1.72	1.71	12.7	11.2	27.8	2	129
1.72	1.70	11.6	9.8	27.5	3	126
1.72	1.70	12.1	10.0	28.2	2	130
1.74	1.71	12.7	8.6	29.0	2	136
1.74	1.72	12.8	12.5	27.2	1	128
1.74	1.73	12.8	7.6	28.2	2	135
1.75	1.71	13.7	13.9	25.9	5	121
1.77	1.70	12.2	16.2	24.1	5	111
1.80	1.77	13.0	9.7	26.5	7	136
1.84	1.76	11.7	16.7	25.5	7	129
1.88	1.73	11.7	16.1	25.2	7	122

*Degree of saturation calculated considering the density of free water.

All the values obtained are shown in Figure 99. With the 52 points determined it is possible to obtain an exponential fit between swelling pressure (P_s, in MPa) and final dry density (ρ_d, in g/cm^3):

$$ln\ P_s = 6.77\ \rho_d - 9.07 \qquad (r^2 = 0.88)$$

The difference between the experimental values and this fitting is 25 percent on average, as is also shown in the figure. This dispersion, which is wider for higher dry densities, is due both to the natural variability of bentonite and to the measurement method used, which does not allow for high degrees of accuracy. Added to this is the fact that the equipment was occasionally used at the limit of its capacity, allowing for a certain deformation of the sample. Swelling pressure is highly sensitive to the above, the influence on the final value obtained of the path applied in determining this pressure having been underlined and demonstrated repeatedly (Gens & Alonso 1992).

Variation depending on type of water

The determination of swelling pressure was performed as described in the previous section on specimens manufactured from the clay with its hygroscopic water content, compacted at various densities but using granitic water to saturate the sample. The results obtained are shown in Table XL, which also includes the theoretical values of swelling pressure for samples of the same final dry density saturated with distilled water, in accordance with the fitting included in the previous section, and the deviation with respect to this theoretical value, the values of deviation being positive when the swelling pressure obtained is higher than the theoretical value.

Taking into account the dispersion of the data obtained for this parameter, due to the measuring technique used, it may be concluded that the values obtained using granitic water do not differ overmuch from those that would have been obtained for the same densities with distilled water, in accordance with the fitting shown in the previous section (Figure 100). Although it is generally accepted that swelling pressure decreases with the saline content of the solution, for montmorillonite compacted at high density the influence of the salinity of the water on the value of swelling pressure is inappreciable, especially in the case of calcium montmorillonite (Pusch 1994).

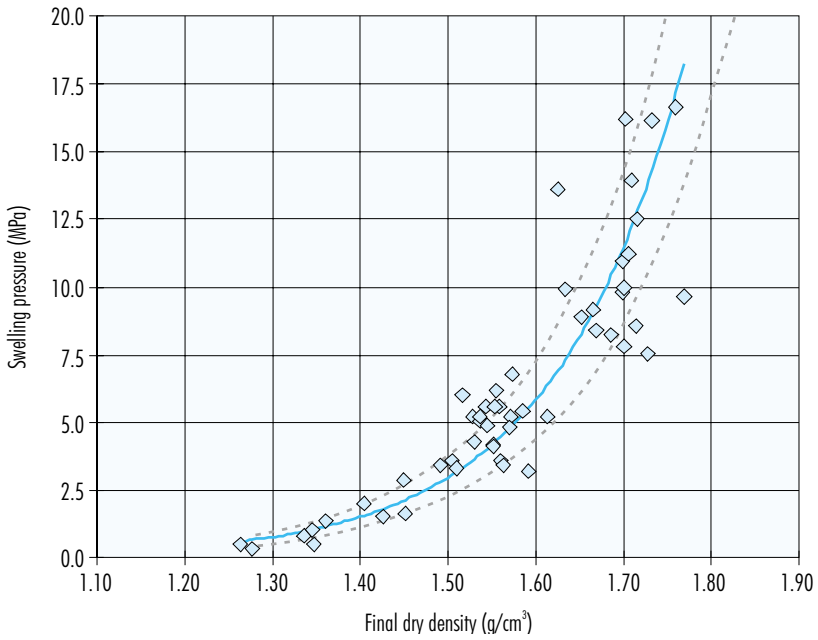

Figure 99. Values of swelling pressure versus dry density at the end of the test, obtained for saturation with distilled water, and exponential fit.

Table XL
Swelling pressure of compacted specimens saturated with granitic water and theoretical values for specimens of the same density saturated with distilled water.

Initial ρ_d (g/cm^3)	Final ρ_d (g/cm^3)	Initial w (%)	Final w (%)	Duration (days)	P_s (MPa)	Theoretical P_s (MPa)	Deviation (%)
1.43	1.41	14.5	36.6	6	1.5	1.6	-8
1.49	1.48	14.8	33.6	6	2.8	2.5	12
1.60	1.58	13.9	28.3	7	7.1	5.0	42
1.72	1.68	13.3	28.0	6	9.2	10.0	-8

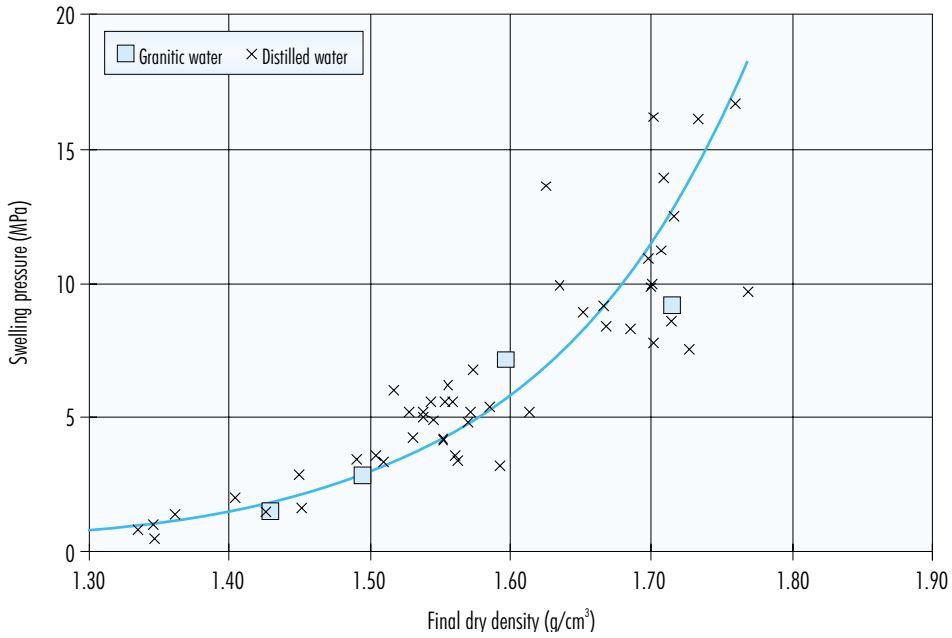

Figure 100. Swelling pressure obtained for clay saturated with distilled and granitic water.

Variation depending on direction of measurement

The determination of swelling pressure described in the previous sections is accomplished in all cases using specimens compacted directly in the oedometer ring and loaded parallel to the compaction force. With a view to checking the influence of the direction of measurement on the value of swelling pressure, various determinations were performed using specimens obtained by trimming certain of the blocks manufactured for the mock-up test within the FEBEX Project (see section "The FEBEX Project" and Figure 68). The trimming was performed using a cylindrical cutter of appropriate dimensions in two different directions: parallel to the block compaction force, *i.e.* vertically as the block is placed in the manufacturing position, and perpendicular to this force, *i.e.* in the horizontal direction. The first type is the one corresponding to the normal direction for test performance. Once the specimen, measuring 9.76 cm^2 in cross section and 1.20 cm in length, is obtained, it

is measured and weighed and inserted in the oedometer ring. The sample is saturated with distilled water from the lower porous stone, a constant volume being maintained through the addition of appropriate loads. Given that the fit between the trimmed specimen and the walls of the cell is not perfect, lateral swelling occurs during saturation, accompanied by a certain reduction in density. This may be calculated since the dimensions of the oedometer ring are fixed and known. This lateral swelling may affect the final value of swelling pressure, as a result of which the values obtained from samples compacted directly in the oedometer ring and from trimmed samples may not be strictly comparable.

Table XLI and Table XLII show the results obtained as a function of the direction of determination, along with the values that would have been obtained from samples of the same final density compacted directly in the oedometer ring and tested in the direction of compaction (fitting included in the section "Variation depending on void ratio"). Also included is the percentage of deviation of the value obtained with respect to the theoretical value, a positive sign indicating that the value obtained is higher than the theoretical value, and *vice versa*. The value of initial dry density reflected in the tables is obtained from the dimensions of the specimen prior to its insertion in the oedometer ring, while the

Table XLI
Values of swelling pressure obtained from samples trimmed perpendicular to compaction force.

Initial ρ_d (g/cm³)	Final ρ_d (g/cm³)	Initial w (%)	Final w (%)	Duration (days)	P_s (MPa)	Theoretical P_s (MPa)	Deviation (%)
1.52	1.44	13.4	36.0	3	1.9	1.8	4
1.64	1.60	14.1	31.0	3	6.1	5.5	11
1.65	1.60	13.7	30.8	3	5.8	5.6	5
1.64	1.63	14.7	30.0	4	6.1	6.7	-8
1.67	1.65	13.5	28.5	4	9.0	7.3	18
1.68	1.65	13.5	28.9	4	8.6	7.2	25
1.66	1.66	13.8	29.5	4	7.0	7.5	-6
1.69	1.67	15.8	28.6	2	8.5	8.3	2

Table XLII
Values of swelling pressure obtained from samples trimmed parallel to compaction force.

Initial ρ_d (g/cm³)	Final ρ_d (g/cm³)	Initial w (%)	Final w (%)	Duration (days)	P_s (MPa)	Theoretical P_s (MPa)	Deviation (%)
1.50	1.48	16.0	36.0	13	2.0	2.5	-20
1.56	1.52	14.4	32.7	3	5.3	3.3	26
1.56	1.51	15.2	31.4	3	4.1	3.2	65
1.65	1.60	16.1	29.4	6	8.3	5.9	42
1.65	1.61	15.7	29.6	6	8.3	6.4	30
1.79	1.72	13.5	28.6	2	10.0	13.5	-26
1.82	1.74	12.3	27.2	2	11.4	14.6	-22

final dry density value is calculated from the final length, with consideration given to the sample's filling on saturation the voids between the wall of the ring and the porous stones, as indeed occurs.

Figure 101 shows the values obtained in both directions along with the theoretical fitting obtained for compacted samples. As has been explained above, the values obtained from compacted and trimmed samples are not exactly comparable, although in this case a comparison between the theoretical value shown in Table XLI and Table XLII has been used to have a reference value with which to determine the difference between swelling pressures measured in one direction or the other. In fact, the values measured in trimmed samples are generally higher than those obtained from compacted samples. Before being inserted in the ring, the trimmed sample has a higher initial dry density than it does once saturated. This initial dry density is responsible for the pressure initially applied in the vertical direction, which is the pressure that has to be counteracted in the oedometer and, therefore, the one that gives the value of swelling pressure. This may be the reason for the differences observed between trimmed and compacted samples. If consideration is given to the initial dry density of the trimmed specimen, instead of that which results from filling of the lateral gap, the swelling pressures of trimmed specimens are lower than those of compacted specimens of the same density, this suggesting that the density in fact conditioning swelling pressure is an intermediate value between the initial and final densities.

Furthermore, the values obtained from samples trimmed parallel to compaction force are on average 14 percent higher than the theoretical values for compacted samples, while those obtained from samples trimmed perpendicular to this force are higher by 6 percent. This difference is not considered to be significant, since the scattering of the values obtained using the oedometer method for swelling pressure determination is large, and most of the values obtained from trimmed samples would fit with the scattering observed with compacted specimens. In any case, if any variation were expected, this should be precisely in the direction observed, *i.e.* the samples tested parallel to compaction should swell more. This is so because if there were any reorganisation of the material during compaction, it would affect the arrangement of laminar particles perpendicular to maximum force, which would

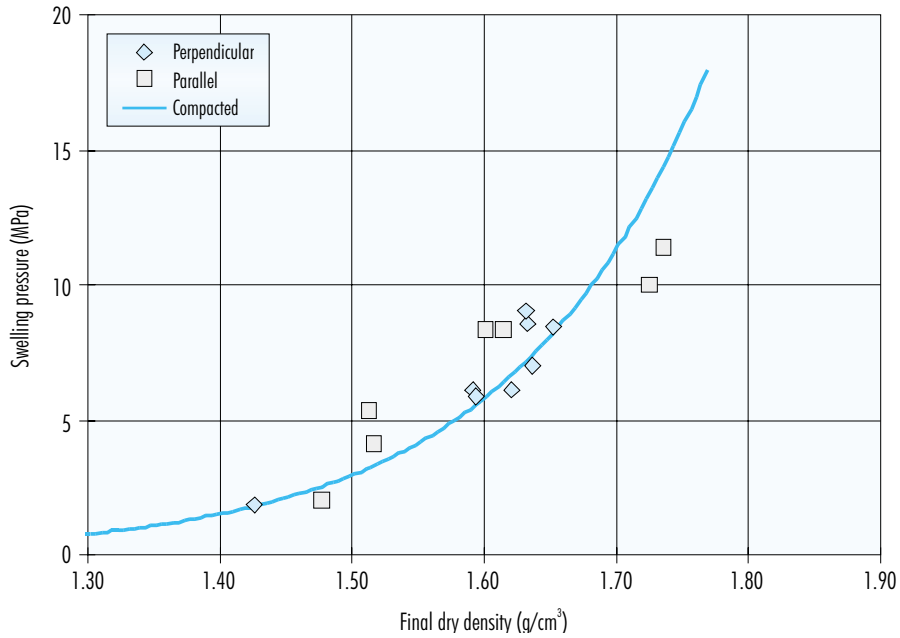

Figure 101. Swelling pressure obtained from specimens trimmed perpendicular and parallel to compaction force, and fitting obtained for compacted samples.

cause greater swelling in the direction parallel to compaction, *i.e.* in the direction of the c-axis of the mineral particles. As has been indicated above, this reorganisation would appear to be improbable, since compaction occurs very rapidly and with the material in the dry condition.

Swelling under load

The saturation (or swelling) under load test makes it possible to determine the strain capacity of the soil when it saturates under a previously established pressure. The test is performed using the oedometric equipment described in the section "OEDOMETER TESTS". The sample is compacted directly in an oedometer ring preventing lateral strain, confined between two porous stones located at the lower and upper parts. The desired load is applied to the sample and the cell is flooded, such that saturation occurs via the lower porous plate. The relation between the increase in final length undergone by the sample in equilibrium with the load applied and its initial length gives the value of strain experienced by the material on saturating under the load at which the test is performed.

In view of the fact that the mechanical behaviour of the clay may be strongly influenced by physico-chemical interaction between the clay particles and the fluid in the pores, the test was performed using both distilled water –used in all cases as a standard– and a saline and a granitic water having a composition similar to that which will be found in the bentonite barrier of the disposal facility, described in the section "WATER USED".

Tests were performed on the compacted clay with its hygroscopic water content at a dry density of 1.60 g/cm^3 and saturated with distilled water. In addition, three series of saturation under load tests were performed, using granitic water, with specimens compacted at a dry density of 1.50, 1.60 and 1.70 g/cm^3; and a further three series were carried out using saline water, with specimens compacted at the same dry densities. In all cases, the specimens were obtained by uniaxial compaction of the clay directly in the oedometer ring. The cross section of the specimens was 11.40 or 9.98 cm^2, and their initial length 1.20 cm. The duration of the tests exceeded 7 days. Table XLIII summarises the characteristics and results of the tests performed using distilled water, while Table XLIV refers to the tests performed using granitic water and Table XLV to those carried out with saline water.

Figures 102, 103 and 104 show the evolution of strain versus time in the tests performed using specimens with a nominal initial dry density of 1.60 g/cm^3 saturated under different loads with distilled water, granitic water and saline water, respectively. The last two figures show how swelling develops more rapidly in the samples subjected to lower loads; this is due to the fact that these samples are able to expand more, this causing a greater increase in pore size and, therefore, in permeability. This confirms the influence of void ratio on the value of permeability.

Table XLIII
Results of swelling under load tests with distilled water.

Pressure (MPa)	Initial ρ_d (g/cm^3)	Initial w (%)	Strain (%)	Duration (days)	Final w (%)	Final ρ_d (g/cm^3)
5.0	1.62	12.8	-17.2	15	39.1	1.39
5.0	1.62	13.0	-17.8	14	38.3	1.37
5.0	1.62	13.3	-12.1	14	38.4	1.44
5.0	1.60	14.6	-17.2	21	40.1	1.37
5.0	1.62	13.2	-17.8	15	39.3	1.37
9.0	1.59	15.0	-13.4	20	37.2	1.40
9.0	1.61	13.7	-14.7	19	36.6	1.40
9.0	1.61	14.2	-15.8	20	36.7	1.39

Table XLIV
Results of swelling under load tests with granitic water.

Pressure (MPa)	Initial ρ_d (g/cm^3)	Initial w (%)	Strain (%)	Duration (days)	Final w (%)	Final ρ_d (g/cm^3)
0.1	1.72	14.0	-28.6	7	35.1	1.34
0.5	1.72	13.9	-20.6	7	32.5	1.43
1.0	1.72	13.1	-18.3	21	32.1	1.46
3.0	1.72	13.0	-10.6	13	28.8	1.55
0.1	1.62	13.1	-25.1	7	41.0	1.29
0.1	1.61	13.1	-24.5	15	38.7	1.29
0.5	1.62	13.4	-14.3	7	38.3	1.41
0.5	1.54	18.4	-13.7	9	39.5	1.35
1.0	1.61	13.6	-10.6	7	36.6	1.46
1.0	1.61	13.0	-8.8	16	34.0	1.48
2.0	1.60	13.7	-3.3	9	32.2	1.54
2.0	1.62	12.5	-6.4	11	29.5	1.52
3.0	1.60	13.3	-1.5	8	30.5	1.57
3.0	1.60	13.3	-1.2	7	30.0	1.58
0.1	1.52	12.7	-22.9	10	46.3	1.23
0.5	1.51	13.5	-12.1	10	40.4	1.34
1.0	1.50	14.2	-8.5	13	34.2	1.38
3.0	1.49	15.0	-1.5	13	32.0	1.46

As was to be expected, the samples compacted at a dry density of 1.50 g/cm^3 undergo a somewhat smaller amount of strain following saturation than those compacted at a dry density of 1.60 g/cm^3 and saturated under the same load, while the samples compacted at a dry density of 1.70 g/cm^3 underwent greater strain on saturating under the same load, in both the tests performed with granitic water and those carried out using saline water.

Figure 105 shows the final values of strain versus the load applied for different initial dry densities, obtained in the saturation tests performed using granitic water. The relation between vertical load (σ, MPa) and strain (ε, %) is logarithmic and depends on initial dry density (ρ_d, g/cm^3); this may be expressed by means of the following equation:

$$\varepsilon = (-6.49\,\rho_d + 16.53)\ln\sigma + (-43.59\,\rho_d + 58.14)$$

The straight lines included in Figure 105 correspond to fittings obtained from this expression.

Figure 106 shows final values of strain versus the load applied for three initial dry densities, obtained from the tests on saturation with saline water. Once again, the relation between load (σ, MPa) and strain (ε, %) is logarithmic and depends on initial dry density (ρ_d, g/cm^3). It may be expressed by means of the following equation:

$$\varepsilon = 6.47\ln\sigma + (-48.71\rho_d + 66.13)$$

The straight lines included in Figure 106 correspond to fittings obtained with this expression.

Table XLV
Results of swelling under load tests with saline water.

Pressure (MPa)	Initial ρ_d (g/cm^3)	Initial w (%)	Strain (%)	Duration (days)	Final w (%)	Final ρ_d (g/cm^3)
0.1	1.71	13.0	-28.9	9	43.8	1.33
0.1	1.70	13.4	-33.1	14	43.7	1.28
0.5	1.72	12.7	-18.4	11	35.2	1.45
0.5	1.69	14.2	-23.0	14	39.3	1.38
1.0	1.70	14.1	-18.2	10	36.6	1.44
1.0	1.71	13.0	-16.3	17	31.9	1.47
3.0	1.68	15.0	-9.7	10	31.9	1.53
3.0	1.71	13.0	-9.5	17	28.5	1.56
0.1	1.60	13.6	-25.9	15	43.2	1.27
0.1	1.58	15.4	-25.8	11	36.8	1.25
0.5	1.61	12.9	-16.2	15	33.6	1.39
0.5	1.63	11.6	-15.7	8	40.4	1.41
1.0	1.60	13.4	-9.9	8	35.1	1.46
1.0	1.61	13.3	-10.6	9	37.1	1.45
2.0	1.59	14.5	-7.2	10	29.5	1.48
2.0	1.60	14.1	-5.7	7	34.0	1.51
3.0	1.59	14.6	-6.1	8	29.2	1.50
3.0	1.59	14.1	-5.1	8	29.3	1.52
0.1	1.50	13.3	-21.1	14	45.3	1.24
0.6	1.50	13.3	-11.9	13	39.4	1.34
1.0	1.51	13.1	-8.2	13	33.4	1.39
3.0	1.50	13.9	1.6	11	32.4	1.52

Figure 107 shows the final strains reached in all the tests performed. This figure also includes the value of swelling pressure for samples with a dry density of 1.60 g/cm^3 saturated with distilled water –calculated in accordance with the expression included in the section "Swelling pressure"–, which corresponds to the load required for deformation to be zero. This value may be seen to fit well with the results obtained in the saturation under load tests. The final strains depend not so much on the type of water used for saturation, but more on initial dry density. Nevertheless, among the samples having an initial dry density of 1.60 g/cm^3, the values of strain obtained with distilled water are higher.

In principle, the salinity of the saturation solution reduces the swelling capacity of the clay, since it prevents osmotic swelling and reduces the development of diffuse double layers. Specifically, Barbour & Fredlund (1989) make a distinction between two

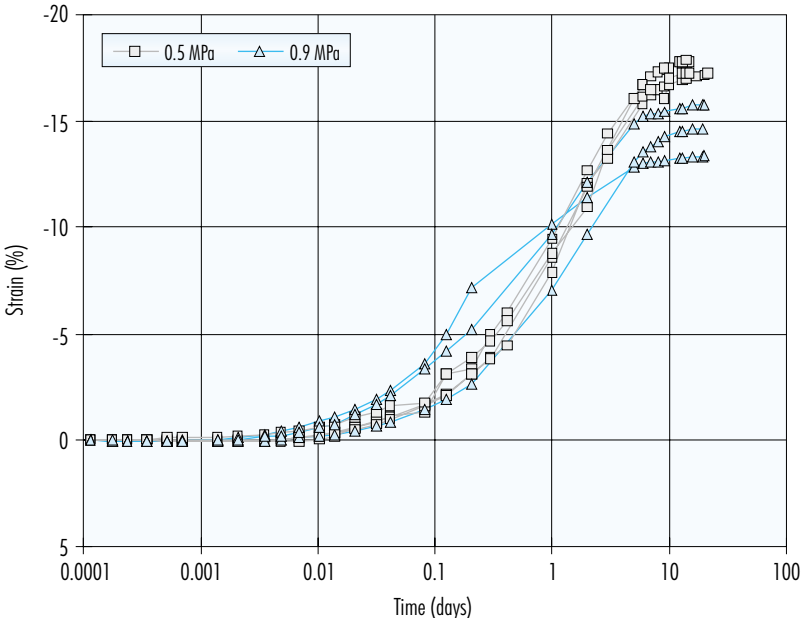

Figure 102. Evolution of strain in saturation tests with distilled water performed using specimens with a nominal initial dry density of 1.60 g/cm³ under different loads.

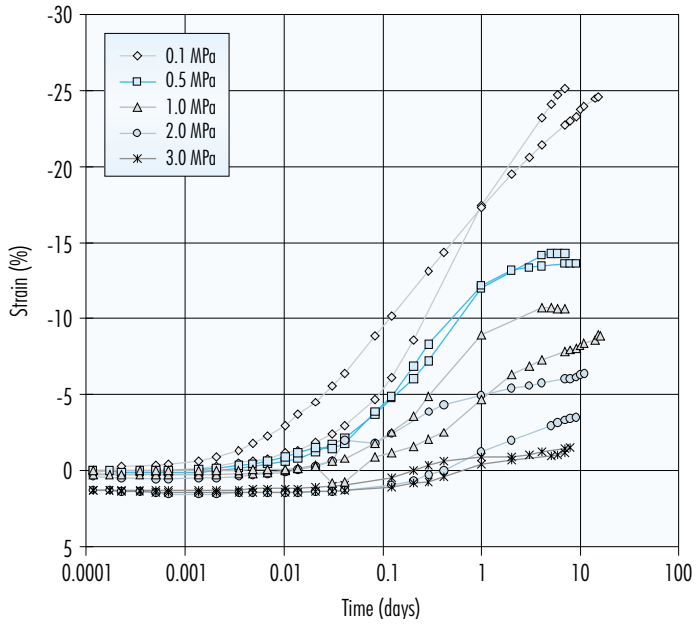

Figure 103. Evolution of strain in saturation tests with granitic water performed using specimens with a nominal initial dry density of 1.60 g/cm³ under different loads.

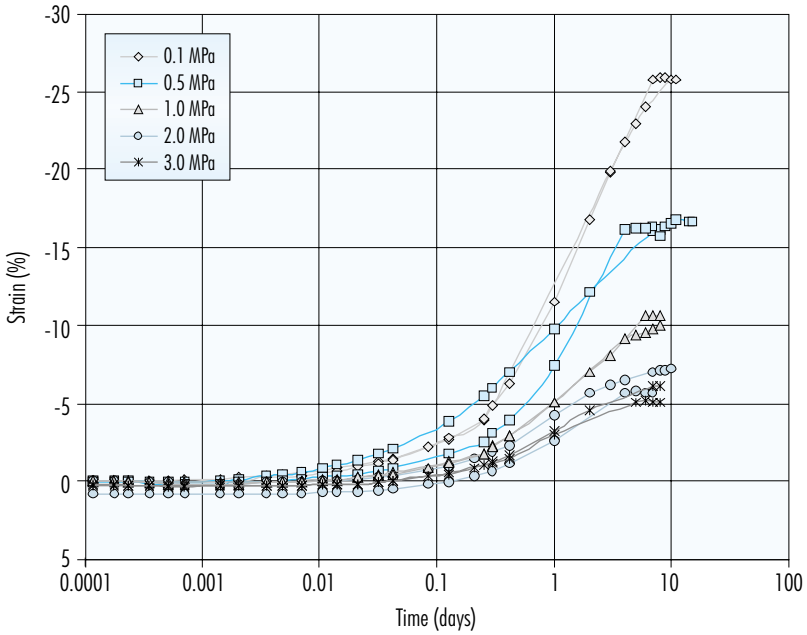

Figure 104. Evolution of strain in saturation tests with saline water performed using specimens with a nominal initial dry density of 1.60 g/cm³ under different loads.

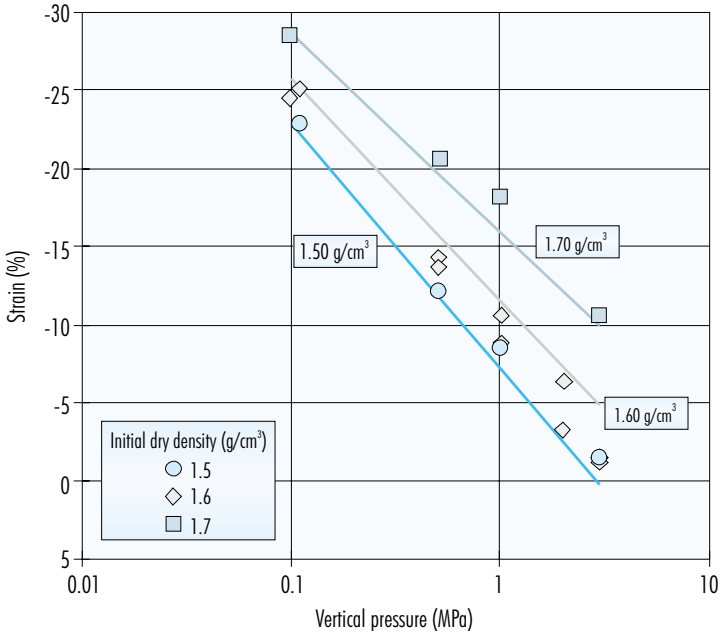

Figure 105. Final strains reached by specimens of different initial dry density following saturation with granitic water under different loads.

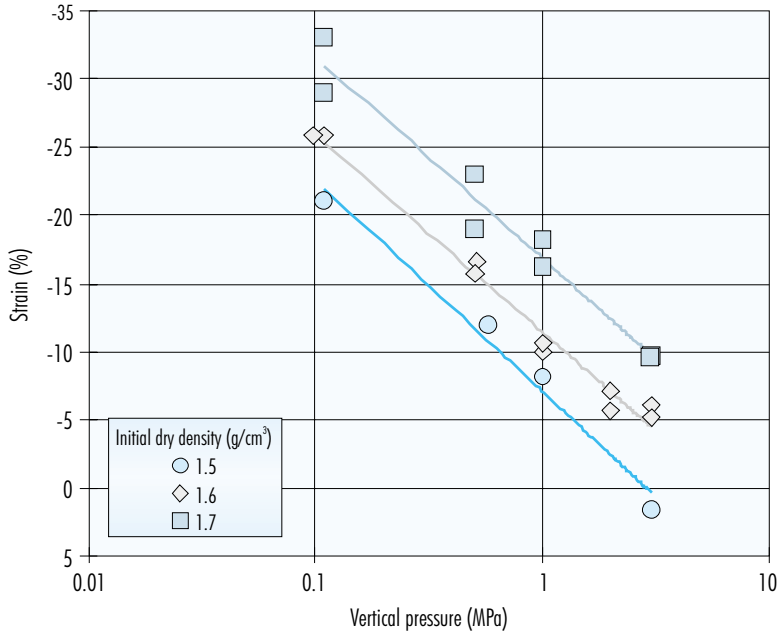

Figure 106. Final strains reached by specimens of different initial dry density following saturation with saline water under different loads.

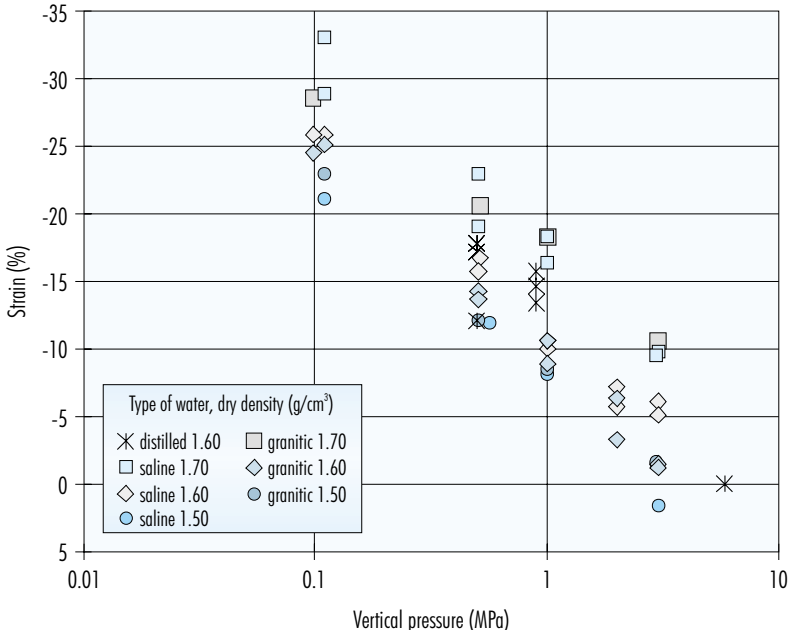

Figure 107. Final strains reached by specimens compacted at different dry densities following saturation under different loads, depending on type of water.

mechanisms responsible for osmotic volume change: osmotic consolidation, the direct result of the suppression of the double layer due to changes in the repulsion between particles, and osmotic flow, which results from differences in concentration of the fluid inside and outside the sample. Both mechanisms depend on the chemistry of the interstitial fluid. Studds *et al*. (1998) find that the swelling capacity of the Wyoming bentonite powder saturated with different solutions decreases as saline concentration increases, although the differences become smaller with increasing vertical pressure, the influence of the molarity of the solution on final strain disappearing with pressures of above 0.2 MPa.

For this reason, it is logical that the samples tested with distilled water should undergo the greatest strain. The fact that no major differences are appreciated between the results obtained with samples saturated with saline and granitic water may be due to the concentration of the saline water being in equilibrium with the mineral phases of the clay, and to the pressures at which saturation occurs being high.

Controlled suction oedometric tests

The results of 20 tests performed in the controlled suction oedometers are shown below. The paths followed were selected with the dual objective of simulating the conditions of different parts of the clay barrier in the disposal facility and of obtaining parameters quantifying its behaviour. Furthermore, all the tests serve overall to establish behaviour patterns that may be of use to check the capacity of the constitutive models and undertake their calibration by back-analysis.

The limitation of oedometric testing is that it does not allow complete insight to be gained into the stress state of the material, since there is no measure of the horizontal confining stress. As a result, difficulties are introduced in the interpretation of the results and in the comparison with the predictions of the models. In the case of unsaturated soils, there is also uncertainty regarding the degree of saturation of the soil, which is always unknown, although the retention curves obtained at constant volume may provide orientative water content values for each suction. However, the most significant trends and features of soil behaviour may be followed with this type of tests (Gens & Alonso 1992), the performance of which is far less complex than that of triaxial tests. Consequently, the objective of performing this series of tests was to identify the main patterns of bentonite behaviour under conditions similar to those of the disposal facility, quantifying to the extent possible the trends observed and contributing to increasing the limited experimental databases on the strain behaviour of highly expansive materials under conditions of high suction.

The Procedure "Controlled suction oedometric testing" was applied, a brief description of which may be found in the section "Controlled suction oedometric testing". All the tests were carried out using specimens compacted uniaxially in the oedometer ring at a nominal dry density of 1.70 g/cm^3, using the clay with its hygroscopic water content. The pressure required to achieve this density is 20 MPa. The initial length of the specimen is 1.20 cm and its cross section 11.40 or 19.24 cm^2. This cross section conditions the maximum vertical pressure applicable in the oedometer, which is 10 MPa in the first case and 5 MPa in the second. Given that all the specimens were compacted using pressures higher than those that can be applied with the equipment, the sample was overconsolidated at the beginning of the tests.

Suction was applied by means of nitrogen pressure for values of between 0.1 and 14 MPa, or by means of solutions of sulphuric acid for values of between 3 and 550 MPa.

The temperature of the tests was kept constant at 20 °C. Wetting/drying and loading/unloading paths were applied, the modification of the vertical load or suction being accomplished gradually in each case. Most of the paths refer to suction change under constant load or to load change under constant suction. The tests end with a process of rapid stepwise unloading, each step lasting one day, as a result of which the deformation does not completely stabilise. Appendix I includes a detailed description of the characteristics and results of each test. In both the tables included in the aforementioned appendix and in the following discussion, only the value of final strain (void ratio) is reflected for each step, although it should be taken into account that each of these values reflects an "equilibrium" that is reached after the sample remains under the same vertical stress and suction conditions for a given period, that normally lasts 20 days. This means that the duration of each test is often longer than a year. The curves for strain versus time for each step in each test are also found in Appendix I.

The tests are referenced in accordance with a key (EDN*_# or EDS*_#) which reflects the following:

- the specific oedometer used for performance of the test: nitrogen or sulphuric acid oedometer, and a number from 1 to 5, since there are 5 test stations of each type (EDN* or EDS*).
- the number of the test performed with that particular equipment (_#).

The following sections present the results obtained. The final void ratio for each step is represented as a funtion of vertical load or corresponding suction. In certain cases, both variables have been represented on the abscissa, due to their having the same units, but using lines of different style for the suction change and vertical load change paths, as indicated by the legend in each case.

Oedometers with suction control by nitrogen pressure

Eight tests of this type were performed, following 4 different paths (E2, E3, E4/1 and E4/2). The maximum applicable suction in these oedometers is 14 MPa, this implying that on the first step of all the tests, suction decreases sharply from the initial value of the compacted sample with its hygroscopic water content –which is some 130 MPa–, to 14 MPa. For this reason, all the samples swell and undergo a decrease in density during the first step of the tests, this being more accentuated in the case of the tests beginning under low load conditions. In these oedometers, the suction may be decreased to 0 MPa by opening the cell to the atmosphere.

The specific paths followed in the tests performed with oedometers with suction control by nitrogen pressure are shown in Figures 108 and 109, in which the initial conditions are marked with a circle.

As may be deduced from the retention curves, in the tests performed with these oedometers the sample remains at all times close to saturation, and in any case with a water content far in excess of the hygroscopic one. Consequently, these tests reproduce the conditions of the bentonite in the areas closest to the external part of the barrier, where saturation will occur very rapidly with no previous desiccation. The tests on wetting under low load simulate situations at the outer part of the barrier, where the gap between the latter and the rock allows for swelling (path E3). The load paths reproduce the compression that the material undergoes as a result of the swelling pressures developed.

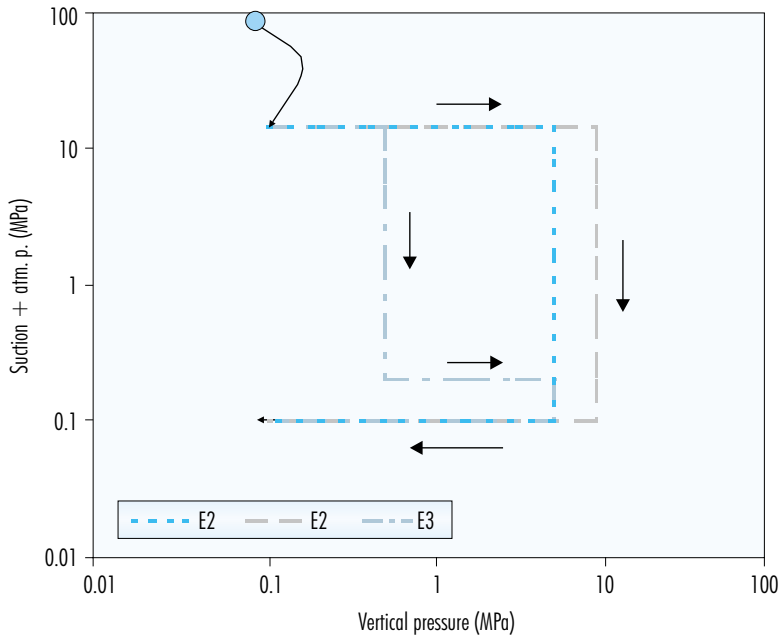

Figure 108. Paths followed in oedometric tests with suction control by nitrogen pressure, types E2 and E3.

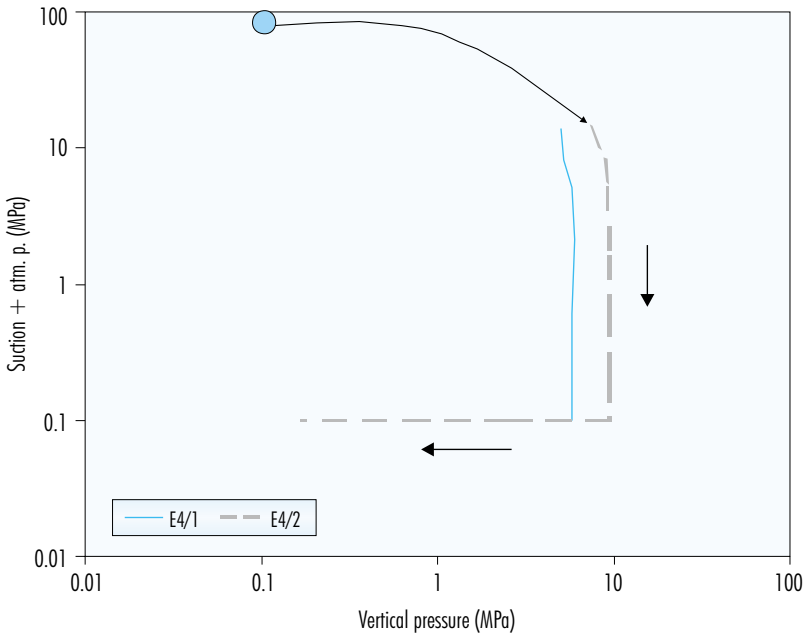

Figure 109. Paths followed in oedometric tests with suction control by nitrogen pressure, type E4.

On paths E4/1 and E4/2 the sample hydrates under a constant high load, which is different in either case. Initially, attempts were made to keep deformation equal to 0 and to determine the swelling pressure of the sample, but this was not achieved due to the loading limitations of the equipment and to the high swelling pressures of the samples.

Path E2

The tests that follow this path begin with stepwise loading of the sample under suction 14 MPa. In tests EDN1_5 and EDN3_10 the load is applied in various steps, while in test EDN5_6 the loading process is quicker. On completion of the loading process, the suction applied is reduced while the maximum value of vertical pressure reached is maintained. The complete path is shown schematically in Figure 110.

The samples for tests EDN1_5 and EDN5_6 had an initial dry density of 1.72 g/cm^3 (e=0.57), while in the case of test EDN3_10 this value was 1.69 g/cm^3 (e=0.60). During the first step there is a decrease in these densities to values of 1.50, 1.55 and 1.55 g/cm^3, respectively. Figure 111 shows the evolution of strain versus time during successive steps on the stretch for load under 14 MPa suction (stretch 1) for the EDN1_5 test. This graph corroborates the importance of the deformation that the sample undergoes during the initial step, when suction changes from 130 to 14 MPa, which is of such a magnitude (14 percent) that it is not counteracted during subsequent loading.

The specific paths followed during these three tests are as follows: while maintaining the maximum suction possible with the equipment (14 MPa), loading of the sample occurs gradually to the maximum possible value (5 MPa in EDN1_5 and 9 MPa in EDN5_6 and EDN3_10, Figure 112). The suction is then reduced gradually to a value of 0, maintaining the same vertical load, this causing an increase in void ratio as shown in Figure 113. This increase in void ratio is small, since the vertical loads applied are high and the degree of saturation does not vary much in the range of suction from 14 to 0 MPa, being very high across this range, as was verified when determining the retention curves at constant volume.

Finally, a stepwise unloading process is accomplished in which void ratio increases logarithmically as load decreases (Figure 114).

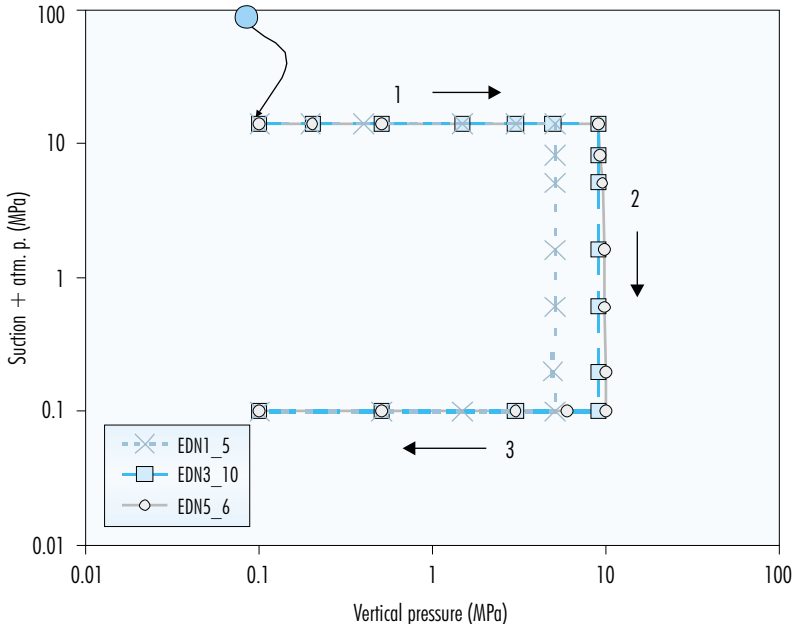

Figure 110. Path E2 followed in oedometers with suction control by nitrogen pressure.

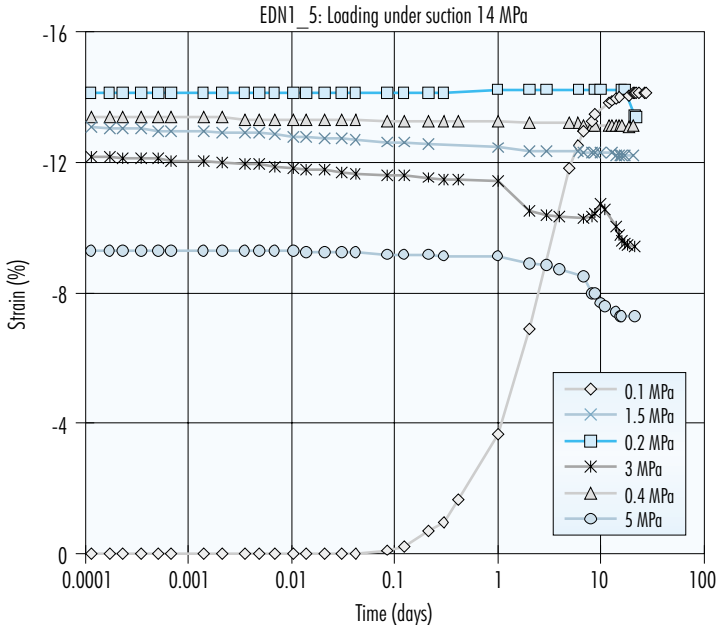

Figure 111. Evolution of strain during the different steps of loading under suction of 14 MPa in test EDN1_5 (path E2, stretch 1). The 0.1 MPa loading step includes strain due to swelling on changing suction from 130 to 14 MPa.

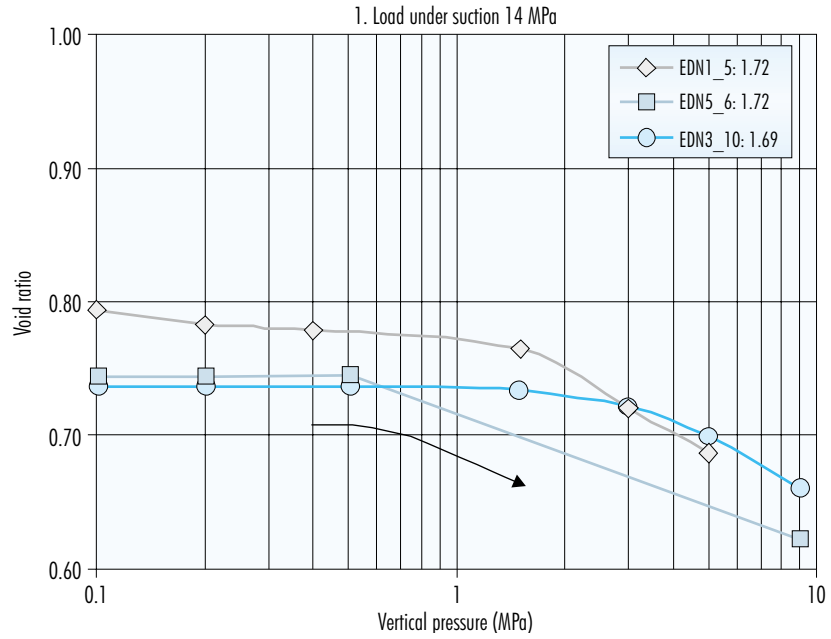

Figure 112. Evolution of void ratio in three tests on a loading path under suction of 14 MPa (initial e 0.57-0.60) (path E2, stretch 1).

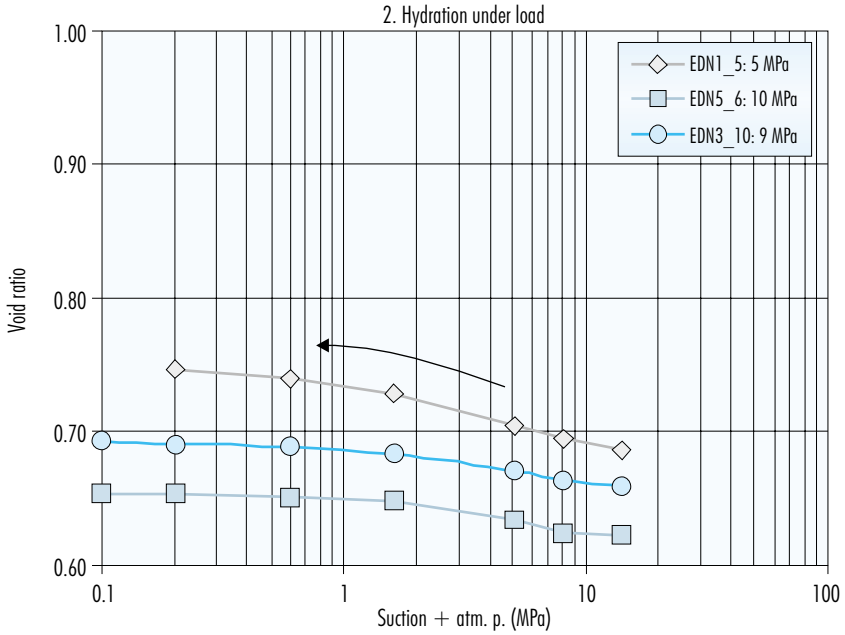

Figure 113. Evolution of void ratio on reducing suction to 0 MPa under a fixed load indicated in the legend (path E2, stretch 2).

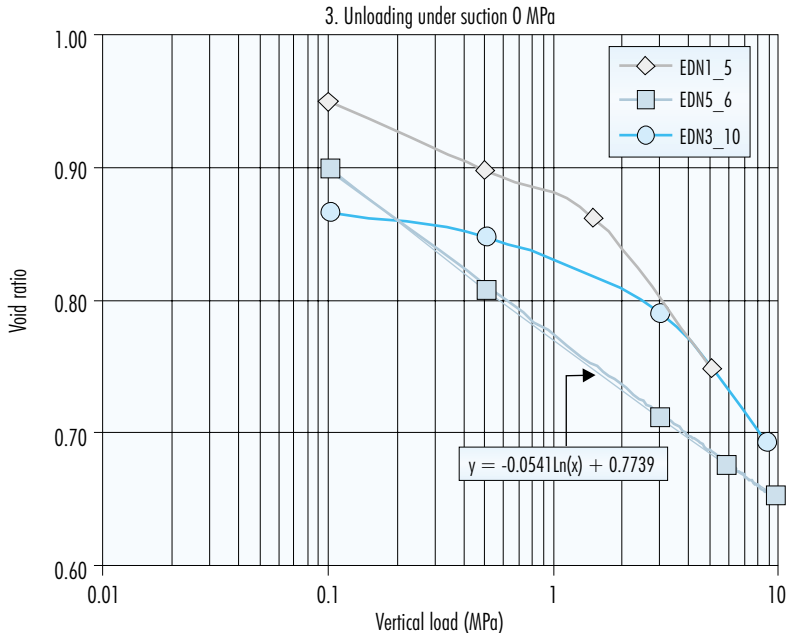

Figure 114. Evolution of void ratio during unloading under suction of 0 MPa (path E2, stretch 3).

Path E3

One test (EDN4_7) was performed following path E3, which is shown schematically in Figure 115.

The path is initiated with a load from 0.1 to 0.5 MPa, with suction maintained at the maximum possible value (14 MPa). The first step includes a decrease in dry density from 1.69 to 1.51 g/cm^3 (stretch 1, Figure 116). Following this minor load, suction is reduced gradually to 0.1 MPa (stretch 2). Once the sample is saturated, loading begins to the maximum possible value (5 MPa, stretch 3), followed finally by rapid, stepwise unloading (stretch 4). The evolution of void ratio during loading is linear, without the initial value being recovered, while during unloading it is logarithmic (Figure 117).

Path E4/1

Tests EDN2_10 and EDN4_6 consist in decreasing suction under high load. While maintaining a constant load (the maximum allowed by the apparatus, 5 MPa), suction is decreased gradually from 14 to 0.1 MPa (EDN2_10) or to 0 MPa (EDN4_6). In both cases, the void ratio varies with suction in accordance with a logarithmic relation shown in Figure 118, that may be extrapolated to the 130 MPa corresponding to the manufacturing value of suction of the sample.

Path E4/2

This test is designed to determine swelling pressure at progressively decreasing values of suction, beginning with a value of 14 MPa and ending with zero suction, following the path shown in Figure 119. The initial dry density of the sample is 1.72 g/cm^3, corresponding to a void ratio of 0.570.

For values of suction of less than 1.5 MPa the loading limit of the apparatus is reached, as a result of which the pressures applied are lower than swelling pressure and the void ratio increases (Figure 120). The increases in void ratio recorded prior to reaching the equipment load limit are due to experimental errors. Once the sample is saturated, on reaching zero suction, a dry density of 1.68 g/cm^3 is attained under the maximum load allowed by the equipment, which is 9.5 MPa. This value of swelling pressure is within the range of values obtained for saturated clay according to the fitting deduced in the section "Swelling pressure". A stepwise process of sample unloading is then performed (Figure 121).

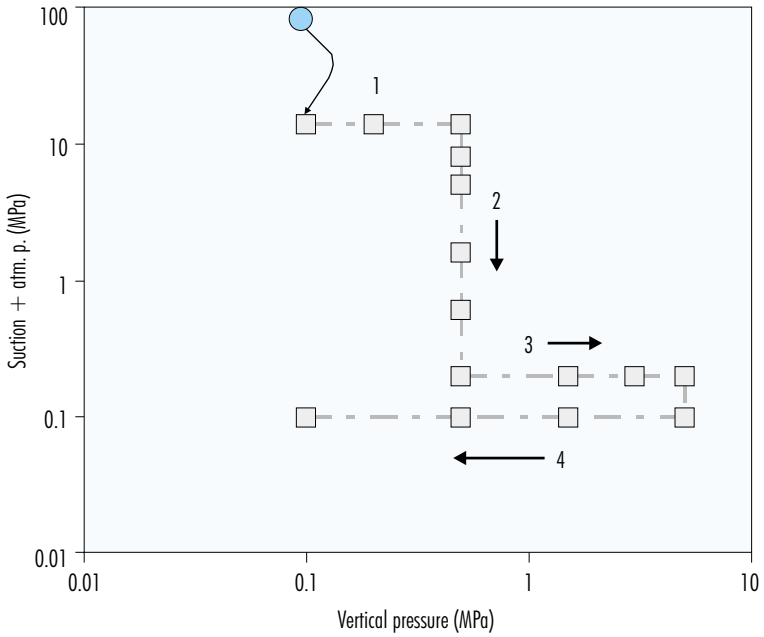

Figure 115. Path E3 followed using oedometer with suction control by nitrogen pressure (test EDN4_7).

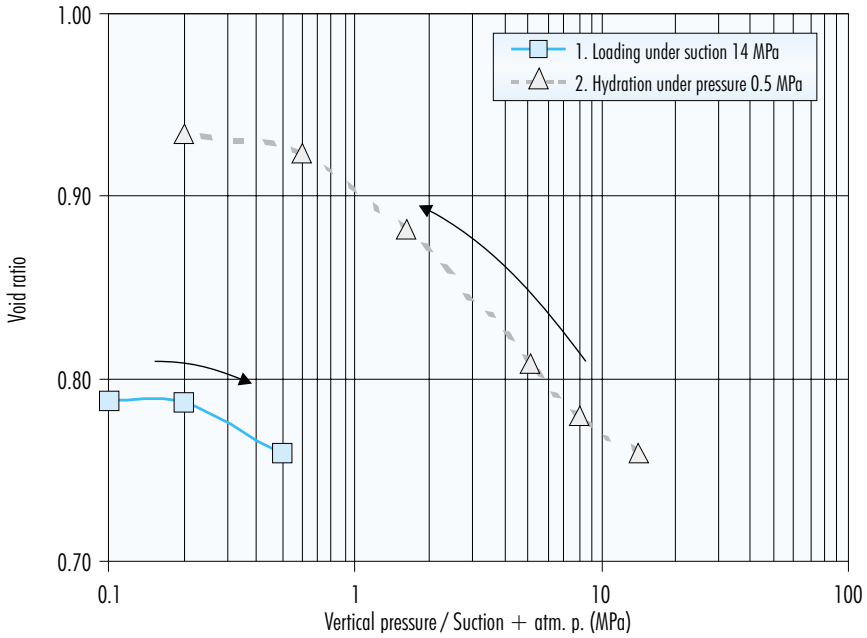

Figure 116. Evolution of void ratio on loading to 0.5 MPa under suction of 14 MPa and on subsequent reduction of suction under a load of 0.5 MPa (test EDN4_7, initial e 0.60).

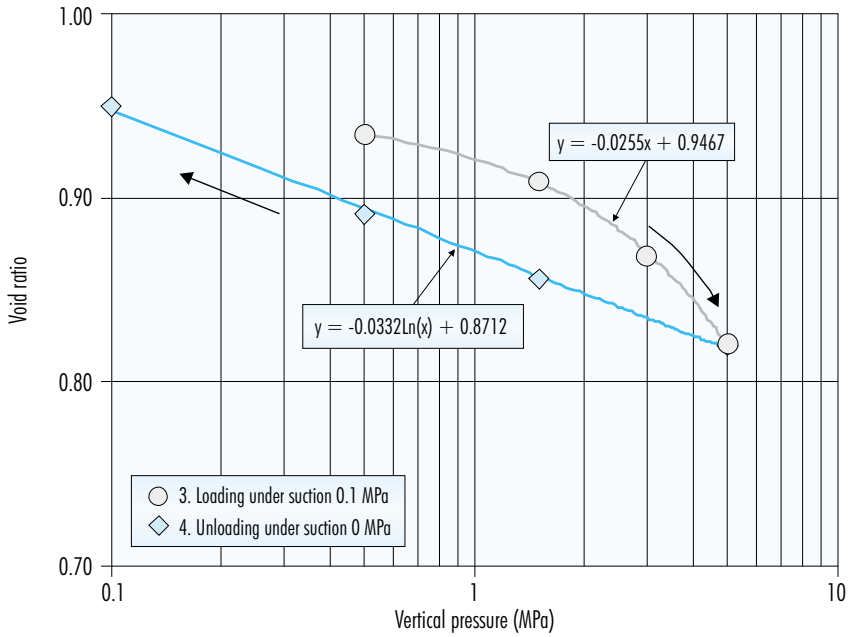

Figure 117. Evolution of void ratio during loading and unloading at saturation (test EDN4_7).

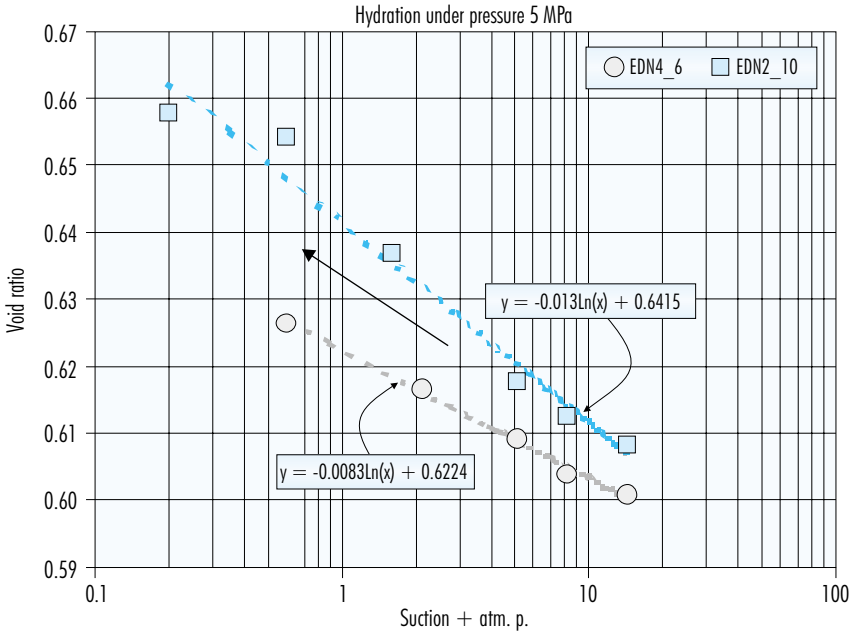

Figure 118. Evolution of void ratio in two tests on decreasing suction under a constant vertical load of 5 MPa (initial e 0.58).

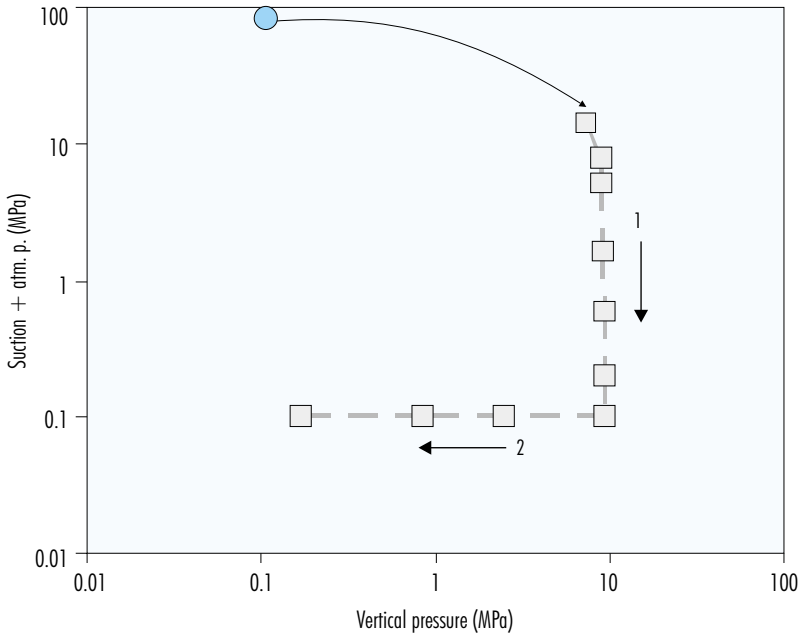

Figure 119. Path E4/2 in oedometer with suction control by nitrogen pressure (test EDN3_9).

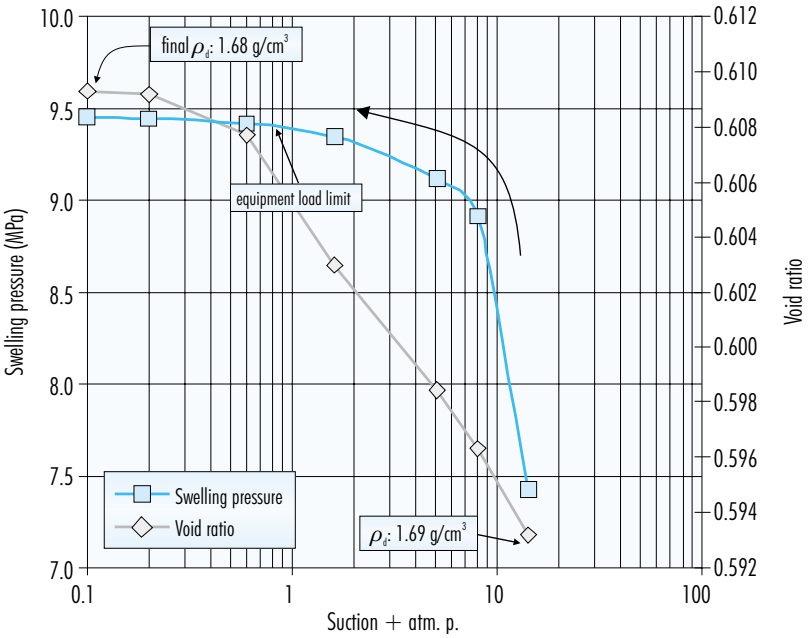

Figure 120. Evolution of void ratio and swelling pressure on decrease of suction from 14 to 0 MPa during test EDN3_9 (initial dry density: 1.72 g/cm^3, e: 0.570).

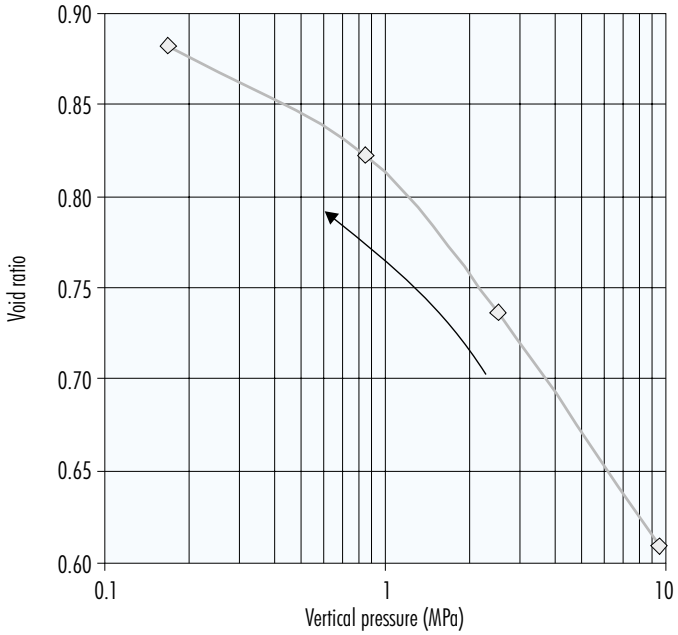

Figure 121. Evolution of void ratio during final unloading at saturation in test EDN3_9.

Oedometers with suction control by solutions

Eight oedometric tests were performed at 20 °C with suction controlled by means of solutions of sulphuric acid, on 7 different paths. The maximum suction applied was 550 MPa. The minimum suction value is achieved by filling the deposit of the oedometric cell with distilled water. Following the performance of a certain number of tests, it was seen that an amount of sulphuric acid from the previous suction step always remained in the deposit, as a result of which the final density of the solution was higher than that of the distilled water, generating a relative humidity corresponding to a suction of between 1.0 and 1.5 MPa. In view of the fact that the final check on the density of the solution of the last step was not performed systematically, a fixed value of 1.3 MPa was taken for the suction applied on pouring distilled water into the deposit.

The paths followed are shown in Figures 122 and 123, in which the initial conditions of the sample are indicated by a circle. Most of the tests performed using these oedometers reproduce the conditions of the bentonite in areas close to the heater, which will undergo some degree of initial desiccation (paths E1/1, E1/2, E2, E3), or in intermediate areas of the barrier, to which the hydration front will take some time to reach, as a result of which the degree of saturation will remain invariable for a period (path E5). Desiccation is simulated by increasing suction under a minor load, since there will initially be a certain gap between the heater and the bentonite, and this will not be compressed. The subsequent load stretches reproduce the compression that the material will undergo due to the swelling pressures developed by the surrounding bentonite, to which the hydration front will have already arrived. Path E6, on the contrary, is analogous to that affecting the bentonite in the area close to the outer part of the barrier, where it initially hydrates under free volume conditions –since there is a gap between the bentonite blocks and the host rock– subsequently being compressed as a result of swelling of the clay placed in areas located further from the edge, as the hydration front progresses towards the centre of the drift.

Paths E1/1, E1/2 and E4 include the determination of swelling pressure. For an unsaturated soil the swelling pressure may be defined as the external load preventing any change in volume when the sample hydrates (Gens & Alonso 1992), this being the meaning given to the term in this work.

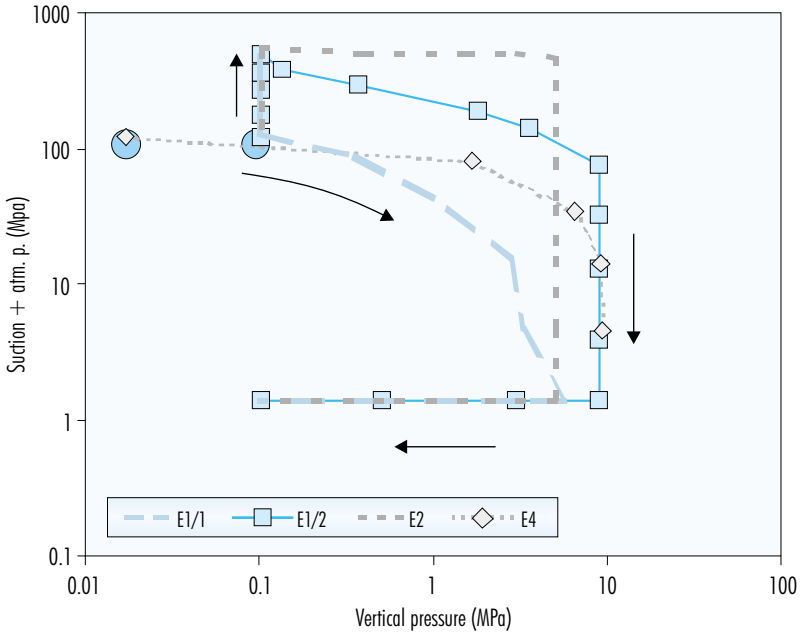

Figure 122. Paths followed in oedometric tests with suction control by solutions of sulphuric acid, types E1/1, E1/2, E2 and E4.

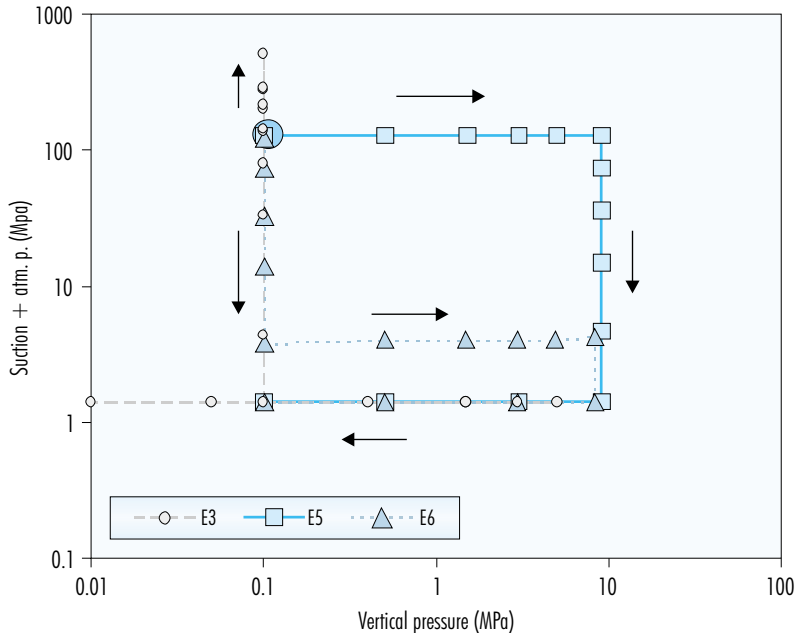

Figure 123. Paths followed in oedometric tests with suction control by solutions of sulphuric acid, types E3, E5 and E6.

On completion of the tests, certain of the samples were analysed using the scanning electron microscope. These samples were seen to contain crystals of gypsum of different morphologies, this not being habitual in the bentonite that was not subjected to treatment or in that used for the oedometric tests performed with control of suction by nitrogen pressure. The origin of these crystals is not clear, and neither is their repercussion on the behaviour of the bentonite.

In view of the fact that these were not found in other types of samples, their origin would appear to be related in some way to the experimental technique. May be during handling of the solution a part could have splashed the sample and reacted with the calcium in the exchange complex. In fact, the agglomerates of smaller sized crystals (2-3 μm) might correspond to neoformations (Figure 124).

On the other hand, other morphologies observed, such as elongated crystals measuring between 10 and 20 μm in length, clusters of acicular crystals and large crystals, do not support this hypothesis (Figure 125).

Path E1/1

Following stabilisation at the suction corresponding to the water content at which the specimens are manufactured (some 130 MPa), test EDS4_6 follows an initial drying path to suctions close to 500 MPa, under a load of 0.1 MPa (Figure 126, stretch 1). The sample is rehydrated under this same load to the initial value of suction (stretch 2), and is then stepwisely loaded as suction decreases, with attempts to maintain the volume of the sample constant (stretch 3), prior to undertaking final unloading (stretch 4).

The initial drying causes the dry density of the sample to increase from a value of 1.70 g/cm^3 to 1.73 g/cm^3. Following the drying, hydration of the sample occurs, as a result of which it recovers the volume lost during desiccation. The evolution of strain at the different steps corresponding to the drying stretch and to wetting under a load of 0.1 MPa is shown in Figure 127, where it may be appreciated that the processes of water transfer due to the effect of change in suction are slow, with no strain observed until after 10 hours. The void ratios at the end of each step on the drying and wetting stretches are shown in Figure 128.

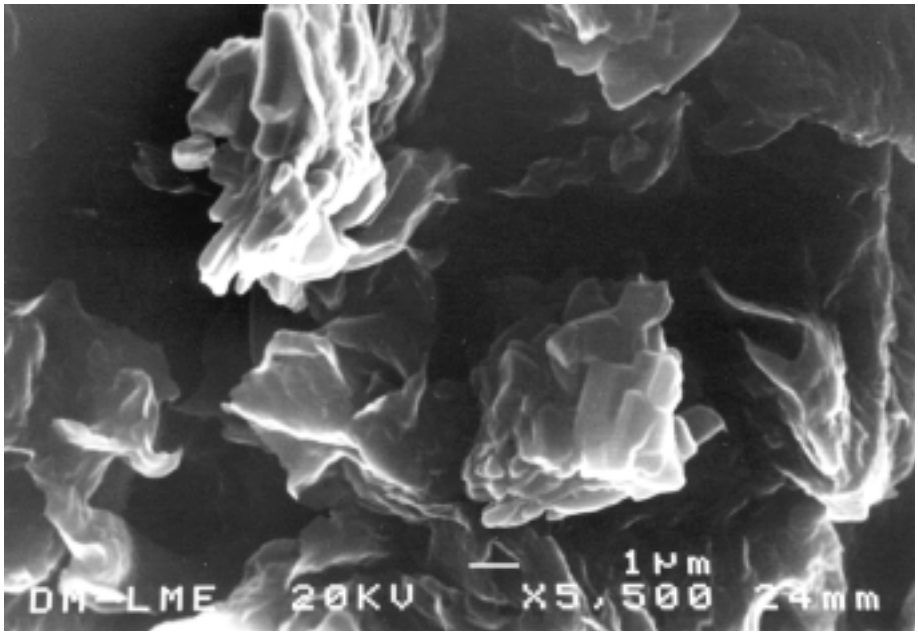

Figure 124. Agglomerates of gypsum crystals of 1-2 μm in the sample from test EDS4_8 (photograph taken with scanning electron microscope with a magnification of 5,500).

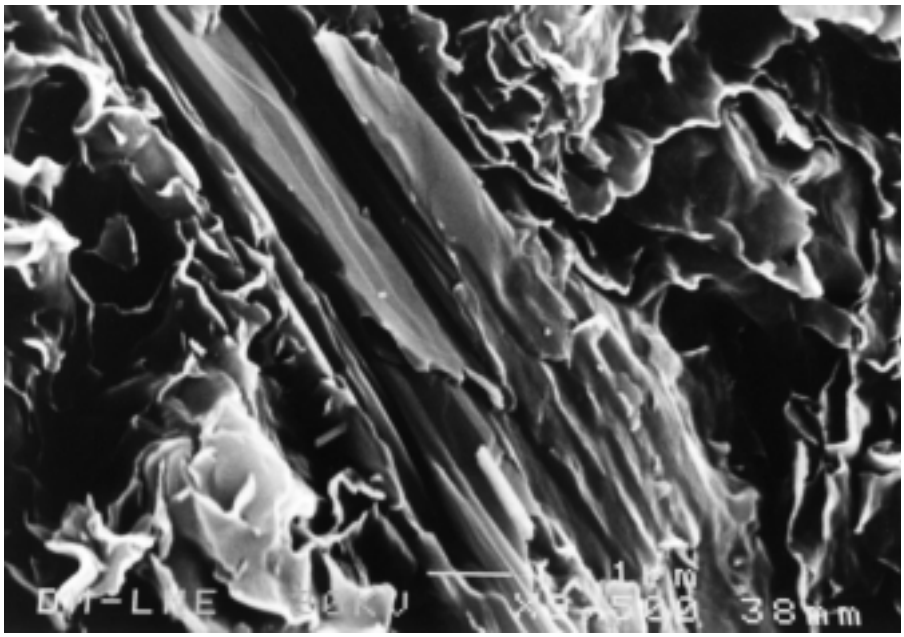

Figure 125. Elongated crystal of gypsum in sample from test EDS2_9 (photograph taken with scanning electron microscope with a magnification of 9,500).

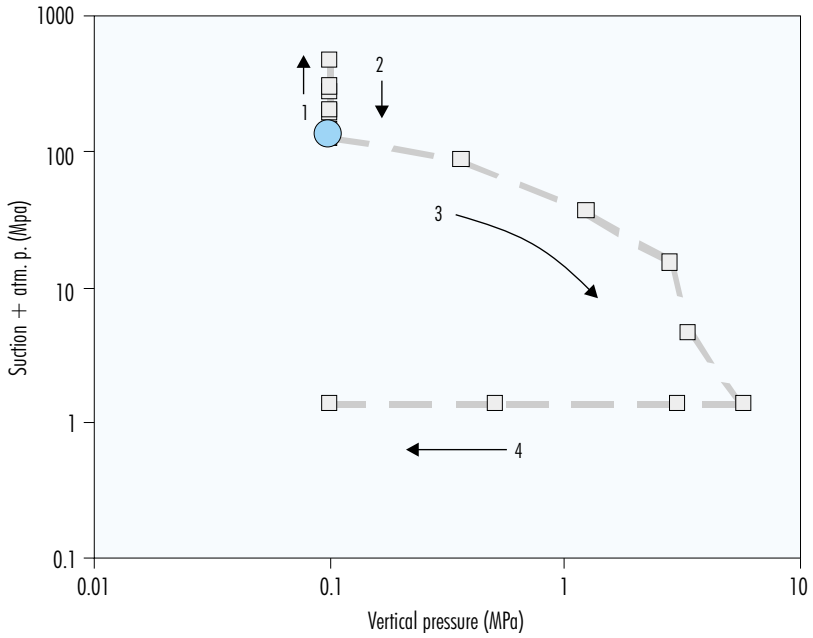

Figure 126. Path E1/1 in oedometer with control of suction by solutions (test EDS4_6).

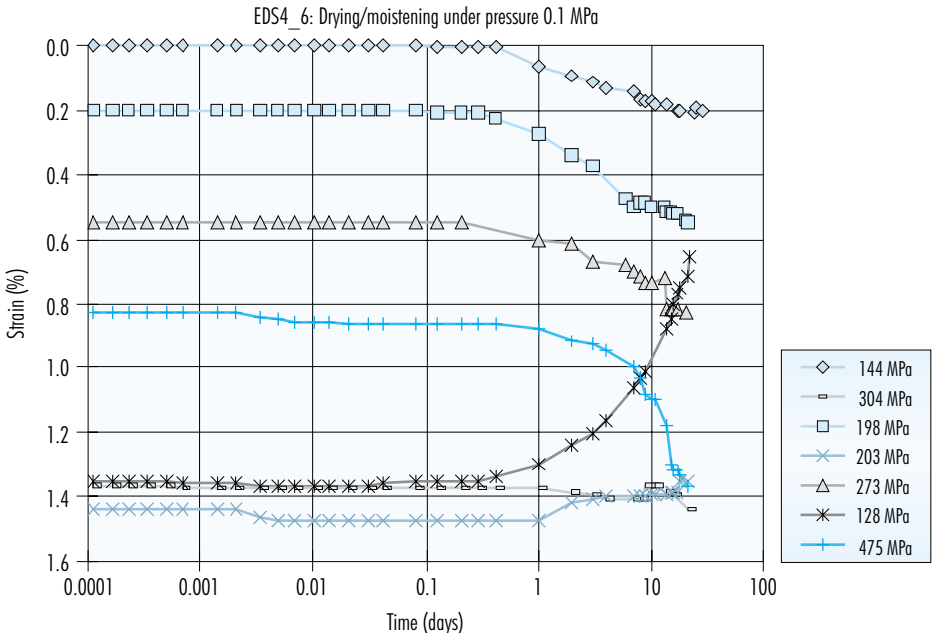

Figure 127. Evolution of strain versus time at the different steps on the drying/wetting path under load of 0.1 MPa in test EDS4_6.

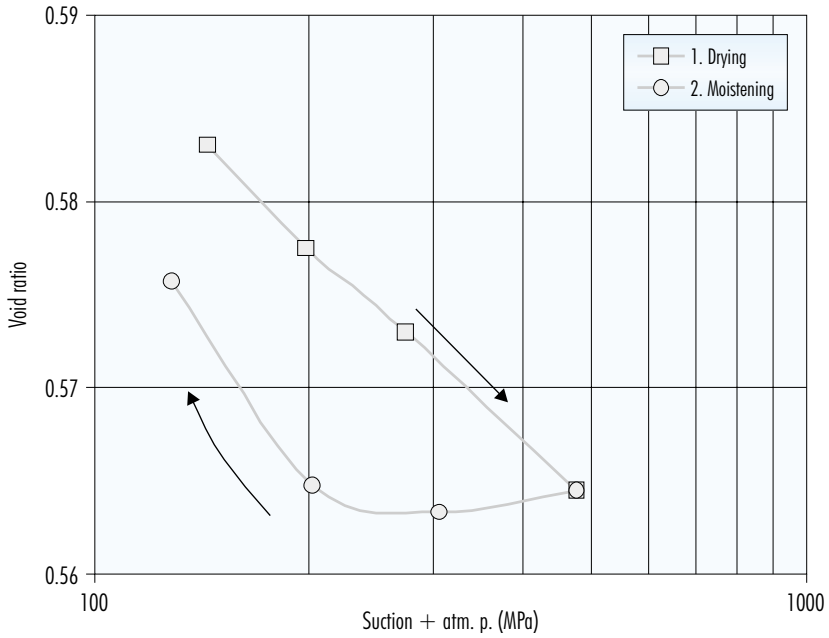

Figure 128. Void ratios corresponding to the different steps of the drying and wetting processes under load of 0.1 MPa in test EDS4_6.

Once the initial dry density has been reached, which occurs at a suction of between 130 and 90 MPa, the volume of the sample is kept approximately constant through the addition of loads, while suction continues to decrease, as a result of which the value of swelling pressure is obtained for gradually decreasing suctions (Figure 129).

At suction values of below 5 MPa, the load capacity of the equipment is insufficient to counteract the swelling of the clay, and because of this there is an important increase in void ratio. For the minimum value of suction, the dry density of the sample decreases to 1.63 g/cm^3, with a swelling pressure of 5.7 MPa, which corresponds to the load limit of the equipment. According to the relation adjusted between dry density and swelling pressure of the saturated sample, the value of swelling pressure for this dry density would be 7.2 MPa, which means that the value observed in this test is lower than the theoretical value, but within the probable range of variation (25 percent, see section "Swelling pressure").

The test finishes with rapid, stepwise unloading once total saturation has been reached (Figure 130), during which there is a logarithmic increase in the void ratio.

Path E1/2

Following stabilisation at the suction corresponding to the water content at which the specimens were manufactured (some 130 MPa), test EDS3_10 follows an initial drying path to a value of suction of 500 MPa, under a load of 0.1 MPa (Figure 131, stretch 1). Following this, suction is reduced as the sample is loaded, with the objective of maintaining its volume constant (stretch 2). Finally, unloading is undertaken (stretch 3).

The drying causes the dry density of the sample to increase from a value of 1.71 g/cm^3 to 1.74 g/cm^3. Following drying, hydration of the sample occurs due to a stepwise decrease in suction. During the process of decreasing suction attempts are made to maintain the volume of the sample reached at the end of desiccation constant, through the addition of appropriate loads. In this way the dry density reached at the end of the drying process is kept constant, as a result of which values of swelling pressure are obtained at decreasing values of suction for a dry density of 1.74 g/cm^3. The values of void ratio obtained on the drying/wetting path and of swelling pressure are shown in Figure 132. It may be observed that for suctions of below 80 MPa, the

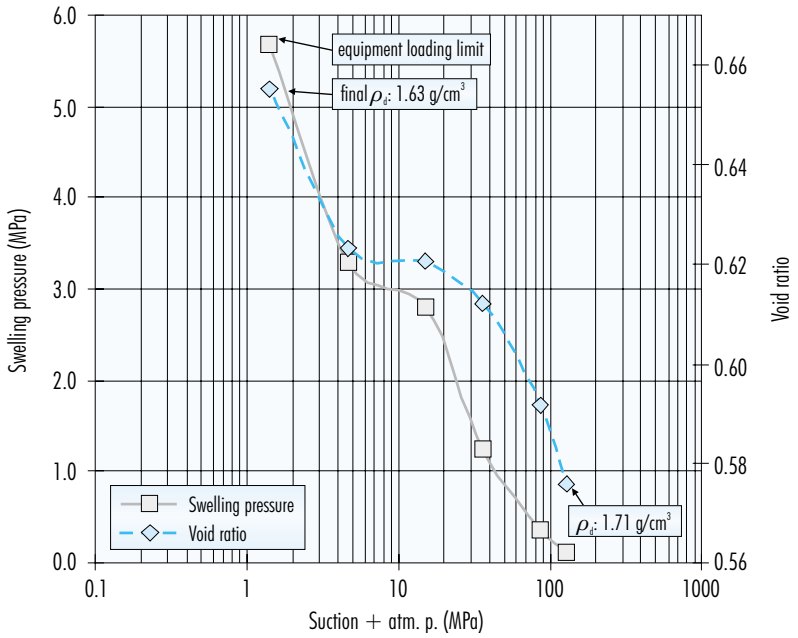

Figure 129. Swelling pressure and variation in void ratio on decreasing suction following intense drying in test EDS4_6.

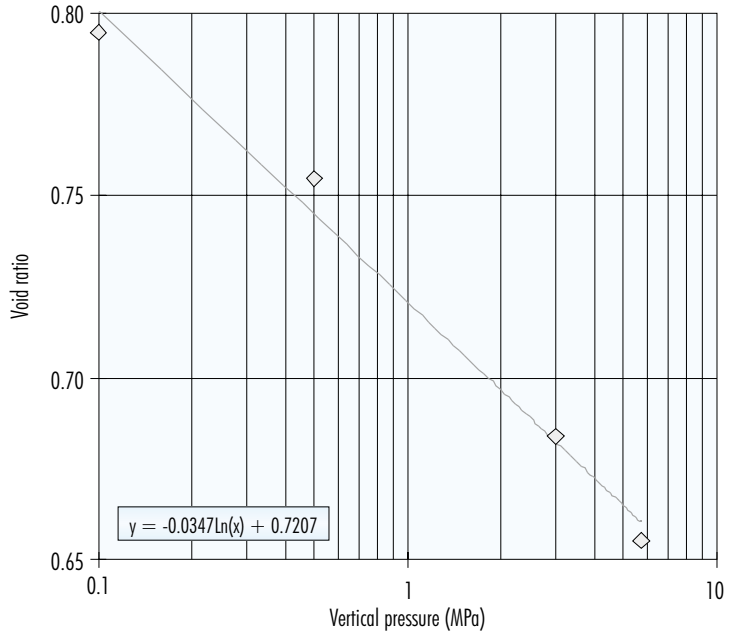

Figure 130. Variation in void ratio on unloading under suction of 1.3 MPa in test EDS4_6.

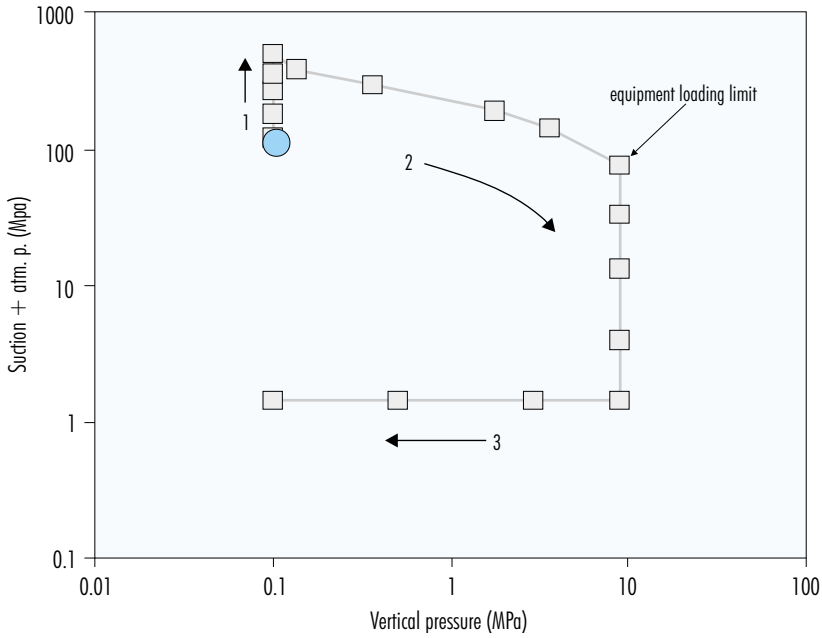

Figure 131. Path E1/2 in oedometer with control of suction by solutions (test EDS3_10).

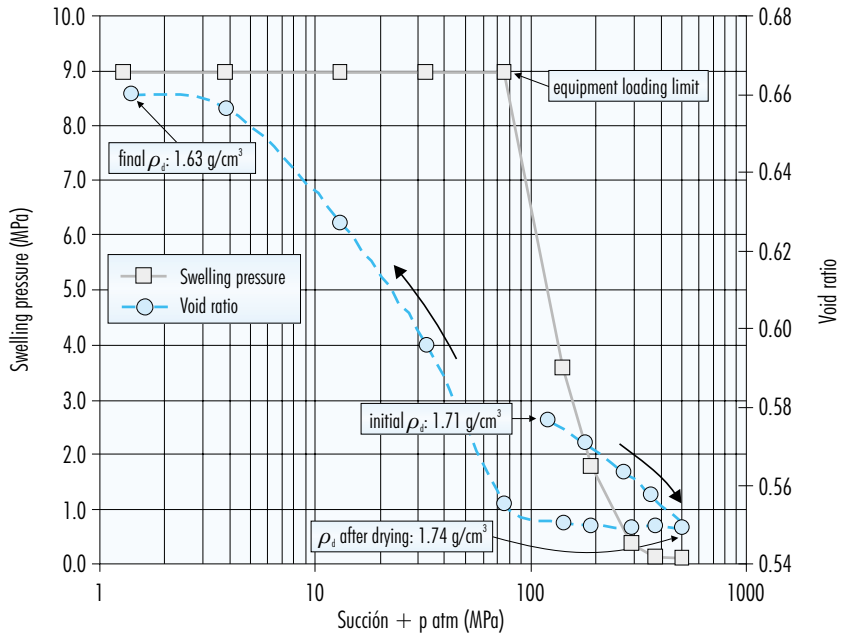

Figure 132. Variation in void ratio during drying and wetting at constant volume, with measurement of swelling pressure, in test EDS3_10.

swelling pressure of the sample exceeds the load limit of the equipment (9 MPa), on account of which its dry density begins to decrease, reaching a value of 1.63 g/cm3 for a suction of 4 MPa, this being maintained to the minimum value of suction. This last item of data suggests that the sample is completely saturated for suctions of 4 MPa, and that consequently there are no pores larger than 0.08 μm (macropores), which is the maximum diameter affected by this suction according to the Jurin-Laplace equation. Furthermore, the possible swelling of the microstructure might be compensated by collapsing of the macrostructure due to the high load applied and to the reduction of the preconsolidation pressure during hydration. The swelling pressure of 9 MPa is higher than the theoretical value for a saturated sample with a dry density of 1.63 g/cm3, which would be 7 MPa (see section "Swelling pressure").

The test finishes with rapid, stepwise unloading of the saturated sample (Figure 133).

Path E2

Path E2 in the oedometer with control of suction by means of solutions consists of 4 stretches, represented in Figure 134. Initially, suction increases under a minor vertical load (stretch 1), the sample is then loaded maintaining the maximum value of suction reached (stretch 2), the suction is subsequently reduced for hydration of the sample under this high load (stretch 3) and the sample is finally unloaded (stretch 4).

Test EDS3_9 begins with a process of drying from the initial suction of 138 MPa to 551 MPa, under a load of 0.1 MPa. This causes a reduction in void ratio from 0.569 (ρ_d: 1.72 g/cm^3) to 0.543, a dry density of 1.75 g/cm^3 being reached. Subsequently, the sample is loaded to 5 MPa keeping the high value of suction reached (more than 500 MPa) constant. This gives rise to a new increase in dry density, which changes to 1.77 g/cm^3. The sample is then hydrated through stepwise reduction of suction, as a result of which dry density decreases to 1.61 g/cm^3.

The void ratios reached at the end of each step on the paths described are shown in Figure 135, in which both the vertical load and suction values are represented on the abscissa. This is because both have the same units, the path referred to by each line being clarified in the legend.

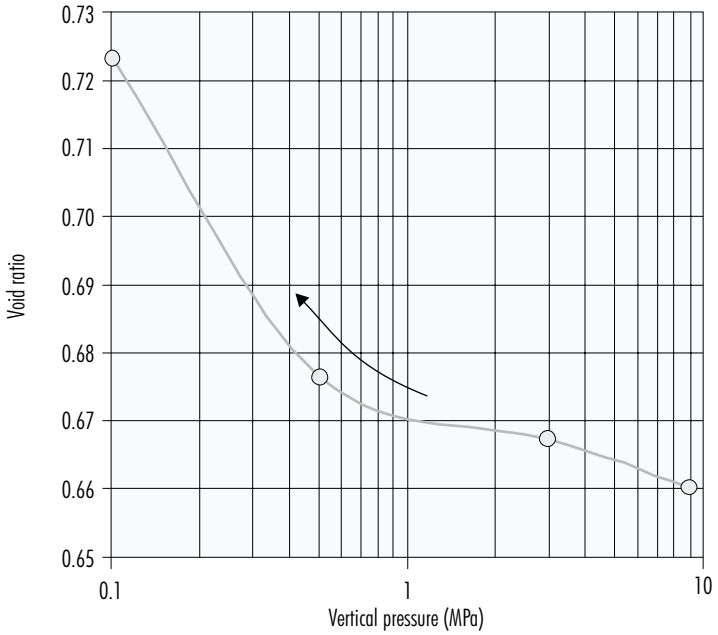

Figure 133. Variation in void ratio on unloading under suction of 1.3 MPa in test EDS3_10.

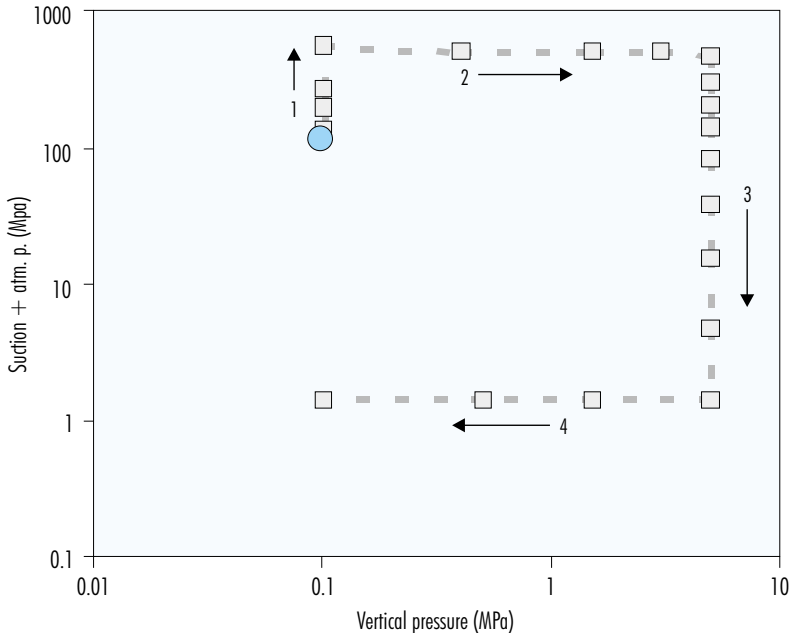

Figure 134. Path E2 in oedometer with suction control by solutions (test EDS3_9).

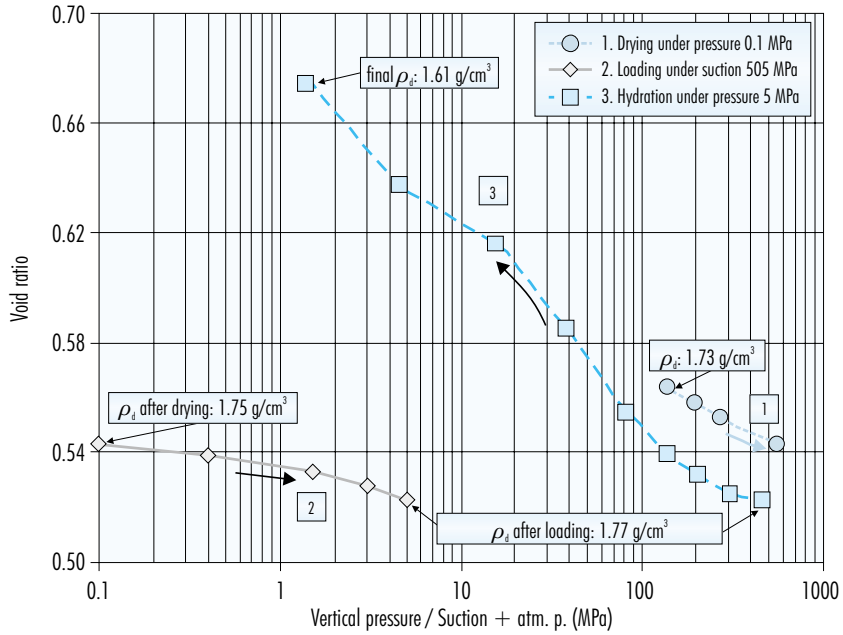

Figure 135. Final void ratios on successive drying, loading and wetting paths in test EDS3_9.

The test finishes with rapid, stepwise unloading of the saturated sample, during which the void ratio increases logarithmically with suction, as shown in Figure 136.

Path E3

Path E3 begins with an increase in the suction to which the sample is subjected under a minor load (Figure 137, step 1), and continues with a decrease in suction to the minimum possible value, with the same load being maintained (stretch 2). The sample is then loaded under this low value of suction (stretch 3), and is finally unloaded (stretch 4).

Test EDS5_5 begins with a process of drying from the initial suction of 138 MPa to a value of 520 MPa, under a load of 0.1 MPa, a reduction in the void ratio from 0.571 (ρ_d: 1.72 g/cm^3) to 0.546 occurring, resulting in a dry density of 1.75 g/cm^3. Subsequently, the sample is hydrated by gradually decreasing suction and maintaining the initial load of 0.1 MPa constant. This gives rise to an important decrease in dry density, which changes to 1.31 g/cm^3. The sample is then loaded to 5 MPa, with which the dry density increases once more to 1.54 g/cm^3.

The void ratios reached at the end of each step on the paths described are shown in Figure 138, in which the values of both vertical load and suction are represented on the abscissa.

The test finishes with rapid, stepwise unloading of the saturated sample, during which the void ratio increases logarithmically with suction, as shown in Figure 139.

The processes of drying and initial wetting were accomplished also in test EDS4_8. The final void ratios on the different steps of this test are shown in Figure 140, in which the values obtained during test EDS5_5 are also included for comparative purposes. The behaviour of the clay is analogous in both tests, the differences in the void ratios being explained by the slight initial disparity of the dry densities of the two samples. Figure 141 is a magnification of the zone of the previous figure corresponding to higher values of suction.

Path E4

Test EDS2_8, which follows path E4, is a swelling pressure test at gradually decreasing values of suction for a sample having an initial dry density of

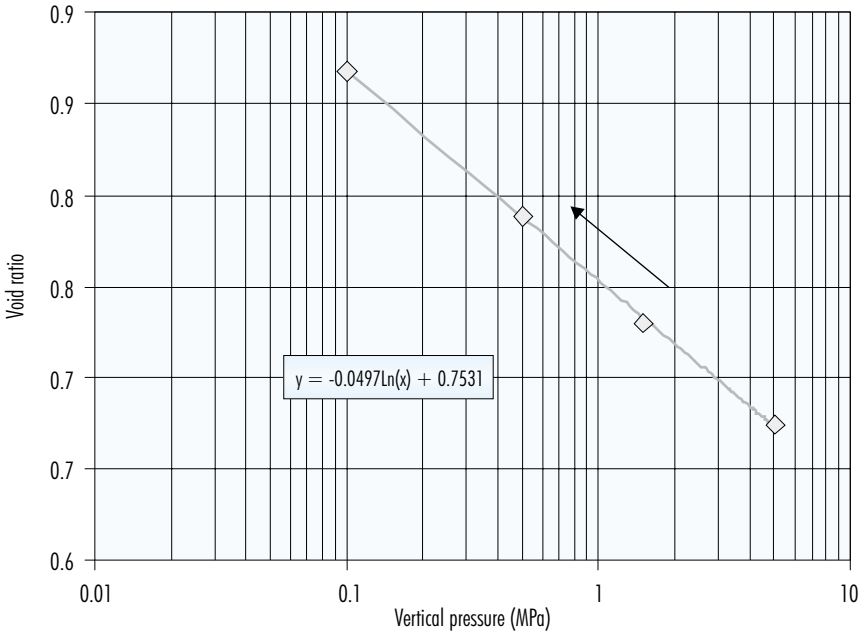

Figure 136. Final void ratios on successive steps of unloading under suction of 1.3 MPa in test EDS3_9.

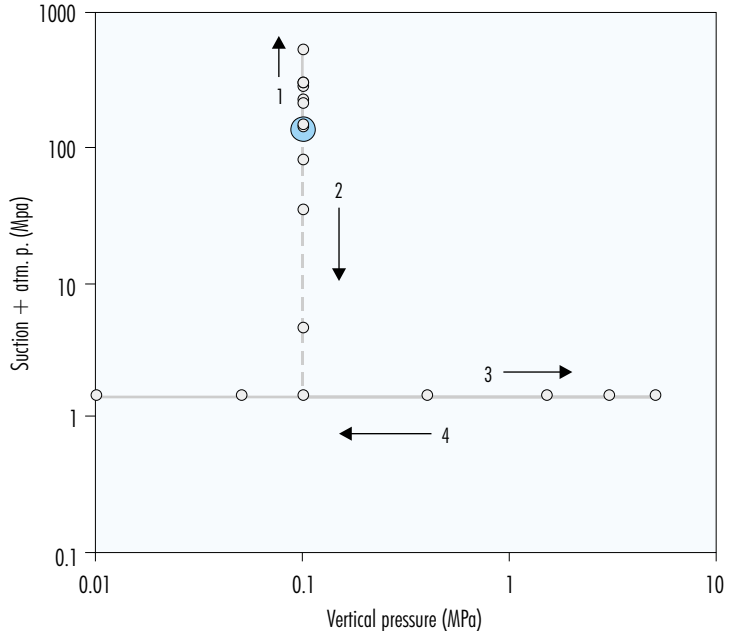

Figure 137. Path E3 in oedometer with control of suction by solutions: tests EDS5_5 and EDS4_8 (the latter only on stretches 1 and 2).

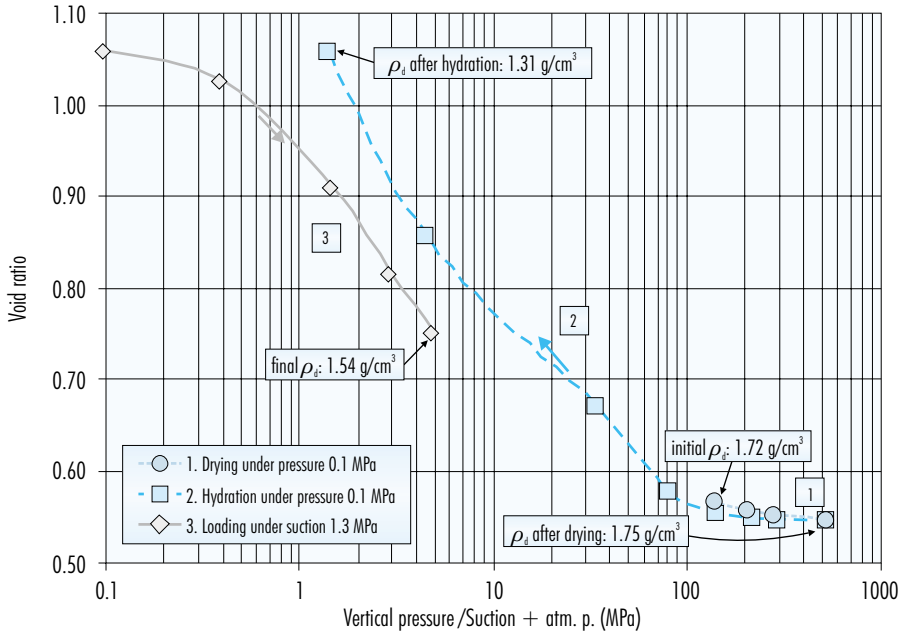

Figure 138. Final void ratios on drying, wetting and loading paths in test EDS5_5.

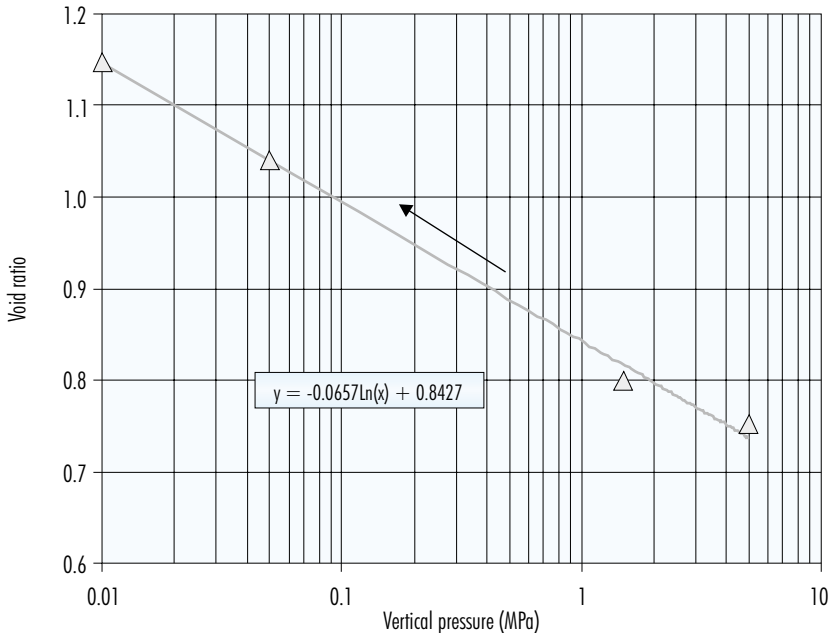

Figure 139. Final void ratios on successive steps of unloading under suction of 1.3 MPa in test EDS5_5.

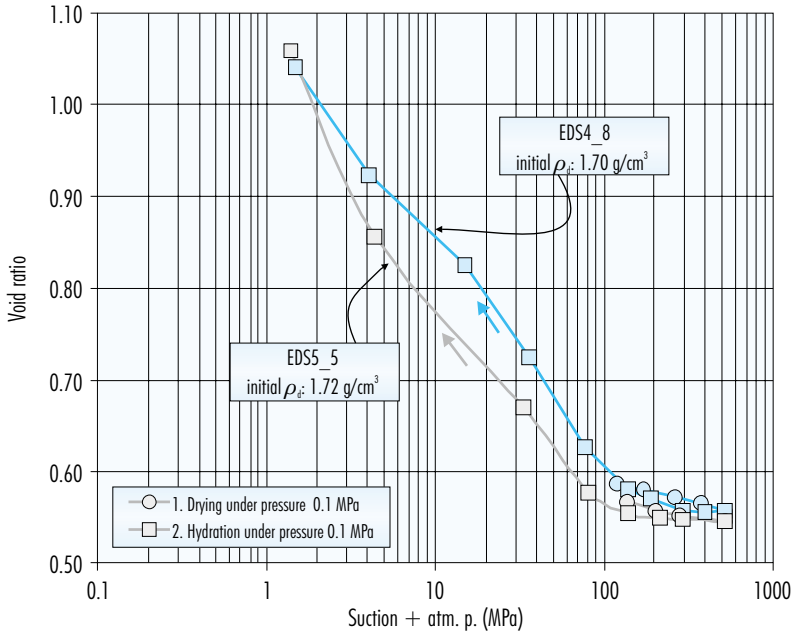

Figure 140. Evolution of void ratio during drying and wetting of the bentonite under a load of 0.1 MPa in two oedometric tests.

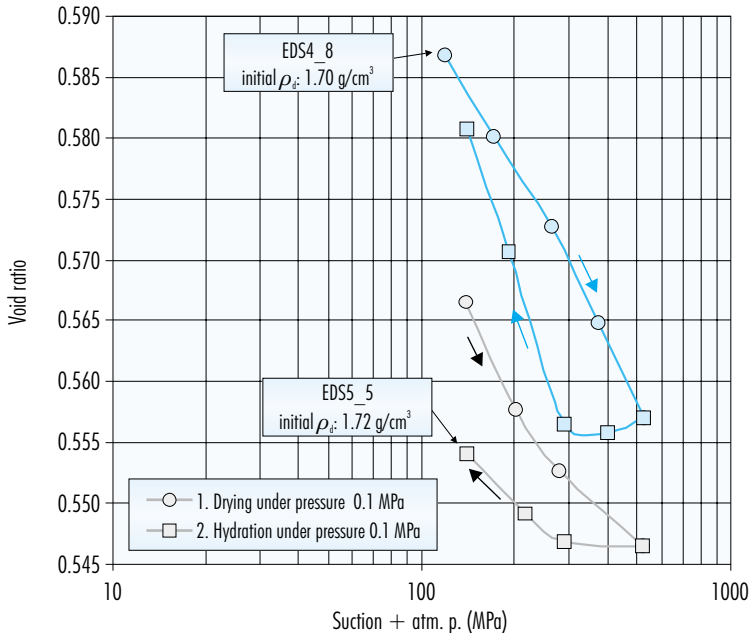

Figure 141. Detail of evolution of void ratios shown in the previous figure for the highest values of suction.

1.73 g/cm^3 (Figure 142). In view of the limitations of the equipment, it was not possible to counteract swelling at lower values of suction, below 14 MPa, as a result of which the final density on the last steps is lower than the initial value, and it was not possible to determine the value of swelling pressure for the initial dry density, but only to maintain maximum load. On the last step equilibrium is reached under a suction of 4.4 MPa with a load of 9.5 MPa, the sample ending with a dry density of 1.70 g/cm^3. According to the fitting shown in the section "Swelling pressure", the swelling pressure of the sample saturated at this density should be 11.5 MPa. Consequently, the value obtained in this test is lower than the theoretical value, but within the possible range of variation (25 percent, see section "Swelling pressure").

Path E5

Path E5 consists in stabilising the sample at the suction corresponding to its equilibrium water content (130 MPa) under a minor load and in subsequently increasing load to the maximum value permitted by the equipment, 9 MPa, maintaining the same value of suction (Figure 143, stretch 1). The suction is then decreased without modifying the high load value reached (stretch 2) and the sample is unloaded once saturated (stretch 3).

The void ratios at the end of the different steps on stretches 1 and 2 of the path are shown in Figure 144. Figure 145 shows the evolution of strain versus time during the different steps involved in the process of decreasing suction under constant load (stretch 2). In both figures it may be observed that during the process of saturation of the sample under a load of 9 MPa, and with suction decreasing from 15.3 to 5.4 MPa, the bentonite undergoes a small decrease in volume ("collapse"), that is recovered when saturation occurs completely.

Once saturation is reached, a process of stepwise unloading is carried out during which the void ratio increases logarithmically (Figure 146).

Path E6

This path consists in a decrease in suction from the initial value to a minor value maintaining a low vertical load (Figure 147, stretch 1). The sample is then loaded under this value of suction (stretch 2) and is finally unloaded (stretch 3).

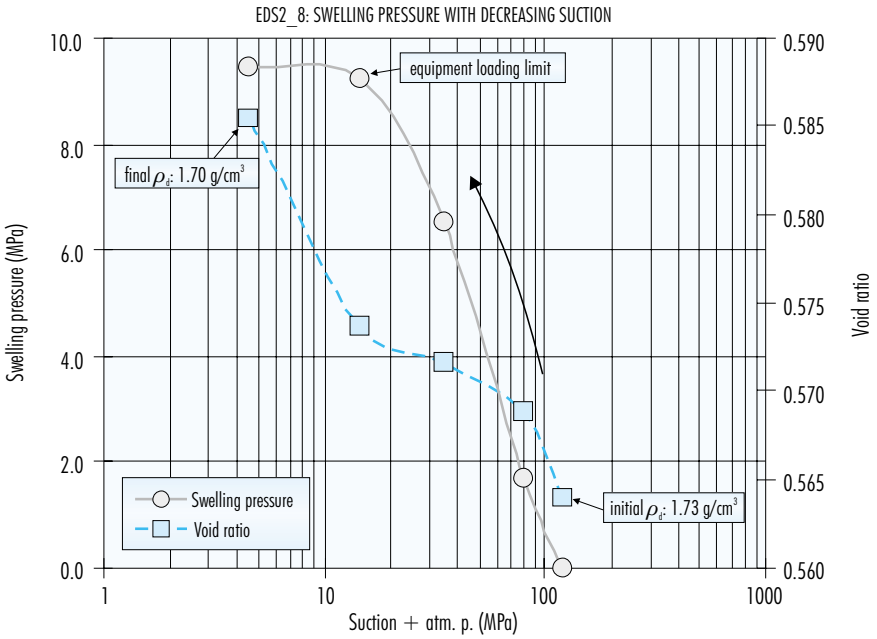

Figure 142. Values of swelling pressure with decreasing suction in test EDS2_8.

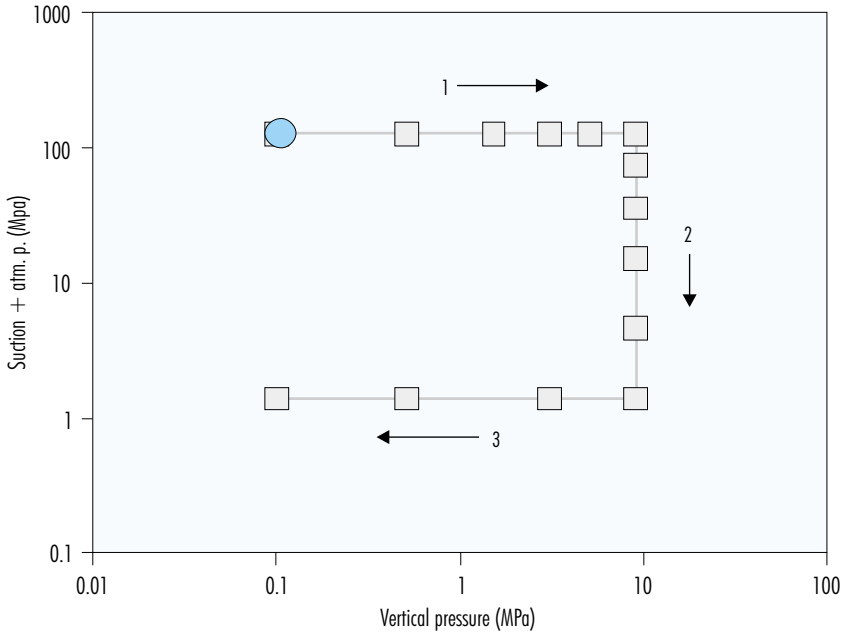

Figure 143. Path E5 in oedometer with control of suction by solutions: test EDS1_10.

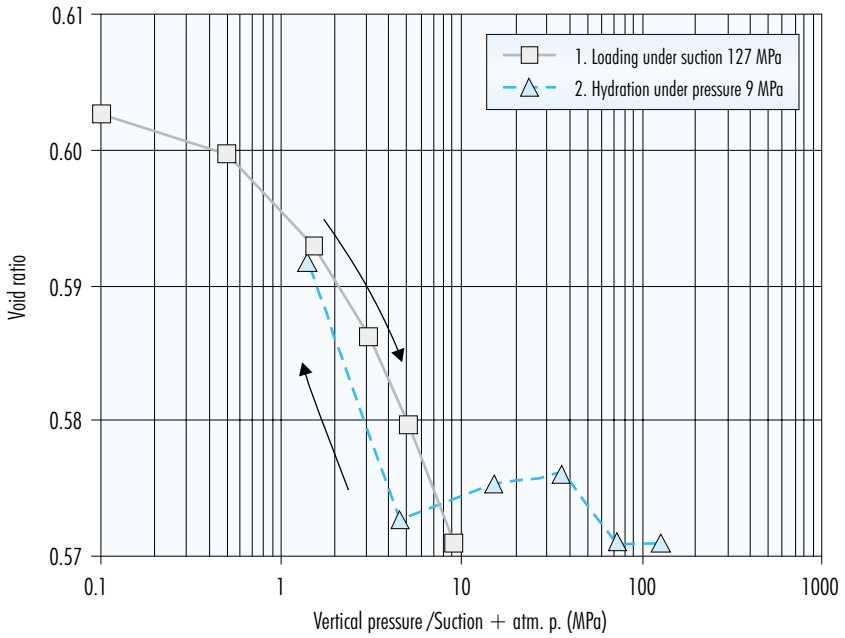

Figure 144. Void ratios corresponding to the different loading steps and subsequent decrease in suction in test EDS1_10.

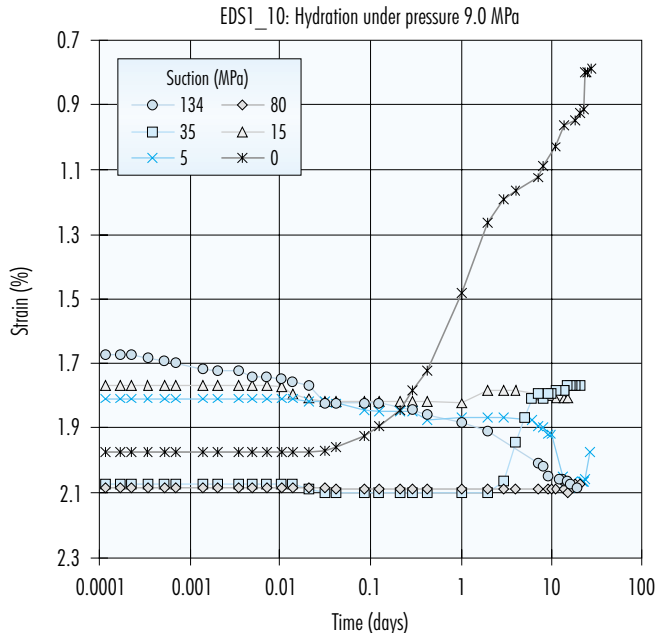

Figure 145. Evolution of strain during the different steps of the process of wetting under a load of 9 MPa in test EDS1_10 (path E5).

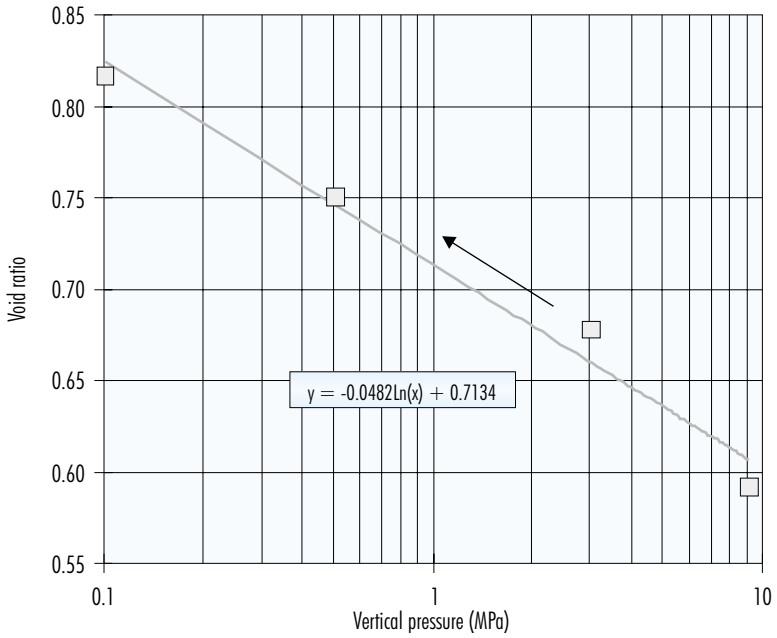

Figure 146. Final void ratio values on the steps corresponding to the process of unloading under a suction of 1.3 MPa in test EDS1_10.

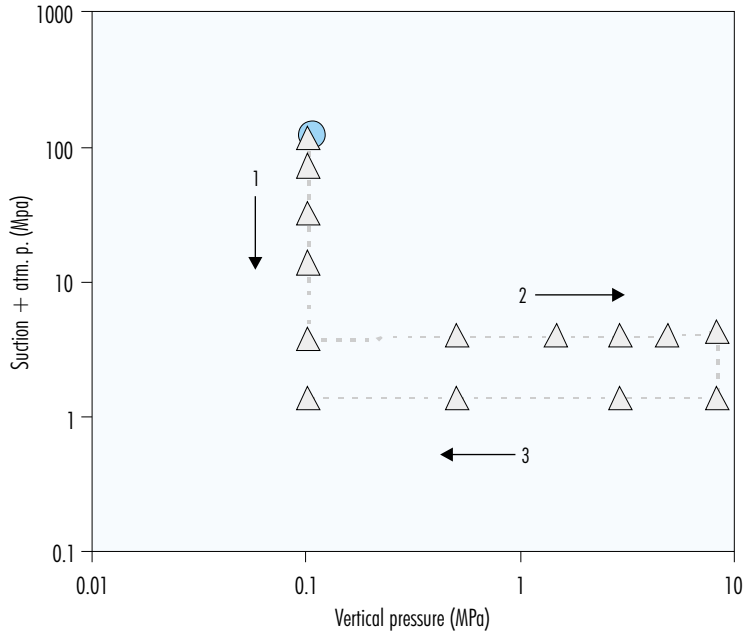

Figure 147. Path E6 in oedometer with control of suction by solutions: test EDS2_9.

This path was followed in test EDS2_9. It begins with stabilisation of the sample at a value of suction corresponding to its hygroscopic water content (130 MPa) under a load of 0.1 MPa and continues with an initial process of wetting to a suction of 4 MPa, maintaining the same vertical load.

During the process of hydration, the dry density of the sample changes from 1.71 to 1.47 g/cm^3. Subsequently, the sample is loaded to 8.4 MPa, as a result of which dry density increases to 1.60 g/cm^3. Suction is then reduced from 4 to 1 MPa, following which the sample is unloaded rapidly and by steps.

The final minor decrease in suction does not cause any appreciable modification of the void ratio, probably because the sample is already completely saturated at a suction of 4 MPa. However, the final unloading under conditions of saturation causes a decrease in dry density to a value of 1.53 g/cm^3.

Figure 148 shows the evolution of void ratio during initial hydration, along with the subsequent loading and final unloading of the sample, the different values of suction and vertical load being represented on the same axis.

Oedometers with suction and temperature control

Path E2 in oedometers with control of suction by means of nitrogen pressure at 20 °C (test EDN1_5) was carried out also at 40 °C (test EDNC_10), at 60 °C (EDNC_11) and at 80 °C (EDNC_12). In addition, a swelling pressure test was performed at different values of suction, at a temperature of 40 °C (test EDNC_9).

The conditions of humidity and temperature to which the sample is subjected during the performance of these tests favour the proliferation of bacteria. This was checked by studying samples subjected to controlled suction oedometric testing under the electron microscope and by comparing them to other samples of the FEBEX bentonite. As was observed with samples of bentonite subjected to thermo-hydraulic treatment (*i.e.* simultaneous heating and hydration), the samples from these oedometric tests showed numerous bacteria of different types, as may be appreciated in Figures 149 and 150. Mingarro *et al*. (2000) estimate a number of between 50,000 and 100,000 bacteria/g for the more hydrated areas of the bentonite subjected to thermo-hydraulic treatment. It has not been possible to determine the re-

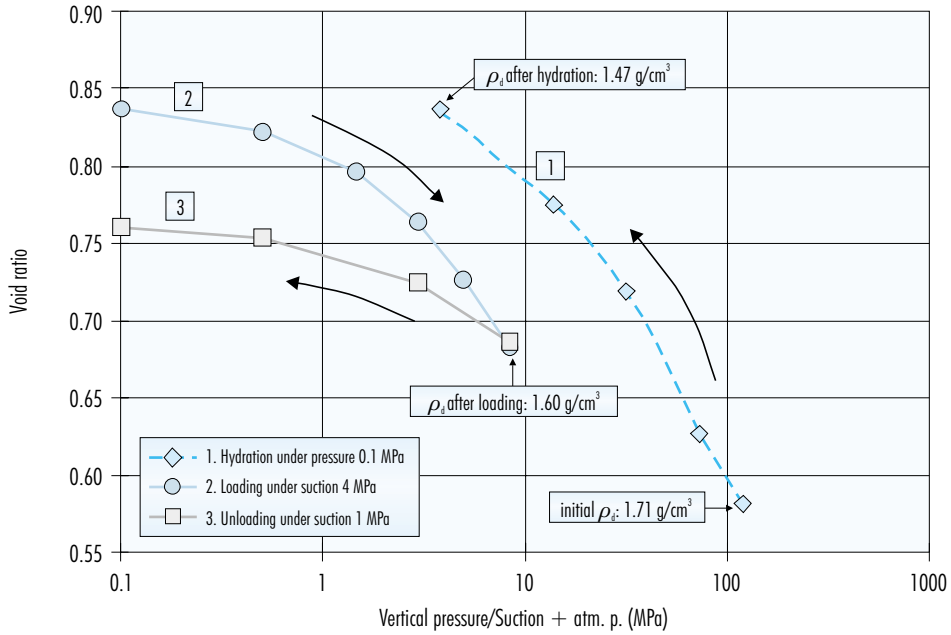

Figure 148. Evolution of void ratio during hydration and subsequent loading and unloading of the sample in test EDS2_9.

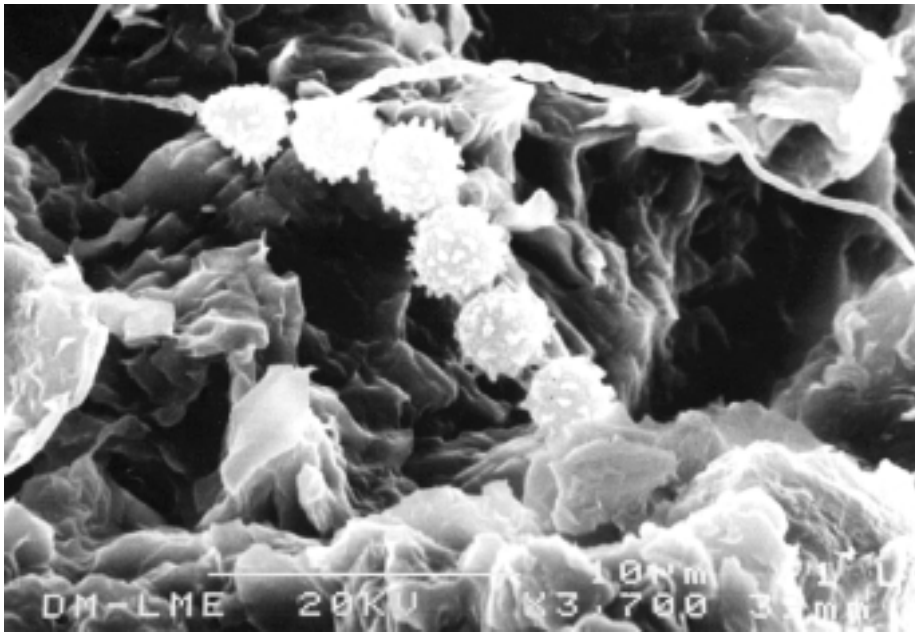

Figure 149. SEM image with magnification of 3,700 of a colony of bacteria in a sample subjected to oedometric testing with controlled suction and temperature.

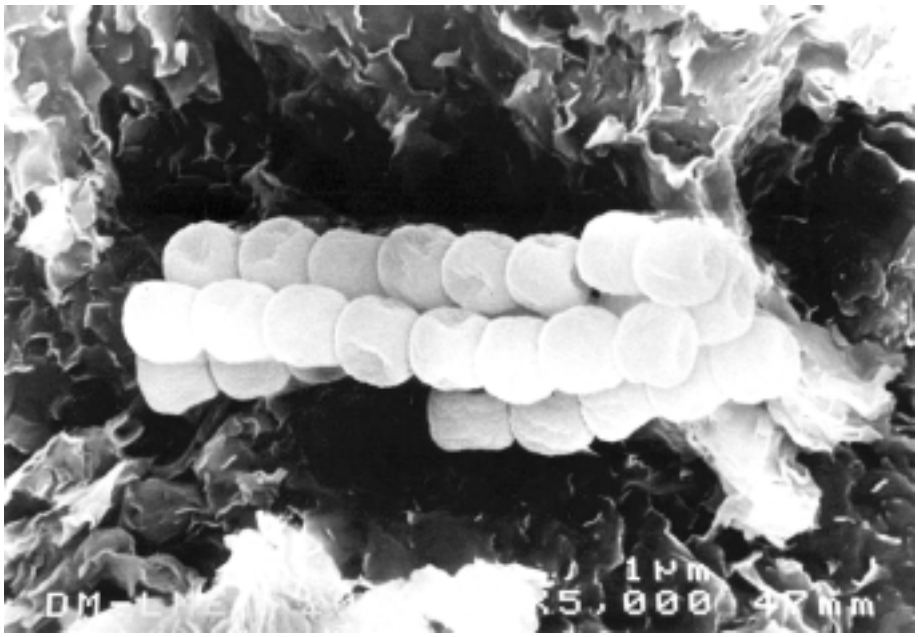

Figure 150. SEM image with magnification of 5,000 of a colony of bacteria in a sample subjected to oedometric testing with controlled suction and temperature.

percussion that this might have on the observed performance of the bentonite.

Swelling pressure

A swelling pressure test was performed for different values of suction in an oedometer with suction control by nitrogen pressure at a temperature of 40 °C, beginning with a value of suction of 0.5 MPa, followed by 5.0 MPa and finally a return to 0.5 MPa (EDNC_9). It is not possible to counteract swelling pressure on the initial step, as a result of which dry density decreases from the initial value of 1.70 g/cm^3 to 1.63 g/cm^3.

Table XLVI includes the values obtained along with the theoretical values of swelling pressure corresponding to each dry density, calculated using the fitting obtained for saturated samples at laboratory temperature (see section "Swelling pressure"). The swelling pressure obtained at 40 °C for a suction of 0.5 MPa is somewhat higher than that obtained at 20 °C for saturated samples, although this difference decreases after the sample is subjected to a

Table XLVI
Test on swelling pressure with controlled suction at 40 °C.

Step	Suction (MPa)	Final ρ_d (g/cm^3)	P_s at 40 °C (MPa)	Theoretical P_s at 20 °C (MPa)
	130	1.70		
1	0.5	1.63	8.4	7.1
2	5.0	1.65	8.1	8.1
3	0.5	1.64	8.1	7.9

process of drying (step 3). Nevertheless, the swelling pressure under a value of suction of 5.0 MPa at 40 °C is the same as that of samples saturated at laboratory temperature. The fact that both swelling pressures are similar suggests an increase in the swelling capacity of the bentonite at this temperature, since this pressure should decrease as suction increases, because there is a reduction in the degree of saturation. In any case, the effect of the temperature would not appear to be relevant, since all the values obtained are within the experimental range of variation.

Path E2

An oedometric test with suction controlled by nitrogen pressure was performed at 40 °C (EDNC_10), along with another at 60 °C (EDNC_11) and a third at 80 °C (EDNC_12), using specimens compacted at a nominal dry density of 1.70 g/cm^3 on path E2 (Figure 151). The same type of test was also performed at 20 °C (EDN1_5).

The first part of the test consists in loading the sample while maintaining the maximum value of suction allowed by the apparatus (14 MPa). During the first step under a load of 0.1 MPa, the dry density of the sample tested at 20 °C changes from 1.72 to 1.50 g/cm^3, that of the sample tested at 40 °C from 1.70 to 1.56 g/cm^3, that of the sample tested at 60 °C from 1.69 to 1.57 g/cm^3 and that of the 80 °C sample from 1.69 to 1.55 g/cm^3. In other words, the swelling that occurs initially when suction decreases from the 130 MPa corresponding to the initial conditions of the clay to the 14 MPa experienced in the oedometer is greater in the test performed at laboratory temperature, as may be appreciated in Figure 152. Figure 153 shows the evolution of void ratio during loading for the tests performed at the different temperatures. During loading, the reduction in the void ratio experienced by the sample tested at the higher temperature is smaller. This is due to the fact that the dry density of this sample is greater because it swelled less during the first step, which in turn may be due to temperature having caused the preconsolidation pressure to increase.

Once the maximum possible load (5 MPa) is reached, the sample is hydrated by gradually reducing suction to 0 MPa. Figure 154 includes the curves showing the evolution of void ratio during hydration. The samples subjected to higher temperatures undergo less swelling, especially for higher values of suction,

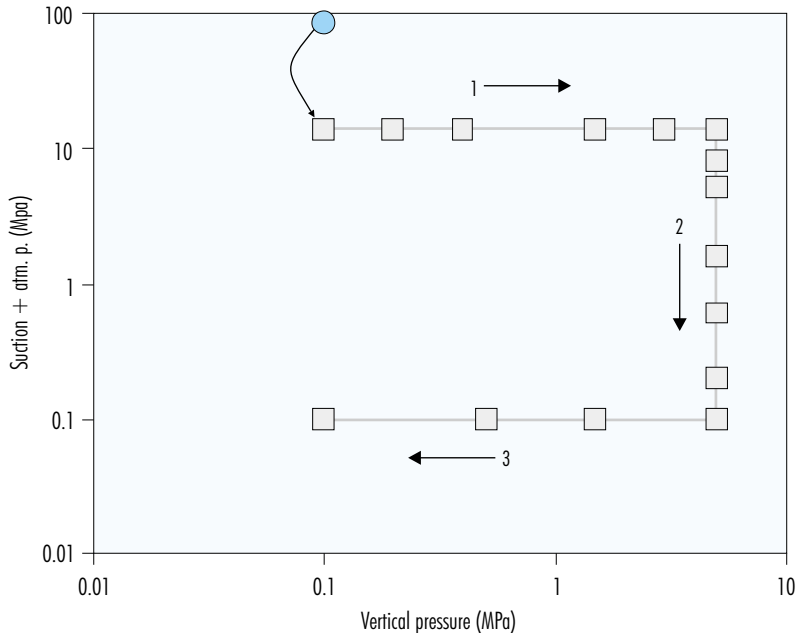

Figure 151. Path E2 in oedometers with control of suction by nitrogen pressure, performed at different temperatures.

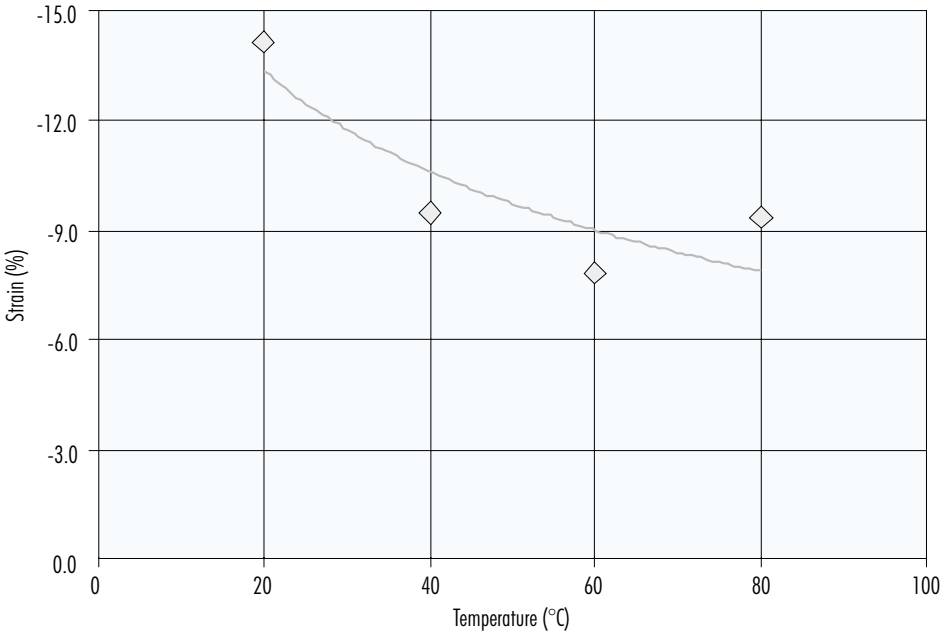

Figure 152. Strain on changing suction from 130 to 14 MPa under a load of 0.1 MPa in tests performed at different temperatures.

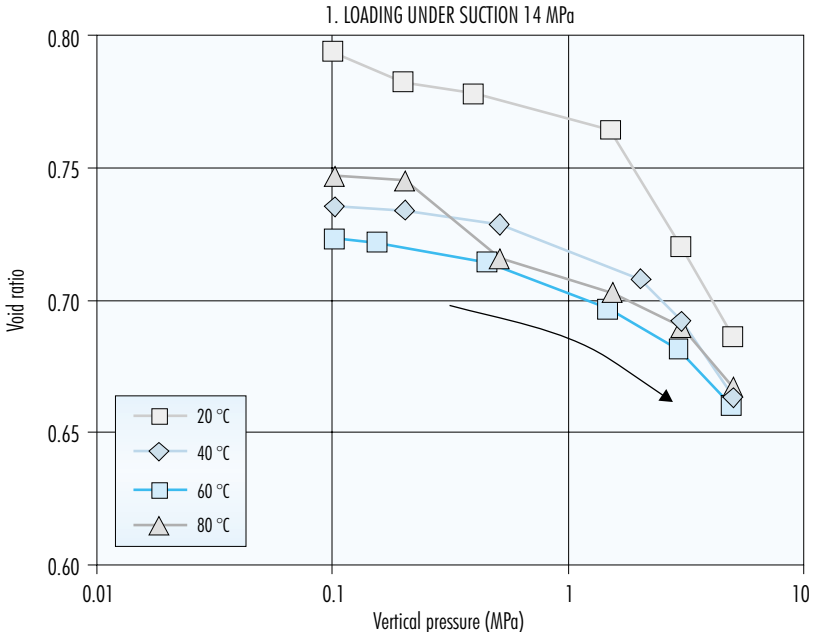

Figure 153. Evolution of void ratio during loading under a suction of 14 MPa in tests performed at different temperatures on path E2 (stretch 1).

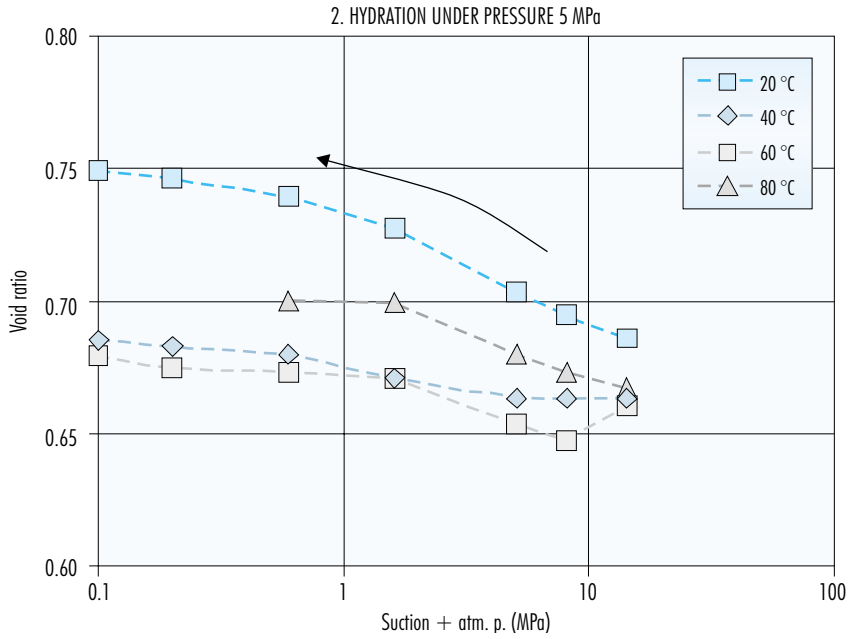

Figure 154. Evolution of void ratio during hydration under a load of 5 MPa in tests performed at different temperatures on path E2 (stretch 2).

although in no case is the increase in void ratio important, since the degree of saturation does not increase much in the range of suction of 14 to 0 MPa (see section "Retention curve"), and furthermore, whatever swelling might occur in the microstructure might be compensated by the collapse of the macrostructure. The effect of increasing preconsolidation pressure with temperature would also contribute to a lower degree of swelling during the hydration of the heated samples. There are no significant differences between the results obtained in the tests performed at 40 and 60 °C, except that the sample tested at 60 °C undergoes a certain degree of collapse when suction decreases from 14 to 8 MPa, this being recovered as suction continues to decrease. The sample tested at 80 °C, however, undergoes greater swelling than those tested at 40 and 60 °C as suction decreases.

The tests conclude with the stepwise unloading of the sample following saturation. The test performed at 80 °C (EDNC_12) had to be interrupted due to a breakdown that occurred prior to this phase being reached. The recovery of the void ratio during unloading is greater in the tests performed at higher temperatures, as is shown in Figure 155: in the test performed at 20 °C, void ratio increased by 26 percent during unloading, this increase amounting to 34 percent in the test performed at 40 °C and to 38 percent in the one carried out at 60 °C, which may be due simply to the fact that the dry densities of the samples subjected to higher temperatures are greater at the beginning of the unloading process. As had been observed, the recovery of void ratio during rapid unloading occurs logarithmically with load (Figure 155).

Consequently, temperature would appear to induce a hardening of the material, which swells less during saturation, this causing an increase in dry density and in preconsolidation pressure, and because of this there is a lower degree of consolidation during subsequent loading.

Analysis of results

Drying paths

The drying of the sample due to the increase of suction to values of close to 500 MPa (Paths E1/1, E1/2, E2 and E3) implies practically no reduction in

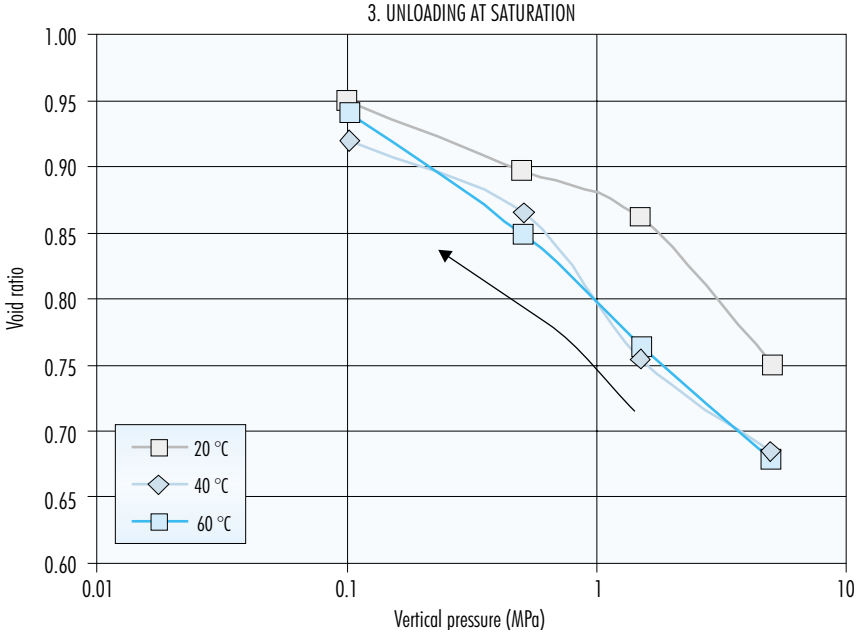

Figure 155. Evolution of void ratio during unloading under conditions of saturation in tests performed at different temperatures on path E2 (stretch 3).

volume, as may be appreciated in Figure 156, which represents the evolution of void ratio during drying under a load of 0.1 MPa for the different tests. In all cases the void ratio (e) decreases with increasing suction (s, MPa) in accordance with a logarithmic relation, for which the following equation may be fitted depending on initial dry density (ρ_d, g/cm3):

$$e = (0.16\,\rho_d - 0.29)\ln s + (-1.68\,\rho_d + 3.53)$$

The lines shown in Figure 156, the slope of which is almost independent from initial dry density, were obtained using this equation.

This minor variation in volume with drying from 120 MPa would appear to indicate that this value of suction is probably above the air entry point, that is to say, the value from which the loss of volume of water due to drying is compensated by the entry of a similar volume of air, with which the loss of water does not translate into loss of total porosity. Values of 100 MPa have been proposed for the point of air entry in montmorillonite (Tessier *et al*. 1992).

Once the drying process is completed, and when suction decreases to the initial value of 130 MPa, the initial dry density is practically recovered, as may be appreciated in Figure 157. Nevertheless, there is an interval of suction, approximately between 500 and 300 MPa, in which the deformations occurring during hydration are very small. This may be due to plastification of the material on drying, this displacing the elastic range. The elastic range would now be between approximately 500 and 300 MPa, when prior to drying it would be below the initial value of 130 MPa. Below these values, the reduction in suction does cause a significant increase in volume.

Furthermore, comparison of the evolution of void ratio during hydration under a minor load, as occurs in tests EDS2_9, EDS4_8 and EDS5_5, indicates that drying does not appear to modify the swelling capacity of the sample during subsequent hydration, due to the small magnitude of the deformations provoked by the drying/wetting cycle. In tests EDS4_8 and EDS5_5 hydration occurs following intense drying to a value of suction of 520 MPa, which did not occur in the case of test EDS2_9. Figure 158 represents the void ratios on the hydration path of test EDS2_9 and on the hydration path following drying in tests EDS4_8 and EDS5_5. The dry density for a suction of approximately 130 MPa is

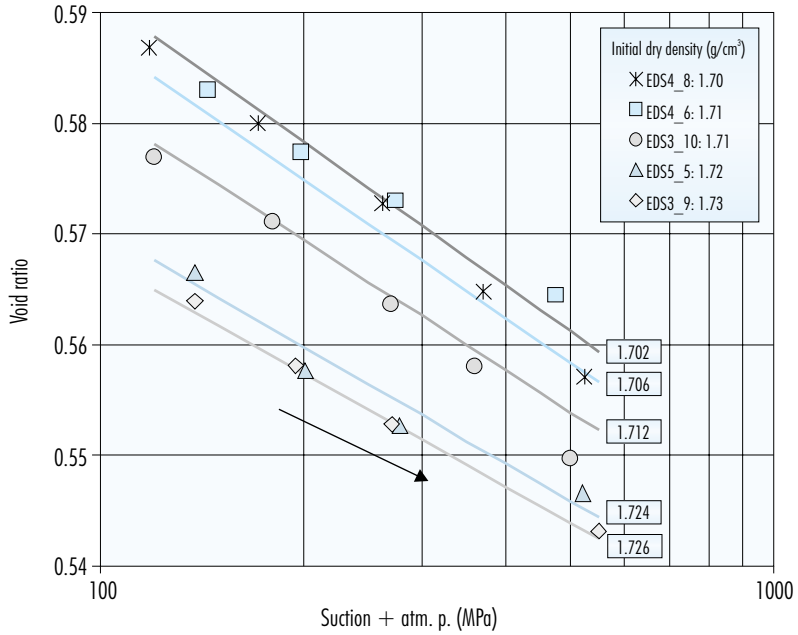

Figure 156. Evolution of void ratio during drying under a vertical load of 0.1 MPa in different tests (initial dry densities are indicated in g/cm³).

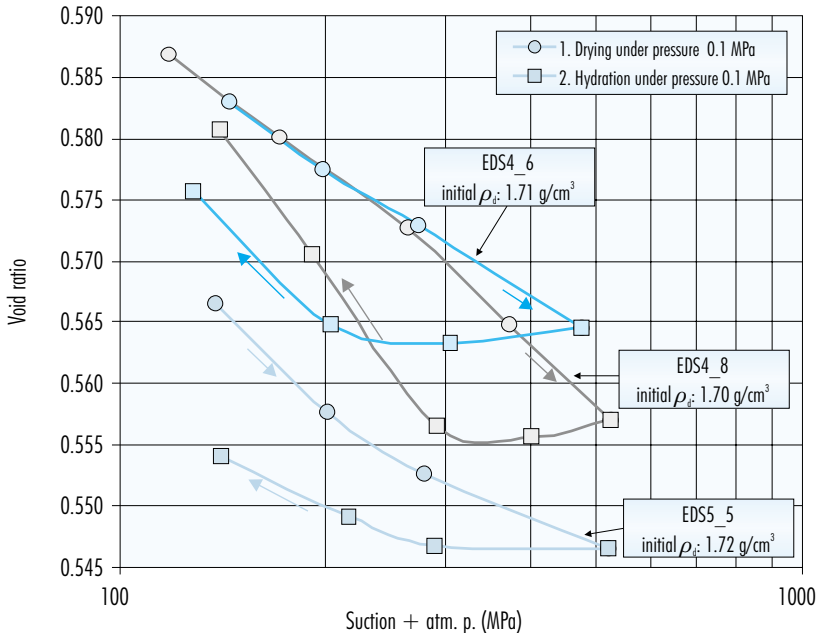

Figure 157. Evolution of void ratio during drying and hydration under a load of 0.1 MPa in different oedometric tests.

1.71 g/cm^3 in the case of tests EDS2_9 and EDS4_8, and 1.74 g/cm^3 for test EDS5_5. The dry density following hydration to a suction of 4 MPa is, however, lower in tests EDS4_8 and EDS5_5 –which included a particularly intense previous process of drying (Figure 156)– than in the case of test EDS2_9. It may also be observed that in the samples subjected to drying there is a very sharp change in slope when suction decreases to below the initial value. The models of microstructural behaviour show that the swelling experienced by a soil on decreasing suction under a given load is higher the higher the suction at the beginning of hydration, and that the relation between the percentage of strain and the decrease in suction increases on reaching lower values of suction, both of which aspects have been confirmed in these tests.

This slightly higher swelling in samples that had undergone previous drying was observed also on the retention curves under free volume conditions, on which the densities reached during the process of wetting after drying are somewhat lower than those experienced on hydration paths (see section "Free volume retention curve"). It might be the case, as was observed in the drying/wetting cycles with granulated samples (section "Atterberg limits, specific surface and granulometry"), that the drying causes a certain disaggregation of the primary particles and an increase in the free surfaces with the capacity to absorb water, and therefore swell. As will be seen below, the values of swelling pressure do not appear to decrease either following drying.

Furthermore, for suctions in excess of 120 MPa, external load does not lead to any important consolidation of the sample, which becomes rigid. This is clearly shown by the fact that the reduction in void ratio induced by load from 0.1 to 5 MPa under a suction of 520 MPa in test EDS3_9 (path E2) is analogous to that which occurs in test EDS1_10 under a suction of 130 MPa (path E5), and equal to 4 percent.

Influence of path

The variety of tests performed has made it possible to underline the repercussion of the type of path on the final value of strain, as well as on the reversibility of the latter. Samples having analogous starting situations and that reach similar final suction and

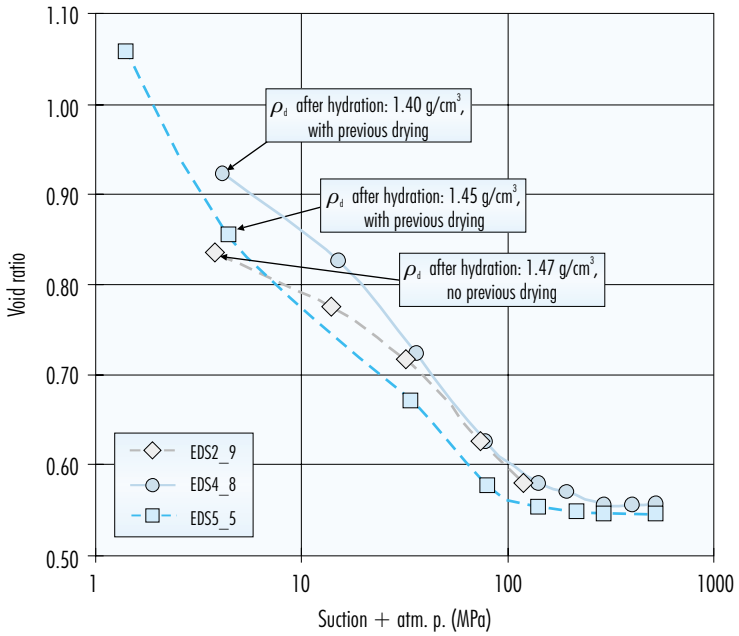

Figure 158. Comparison of the evolution of void ratio during hydration under a load of 0.1 MPa in three oedometric tests, two of which had previously included drying to a suction of 520 MPa.

load conditions, albeit via different situations of stress, show very different deformational behaviour. This section compares the results of pairs of tests performed on paths having common starting and end points, or some common intermediate point. In the interests of greater clarity, the figure showing the results also includes the paths –or stretches of paths- being compared.

Thus, for example, paths E2 (test EDN1_5) and E3 (test EDN4_7) start with the sample in the same conditions: suction 14 MPa and vertical load 0.1 MPa. On path E2 the sample is gradually loaded to 5 MPa and is then hydrated by decreasing suction under this high load (Figure 110). On path E3, however, the sample is initially loaded only to a minor value (0.5 MPa), under which hydration occurs. On reaching the minimum value of suction, 0.1 MPa, loading of the sample to 5 MPa is accomplished (Figure 115). Consequently, at this point the conditions of both tests are the same: suction 0.1 MPa and load 5 MPa. However, the void ratios are very different, as may be appreciated in Figure 159, which underlines the importance of the path followed as regards the final value of strain.

On the loading path in test EDN1_5 there is a change in slope that would appear to correspond to the "preconsolidation pressure", the value of which must have decreased during the hydration that occurs when the sample is placed in the oedometer under low values of load and suction during the initial step, due to the increase in volume associated with decreasing suction. From this value onwards, irreversible volume reduction strains would occur. Furthermore, the microstructural deformation that occurs on hydration is larger the smaller the load applied. The effect of increasing deformability under load in the more saturated sample (test EDN4_7) does not compensate for the greater expansion caused previously as a result of hydration under low load. In this respect, there is an increase in void ratio in test EDN4_7 that subsequent loading is not capable of counteracting.

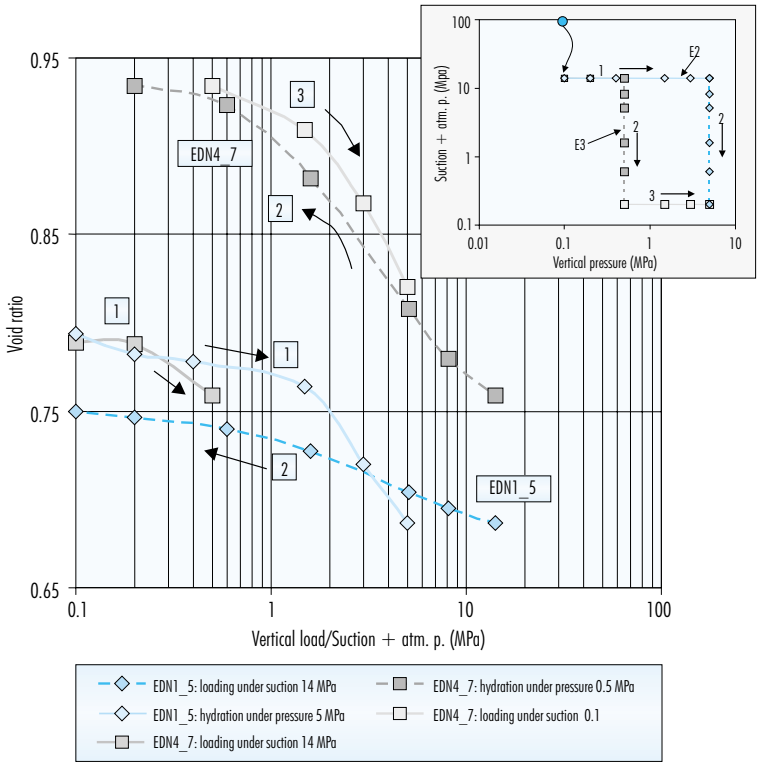

Figure 159. Comparison of void ratios at the end of each step on paths E2 (test EDN1_5) and E3 (test EDN4_7) performed in oedometers with control of suction by nitrogen pressure.

In the tests performed with control of suction by nitrogen pressure the sequence in which loads are applied prior to saturation also has an influence on final strain. This may be appreciated by comparing paths E2 and E4/1, on which hydration of the sample occurs due to the reduction of suction from 14 MPa under a vertical load of 5 MPa. On path E2 (test EDN1_5) the loading of the sample prior to hydration is accomplished stepwise. This means that on the first step an important increase in void ratio is possible (Figure 112), since for the maximum suction that may be applied using these oedometers (14 MPa) the bentonite has high water uptake capacity, especially if not loaded. On path E4/1 (tests EDN2_10 and EDN4_6) however, the entire load is applied at the beginning of the test, which restricts the decrease in initial density. This initial difference in the way load is applied modifies the behaviour of the material during subsequent hydration, as may be appreciated in Figure 160. In the test following path E2, the void ratio of the sample at the onset of hydration is higher than in the tests performed on path E4/1, and besides, the increase in void ratio that occurs during hydration is also higher.

The influence of the magnitude of vertical load during hydration on the deformational behaviour of the sample is even clearer if the results of tests performed in oedometers with suction control by solutions of sulphuric acid are compared. For example, paths E5 and E6 start and finish at the same values of load and suction, but while in the first the sample is loaded prior to hydration, on path E6 hydration occurs prior to loading. This translates into a major difference in final void ratios in the two tests, as is shown by Figure 161. The load in test EDS1_10 (path E5, stretch 1) occurs with the sample at its hygroscopic water content, since the suction applied corresponds to the value of relative humidity in the laboratory (130 MPa), therefore the sample is not saturated (the maximum dry density reached during loading is 1.72 g/cm3, which for a water content of

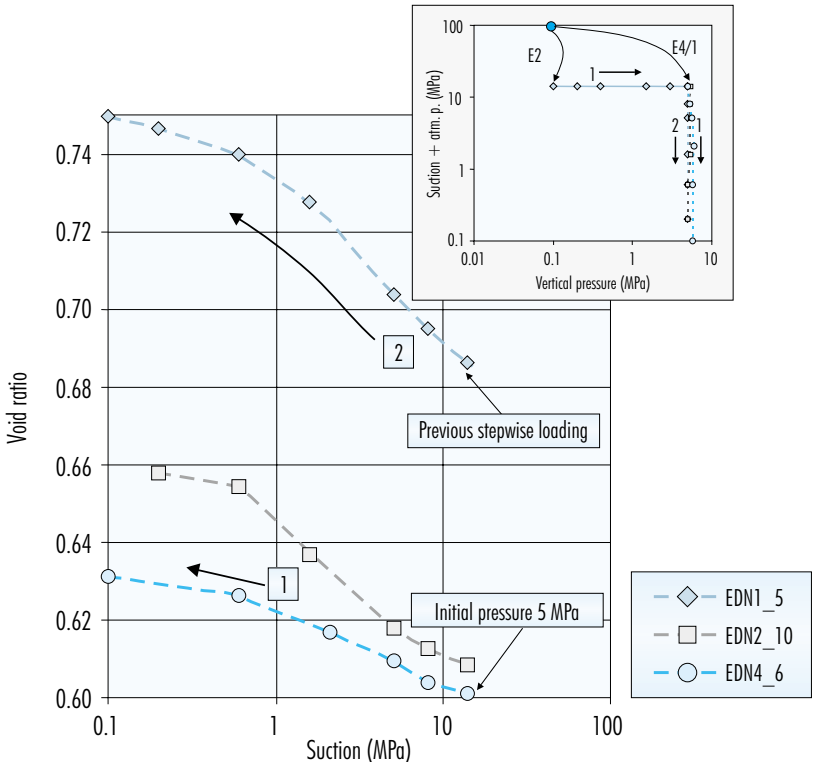

Figure 160. Evolution of void ratio during hydration under a load of 5 MPa on paths E2 (test EDN1_5) and E4/1 (tests EDN2_10 and EDN4_6).

14 percent –assuming that water content remains at its initial value–, corresponds to a degree of saturation of 66 percent). Furthermore, the sample is overconsolidated, as a result of which dry density increases only from 1.68 to 1.72 g/cm^3. Neither is there any significant increase in void ratio during subsequent hydration, since the decrease in suction takes place under a very high vertical load compared to swelling pressure (9 MPa, as opposed to a value of swelling pressure of 13 MPa for a dry density of 1.72 g/cm^3, in accordance with the fitting included in the section "Swelling pressure"), as a result of which the final value of dry density is larger than at the beginning of the test. On path E6 (test EDS2_9), however, hydration occurs under a very low vertical load, 0.1 MPa, this allowing the sample to expand until a dry density of 1.47 g/cm^3 is reached. The subsequent loading, which takes place under a suction of 4 MPa, occurs with the sample saturated (see section "Retention curve") and gives rise to an important degree of consolidation –since the dry density is lower than in the other test and the preconsolidation pressure must have decreased during previous hydration–, although it is not sufficient for the dry density to increase to its initial value. This is due to the fact that hydration causes irreversible strains, which are larger the lower the load applied during it.

The influence of the path on the final values of strain is also important after intense drying. This is made clear when comparing paths E2 and E3 in oedometers with suction control by means of solutions. Both begin and end under identical conditions of suction and vertical load (initial suction: 138 MPa, initial vertical load: 0.1 MPa, final suction: 1 MPa, final vertical load: 5 MPa) and begin with a gradual increase in suction to more than 500 MPa under a load of 0.1 MPa. However, on path E2 (test EDS3_9), loading of the sample to 5 MPa occurs after drying, followed by stepwise hydration to a suction value of 1 MPa; while on path E3 (test EDS5_5) the sample is hydrated after drying by decreasing suction to 1 MPa and is then loaded to 5 MPa (Figure 162).

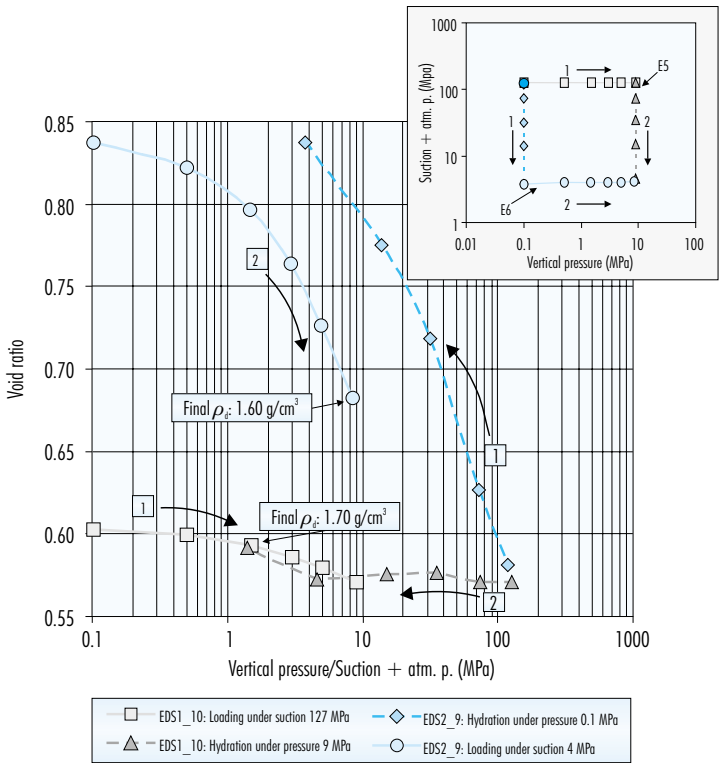

Figure 161. Comparison of void ratios at the end of each step on paths E5 (test EDS1_10) and E6 (test EDS2_9).

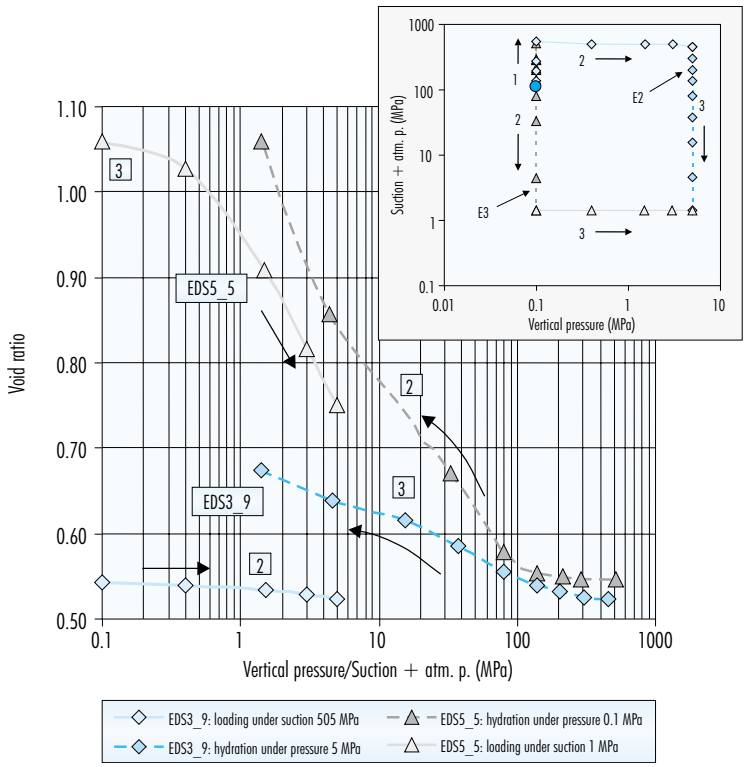

Figure 162. Comparison of void ratios at the end of each step on paths E2 (test EDS3_9) and E3 (test EDS5_5) (the initial drying of both tests is not represented).

Analogous to what was observed on path E6, the hydration of the sample under a small load on path E3 causes an important increase in void ratio, which cannot be counteracted with the subsequent vertical loading, as a result of which the value of dry density remains at 1.54 g/cm3. On path E2 (test EDS3_9), the loading of the sample subjected to an important value of suction, and therefore with a very small value of water content (lower than 6 percent according to the retention curves), hardly causes consolidation. In fact, the consolidation induced by loading from 0.1 to 5 MPa under a suction of 520 MPa amounts to 4 percent, analogous to that occurring in test EDS1_10 under a suction of 130 MPa (path E5). The dry density at the end of the loading cycle in test EDS3_9 is 1.77 g/cm3, which would correspond to a swelling pressure of 18 MPa. Consequently, the 5 MPa load under which the decrease in suction occurs is very far from the value of swelling pressure for this sample, this allowing the void ratio to increase considerably during hydration.

Despite the above, this increase in void ratio is insufficient to equal the dry density under the same final conditions in test EDS5_5.

In test EDS1_10 hydration occurs under a load of 9 MPa, while in test EDS3_9 it takes place under a lower load. In addition, the dry density at the beginning of hydration in test EDS3_9 (1.77 g/cm3) is higher than in test EDS1_10 (1.72 g/cm3), due to the drying that occurs at the beginning of the former. These two circumstances, higher dry density and the lower load under which hydration occurs (far from the value of swelling pressure of the sample), allow for greater recovery of void ratio in test EDS3_9 and contribute to the fact that in this test the collapse observed in test EDS1_10 does not occur. Another fundamental difference between the two tests is the water content of the sample on the initiation of hydration, which must be around 6 percent for test EDS3_9 and 14 percent for test EDS1_10 (see section "Retention curve"). Figure 163

compares the results of the two tests. It may be appreciated that for high suctions there is little change in rigidity in response to loads.

The collapse observed in test EDS1_10 may be explained as being the result of transfers between the micro and macrostructure. Under a vertical load of 9 MPa, only a limited quantity of water is able to enter the sample during hydration, which initially affects only the microstructure, because of the high values of suction involved. When suction decreases to 15 MPa, the mesopores begin to be affected, and when saturation occurs there is a loss of macrostructure strength and its collapse. When total saturation is reached, the clay continues to swell, since the interlamina has a greater availability of water from the mesopores (under a load of 9 MPa and with suction below 4 MPa, the macropores will probably have disappeared).

What has been presented in this section leads to the conclusion that when the sample is hydrated under a low vertical load (tests EDN4_7, EDN1_5, EDS2_9 and EDS5_5) void ratio increases considerably, and the vertical load subsequently applied is incapable of counteracting the swelling, despite the decrease in preconsolidation pressure. However, if swelling is prevented during saturation by loading the sample previously or simultaneously (tests EDS1_10, EDS3_9, EDN1_5, EDN4_6 and EDN2_10), the final volume change is smaller. This behaviour is an example of the irreversible macroscopic deformation induced by microscopic swelling, the magnitude of which depends on the stress path and agrees with the results reported by Brackley (1975) and Justo *et al*. (1984).

A quantitative demonstration of this behaviour is obtained by comparing the slopes of the straight lines that relate void ratio with suction (plus atmospheric pressure in MPa) –on a semilogarithmic scale– for hydration under different loads (index C_m of Fredlung & Rahardjo (1993), analogous to the λ_s index in Alonso *et al*. (1990)). The linear section of this relation spans the range of suctions 0.5 to 140 MPa, since for suctions of less than 0.5 MPa or in excess

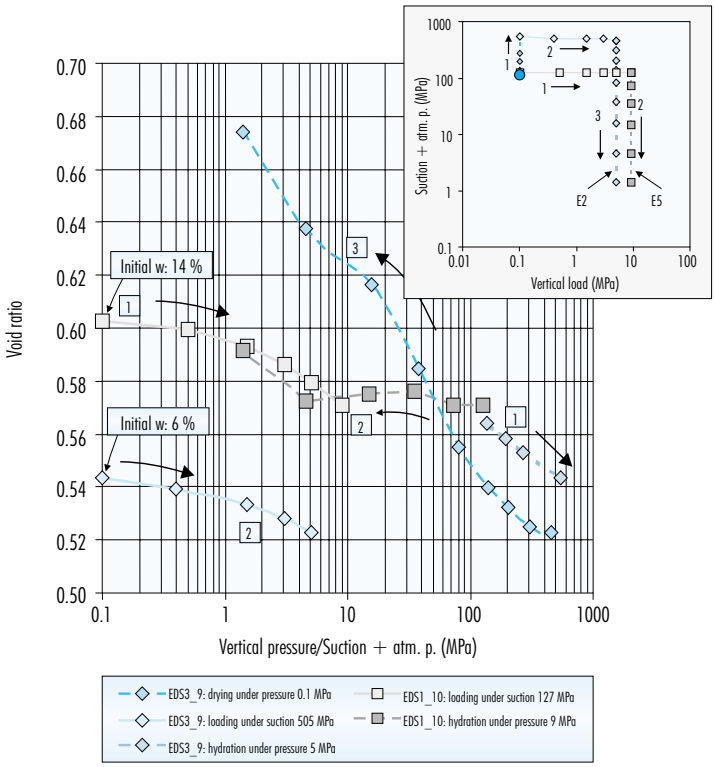

Figure 163. Comparison of void ratios at the end of each step on paths E2 (test EDS3_9) and E5 (test EDS1_10).

of 140 MPa, the changes in volume decrease in intensity. Table XLVII shows the values of this slope for the different tests, indicating the range of suction for which the relation is linear and the value of dry density at the beginning of the path. Also included are the slopes of the straight line relating void ratio and suction (plus atmospheric pressure in MPa) –on a semilogarithmic scale– for the drying paths between 120 and 520 MPa.

The values obtained are of the order of those reported by Fredlund & Rahardjo (1993) for different types of clay soils, between –0.07 and –0.29.

It may be observed that the values of the slope for the drying paths are much lower than those on the hydration paths for the same load. This indicates the low degree of deformability of the soil on exceeding a given value of suction, as was observed during analysis of the drying paths above 120 MPa in the previous section.

The values corresponding to the hydration paths are represented in Figure 164, where a logarithmic relation may be obtained between the magnitude of strain (indicated as variation in void ratio, Δe) associated with a given change in suction (s) and the load applied during the process (σ), the strain being greater the lower the load. This may be expressed by means of the following:

$$\Delta e / \Delta \log s = 0.044 \ln \sigma - 0.113 \quad (r^2 = 0.93)$$

The behaviour observed agrees with the models that maintain that the microstructural expansion due to decreasing suction is greater the lower the load applied, this giving rise to a reorganisation of the macrostructure which causes the void ratio to increase more as the load applied is lower. As a result, there is a plastic increase in volume and a softening of the material that modify the subsequent effect of the load applied to it (Gens & Alonso 1992), as was observed during the tests described above.

Preconsolidation pressure

As was pointed out at the beginning of this chapter, the samples tested in oedometers with suction control were uniaxially compacted under a load of 20 MPa to obtain a nominal dry density of 1.70 g/cm^3.

Table XLVII
Slope of the "void ratio/log suction" relation for paths of changing suction under constant load.

Test	Load (MPa)	Path (MPa)	Initial ρ_d (g/cm^3)	$\Delta e/\Delta \log s$
EDN1_5	5	14-0.5	1.57	-0.041
EDN3_10	9	14-0.5	1.59	-0.022
EDN5_6	10	14-0.5	1.55	-0.023
EDN4_7	0.5	14-0.5	1.51	-0.125
EDN4_6	5	14-0.5	1.71	-0.034
EDN2_10	5	14-0.5	1.71	-0.019
EDS3_9	5	139-1	1.76	-0.067
EDS5_5	0.1	141-1	1.74	-0.247
EDS4_8	0.1	140-1	1.72	-0.233
EDS2_9	0.1	119-1	1.71	-0.173
EDS4_6	0.1	144-475	1.70	-0.035
EDS3_9	0.1	138-506	1.72	-0.034
EDS5_5	0.1	138-520	1.72	-0.034
EDS4_8	0.1	118-523	1.71	-0.046

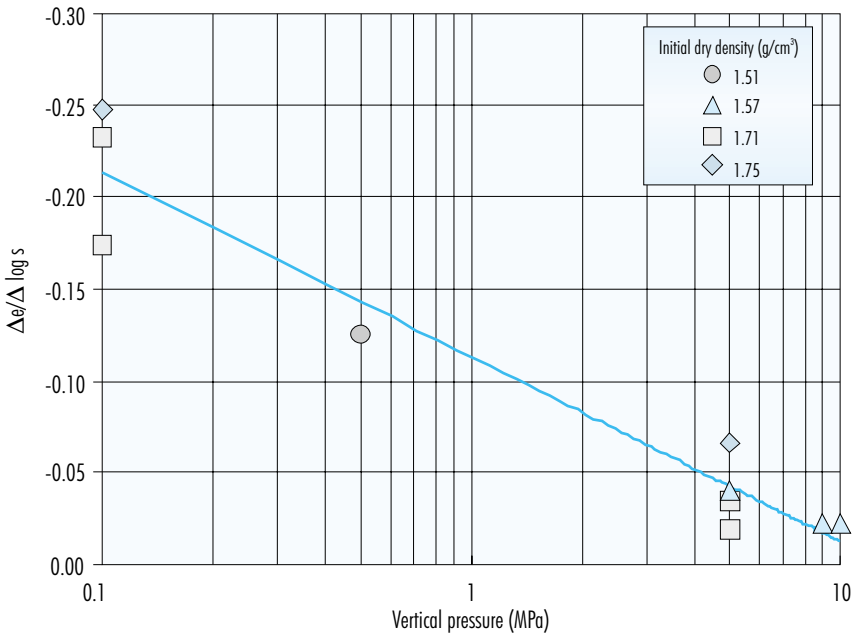

Figure 164. Slope of the "void ratio/log suction" relation for the paths of hydration under different loads indicated in Table XLVII.

In view of the maximum load that may be achieved with the oedometric equipment, which is around 10 MPa, this implies that the samples are overconsolidated at the beginning of the tests, as long as the initial suction (130 MPa) is not reduced. However, the modification of the structure of the sample, for example as a result of hydration under low load –with which more open structures with higher levels of porosity are obtained–, may cause the value of preconsolidation to decrease.

This has been analysed through determination of the preconsolidation pressure (σ'_p) in the graphs showing the evolution of void ratio due to increasing load under constant suction. The values obtained are included in Table XLVIII. In all the tests (with the ex-

Table XLVIII
Preconsolidation pressure for different tests.

Test	Suction (MPa)	Overload[1] (MPa)	ρ_d[2] (MPa)	σ'_p (MPa)
EDN1_5	14	0.1	1.50	1.5
EDN3_10	14	0.1	1.55	3.0
EDN4_7	0.1	0.5	1.40	1.3
EDS5_5	1.3	0.1	1.31	1.0
EDS1_10	127		1.68	20
EDS2_9	3.9	0.1	1.47	1.5

[1]*Overload during previous hydration.*
[2]*Dry density at the end of the first load step.*

ception of EDS1_10), loading was preceded by hydration under an overload, which is also indicated in the table. This causes a significant decrease in dry density. In test EDS1_10, loading occurred under conditions of hygroscopic water content (suction approximately 130 MPa), without previous hydration, on account of which the preconsolidation pressure is considered to be that corresponding to compaction.

These values are represented in Figure 165. It may be observed that, as suction decreases and the value of dry density is lower, in other words, the structure more open, the preconsolidation pressure decreases from the initial value of 20 MPa to values of between 1 and 3 MPa, these being smaller the lower the dry density at the initiation of loading. Likewise, when previous hydration takes place under conditions of higher overload, the preconsolidation pressure tends to be higher, because the resulting structure is not so open (test EDN4_7). Gens & Alonso (1992) attribute this type of behaviour to the microstructural deformations that occur during swelling, which, as has been pointed out, are greater the lower the overload under which hydration takes place. The swelling of the microstructure affects the skeleton of the soil, causing softening and a reduction of the area showing elastic behaviour (displacement of the loading/collapse (LC) surface towards lower values of load), as a result of which preconsolidation pressure would be reduced. This reduction will be more important the lower the load under which previous hydration was performed.

A determination was made also of the slope values of the straight lines relating void ratio to load (in MPa) –on a semilogarithmic scale– on paths with loading under constant suction (C_t index in Fredlung & Rahardjo (1993), equivalent to the compression index (C_c) in saturated soils) and the values of this slope on paths with unloading under constant suction (equivalent to the swelling index (C_s) in saturated soils). The values obtained are shown in Table XLIX, along with the specific path to which they correspond. The values of compression index may be classified in two groups, depending on whether they correspond to paths on which the load value remains below or above preconsolidation pressure, in other words paths on which the sample is overconsolidated or not, as shown in Figure 166.

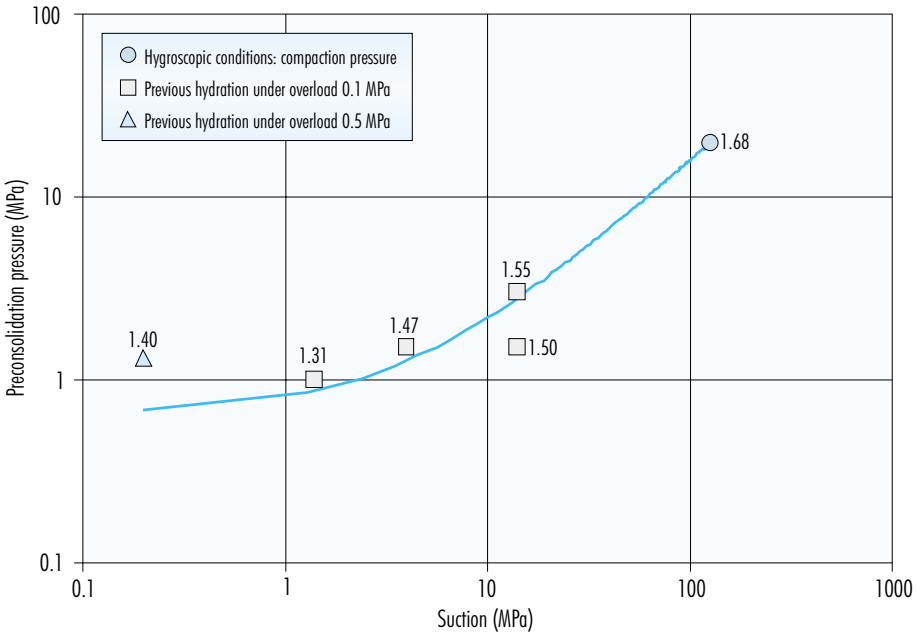

Figure 165. Preconsolidation pressure for different tests with loading under constant suction, indicating dry density at the end of the first loading step in g/cm³.

Table XLIX
Compression and swelling indexes obtained in oedometric test with controlled suction.

Test	Suction (MPa)	Path (MPa)	C_c / C_s	Overconsolidation Y/N
EDN4_7	0.1	3.0 – 5.0	-0.214	N
EDS5_5	1.3	1.5 – 5.0	-0.302	N
EDS2_9	3.9	3.0 – 8.4	-0.180	N
EDN1_5	14	1.5 – 5.0	-0.149	N
EDN3_10	14	3.0 – 9.0	-0.129	N
EDS1_10	127	0.5 – 9.1	-0.023	Y
EDS3_9	505	3.0 – 5.1	-0.012	Y
EDN1_5	0	5.0 – 0.1	-0.112	Y
EDN5_6	0	9.9 – 0.1	-0.125	Y
EDN3_10	0	9.0 – 0.1	-0.083	Y
EDN4_7	0	5.0 – 0.1	-0.076	Y
EDN3_9	0	9.5 – 0.2	-0.156	Y
EDS4_6	1.3	5.7 – 0.1	-0.080	Y
EDS3_10	1.3	9.0 – 0.1	-0.030	Y
EDS3_9	1.3	5.1 – 0.1	-0.114	Y
EDS5_5	1.3	5.0 – 0.01	-0.151	Y
EDS1_10	1.3	9.1 – 0.1	-0.111	Y
EDS2_9	1.3	8.4 – 0.1	-0.038	Y

It may be appreciated that the compression index tends to decrease as suction increases, and is significantly lower in the case of overconsolidated samples. Despite this, these indexes of load-induced strain are greater than the indexes of strain due to the effect of changing suction (C_m) included in Table XLVII.

Although swelling indexes habitually amount to 10-20 percent of compression indexes (somewhat higher in expansive clays), in these tests, for the low values of suction, they averaged 50 percent of the compression indexes. In other words, the values encountered are high in relation to those of the compression index.

Unloading

Most of the oedometric tests performed ended with a process of rapid, stepwise unloading of the sample once the minimum value of suction was reached. This value of suction was 0 MPa in the case of the oedometric tests performed with control of suction by nitrogen pressure and 1.3 MPa for those carried out with suction control by solutions. The process of unloading was performed over 3 or 4 steps, the duration of which was one day, three days as maximum. When the removal of load is accomplished following these patterns, the increase in void ratio (e) that occurs with decreasing load (σ, MPa) is logarithmic, as has been demonstrated in the previous sections:

$$e = a \ln \sigma + b$$

The parameters a and b in this equation, adjusted for each test, are shown in Table L, which also indicates the dry density of the sample on initiation of the unloading process, the suction under which this process is performed and the swelling index (C_s).

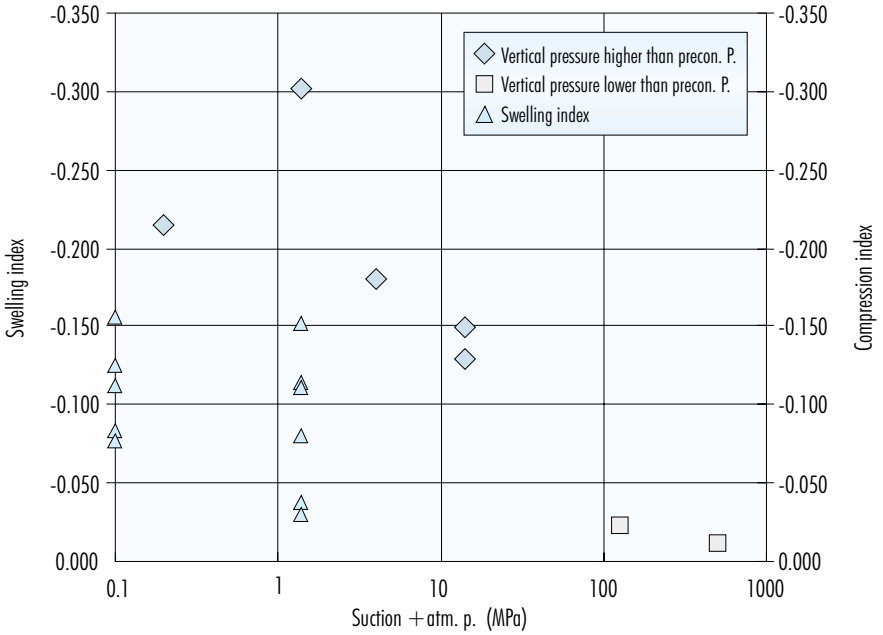

Figure 166. Compression and swelling indexes obtained on paths of loading and unloading under constant suction (precon. P. = preconsolidation pressure).

Table L
Parameters of fitting of the logarithmic equation relating void ratio to load during final unloading in the tests.

Test	Temperature (°C)	ρ_d^1 (g/cm³)	Suction (MPa)	a	b	C_s
EDN4_7	20	1.48	0	-0.033	0.871	-0.08
EDN5_6	20	1.61	0	-0.055	0.773	-0.12
EDS1_10	20	1.70	1	-0.048	0.713	-0.11
EDS3_9*	20	1.61	1	-0.050	0.753	-0.11
EDS4_6*	20	1.63	1	-0.035	0.721	-0.08
EDS5_5*	20	1.54	1	-0.066	0.843	-0.15
EDNC_10	40	1.60	0	-0.063	0.791	-0.15
EDNC_11	60	1.61	0	-0.068	0.793	-0.16

[1] Dry density on initiation of unloading.
** Tests including intense drying.*

In those cases in which the unloading steps extended longer than foreseen, the evolution of void ratio no longer followed this trend (tests EDN1_5, EDN3_9, EDN3_10 and EDS3_10), this indicating that equilibrium had not been attained after 24 hours.

The unloading process in those tests that followed a path including intense drying of the sample as a result of increasing suction (EDS3_9, EDS4_6 and EDS5_5) may be fitted to an equation that includes the value of dry density at the beginning of unloading (ρ_d^1, g/cm^3):

$$e = 0.31\rho_d^1 - 0.55) \times \ln\sigma + (-1.34\,\rho_d^1 + 2.92)$$

Figure 167 shows the results of unloading for various tests and the fittings obtained using the previous equation for tests in which there was previous drying as a function of their dry density at the beginning of unloading. The figure also includes a fitting obtained for tests performed at temperatures in excess of 20 °C (40 and 60 °C) with a dry density on initiation of the unloading process of 1.60 g/cm^3:

$$e = -0.065\ln\sigma + 0.792$$

Swelling pressure

Several tests were performed for the measurement of swelling pressure at decreasing values of suction. As has been indicated above, the swelling pressure of an unsaturated soil was considered to be the external load under which the sample undergoes no change in volume during hydration. Although the nominal dry density at the beginning of the tests is 1.70 g/cm^3, the load capacity of the equipments –maximum 10 MYPa– did not allow this to be kept constant throughout the entire determination, since the theoretical swelling pressure for a saturated sample of this density is 11.5 MPa (see section "Swelling pressure"). For this reason, in most cases the values of swelling pressure obtained correspond to samples whose dry density undergoes some reduction during hydration.

The specific paths followed and the results of each test are shown in Figure 168, which includes the theoretical values of swelling pressure for saturated samples of the same dry density.

These values were calculated by means of the fitting obtained from the results of swelling pressure tests on samples manufactured by compacting the clay with its hygroscopic water content at different dry densities and saturated with distilled water (section "Swelling pressure: Variation depending on void ratio"):

$$\ln P_s = 6.77\rho_d - 9.07 \qquad (r^2 = 0.88)$$

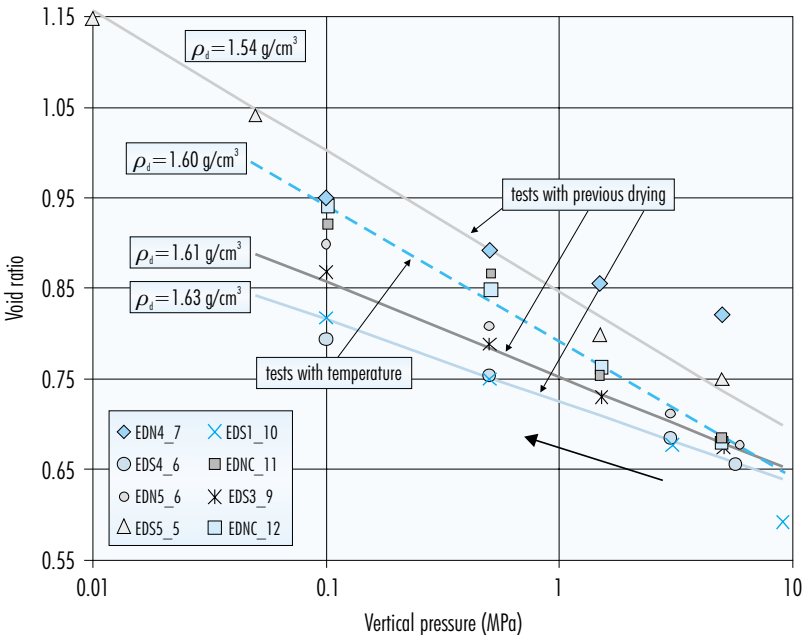

Figure 167. Evolution of void ratio during unloading at saturation in different tests and logarithmic fittings (the values of dry density on initiation of unloading are also shown).

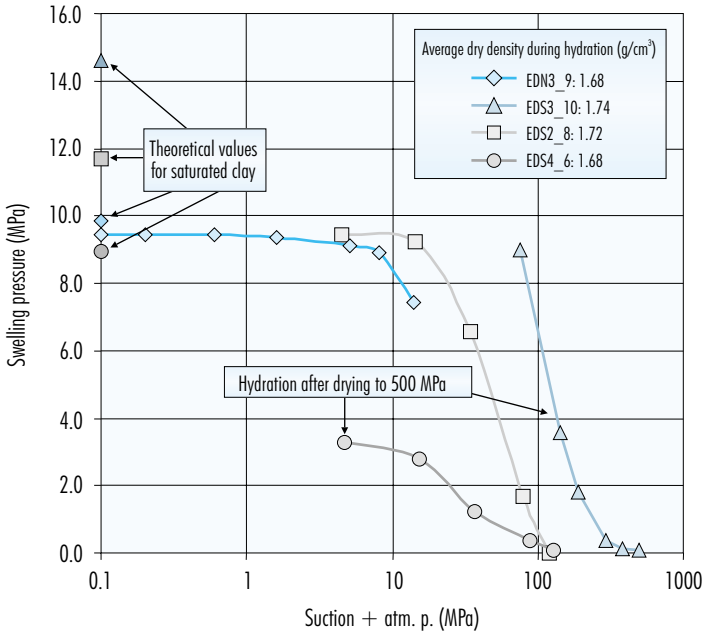

Figure 168. Swelling pressure obtained for decreasing suction on paths E4/2 (test EDN3_9), E4 (test EDS2_8), E1/2 (test EDS3_10) and E1/1 (test EDS4_6).

When comparing the values of swelling pressure for saturated samples obtained from oedometer testing with controlled suction with the theoretical values calculated using this fitting, it is necessary to bear in mind that the difference observed between the experimental values and the fitting averaged 25 percent.

In the figure it may be appreciated that the swelling pressure of the unsaturated sample shows a logarithmic increase between 130 MPa (the suction corresponding to hygroscopic water content) and 10 MPa, but that below this value the increase is attenuated. The data obtained point to the sample's being completely saturated for suctions of 4 MPa, or to the increase in the degree of saturation corresponding to the decrease in suction from 4 to 0 MPa being small –as may be deduced from the retention curves–, as a result of which the sample reaches its equilibrium porosity under the load applied, with no further increases in swelling pressure. Even though the microstructure were to undergo some degree of swelling, the development of collapse in the macrostructure for these high loads and low suctions would contribute to the volume of the sample not varying.

Throughout the entire interval of suction tested, swelling pressure depends on dry density, and is higher the greater the latter. Furthermore, for suction in excess of 200 MPa hardly any swelling pressure is developed.

In test EDN3_9 (path E4/2 in oedometers with control of suction by nitrogen pressure), the equipment loading limit is reached for suctions of below 1.5 MPa, without this implying any significant reduction in the dry density of the sample. On reaching zero suction, the saturated sample has a dry density of 1.68 g/cm^3 under the maximum load allowed by the equipment, which is 9.5 MPa. This value of swelling pressure is of the order of the values obtained for saturated clay of the same density, in accordance with the fitting shown above.

In test EDS2_8 (path E4 in oedometers with suction control by means of solutions), which is initiated with a dry density of 1.73 g/cm^3, it was not possible to counteract swelling for suctions below 14 MPa. On the last step, equilibrium is reached under a suction of 4.4 MPa with a load of 9.5 MPa, the sample remaining with a dry density of 1.70 g/cm^3. The theoretical swelling pressure of the saturated sample at

this density should be 11.5 MPa. In view of the minor variation in swelling pressure for low values of suction measured in other tests, a value of swelling pressure somewhat lower than the theoretical value would have been obtained in this test, albeit within the deviation expected.

Two swelling pressure tests were also performed after subjecting the sample to intense drying by increasing suction to values in excess of 500 MPa in the oedometers with suction control by solutions. These tests were EDS3_10 (path E1/2) and EDS4_6 (path E1/1). In the first of these, the swelling pressure of the sample is determined with the dry density attained at the end of drying, 1.74 g/cm^3, which is, therefore, higher than in the rest of the tests. In test EDS4_6, suction is decreased once more following drying, and when the initial value of 130 MPa is reached, the loads required to determine swelling pressure are applied.

The value of swelling pressure for a suction of 4.7 MPa obtained in test EDS4_6 is 3.3 MPa, much lower than that which would correspond to a saturated sample of the same dry density, 1.66 g/cm^3 (8.7 MPa). Below this suction, the dry density of the sample decreases, due to the load limitations of the equipment, reaching a value of 1.63 g/cm^3 for a suction of 1.3 MPa, under a load of 5.7 MPa, which is also lower than the theoretical value of swelling pressure for the saturated sample, which would be 7.2 MPa (not represented in the figure). In any case, the final value of swelling pressure obtained remains within the experimentally verified margins of deviation.

In test EDS3_10, however, it is observed that for suctions below 80 MPa, the swelling pressure of the sample exceeds the loading limit of the equipment (9 MPa), as a result of which its dry density begins to decrease, reaching a value of 1.63 g/cm^3 for a suction of 4 MPa, which is maintained to the minimum value of suction. This swelling pressure of 9 MPa is higher than the theoretical value for a saturated sample with a dry density of 1.63 g/cm^3, which would be 7.2 MPa, but is also within the range of scattering observed for the FEBEX bentonite.

Consequently, the results of the two swelling pressure tests performed on previously desiccated samples have been scattered, although in both cases the values obtained are within the theoretical range of variation of this parameter for the FEBEX bentonite. This suggests that drying by increasing suction to 500 MPa does not cause any modification in swelling pressure that might be appreciated with the experimental techniques available. Test EDS3_10 suggests that the swelling pressure developed after drying is even greater than in the case of the untreated sample, which agrees with the high swelling capacity recorded in samples previously subjected to high values of suction (see section "Drying paths").

Thermal characterisation

Thermal conductivity

Thermal conductivity was measured using the Kemtherm QTM-D3 equipment, which operates in accordance with the transient hot wire method. The measurement is performed at laboratory temperature in triplicate for each sample. Small blocks of clay (10x4x3 cm) were used, obtained by uniaxial compaction at nominal dry densities of 1.60, 1.65, 1.70 and 1.75 g/cm^3. The granulated clay was used for compacting, either at hygroscopic water content or with added water. In this last case, the samples remained in closed plastic bags for several days, following mixing of the clay and water, to guarantee a homogeneous distribution of the water. The compaction pressures were between 12 and 35 MPa, depending on dry density, for the blocks manufactured from the clay with its hygroscopic water content. In the case of the blocks manufactured from clay with a water content of 20 percent, the compaction pressures were between 23 MPa, for the lower dry densities, and 65 MPa, for the higher densities. Following the measurement of thermal conductivity, certain of these blocks were oven dried at 100 °C for 24 hours and, after cooling, their thermal conductivity was determined again. On completion of the measurements, all the blocks on which the determination had been performed, both those dried and those not, were reweighed and measured and their water content determined by oven drying, to check actual water content and the change in density.

In most of the tests, the measurement was accomplished by applying the probe to the compaction surface of the block, therefore the value obtained is the one for conductivity in the direction parallel to the force of compaction. However, with a view to gaining insight into the influence of the direction of measurement on the value of thermal conductivity, and consequently the anisotropy of this property, certain of the samples were measured on two adjacent faces, *i.e.* parallel and perpendicular to compaction force.

The average values of thermal conductivity, measured in two directions with respect to compaction (λ parallel, λ perpendicular), dry density (ρ_d), water content (w), degree of saturation (S_r) and volumetric water content (θ) of each block are shown in the following tables. The data have been grouped on the basis of the dry density of the specimen, this having allowed four ranges of density to be distinguished:

- Specimens with a dry density of between 1.49 and 1.55 g/cm^3, with an average value of 1.53 g/cm^3. The results of the tests performed using these specimens are shown in Table LI.
- Specimens with a dry density of between 1.58 and 1.65 g/cm^3, with an average value of 1.61 g/cm^3. The results of the tests performed using these specimens are shown in Table LII.
- Specimens with a dry density of between 1.66 and 1.74 g/cm^3, with an average value of 1.70 g/cm^3. The results of the tests performed using these specimens are shown in Table LIII.
- Specimens with a dry density of 1.75 g/cm^3. The results of the tests performed using these specimens are shown in Table LIV.

The blocks having a water content of close to 0 percent are those which were oven dried following compaction at a different water content. This process of drying implies an increase in dry density due to shrinkage. The density on completion of the determination is the one indicated in the tables. The slight uptake of water observed (values of water content somewhat higher than 0 percent) occurs during the measuring process, which takes place under laboratory temperature and relative humidity conditions.

Figure 169 includes a graphic representation of the values of thermal conductivity in the direction parallel to compaction force versus water content for the different intervals of density. Thermal conductivity (λ, W/m·K) may be related exponentially to water content (w, %) in the interval studied. This relation, which also includes the contribution made by dry density (ρ_d, g/cm^3), is expressed as follows:

$$\ln \lambda = \ln(0.8826\,\rho_d - 0.8909) + 0.003\,w$$

The fittings shown in Figure 169 are obtained using this equation.

The values of thermal conductivity are of the same order as those encountered by other authors for similar materials. Beziat *et al.* (1988) report values of thermal conductivity for a calcium smectite, compacted over an interval of densities and with a water content similar to those used in this study, of between 0.57 and 1.32 W/m·K. Pusch (1994) gives a value of 0.7 W/m·K for bentonite compacted with hygroscopic water content, and of 1.5 W/m·K for bentonite compacted at the same density but completely saturated. Both works point to an important increase in thermal conductivity with water content and density.

Table LI
Thermal conductivity (λ) of specimens with dry densities of between 1.49 and 1.55 g/cm^3 (average dry density of 1.53 g/cm^3).

ρ_d (g/cm^3)	w (%)	S_r^* (%)	λ parallel (W/m K)	λ perpend. (W/m K)	θ
1.53	0.1	0.00	0.48		0.00
1.55	0.9	0.03	0.48		0.01
1.55	0.9	0.03	0.50		0.01
1.53	1.7	0.06	0.50		0.03
1.49	14.2	0.48	0.75		0.24
1.51	15.0	0.51	0.76	0.71	0.26
1.54	18.1	0.64	0.92		0.33
1.52	20.0	0.70	0.91	0.90	0.36
1.52	25.0	0.87	1.09	1.15	0.48

**Degree of saturation calculated considering the density of free water.*

Table LII
Thermal conductivity (λ) of specimens with dry densities of between 1.58 and 1.65 g/cm^3 (average dry density of 1.61 g/cm^3).

ρ_d (g/cm^3)	w (%)	S_r^* (%)	λ parallel (W/m K)	λ perpend. (W/m K)	θ
1.58	0.1	0.00	0.48		0.00
1.60	1.0	0.04	0.55		0.02
1.59	1.1	0.04	0.58		0.02
1.60	2.0	0.08	0.57		0.03
1.63	12.6	0.52	0.73		0.23
1.60	13.1	0.51	0.68		0.24
1.60	13.3	0.52	0.61		0.24
1.64	13.8	0.57	0.91		0.26
1.58	15.0	0.57	0.81	0.73	0.27
1.63	15.0	0.62	0.95	0.89	0.28
1.65	15.0	0.64	1.00	0.89	0.28
1.59	15.4	0.60	0.70		0.28
1.59	15.5	0.60	0.70		0.28
1.60	15.5	0.61	0.78		0.29
1.61	18.6	0.74	1.12		0.36
1.59	20.0	0.77	1.12	0.99	0.38
1.65	20.0	0.85	1.18	1.16	0.40
1.60	20.4	0.80	1.22		0.39
1.63	25.3	1.04	1.27		0.52
1.64	25.4	1.06	1.31		0.52
1.62	26.0	1.05	1.27		0.53
1.62	26.2	1.06	1.30		0.54
1.60	26.6	1.04	1.25		0.54
1.61	27.1	1.08	1.28		0.55
1.59	27.4	1.06	1.26		0.56

The increase in thermal conductivity with water content for a given density (and consequently porosity) is due to the fact that the thermal conductivity of water (0.58 W/m·K) is higher than that of air (0.025 W/m·K), 23 times higher, as a result of which the increase in the water content of the pores translates into an increase in overall thermal conductivity. Furthermore, this increase is seen not to be linear. This is because below a given value of water content, water is adsorbed or forms a film over the mineral particles. For higher water contents, filling of the pores begins, with water "bridges" being formed be-

Table LIII
Thermal conductivity (λ) of specimens with dry densities of between 1.66 and 1.74 g/cm^3 (average dry density of 1.70 g/cm^3).

ρ_d (g/cm^3)	w (%)	S_r^* (%)	λ parallel (W/m K)	λ perpend. (W/m K)	θ
1.67	0.1	0.00	0.64		0.00
1.72	0.5	0.02	0.63		0.01
1.70	1.2	0.06	0.68		0.02
1.74	1.4	0.07	0.72		0.02
1.66	1.9	0.08	0.62		0.03
1.73	11.9	0.57	0.83		0.23
1.72	12.9	0.61	0.81		0.25
1.70	13.1	0.60	0.79		0.25
1.67	13.4	0.58	1.05		0.25
1.74	13.7	0.67	0.90		0.27
1.70	14.4	0.66	1.03		0.28
1.69	15.0	0.68	0.95	0.95	0.29
1.71	15.0	0.70	0.94		0.29
1.70	16.8	0.77	1.19		0.33
1.71	17.0	0.80	1.23		0.34
1.67	20.0	0.88	1.14	1.17	0.40
1.72	20.0	0.95	1.43	1.39	0.41
1.73	21.6	1.04	1.22		0.45
1.70	21.8	1.00	1.27		0.45
1.69	22.3	1.01	1.25		0.46
1.71	22.6	1.05	1.25		0.47
1.69	22.7	1.03	1.27		0.47

*Degree of saturation calculated considering the density of free water.

Table LIV
Thermal conductivity (λ) of specimens with a dry density of 1.75 g/cm^3.

ρ_d (g/cm^3)	w (%)	S_r^* (%)	λ parallel (W/m K)	θ
1.76	16.2	0.82	1.27	0.33
1.75	20.4	1.01	1.24	0.43
1.76	20.5	1.04	1.23	0.43

*Degree of saturation calculated considering the density of free water.

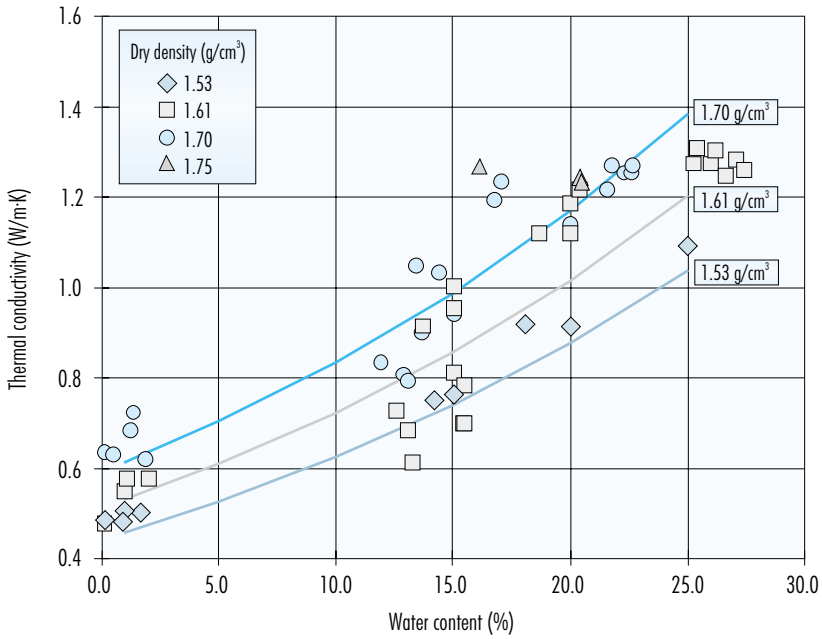

Figure 169. Thermal conductivity versus water content for different dry densities.

tween the voids filled with air, on account of which thermal conductivity increases in a significant amount. Above a certain value of water content, the increases in water content have a slight effect on the value of conductivity (Tindall & Kunkel 1999).

The increase in density contributes also to the increase in thermal conductivity, due to the fact that the decrease in porosity implies a reduction of the space occupied by water or air, components that both have a much lower conductivity than the mineral particles.

Figure 170 shows the values of thermal conductivity for the specimens, this having been measured parallel and perpendicular to compaction. There is no important variation in thermal conductivity in either direction with respect to the other, although it is usually slightly higher when measured parallel to the compaction force. This difference decreases as water content increases, and the ratio may even be inverted for a water content of 25 percent. This lack of anisotropy, already observed in relation to other properties (permeability, retention curve) confirms that there is no reorganisation of aggregates during compaction. Heat dissipation across the barrier of the disposal facility will occur mainly in the radial direction, *i.e.* perpendicular to the block compaction force.

Figure 171 shows all the values of thermal conductivity (λ, W/mK), grouped by density intervals, versus the degree of saturation (S_r). A correlation has been determined between the degree of saturation (S_r) and the coefficient of thermal conductivity. A sigmoidal type equation has been used for this purpose (Boltzmann):

$$\lambda = \frac{A_1 - A_2}{1 + e^{(Sr - x0)/dx}} + A_2$$

where A_1 represents the value of λ for $S_r=0$, A_2 the value of λ for $S_r=1$, x_0 the degree of saturation for which thermal conductivity is the average of the two extreme values and dx is a parameter. This equation was chosen because it accurately represents the behaviour of conductivity versus water content (degree of saturation), which as has been seen above, are directly related but not in a linear fashion.

The fitting obtained, with an r^2 of 0.923, gives the following values for each parameter:

$$A_1 = 0.57 \pm 0.02$$

$$A_2 = 1.28 \pm 0.03$$

$$x_0 = 0.65 \pm 0.01$$

$$dx = 0.100 \pm 0.016$$

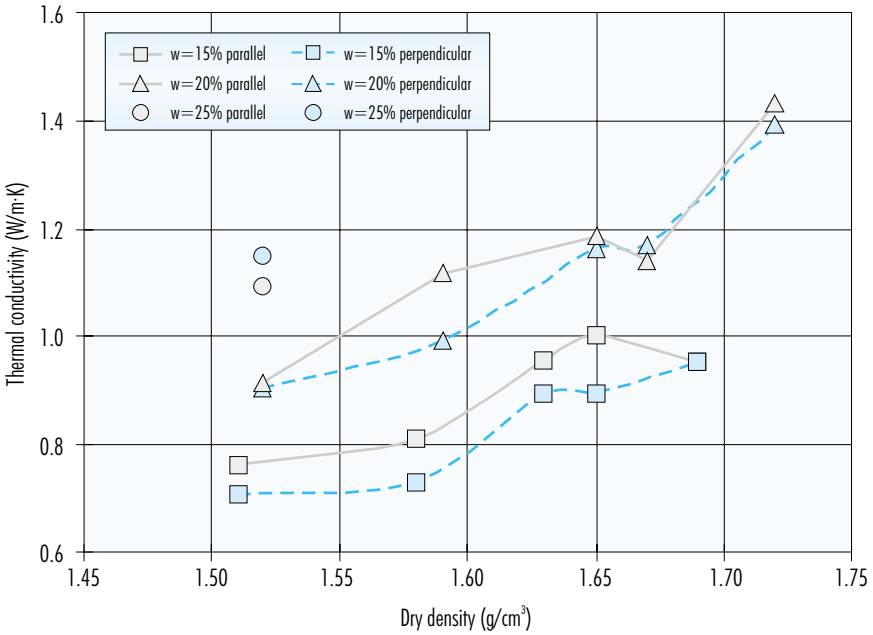

Figure 170. Thermal conductivity, measured parallel and perpendicular to the compaction surface, as a funtion of the dry density and water content of the blocks.

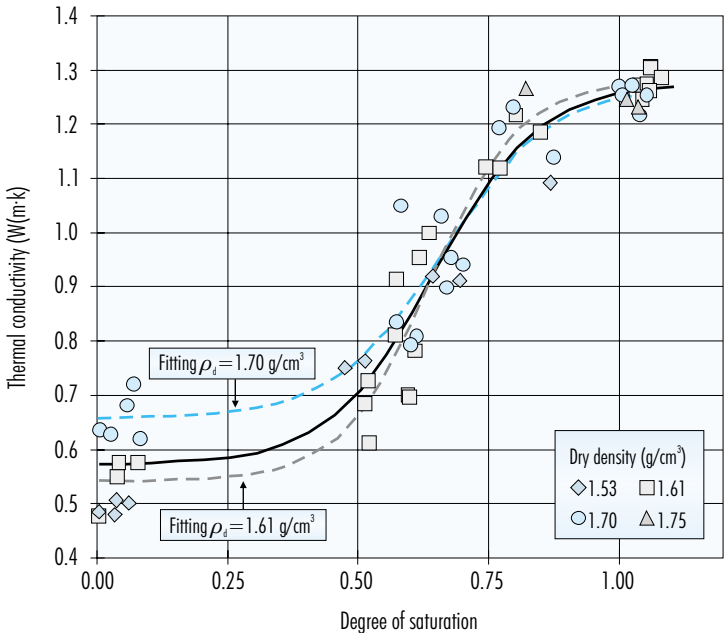

Figure 171. Thermal conductivity versus degree of saturation and fitting for all the points (continuous line) and two intervals of density.

The figure also includes the fittings obtained with the values corresponding to two intervals of density.

A clear distinction depending on dry density may be observed for the low degrees of saturation, the thermal conductivity of samples having a higher dry density being greater for a given degree of saturation. However, this difference is attenuated as the degree of saturation increases. The parameters of the fittings for dry densities of 1.61 and 1.70 g/cm^3 in Figure 171 are shown in Table LV. Parameter A_1 (thermal conductivity of the dry sample) is higher for samples with higher dry densities, while parameter A_2 (thermal conductivity of the saturated sample) is somewhat lower. This is due to the fact that the thermal conductivity of a sample of low density undergoes a greater increase as saturation occurs than does one of higher dry density, since the porosity of the former is greater and the sample may take up more water; in fact, samples with lower dry densities require more water to reach saturation. The repercussion of water content on the value of thermal conductivity is particularly important, the coefficient of correlation between water content and thermal conductivity being 0.89, while the same coefficient between dry density and thermal conductivity is only 0.39.

It should be remembered that the blocks used to determine thermal conductivity were compacted from clay with a given water content, subjected to high pressures. In other words, they did not saturate under free volume conditions. This fact may condition the structure of the water in the clay and its properties.

Table LV
Coefficients of Boltzman type fittings between thermal conductivity and degree of saturation.

Coefficients of fitting	Interval of dry density 1.58-1.65 g/cm^3	Interval of dry density 1.66-1.74 g/cm
r^2	0.953	0.901
A_1	0.54±0.03	0.66±0.03
A_2	1.28±0.03	1.27±0.04
x_0	0.64±0.02	0.66±0.03
dx	0.085±0.016	0.103±0.036

página en blanco

7. Conclusions

7. Conclusions

Various aspects of the thermo-hydro-mechanical behaviour of a bentonite from the Cortijo de Archidona deposit (Almería) were studied, this having been selected as the Spanish reference material for the sealing of a disposal facility for high level radioactive wastes. The main conclusions obtained during the study are summarised below, classified depending on the area of application.

Experimental procedures and techniques

The determination of basic physical parameters in highly expansive materials requires modification of the conventional techniques established in the UNE Standards and in other habitual laboratory procedures. The following observations were made in relation to the suitability of the methods and the interpretation of the results obtained:

- The high water absorption capacity of bentonite makes it necessary, for determination of the liquid limit, to increase the hydration time of the paste to 48 hours, in order to ensure complete hydration. For the same reason, and in relation to obtaining the granulometric distribution, the suspension period was extended to 48 hours, instead of the 18 established in the Standard. In view of the specific characteristics of aggregation of this bentonite (see section "Atterberg limits, specific surface and granulometry"), the treatment for dispersion prior to granulometric analysis was intensified to include mechanical agitation and ultrasonic cycles.
- The porosimetry data obtained by mercury intrusion should be evaluated taking into account the percentage of pores that cannot be quantified using this method, due to their being excessively small or not interconnected. In the case of the FEBEX bentonite, this percentage may constitute a majority, reaching around 67 percent.
- The method developed for the determination of hydraulic conductivity involves experimental difficulties for the higher dry densities (as from 1.70 g/cm^3), for which the water flows are small and difficult to measure, this causing greater scattering of the data obtained. The relation between flow and hydraulic gradient is linear for the interval of gradients of between 2,800 and 26,400 m/m, this underlining the validity of Darcy's law for this interval in the case of bentonite compacted at dry densities of between 1.30 and 1.84 g/cm^3.
- In expansive materials, the value of intrinsic permeability for a given porosity varies extraordinarily with the type of fluid used for determination, depending on whether it reacts or not with the clay. For this reason, the values of intrinsic permeability of the dry sample obtained with gas are much higher than those obtained with water for the saturated sample.
- The retention curve of expansive materials depends on the confinement condition of the material during determination, higher water contents being obtained for a given value of suction if the determination is performed under free volume conditions than if the sample is confined. This difference is particularly significant for the low suctions at which swelling occurs. For this reason, when conventional methods are applied for the determination of retention curves for such materials, no results representative of the conditions of the bentonite in an engineered barrier, where it is confined, are obtained.
- Although good results were obtained regarding the retention curves for confined conditions determined using oedometers with controlled suction, this method has been seen to allow for certain variation of the sample volume, which is not always detected. This means that the curves determined in this way do not correspond to a single density, but to an interval of densities. For this reason, the use of the non-deformable cells designed is considered to be more advisable, due both to the simplicity of their use and to the accuracy of the results obtained.
- The determination of the swelling pressure of highly expansive materials in conventional oedometers poses a series of technical difficulties. Given the "limited" loading capacity of these systems, it is necessary to reduce the diameter of the specimen in order to achieve the pressures that have to be applied. This reduces the representativeness of the sample, therefore it is advisable to work with specimen lengths of at least 1.20 cm, even though testing times are extended. Nevertheless, the loading limit of the equipment is frequently reached, which, along with the low degree of accuracy of the method, leads to high scattering of the values obtained, especially for the higher dry densities. The effect of accidental deformation of the soil during testing on the value of swelling pressure may also contribute to this scattering.

- The results obtained in the determination of hydraulic conductivity and swelling pressure are conditioned by the way in which the specimens are prepared: specimens compacted directly in the test rings have a more homogeneous density, while those trimmed from larger blocks and subsequently placed in the test rings have lower densities at their borders, due to the fact that the space between the specimen and the ring is filled on saturation. This causes overall dry density to be lower than that in the central part of the specimen, which conditions flow and swelling. For this reason, trimmed specimens of the same average density as compacted specimens have slightly lower hydraulic conductivities and higher swelling pressures. This observation should be taken into account when addressing studies in which the hydraulic properties of samples prepared in different ways are compared. For example, following dismantling of the FEBEX Project large-scale tests, the hydraulic conductivity and swelling pressure of samples from the blocks installed in the barrier will be determined. For the performance of tests on the undisturbed sample it will be necessary to trim specimens of an appropriate size from the blocks. This should be taken into account when comparing the results obtained with the standard results for the untreated sample, since the properties of the latter were determined using specimens compacted directly in the test rings.
- The method of controlling suction by solutions of sulphuric acid in the oedometric tests has shown itself to be more adequate for the study of this material than the one in which control is accomplished by means of nitrogen pressure. This is due to the fact that the range of suction that may be applied using the latter method is very small compared to the suction of the bentonite, as a result of which in oedometric tests performed with suction control by nitrogen pressure, it is possible to investigate the behaviour of the bentonite only under conditions close to saturation. Furthermore, this method implies a larger number of experimental difficulties and is more open to failures (breakdown of membrane, leakage across the loading ram or valve of the cell).
- The manufacturing of high density specimens of bentonite requires the application of uniaxial loads of around 20 MPa. These loads are far higher than the loading limit of normal oedometric systems (10 MPa). For this reason, when working with bentonite compacted at high density using conventional oedometric equipment, it remains predominantly in the elastic domain, except in cases in which there is an important increase in the porosity of the sample as a result of hydration under low load, with which preconsolidation pressure is reduced.
- It has been seen in oedometric tests with suction and temperature control that particularly numerous populations of bacteria develop in the clay, probably due to the high humidity and temperature conditions. Likewise, the electron microscopy study of certain samples of bentonite from oedometric tests with suction control by sulphuric acid solutions has revealed the presence of abundant crystals of gypsum of different morphologies, the origin of which has not been determined. The influence that these two aspects might have on the deformational behaviour observed in the clay remains to be determined.

Thermo-hydro-mechanical characterisation of expansive clays

This section refers to the characteristics of the bentonite studied, both those which are specific to it and those that are extendable to other expansive clays, and includes an interpretation of the behaviour observed. Most of the determinations were carried out on bentonite compacted at dry densities of between 1.80 and 1.50 g/cm^3, this covering from the initial density of the compacted blocks used for the FEBEX Project mock-up test to the density of the emplaced barrier once saturated, including even the local variations to be expected.

The FEBEX bentonite consists of smectite to more than 90 percent. However, its plasticity is relatively low ($w_L = 102 \pm 4$ %), as is the percentage of particles measuring less than 2 μm (67 ± 3 %). The electron microscope study has shown that the microstructure most frequent in the bentonite is made up of piles of smectite laminae that appear to pseudomorphise the original mineral grains of the volcanic rock. These purely smectitic piles might be responsible for the low plasticity and for the granulometry, which is too coarse for a clay material. Treatment by successive cycles of drying and mixing with water appears to disintegrate this structure, giving rise to gradually higher liquid limit val-

ues (up to 172 percent), fractions of less than 1.4 μm (up to 85 percent) and external specific surface (which changes from 32 to 57 m^2/g), this indicating an increase in the number of accessible reactive surfaces. As a result of this microstructural change, the material tested and dried in the laboratory should not be used for the performance of new thermo-hydro-mechanical tests.

The FEBEX bentonite compacted with its hygroscopic water content possesses a percentage of pores measuring less than 0.006 μm of around 67 percent, this meaning that a percentage of pores of this order is in the intra-aggregate porosity domain (below 0.002 μm). The rest of the porosity is distributed among three families –identified by mercury intrusion– of which the most abundant (18 percent) is that of the "small" pores, which actually occupy the domain of mesoporosity. The families of medium-sized and large pores form part of the macroporosity. This distribution may undergo modifications depending on the degree of saturation. No modifications to this distribution depending on dry density have been observed in the range between 1.67 and 1.78 g/cm^3.

When the clay saturates at a constant volume, expansion being prevented, the water entering acquires a density in excess of 1.00 g/cm^3, possibly reaching values of up to 1.36 g/cm^3. The density of the water increases as water content decreases and, especially, as the dry density of the clay increases, this possibly being due to the reduction in porosity complicating the development of diffuse double layers. This hypothesis would explain how fictitious degrees of saturation in excess of 100 percent are reached when they are calculated using the density of free water.

Permeability

- The increase of the dry density of the sample gives rise to an exponential decrease in saturated permeability (and of intrinsic permeability), with two intervals of different hydraulic behaviour being distinguished, the point of separation of the two being a value of dry density of 1.47 g/cm^3. The increase in hydraulic conductivity with decreasing density is clearer for dry densities below this value, this being due to the fact that, as the swelling capacity of the clay decreases, there is a growth in the size of the flow channels and, therefore, in effective porosity and permeability.
- Hydraulic conductivity increases slightly (half an order of magnitude) when saline water –of a composition similar to that of the interstitial water of the bentonite– is used instead of granitic or distilled water as the permeating agent, especially in the case of low densities.
- The permeability to gas of compacted specimens with the same water content also decreases exponentially as dry density increases, as long as the degree of saturation is kept below a certain threshold value (between 65 and 80 percent, depending on dry density). The decrease in the permeability to gas for degrees of saturation above this threshold is particularly sharp, this marking the discontinuity of the gaseous phase. However, the parameter that presents the best correlation with the value of permeability to gas is the accessible pore volume ($e\ (1-S_r)$). A potential relation may be established between the two.
- The intrinsic permeability of samples having the same porosity varies with the degree of saturation, with differences of up to eight orders of magnitude between dry and saturated samples. This is due to the fact that the water causes the clay laminae to expand, thus reducing the size of the pores between aggregates. Clay hydrated under confined conditions shows the same overall volume of pores as a dry sample of the same dry density, although the spaces between aggregates are reduced or disappear due to the swelling of the clay particles. This variation in the average diameter of the pores available to flow explains the major difference in the values of intrinsic permeability in dry and saturated samples. On the other hand, the intrinsic permeability for a given degree of saturation depends on the dry density of the sample.

Retention of water

The retention curves of the bentonite compacted in the dry density range of 1.60-1.75 g/cm^3 were determined under confinement and free volume conditions at a temperature of 20 °C. For dry densities of between 1.65 and 1.70 g/cm^3, the retention curve was determined under constant volume conditions at 40 °C. In all cases, the initial water content of the clay was that corresponding to hygroscopic water content.

The suction of the FEBEX bentonite is very high, this constituting a measure of its great water avidity and

retention capacity. It is fundamentally of the matric type, with the contribution made by osmotic suction being inappreciable.

The behaviour of trimmed and compacted specimens reflects the same patterns, so the way in which the specimens are prepared may be said not to modify retention capacity.

The water retention capacity of the clay is conditioned to a large extent by the state of confinement. For this reason, there are major differences between the retention curves determined under free volume conditions and those determined under conditions of confinement. These differences affect only those paths, or sections of paths, on which the dry density of the sample is lower than the initial value, in other words, the hydration paths and part of the paths of wetting after drying, since once shrinkage begins to occur it is no longer possible to speak of confined volume. The most significant features of behaviour under these two conditions are as follows:

- The difference between the water contents reached for a given value of suction under free volume and confined conditions becomes more appreciable for suctions below a given value, which depends on dry density. For the interval of dry densities analysed, this value is between 30 and 8 MPa. Above these values, suction would be controlled by the micros- tructure and would be independent from dry density (intra-aggregate suction), while below them it would be controlled by the macrostructure (inter-aggregate suction).
- The degrees of saturation reached by confined samples are higher than those reached by samples under free volume conditions for the same value of suction. In fact, the confined samples reach total saturation, while those tested under free volume conditions do not. Thus, the maximum degree of saturation on the free volume paths is between 60 and 80 percent, depending on dry density.
- The suction/water content relation determined under free volume conditions may be expressed by means of a logarithmic law: the water content of the sample decreases on drying paths (increasing suction) and increases on wetting paths (decreasing suction). In turn, the modification of dry density depending on suction on these paths follows a potential law, increasing during drying and decreasing during wetting. The influence of initial dry density on the values of water content and dry density reached on each suction step is small. The repercussion of initial dry density on the water content reached becomes clearer as suction decreases. However, the values of dry density tend towards a value equal to 1 g/cm^3 for a suction of 0.1 MPa, regardless of the initial value of dry density.
- Consequently, in the case of saturation under free volume conditions, the retention capacity of the clay is influenced to some extent by the average size of the pores. The lower this size is, *i.e.* the greater the dry density, the higher the water content for a given value of suction on the wetting path, since there will be a higher volume of pores with the diameter affected by each suction value. In the case of saturation under a constant volume, however, retention capacity is restricted by total porosity. For this reason, the higher the dry density, the lower the water content reached for a given value of suction, especially when the sample approaches saturation.
- On both wetting paths and those including wetting after drying under free volume conditions, the degree of saturation for a given suction is greater for samples having a higher initial dry density. In view of the decrease in density that accompanies the increase in water content that occurs with decreasing suction, the degree of saturation remains approximately constant for an interval of suction of between 0.5 and 100 MPa. The upper value corresponds to the air entry point of the microstructure, as from which the water entering the clay on wetting paths ceases to replace the air, which no longer exists the material, this causing an increase in volume equal to the increase in the volume of water and a significant decrease in dry density. The value of 0.5 MPa, below which there is an increase in the degree of saturation, corresponds to the initiation of saturation of pores larger than 0.59 μm, belonging to the domain of macroporosity (medium-sized pores), and consequently to the point at which air exits the macrostructure. This latter value cannot be identified on the curves determined at constant volume, probably because during saturation, the macroporosity, which is invaded by the expansion of the microporosity, disappears, a reduction in average pore size occurring as saturation is approached.

- Consequently, for compacted clays of some degree of expansibility, on free volume paths, it is more advisable to use water content than degree of saturation as a state variable for certain intervals of suction.
- In the case of processes of wetting after drying under free volume conditions, the water content reached is slightly lower than on wetting paths, although the difference between the two values decreases with suction, the ratio being inverted at lower values of suction.
- The retention curves at constant volume show hysteresis, as a result of which the water content on wetting paths is lower than on the drying paths that follow.
- The effect on the retention curves of increasing temperature to 40 °C is not particularly appreciable, although it would appear to point to a slightly higher retention capacity at 40 °C than at 20 °C under confined conditions, this being contrary to what has been observed by other authors on curves determined under free volume conditions.

Swelling

The swelling pressure of bentonite relates to dry density by way of an exponential law, without any repercussion having been identified as regards the use of distilled or granitic water to saturate the sample.

In saturation under load tests, the relation between vertical load and the strain experienced by the clay on saturating is logarithmic in type, and depends on initial dry density. However, the final strains do not depend to any great extent on the type of water used to saturate (distilled, granitic or saline), although for an initial dry density of 1.60 g/cm^3, the final strains reached on saturating with distilled water are slightly larger. This lack of influence of the salinity of the water on the value of strain may be due, on the one hand, to the saline water used being in equilibrium with the mineralogical composition of the clay and, on the other, to the vertical loads used being high (between 0.1 and 3.0 MPa), which might complicate osmotic processes.

Thermal conductivity

The thermal conductivity at laboratory temperature of the compacted blocks of clay increases with dry density and, especially, with water content. For the dry clay it has a value of 0.57 W/m·K, and for the saturated clay of 1.27 W/m·K. The thermal conductivity of dry samples is higher for those having higher dry densities, while in the case of saturated samples, thermal conductivity is higher for those having lower dry densities. This is due to the fact that samples of lower density need higher water contents to saturate, and the liquid phase has a greater repercussion on the value of thermal conductivity than the solid phase.

Anisotropy

The compacted blocks do not show anisotropy with respect to either hydraulic conductivity, swelling pressure or retention capacity. In other words, these properties give analogous values when determined in the direction parallel to compaction force or perpendicular to it. This observation suggests that there is no reorganisation of the laminar particles during manufacturing of the blocks, probably because the compaction process is rapid and takes place in the absence of free water, since the material is compacted with its hygroscopic water content. Furthermore, smectite –the major constituent of bentonite– is a mineral that has irregularly shaped crystals and, therefore, a low reorientation capacity. The relative variety of the granulometric distribution (with a silt fraction of 22 percent) is also an obstacle to particle orientation. In any case, when the sample is saturated during the determinations, the microstructure would tend to homogenise. Thermal conductivity does not show any significant anisotropy, despite the fact that its measurement is not necessarily accomplished with the sample saturated. Furthermore, the low degree of anisotropy observed in the values of thermal conductivity decreases as the water content of the sample increases.

Deformability under unsaturated conditions

It is a feature of the oedometric tests performed that they have covered a very wide range of suctions, from 0 to 500 MPa, as a result of which practically all the hydration states of the bentonite have been explored. The literature contains hardly any experimental data on such high levels of suction. The tests dealt with in this work underline the fact that the deformational behaviour of bentonite is dominated by its microstructure, and by the repercussion of microstructural deformations on the macrostructure.

The drying of the sample by decreasing suction to values of around 500 MPa –which implies a decrease in water content to values close to 4 percent– involves practically no variation in volume, although void ratio decreases logarithmically with increasing suction, depending on dry density. This minor variation in volume with drying from 120 MPa would appear to indicate that below this value of suction will be the air entry point, that is to say, the value from which the loss of volume of water due to drying is compensated by the entry of a similar volume of air, as a result of which the loss of water content does not translate into a loss of total porosity. Furthermore, for suctions above this value, the external load does not cause any important consolidation in the sample, which becomes rigid.

Likewise, drying of the sample by increasing suction to 500 MPa does not modify either its swelling capacity during subsequent hydration or its swelling pressure once saturated. On the contrary, decreasing suction causes greater strain in the sample the higher the initial value of suction, on account of which samples subjected to drying may swell more, as predicted by the microstructural behaviour models.

Strains due to swelling increase as lower values of suction are reached.

The variety of the tests performed has made it possible to highlight the impact that the type of path has on the final value of strain, as well as on its reversibility. When the sample hydrates under a low vertical load, void ratio increases to a large extent, and the vertical load applied subsequently is incapable of counteracting this swelling; in other words, the deformation induced is irreversible. However, if swelling is prevented during saturation, by previously or simultaneously loading the sample, the final change in volume is smaller. Furthermore, if hydration of the sample occurs from a low degree of saturation and under an important overload, the sample may experience minor reversible collapse. The influence of the path on the final values of strain is also important after intense drying. This behaviour is an example of the irreversible macroscopic deformation that is induced by microstructural swelling. The change in volume during hydration –whose main component is microstructural– decreases in intensity the higher the overload under which it occurs. Specifically, a logarithmic law has been identified relating the variation in volume due to changing suction with overload. This expansion in the microstructure as a result of hydration under low load gives rise to a reorganisation of the macrostructure, which becomes more porous, a plastic and consequently irreversible increase in volume occurring. The load subsequently applied in the tests was insufficient to counteract the above.

During this microstructural expansion there is also a decrease in preconsolidation pressure, which becomes smaller the lower the dry density reached during hydration, which in turn is related to the overload under which the latter occurs and the intensity of hydration, in other words, to the value to which suction has decreased during the process. Consequently, preconsolidation pressure will decrease more during hydration the lower the overload under which it occurs and the higher the degree of saturation reached. The value of preconsolidation pressure was determined for different suctions, the values identified ranging from 20 MPa, corresponding to the pressure of specimen manufacturing, to 1 MPa.

The importance of the stress path as regards the value of final strain, referred to in earlier paragraphs, underlines the fact that the analysis of the behaviour of highly expansive materials cannot be accomplished by means of state surfaces, since these would differ even in the case of monotonic deformations (only increase or only decrease in volume), depending on the sequence and intensity of the stresses applied (load and suction). In order to correctly model the behaviour of compacted bentonite, in the case of arbitrary load and suction change paths, it is necessary to use elasto-plastic type models incorporating the interaction between the microstructure and the macrostructure of the soil.

The deformability due to increasing load decreases in the case of high values of suction, and especially in overconsolidated samples.

The swelling pressure of the unsaturated sample increases logarithmically in the interval of suctions of between 130 MPa (the suction corresponding to hygroscopic water content) and 10 MPa, although below this value the increase is attenuated, probably because for lower values of suction the confined sample is practically saturated, and because the strains due to microstructural swelling are compensated by strains caused by macrostructural collapse. Across this entire range of suction, swelling pressure depends on dry density, and increases with it. On the other hand, for suctions in excess of 200 MPa, there is hardly any development of swelling pressure.

The increase in temperature to 80 °C in the controlled suction oedometric tests performed would

appear to induce a hardening of the material, increasing its preconsolidation pressure and limiting its swelling capacity.

When the saturated sample is unloaded rapidly and in a stepwise fashion, the increase in void ratio that occurs on reduction of the load is logarithmic, and dependent on the dry density at the beginning of the process. The swelling indexes obtained during these processes of unloading are very high, corresponding to a 50 percent of the compression indexes.

Bentonite as an engineered barrier

The bentonite installed in the disposal facility in the form of high density blocks manufactured by uniaxial compaction of clay granulate with its hygroscopic water content, has a fundamentally high value of suction, and consequently a high degree of water avidity. This will be the fundamental force driving the saturation of the barrier with the water from the surrounding massif. However, as the clay saturates, its intrinsic permeability will decrease, as the size of the flow channels becomes smaller, this being accompanied by a decrease in the suction gradient responsible for the flow of water, as a result of which the saturation process will become steadily slower. This reduction in flow will be compensated only in part by the increase in relative permeability occurring with increasing saturation.

Simultaneously with hydration there will be expansion of the bentonite in those areas in which there is space for this to occur. In this way, the swelling and high level of suction of the bentonite will also prevent the joints between blocks becoming preferential channels for the flow of water, since water coming into contact with the bentonite will be immediately absorbed, causing the latter to expand and to seal any type of joint. Likewise, the gap between the bentonite and the wall of the drift will be closed by this same process. In those areas in which the bentonite is confined, the swelling pressure exercised by the clay will increase logarithmically with saturation, causing compression of the drier areas and an increase in their density, as described in the section "BENTONITE UNDER DISPOSAL FACILITY CONDITIONS".

The controlled suction oedometric tests have shown that during the hydration of the compacted bentonite irreversible strains may occur, these being larger the lower the overload. In the barrier, and due to its being confined, the overload of the bentonite will in all cases be important, therefore irreversible strains are not expected to occur during hydration, except at the joints between the blocks and at the periphery, where the space between the bentonite and the rock may be sufficient to allow for free expansion of the clay. As a result, there would be an outer ring in which the bentonite would have a lower dry density –which would no longer be recovered– and a higher water content. This ring might constitute a source of water supply and would ensure its homogeneous distribution across the entire surface of the barrier.

Furthermore, the drying of the bentonite that occurs in the vicinity of the canister due to increasing temperature, as long as water content does not decrease below 4-6 percent, will not cause any significant reduction in volume, since above the value of suction corresponding to hygroscopic water content the sample becomes very rigid. This will prevent the formation of shrinkage cracks and preferential flow channels from becoming important.

The high suction generated by drying may, with increasing hydraulic gradients, speed up the arrival of water to the internal areas of the barrier. It has been seen that drying to water contents of 4-6 percent does not reduce the swelling capacity of the bentonite, as a result of which the hydro-mechanical properties of the material will not be altered following the transient period, and with the arrival of water the bentonite will expand and the canister will be confined.

Once the barrier is saturated, and taking into consideration that the dry density of the assembly is between 1.60 and 1.65 g/cm^3, its permeability will be between 10^{-13} and 10^{-14} m/s, and its swelling pressure between 4 and 10 MPa. The possible increase in the density of the water on entering the compacted bentonite may cause the volume of water required to saturate the barrier to increase by up to 20 percent over that foreseen by the calculations considering the density of the water to be equal to 1.00 g/cm^3.

The thermal conductivity of the saturated blocks of FEBEX bentonite –between 1.2 and 1.3 W/m·K– is sufficient to favour the dissipation of the heat generated by decay of the radioactive wastes. In any case, the impact of temperature on the properties analysed does not appear to be drastic.

Subsequent research

Taking into account the results obtained in this work, the difficulties encountered during its performance

and the knowledge required to assess the behaviour of bentonite as a sealing material, it is estimated that future research efforts should focus on the following aspects:

- The sensitivity analyses of the models of long-term barrier performance have shown the repercussion of the retention curve on the estimation of barrier saturation times. In order to reduce the uncertainties associated with this characteristic of the material, the retention curves of the bentonite at constant volume and depending on temperature should be determined more accurately. The technique developed during the final stages of this work for determination of the retention curve at constant volume by means of non-deformable cells offers the possibility of obtaining more accurate data making it possible to confirm certain hypotheses regarding the water retention characteristics of bentonite. Thus, for example, the limits of the intra and inter-aggregate suction domain depending on dry density, the exact values of suction as from which the bentonite becomes saturated depending on dry density and the scope of phenomena of hysteresis.
- Another property that fundamentally conditions the hydraulic performance of the barrier and saturation time is the unsaturated permeability of the bentonite. The determination of this parameter is addressed indirectly by the back-analysis of infiltration tests, in other words through the application of a model to a well defined problem. In view of the specific characteristics of this approach, it has not been applied in this study, although knowledge of it is a priority issue.
- Although this work has included analysis of the repercussion of hydration water on certain properties, this study has not been systematic and has been limited to two types of water (granitic and saline). It is considered advisable to analyse the influence of the saline concentration of the hydration water on the hydro-mechanical properties of the clay. This concentration might be high, due to the dissolution and transport of salts present in the bentonite and involved in the process of saturation.
- The thermal aspects of the behaviour of the bentonite have not been studied sufficiently, due to the added complexity of the experimental techniques. The influence of dry density and water content on most of the properties of the FEBEX bentonite has been tested and is known, but the tests were performed at laboratory temperature. The retention curve, permeability and swelling pressure are among the key properties of the sealing material for which the influence of temperature should be identified. As has been said, knowledge of the first two is decisive for prediction of the rate of hydration of the barrier. Furthermore, the swelling pressure that will be developed by the material is one of the design parameters of the disposal facility.
- The studies of the thermo-hydro-mechanical behaviour of the bentonite should at all times bear in mind the microstructural aspects of the material, therefore it is appropriate to use complementary techniques allowing the observations made to be explained, such as the determinations of porosity (especially by gas adsorption) and optical and electron microscope studies. Knowledge of porosimetry and specific surface might allow insight to be gained into the volume of water that may exist, in the form of free or adsorbed water, and information to be obtained indirectly on the retention curve and relative permeability.
- Knowledge of the density of the water as it becomes part of the water saturating the compacted bentonite is a key factor as regards determination of the volume of water required to saturate the engineered barrier, and because of this detailed studies should be performed using appropriate experimental techniques in an attempt to confirm the variation of water density with the density and water content of the material.

8. References

8. References

AITCHISON, G.D.(1959): The strength of quasi-saturated and unsaturated soils in relation to the pressure deficiency in the pore water. *Proc. 4th Int. Conf. Soil Mech. Found.. Eng*. London. 135-139.

AITCHISON G.D. & MARTIN, R. (1973): A membrane oedometer for complex stress-path studies in expansive clays. *Proc. 3rd. Int. Conf. Expansive Soils*. Haifa. 161-167.

AITEMIN (1999): Sensors data report (In situ experiment) nº 15. *FEBEX report* 70-AIT-L-5-21. Madrid. 160 pp.

ALLEN, T.(1981): Particle size measurement. 3rd. Edition. *Chapman & Hall*. London.

ALONSO, E.E.; GENS, A. & HIGHT, D.W.(1987): Special problem soils. *Proc. 9th Int. Conf. Soil Mech. Found.. Eng*. Dublin. General Report, session 5, 5.1-5.60.

ALONSO, E.E.; GENS, A. & JOSA, A.(1990): A constitutive model for partially saturated soils. *Géotecnique* 40(3): 405-430.

ARYA, L.M.; LEIJ, F.J.; SHOUSE, P.J. & VAN GENUCHTEN, M. Th.(1999): Relationship between the hydraulic conductivity function and the particle-size distribution. *Soil Sci. Soc. Am. J.* 63: 1063-1070.

ARNOLD, M(1984): The genesis, mineralogy and identification of expansive soils. *Proc. 5th Int. Conf. Expansive Soils*. Adelaida. 32-41.

ASTM D2435 (1980): Standard Test Method for One-dimensional Consolidation Properties of Soils. Annual Book of ASTM Standards, vol. 04.08, Soil and Rock; Building Stones, Sect. 4, *ASTM*, Philadelphia, PA.

ASTM D4546 (1985): Standard Test Method for One-Dimensional Swell or Settlement Potential for Cohesive Soils. Annual Books of ASTM Standards. Vol 04.08. Soil and Rock; Building Stones, Sect. 4, *ASTM*, Philadelphia, PA.

ASTM D3663-99: Standard Test Method for Surface Area of Catalysts and Catalyst Carriers.

ASTUDILLO, J; OLMO, C. DEL; RIVAS, P.; MARTÍN, P.L.; VILLAR, M.V.; PÉREZ DEL VILLAR, L.; PARDILLO, J.; DARDAINE, M. & LAJUDIE, A.(1995): Field test for the demonstration of the emplacement feasibility of clay buffer material as engineered barrier, in crystalline formation. Volume 1, 2 & 3. *Nuclear Science and Technology. EUR* 15692/3. Luxembourg.

ATKINSON, J.H. & BRANSBY, P.L.(1977): The mechanics of soils. An introduction to critical state soil mechanics. University Series in Civil Engineering. *McGraw-Hill*. 374 pp.

BARBOUR, S.L. & FREDLUND, D.G.(1989): Mechanisms of osmotic flow and volume change in clay soils. *Can. Geotech. J.* 26: 551-562.

BEN RHAIEM, H.; TESSIER, D. & PONS, CH.H.(1986): Comportement hydrique et évolution structurale et texturale des montmorillonites au cours d'un cycle de dessiccation-humectacion: Partie I. Cas des montmorillonites calciques. *Clay Minerals* 21:9-29.

BERNIER, F.; VOLCKAERT, G.; ALONSO, E. & VILLAR, M.V.(1997): Suction-controlled experiments on Boom clay. *Eng. Geol*. 47(4): 325-338.

BEZIAT, A., DARDAINE, M. & GABIS, V.(1988): Effect of compaction pressure and water content on the thermal conductivity of some natural clays. *Clays and Clay Minerals* 36(5): 462-466.

BISHOP, A.W. & DONALD, I.B.(1961): The experimental study of partly saturated soil in the triaxial apparatus. *Proc. 5th Int. Conf. Soil Mechanics* 1: 13-21. Paris.

BISHOP, A.W. & BLIGHT, G.E.(1963): Some aspects of effective stress in saturated and partly saturated soils. *Géotechnique* 13(3): 177-197.

BISHOP, A.W. & WESLEY, L.D.(1975): A hydraulic triaxial apparatus for controlled stress path testing. *Géotechnique* 25(4): 657-670.

BLACK, W.P.M. & CRONEY, D.(1957): Pore water pressure and moisture content studies under experimental pavements. *Proc. 4th Int. Conf. Soil Mech. Found. Eng*. London. Vol. 2: 94-103.

BLATZ, J. & GRAHAM, J.(2000): A system for controlled suction in triaxial tests. *Géotechnique* 50(4): 465-469.

BOCKING, K.A. & FREDLUND, D.G.(1980): Limitations of the axis translation technique. *Proc. 4th Int. Conf. Expansive Soils*. Denver. 117-135.

BRACKLEY, I.J.(1975): Swell under load. *Proc. 6th Regional Conf. for Africa on Soil Mechanics and Foundation Engineering* 1: 71-79.

BRANDL, H.(1992): Mineral liners for hazardous waste containment. *Géotechnique* 42(1): 57-65.

BRUNAUER, S.; EMMET, P.H. & TELLER, E.(1938): Adsorption of gases in multimolecular layers. *J. Amer. Chem. Soc*. 60: 309-319.

BUCHAN, G.D.(1991): Soil temperature regime. In: SMITH, K.A. & MULLINS, C.E.(eds.): Soil Analysis. Physical Methods. *Dekker*. New York. 551-612.

BURDINE, N.T.(1953): Relative permeability calculations from pore-size distribution data. *Petr. Trans. Am. Inst. Mining Metall. Eng*. 198: 71-77.

CABALLERO, E.; REYES, E.; LINARES, J. & HUERTAS, F. (1985): Hydrothermal solutions related to bentonite genesis, Cabo de Gata region, Almería, SE Spain. *Minerl. Petrogr. Acta* 29A:187-196.

CHEN, F.H.(1988): Foundations on Expansive Soils. *Developments in Geotechnical Engineering* 12. *Elsevier*. Amsterdam. 280 pp.

COLEMAN, J.D. & MARSH, A.D.(1961): An investigation of the pressure membrane method for measuring the swelling properties of soils. *J. Soil Sci.* 12: 343-362.

COREY, A.T.(1957): Measurement of air and water permeability in unsaturated soil. *Proc. Soil Sci. Soc. Amer.* 21(1): 7-10.

CRONEY, D.(1952): The movement and distribution of water in soils. *Géotechnique* 3(1): 1-16.

CRONEY, D. & COLEMAN, J.D.(1960): Pore pressure and suction in soil. In: Pore pressure and suction in soils conf. *Butterworths*. Londres. 31-37.

CUADROS, J.; HUERTAS, F.; DELGADO, A. & LINARES, J.(1994): Determination of hydration (H_2O^-) and structural (H_2O^+) water for chemical analysis of smectites. Application to Los Trancos smectites, Spain. *Clay Minerals* 29: 297-300.

CUÉLLAR, V.(1978): Análisis crítico de los métodos existentes para el empleo de arcillas expansivas en obras de carretera y recomendaciones sobre las técnicas para su uso habitual en España. *Laboratorio de Transporte y Mecánica de Suelo*. Madrid. 321 pp.

CUEVAS, J.(1992): Caracterización de esmectitas magnésicas de la Cuenca de Madrid como materiales de sellado. Ensayos de alteración hidrotermal. ENRESA. Publicación Técnica Nº 04/92. Madrid. 183 pp.

CUEVAS, J.; VILLAR, M.V.; MARTÍN, M.; COBEÑA, J.C.; LEGUEY, S. & RIVAS, P.(1999): Thermo-hydro-geochemical tests in small cells. CIEMAT/DIAE/54111/4/99. FEBEX report 70-IMA-M-0-5. Madrid. 44 pp.

CUI, Y.J.(1993): Etude du comportement d'un limon compacté non-saturé, et de sa modélisation dans un cadre élasto-plastique. *Thèse de l'Ecole Nationale des Ponts et Chaussées*. París.

DANIEL, D.E.(1982): Measurement of hydraulic conductivity of unsaturated soils with thermocouple psychrometers. *Soil Sci. Soc. Am. J.* 46(6): 1125-1129.

DELAGE, P.(1987): Aspects du comportement des sols non saturés. *Revue Française de Géotechnique* 40: 33-43.

DELAGE, P.(1993): Experimental techniques. In: Unsaturated soils – Recent developments and applications. *CEEC Course*, Barcelona, June 15-17.

DELAGE, P.; SURAJ DE SILVA, G.P.R. & DE LAURE, E.(1987): Un nouvel appareil triaxial pour les sols non-saturés. *Proc. 9th European Conf. Soil Mech. Found.Eng.* Dublin. Vol 1: 25-28.

DELAGE, P.; SURAJ DE SILVA, G.P.R. & VICOL, T.(1992): Suction controlled testing of non saturated soils with an osmotic oedometer. *Proc. 7th Int. Conf. On Expansive Soils*. Dallas. 260-211.

DELAGE, P.; HOWAT, M.D. & CUI, Y.J.(1998): The relationship between suction and swelling properties in a heavily compacted unsaturated clay. *Eng. Geol*. 50: 31-48.

DELGADO, A.(1993): Estudio isotópico de los procesos diagenéticos e hidrotermales relacionados con la génesis de bentonitas (Cabo de Gata, Almería). *Ph. D. Thesis*. Universidad de Granada. 413 pp.

DIAMOND, S.(1970): Pore size distribution in clays. *Clays and Clay Minerals* 18: 7-23.

DINEEN, K.(1997): The influence of soil suction on compressibility and swelling. *Ph. D. Thesis*. Univ. of London.

DINEEN, K. & BURLAND, J.B.(1995): A new approach to osmotically controlled oedometer testing. *In*: ALONSO, E.E. & DELAGE, P.(eds.): Unsaturated Soils. *Balkema*. Rotterdam.

DIRKSEN, C.(1991): Unsaturated hydraulic conductivity. In: SMITH, K.A. & MULLINS, C.E.(eds.): Soil Analysis. Physical Methods. *Marcel Dekker*, New York. 209-269.

ECHAGÜE, G. *et al.*(1989): Tratamiento y gestión de residuos radiactivos. *Ilustre Colegio Oficial de Físicos*. Madrid. 248 pp.

ENRESA (1994): Almacenamiento geológico profundo de residuos radiactivos de alta actividad (AGP). Conceptos preliminares de referencia. *Publicación Técnica ENRESA* 07/94. Madrid. 60 pp.

ENRESA (1995): Almacenamiento geológico profundo de residuos radiactivos de alta actividad (AGP). Diseños conceptuales genéricos. *Publicación Técnica ENRESA* 11/95. Madrid. 105 pp.

ENRESA (1997): FEBEX. Etapa preoperacional. Informe de síntesis. *Publicación Técnica ENRESA* 9/97. Madrid. 189 pp.

ENRESA (1998): FEBEX. Bentonita: origen, propiedades y fabricación de bloques. *Publicación Técnica ENRESA* 04/98. Madrid. 146 pp.

ENRESA (2000): FEBEX Project. Full-scale engineered barriers experiment for a deep geological repository for high level radioactive waste in crystalline host rock. Final Report. *Publicación Técnica ENRESA* 1/2000. Madrid. 354 pp.

ESCARIO, V. (1965): International Panel Report "Engineering effects of moisture changes in soils". *Concluding Proc. Int. Research and Engineering Conf. Expansive Clay Soils*. Texas A & M Univ.

ESCARIO, V.(1967): Measurement of the swelling characteristics of a soil fed with water under tension. Int. Cooperative Research on the Prediction of Moisture Content under Road Pavements. *OCDE Working Group*. Madrid meeting.

ESCARIO, V.(1969): Swelling of soils in contact with water at a negative pressure. *Proc. 2nd Int. Conf. Expansive Clay Soils*. Texas A & M Univ. 207-217.

ESCARIO, V. (1980): Suction controlled penetration and shear tests. Proc. 4th Int. Conf. Expansive Soils II: 781-797. Denver.

ESCARIO, V. & SÁEZ, J.(1973): Measurement of the properties of swelling and collapsing soils under controlled suction. Proc. 3rd Int. Conf. Expansive Soils 2: 195-200. Haifa.

ESCARIO, V. & SÁEZ, J.(1986): The shear strength of partly saturated soils. *Géotechnique* 36(3): 453-456.

ESTEBAN, F.(1990): Caracterización experimental de la expansividad de una roca evaporítica. Identificación de los mecanismos de hinchamiento. *Ph. D. Thesis*. Universidad de Cantabria. 395 pp.

ESTEBAN, F. & SÁEZ, J.(1988): A device to measure the swelling characteristics of rock samples with control of suction up to very high values. *ISRM Symposium on Rock Mechanics and Power Plants* 2. Madrid.

EUROPEAN COMISSION (1995): Community´sresearch and development programme on radioactive waste management and storage. Shared-cost action (1990-1994). *Nuclear science and technology series. EUR* 16548. Luxembourg. 680 pp.

EVERETT, D.H. & HAYNES, J.M.(1973): Capillarity and Porous Materials: Equilibrium Properties. *Colloid Science* 1: 123-172.

FERNÁNDEZ SOLER, J.M.(1992): El volcanismo calco-alcalino de Cabo de Gata (Almería). *Ph. D. Thesis*. Universidad de Granada. 243 pp.

FERNÁNDEZ, A.M. & CUEVAS, J.(1998): Estudios del agua intersticial de la arcilla FEBEX. *CIEMAT report. FEBEX report* 70-IMA-L-9-44. Madrid. 40 pp.

FERNÁNDEZ, A.M.; RIVAS, P. & CUEVAS, P.(1999): Estudio del agua intersticial de la arcilla FEBEX. *CIEMAT report. FEBEX report 70-IMA-L-0-44*. Madrid. 144 pp.

FREDLUND, D.G. & HASAN, J.U.(1979): One-dimensional consolidation theory: unsaturated soils. *Can. Getech. J.* 16:521-531.

FREDLUND, D.G. & MORGENSTERN, N.R.(1977): Stress state variables for unsaturated soils. *J. Soil Mech. and Foundation Eng. A.S.C.E*. GT5: 447-466.

FREDLUND, D.G. & RAHARDJO, H.(1993): Soil Mechanics for Unsaturated Soils. *John Wiley & Sons*. New York.. 517 pp.

FREDLUND, D.G.; MORGENSTERN, N.R. & WIDGER, R.A.(1978): The shear strength of unsaturated soils. *Can. Geotech. J.* 15(3): 313-321.

FREDLUND, D.G.; SATTLER, P.J. & GAN, J.K.-M.(1992): *In situ* suction measurements using thermal sensors. *Proc. 7th Int. Conf. On Expansive Soils*: 325-330.

GARDNER, R.(1956): Calculation of capillary conductivity from pressure plate outflow data. *Proc. Soil Sci. Soc. Am.* 20: 317-320.

GEHLING, W.Y.Y.(1994): Suelos expansivos. Estudio experimental y aplicación de un modelo teórico. *Ph. D. Thesis*. Universidad Politécnica de Cataluña.

GENESTE, PH.; RAYNAL, M.; ATABEK, R; DARDAINE, M. & OLIVER, J.(1990): Characterization of a French clay barrier and outline of the experimental progamme. *Engineering Geology* 28: 443-454.

GENS, A. & ALONSO, E.(1992): A framework for the behaviour of unsaturated clay. *Canadian Geotech. J.* 29:1013-1032.

GENS, A.; ALONSO, E.E. & JOSA, A.(1979): Elasto-plastic modelling of partially saturated soils. *Proc. 3rd Int. Symp. on Numerical Models in Geomechanics*, Niagara Falls, 163-170.

GILI, J.A.(1987): Modelo microestructural de medios granulares no saturados. *Ph. D. Thesis*. Universidad Politécnica de Cataluña. Barcelona.

GMITRO & VERMEULEN (1964): *An I. Ch. E. J.* 10(5):740.

GOGUEL, J.; CANDÈS, P. & IZABEL, C.(1987): Stockage des déchets radioactifs en formations géologiques. Critères techniques de choix de site. *Rapport du groupe de travail présidé par le professeur Goguel*. Ministère de l'Industrie, des P. & T. et du Tourisme. 245 pp.

GRIM, R.E.(1968): Clay Mineralogy. 2nd ed. *McGraw-Hill Book Company*. New York. 596 pp.

GÜVEN, N.(1990): Longevity of bentonite as buffer material in a nuclear-waste repository. *Eng. Geol.* 28(3-4): 233-248.

HAIJTINK, B. & DAVIES, C.(comp.)(1998): *In situ* testing in underground research laboratories for radioactive waste disposal – Proceedings of a Cluster seminar held in Alden Biessen, Belgium, 10-11 December 1997. *Nuclear Science and Technology. EUR* 18323. Luxembourg. 339 pp.

HILF, J.W.(1956): An investigation of pore water pressure in compacted cohesive soils. *US Bureau of Reclamation Tech. Memo* 654. Denver.

HOLTZ, W.G. & GIBBS, H.J.(1956): Engineering properties of expansive clays. *Transactions ASCE* 121: 641-677.

HUECKEL, T. & PEANO, A.(1996): Thermomechanics of Clays and Clay Barriers, 3rd. International Workshop on Clay Barriers, ISMES, Bergamo, Italy, October 22-23, 1993 – Introduction. *Eng. Geol.* 41 (1-4): 1-4.

HURLBUT, C.S. & KLEIN, C.(1982): Manual de mineralogía de Dana. 3ª ed. *Reverté*. Barcelona. 564 pp.

ISSC (1965): Review panel: Engineering concepts of moisture equilibria and moisture changes in soil. *Proc. Symp. Moiture equilibria and moisture change in soils beneath covered areas*. Butterworths: 7-21.

JACKSON, R.D. & TAYLOR, S.A.(1965): Heat Transfer. In: BLACK, C.A. (ed): Methods of soil analysis. Agronomy Series 9. *American Society of Agronomy*. Madison.

JENNINGS, J.E.B. & BURLAND, J.B.(1962): Limitations to the use of effective stresses in partly saturated soils. *Géotechnique* 12(2): 125-144.

JIMÉNEZ, J.A. & JUSTO, J.L., de(1971): Geotecnia y Cimientos I. Propiedades de los suelos y de las rocas. *Ed. Rueda*. Madrid. 422 pp.

JIMÉNEZ, J.A. & SERRATOSA, J.M.(1953): Compressibility of clays. *3er Congreso Internacional de Mecánica de Suelos* vol. 1: 192-198. Zürich.

JOSA, A.C.(1988): Un modelo elastoplástico para suelos no saturados. *Ph. D. Thesis*. ETSICCP. Universidad Politécnica de Cataluña.

JOSA, A.; ALONSO, E.E.; LLORET, A. & GENS, A.(1987): Stress-strain behaviour of partially saturated soils. *Proc. 9th Europ. Conf. Soil Mech. Found. Eng*. Dublin. 561-564.

JUSTO, J.L.; DELGADO, A. & RUIZ, J.(1984): The influence of stress-path on the collapse-swelling of soils in the laboratory. *Proc. 5th Int. Conf. on Expansive Soils*, Adelaida. 67-71.

KÄRNBRÄNSLEHANTERING, S.(1999): Äspö Hard Rock Laboratory. Annual Report 1998. *SKB Technical Report* TR-99-10. Stockholm. 165 pp.

KARNLAND, O.(1996): Äspö Hard Rock Laboratory. Test plan for long term tests of buffer material. *Progress Report* HRL-96-22. *SKB*. Stockholm. 34 pp.

KASSIFF, G. & BEN SHALOM, A.(1970): Apparatus for measuring swell potential under controlled moisture intake. *A.S.T.M. Jnl. Mater.* 5(4): 3-15.

KASSIFF, G. & BEN SHALOM, A.(1971): Experimental relationship between swell pressure and suction. *Géotechnique* 21(3): 245-255.

KEELING, P.S.(1961): The examination of clays by IL/MA. *Trans. Brit. Ceram. Soc.* 60: 217-244.

KHEMISSA, M.(1992): Mesure de la perméabilité des argiles sous contrainte et température. *Revue Française de Géotechnique* 82(1): 11-22.

KIRKHAM, D.(1946): Field method for determination of air permeability of soil in its undisturbed state. *Soil Sci. Soc. Am. Proc.* 11:93-99.

KLUTE, A. (1965): Laboratory measurements of hydraulic conductivity of saturated soil. In: BLACK, C.A.(Ed.): Methods of Soil Analysis. *Agronomy Series n. 9. American Society of Agronomy, Inc*. 210-221.

KLUTE, A. & DIRKSEN, C.(1986): Hydraulic conductivity and diffusivity: Laboratory methods. In: KLUTE, A.(ed.): Methods of Soil Analysis, Part I, Physical and Mineralogical Methods. *Am. Soc. Agron.* 2nd ed. Madison.

KOMORNIK, A. & ZEITLEN, J.G.(1965): An apparatus for measuring the lateral soil pressure in the laboratory. *Proc. 6th Int. Conf. Soil Mech. and Found. Eng*. Mexico. Vol. 1: 141-148.

KOMORNIK, A.; LIVNEH, N. & SMUCHA, S.(1980): Shear strength and swelling of clays under suction. *Proc. 4th Int. Conf. Expansive Clays*. Denver. Vol. 1: 206-226.

KOOL, J.B.; PARKER, J.C. & VAN GENUCHTEN, M. Th.(1985): Determining soil hydraulic properties from one-step outflow experiments by parameter estimation, 1. Theory and numerical studies. *Soil Sci. Soc. Am. J.* 49: 1348-1354.

KRAHN, J. & FREDLUND, D.G.(1972): On total, matric and osmotic suction. *Soil Science* 114(5): 339-348.

KRAZYNSKI, L.M.(1973): The need for uniformity in testing of expansive soils. *Proc. Workshop on Expansive Clays and Shales in Highway Design and Construction*. Vol. 1. 98-128.

KYOTO ELECTRONICS Manufacturing Co.(1987): Kemtherm QTM-D3 Quick Thermal Conductivity Meter Instruction Manual.Tokyo. 19 pp.

LAJUDIE, A.(1986): Mesure et analyse d'identification et de caractérisation de l'argile de Fourge-Cahaignes. *N.T. SESD/87.31*. CEA-Fontenay-aux-Roses. Paris.

LAMBE, T.W. & WHITMAN, R.V.(1979): Soil Mechanics. *Wiley*. New York. 553 pp.

LAWRENCE, G.P., PAYNE, D. & GREENLAND, D.J.(1979): Pore size distribution in critical pint and freeze dried aggregates from clay subsoils. *J. Soil Sci.* 30: 499-516.

LEONE, G.; REYES, E.; CORTECCI, G.; POCHINI, A. & LINARES, J.(1983): Genesis of bentonites from Cabo de Gata, Almería, Spain: a stable isotope study. Clay Minerals 18: 227-238.

LIDE, D.R.(1995): CRC Handbook of Chemistry and Physics. 75th ed. *CRC Press*.

LINARES, J. *et al.*(1993): Investigación de bentonitas como materiales de sellado para almacenamiento de residuos radiactivos de alta actividad. *Publicación Técnica ENRESA* 01/93. Madrid. 324 pp.

LINARES, J. *et al.*(1996): Alteración hidrotermal de las bentonitas de Almería. *Publicación Técnica ENRESA* 06/96. Madrid. 151 pp.

LLORET, A.(1982): Comportamiento deformacional del suelo no saturado bajo condiciones drenadas y no drenadas. *Ph. D. Thesis*. Universidad Politécnica de Cataluña.

LLORET, A. & ALONSO, E.(1980): Consolidation of unsaturated soils including swelling and collapse behaviour. *Géotechnique* 30(4): 449-477.

LUIS Y LUIS, P.(1990): Determinación de propiedades físico-químicas de materiales cerámicos. *Final Report*. UCM. Depto. de Ingeniería Química. Madrid. 208 pp.

LYTTON, R.L.(1967): Isothermal water movement in clay soils. *Ph. D. Dissertation*. University of Texas. Austin. 231 pp.

MARSHALL, T.J.(1958):A relation between permeability and size distribution of pores. *J. Soil Science* 9:1-8.

MARTIN, R.T.(1962): Adsorbed water on clay: a review. *9th Nat. Conf. On Clays and Clay Minerals*. Pergamon. Oxford. 28-70.

MARTÍN, P.L.(1999): Ensayo en maqueta: informe final. Instalación y operación. Versión 0. *CIEMAT report. FEBEX report* 70-IMA-M-9-4. Madrid.

MARTÍN, P.L. & DARDAINE, M.(1990): Resultados preliminares de compactación uniaxial industrial sobre dos bentonitas españolas seleccionadas: MAC-C de la Cuenca de Madrid y S-2 de la zona de Almería. Resultados de la Fase I. Contrato CEA/ENRESA A2845. *Rapport Technique RDD* 98/17. 57 pp.

MARTÍN, P.L.; DARDAINE, M. & LAJUDIE, A.(1990): Resultados de compactación uniaxial industrial sobre una bentonita española seleccionada: S-2 de la zona de Almería. Resultados de la Fase I. Contrato CEA/ENRESA A2845. *Rapport Technique DSD* 90/18. 53 pp.

MATYAS, E.L.(1967): Air and water permeability of compacted soils. In: Permeability and Capillary of Soils. *ASTM STP* 417. 160-175.

MATYAS, E.L. & RADHAKRISHNA, H.S.(1968): Volume change characteristics of partially saturated soils. *Géotechnique* 18: 432-448.

McNEAL, B.L. & COLEMAN, N.T.(1966): Effect of solution composition on soil hydraulic conductivity. *Soil Sci. Soc. Amer. Proc.* 308-317.

MEYER, D. & HOWARD, J.J.(eds.)(1983): Evaluation of clays and clay minerals for application to repository sealing. *Technical Report* ONWI-486. DE83 017788. DOE. 180 pp.

MICROMERITICS (1985): Instruction Manual Poresizer 9310. V 1.00. Norcross, GE.

MILLINGTON, R.J. & QUIRK, J.P.(1961): Permeability of porous solids. *Trans. Faraday Soc.* 57: 1200-1206.

MINGARRO, M; RODRÍGUEZ, V. & GARCÍA BACHILLER, J.(1997): Estudios microbiológicos de la arcilla FEBEX. *CIEMAT/IMA/*54223/4/00 report. *FEBEX report* 70-IMA-L-0-68. Madrid.

MINGARRO, E.; RIVAS, P.; VILLAR, L.P. del; CRUZ, B. de la; GOMEZ, P.; HERNANDEZ, A.; TURRERO, M.J.; VILLAR, M.V.; CAMPOS, R.; COZAR, J.(1991): Characterization of clay (bentonite)/crushed granite mixtures to build barriers against the migration of radionuclides: diffusion studies and physical properties. Task 3-Characterization of radioactive waste forms. A series of final reports (1985-1989)-No.35. *Nuclear science and technology series*. *Commission of the European Communities*. Luxembourg. 136 pp.

MITCHELL, J.K.(1976): Fundamentals of soil behavior. *John Wiley & Sons, Inc*. New York. 422 pp.

MOORE, D.M. & REYNOLDS, R.C.(1989): Identification of mixed-layered clay minerals. In: X Ray Diffraction and the Identification and Analysis of Clay Minerals. *Oxford University Press*. 202-240.

MUALEM, Y.(1976): A new model for predicting the hydraulic conductivity of unsaturated porous media. *Water Resour. Res*. 12: 513-522.

MULTON, J.-L.; BIZOT, H. & MARTIN, G.(1981): Eau (teneur, activité, absorption, propriétés fonctionnelles)-humidités relatives. In: DEYMIÉ, B.; MULTON, J.-L. & SIMON, D.(coord.): Tecniques d'analyse et de contrôle dans les industries agroalimentaires. Sciences et Techniques Agro-alimentaires 4: 1-60. Technique et Documentation. *Apria*.

NAVARRO, V.(1996): Modelo de comportamiento mecánico e hidráulico de suelos no saturados en condiciones no isotermas. *Ph. D. Thesis*. Universidad Politécnica de Cataluña. Barcelona.

NEERDAEL, B.; MEYNENDONCKX, P. & VOET, M.(1992): The Bacchus backfill experiment at the Hades underground research facility at Mol, Belgium. Final Report. *Nuclear Science and Technology Series. EUR* 14155. Luxembourg, 62 pp.

NEWMAN, A.C.D. & BROWN, G.(1987): The chemical constitution of clays. In NEWMAN, A.C.D.(ed.): Chemisty of clays and clay minerals. *Mineralogical Society Monograph* 6. Longman Scientific & Technical.

OLPHEN, M. & FRIPIAT, J.J.(1979)(eds.): Data Handbook for Clay Materials and Other Non-metallic Minerals. *Pergamon Press*. 203-216.

OLSEN, H.W.(1962): Hydraulic flow through saturated clays. *9th Nat. Conf. On Clays and Clay Minerals. Pergamon*. Oxford. 170-182.

PEREZ DEL VILLAR, L.(1989a): Caracterización mineralógica y geoquímica de algunas muestras de bentonita procedentes de la Cuenca terciaria de Madrid (Yuncos, Toledo). *CIEMAT report*. Madrid. 29 pp.

PEREZ DEL VILLAR, L.(1989b): Caracterización mineralógica y geoquímica de algunas muestras de bentonita procedentes de la provincia de Almería. *CIEMAT report*. Madrid. 29 pp.

PEREZ DEL VILLAR, L.; de la CRUZ, B. & COZAR, J.S. (1991): Estudio mineralógico, geoquímico y de alterabilidad de las arcillas de Serrata de Níjar (Almería) y del Cerro del Monte (Toledo). *CIEMAT report*. Madrid. 51 pp.

PINTADO, X.; LEDESMA, A. & LLORET, A.(1998): Back-analysis of thermohydraulic bentonite properties from laboratory tests. *Int. Workshop on Key Issues in Waste Isolation Research*. Barcelona.

POUSADA, E.(1984): Deformabilidad de las arcillas expansivas bajo succión controlada. *Ph. D. Thesis. Cuadernos de investigación* C8. *CEDEX*. Madrid. 274 pp.

PROST, R.; KOUTIT, T.; BENCHARA, A. & HUARD, E.(1998): State and location of water adsorbed on clay minerals: consequences of the hydration and swelling-shrinkage phenomena. *Clays and Clay Minerals* 46(2): 117-131.

PUSCH, R.(1979): Highly compacted sodium bentonite for isolating rock-deposited radioactive waste products. *Nuclear Technology* 45: 153-157.

PUSCH, R.(1985): Final Report of the Buffer Mass Test - Volume III: Chemical and physical stability of the buffer materials. *Stripa Project* 85/14. *SKB*. Stockholm. 65 pp.

PUSCH, R.(1994): Waste disposal in rock. *Developments in Geotechnical Engineering* 76. *Elsevier*. Amsterdam. 490 pp.

PUSCH, R. & BÖRGESSON, L.(1985): Final Report of the Buffer Mass Test - Volume II: Test results. *Stripa Project* 85/12. *SKB*. Stockholm. 195 pp.

PUSCH, R.& GRAY, M.N.(1989): Sealing of radioactive waste repositories in crystalline rock. *OECD-NEA/ CEC Workshop "Sealing of Radioactive Waste Repositories"*. Braunschweig.

PUSCH, R.; KARNLAND, O. & HÖKMARK, H.(1990): GMM -A general microstructural model for qualita-

tive and quantitative studies on smectite clays. *SKB Technical Report 90-43*. 94 pp.

PUSCH, R.; MUURINEN, A.; LEHIKOINEN, J.; BORS, J. & ERIKSEN, T.(1999): Microstructural and chemical parameters of bentonite as determinants of waste isolation efficiency. Final report. *Nuclear science and technology series. EUR* 18950. Luxembourg. 121 pp.

PUSCH, R.; NILSSON, J. & RAMQVIST, G.(1985): Final Report of the Buffer Mass Test – Volume I: scope, preparative field work, and test arrangement. *Technical Report Stripa Project* 85-11. SKB, Stockholm. 190 pp.

RICHARDS, L.A.(1941): A pressure membrane extraction apparatus for soil suction. *Soil Science* 51: 377-386.

RICHARDS, B.G. (1965): A thermistor hygrometer for the direct measurement of the free energy of soil moisture. CSIRO Soil Mechanics Section. *Technical Report* Nº5. Melbourne.

RICHARDS, B.G. (1967): Moisture flow and equilibria in unsaturated soils for shallow foundations. Permeability and Capillarity of Soils. *ASTM. STP* 417: 4-34.

RICHARDS, B.G. (1978): Application of an experimentally based non-linear constitutive model of soils in laboratory and field tests. *Aust. Geomech. Jnl.* G8: 20-30.

RICHARDS, B.G.(1984): Finite element analysis of volume change in expansive clays. *Proc. 5th Int. Conf. on Expansive Soils*. Adelaida. 41-45.

RICHARDS, B.G.; PETER, P. & MARTIN, R. (1984): The determination of volume change properties in expansive soils. *Proc. 5th Int. Conf. on Exp. Soils.* Adelaide. 179-186.

RIDLEY, A.M. & BURLAND, J.B.(1993): A new instrument for the measurement of soil moisture suction. *Géotechnique* 43(2): 321-324.

RIDLEY, A.M. & BURLAND, J.B.(1995): Measurement of suction in materials with swell. *Applied Mechanics Reviews* 48(9).

RIVAS, P; VILLAR, M.V.; CAMPOS, R.; PELAYO, M.; MARTIN, P.L.; GOMEZ, P.; TURRERO, M.J.; HERNANDEZ, A.I.; COZAR, J.S. & MINGARRO, E.(1991): Caracterización de materiales de relleno y sellado para almacenamiento de residuos radiactivos: bentonitas españolas. *CIEMAT-DT-TG report*. Madrid. 196 pp.

ROLFE, P.F. & AYLMORE, L.A.G.(1977): Water and salt flow through compacted clays: I. Permeability of compacted illite and montmorillonite. *Soil Sci. Soc. Am. J.* 41: 489-495.

ROMERO, E.(1999): Characterisation and thermo-hydro-mechanical behaviour of unsaturated Boom-clay: An experimental study. *Ph. D. Thesis.* Universidad Politécnica de Cataluña. Barcelona. 405 pp.

ROMERO, E.; GENS, A. & LLORET, A.(1999): Water permeability, water retention and microstructure of unsaturated compacted Boom Clay. *Engineering Geology* 54: 117-127.

ROSS, C.S. & HENDRICKS, S.B.(1945): Minerals of the montmorillonite group – Their origin and relation to soils and clays. *US Geological Survey Professional Paper* 205-B. 79 pp.

SAIX, C. & JOUANNA, P.(1990): Appareil triaxial pour l'étude du comportement thermique de sols non saturés. *Can. Geotech. J.* 27: 119-128.

SALO, J.-P. & KUKKOLA, T.(1989): Bentonite pellets, an alternative buffer material for spent fuel canister deposition holes. *Workshop "Sealing of Radioactive Waste Repositories"*. Braunschweig.

SCHAAP, M.G.(1999): Rosetta help file: Predicting soil hydraulic parameters form basic soil data. http://www.ussl.ars.usda.gov/MODELS/rosetta.

SELVADURAI, A.P.S.(1997): Hydro-thermo-mechanics of engineered clay barriers and geological barriers (Foreword). *Eng. Geol*. 47: 311-312.

SING, K.S.W.; EVERETT, D.H.; HAUL, R.A.W.; MOSCOU, L.; PIEROTTI, R.A.; ROUQUÉROL, J. & SIEMIENIEWSKA, T.(1985): Reporting physisorption data for gas/solid systems with special reference to the determination of surface area and porosity. *Pure & Appl. Chem*. 57(4): 603-619. IUPAC.

SPOSITO, G. & PROST, R.(1982): Structure of water adsorbed on smectites. *Chem. Rev*. 82:554-573.

STEPKOWSKA, E.T.(1990): Aspects of the clay/electrolyte/water system with special reference to the geotechnical properties of clays. *Eng. Geol.* 28(3-4): 249-268.

STUDDS, P.G.; STEWART, D.I. & COUSENS, T.W.(1998): The effects of salt solutions on the properties of bentonite–sand mixtures. *Clay Minerals* 33: 651-660.

TESSIER, D.; LAJUDIE, A. PETIT, J.-C.(1992): Relation between the macroscopic behaviour of clays and their microstructural properties. *Appl. Geochem.* 1: 151-161.

THOMÉ, F.(1993): Comportamiento de los suelos parcialmente saturados bajo succión controlada. *Ph. D. Thesis*. *Cuadernos de investigación C36. CEDEX.* Madrid. 241 pp.

TINDALL, J.A. & KUNKEL, J.R.(1999): Unsaturated Zone Hydrology for Scientists and Engineers. *Prentice Hall.* Upper Saddle River. 624 pp.

TISOT, J.P. & ABOUSHOOK, M.(1983): Triaxial study of swelling characteristics. *Proc. 7th Asian Conf. Soil Mech. Found. Eng*. 1: 94-97. Manila.

TSIGE, M.(1999): Microfábrica y mineralogía de las arcilla azules del Guadalquivir: influencia en su comportamiento geotécnico. *Ph. D. Thesis*. *Monografías M66. CEDEX*. Madrid. 294 pp.

TUNCER, E.R.(1988): Pore size distribution characteristics of tropical soils in relation to engineering properties. *2nd Inst. Conf. on Geomechanics in Tropical Soils* 1: 63-70. Singapore.

UNE 7045(1952): Determinación de la porosidad de un terreno.

UNE 103-104-93: Determinación del límite plástico de un suelo. *AENOR*.

UNE 103-300-93: Determinación de la humedad de un suelo mediante secado en estufa. *AENOR*.

UNE 103-103-94: Determinación del límite líquido de un suelo por el método del aparato de Casagrande. *AENOR*.

UNE 103-302-94: Determinación de la densidad relativa de las partículas de un suelo. *AENOR*.

UNE 103-101-95: Análisis granulométrico de suelos por tamizado. *AENOR*.

UNE 103-102-95: Análisis granulométrico de suelos finos por sedimentación. Método del densímetro. *AENOR*.

UPC (1998): FEBEX. Preoperational thermo-hydro-mechanical (THM) modelling of the "in situ" test. *Publicación técnica ENRESA* 09/98. Madrid. 99 pp.

VANAPALLI, S.K.; FREDLUND, D.G. & PUFAHL, D.E.(1999): The influence of soil structure and stress history on the soil-water characteristics of a compacted till. *Géotechnique* 49(2): 143-159.

VAN GENUCHTEN, M. TH.(1980): A closed-form equation for predicting the hydraulic conductivity of unsaturated soils. *Soil Science Society of America Journal* 44: 892-898.

VAN GENUCTHEN, M. Th.; LEIJ, F.J. & YATES, S.R.(1991): The RETC code for quantifying the hydraulic functions of unsaturated soils. U.S. Salinity Laboratory IAG-DW12933934. U.S. Environmental Protection Agency EPA/600/2-91/065. Riverside.

VICOL, T.(1990): Comportement hydraulique et mécanique d'un limon non saturé. Application à la modélisation. *Thèse de Doctorat de l'Ecole Nationale de Ponts et Chausées*. Paris. 257 pp.

VILLAR, M.V.(1995a): Thermo-Hydro-Mechanical characterization of the Spanish reference clay material for engineered barrier for granite and clay HLW repository: Laboratory and small mock-up testing. *Publicación Técnica ENRESA* 03/95.

VILLAR, M.V.(1995b): First results of suction controlled oedometer tests in highly expansive montmorillonite. In: E.E. ALONSO & P. DELAGE(eds): Unsaturated soils. *Proc. 1st Int. Conf. Unsaturated Soils* (Paris). *Balkema*. Rotterdam. 207-213.

VILLAR, M.V.(1997): Muestreo y caracterización de bloques para el ensayo maqueta del Proyecto FEBEX. *CIEMAT/IMA*/54A15/7/97 report. Madrid.

VILLAR, M.V. & DARDAINE, M.(1990): Contribución a la selección de una arcilla española como material de relleno de un almacenamiento de combustible irradiado en roca dura. Resultados de la Fase I. Contrato CEA/ENRESA A2845. *Rapport Technique DRDS* nº 244 marzo 1990. CEA.

VILLAR, M.V. & MARTIN, P.L.(1996): Suction controlled oedometer tests in montmorillonite clay. Preliminary results. In: S.P. Bentley(ed): Enginering geology of waste disposal. *Geological Society Engineering Geology Special Publ*ication No. 11. The Geological Society. London. 309-311.

VILLAR, M.V.& MARTÍN, P.L.(1999): Efectos sobre el suelo y acuíferos del vertido de las minas de Aznalcóllar: Caracterización física de las muestras de suelo. Version 0. *CIEMAT/DIAE*/54012/3/99 *Technical Report*. Madrid. 27 pp.

VILLAR, M.V. & RIVAS, P.(1994): Hydraulic properites of montmorillonite-quartz and saponite-quartz clay mixtures. *Applied Clay Science* 9: 1-9.

VILLAR, M.V.; FERNÁNDEZ, A.M. & CUEVAS, J.(1997): Caracterización geoquímica de bentonita compactada: Efectos producidos por flujo termohidraúlico. Versión 1. *CIEMAT/IMA*/54A15/6/97 *report*. *FEBEX report* 70-IMA-M-0-2. Madrid.

VOLCKAERT, G.; BERNIER, F.; ALONSO, E.; GENS, A.; SAMPER, J.; VILLAR, M.V.; MARTÍN, P.L.; CUEVAS, J.; CAMPOS, R.; THOMAS, H.R.; IMBERT, C. & ZINGARELLI, V.(1996): Thermal-hydraulic-mechanical and geochemical behaviour of the clay barrier in radioactive waste repositories (model development and validation). *Nuclear science and technology*. *EUR* 16744. Commission of the European Communities. Luxembourg. 722 pp.

VOLCKAERT, G.; ORTIZ, L.; DE CANNIÈRE, P.; PUT, M.; HORSEMAN, S.T.; HARRINGTON, J.F.; FIORAVANTE, V. & IMPEY, D.(1995): MEGAS – Modelling and experiments on gas migration in repository host rocks. Final Report Phase I. *EUR* 16235.

WAN, A.W.L.; GRAY, M.N. & GRAHAM, J.(1995): On the relations of suction, moisture content, and soil structure in compacted clays. In: E.E. ALONSO & P. DELAGE(eds): Unsaturated soils. Proc. 1st Int. Conf. Unsaturated Soils (Paris). *Balkema*. Rotterdam. 215-222.

WHEELER, S.J.(1986): The stress-strain behaviour of soils containing gas bubbles. *PhD*. *Thesis*. University of London.

WHEELER, S.J.(1988): The undrained shear strength of soils containing large gas bubbles. *Géotechnique* 38(3): 399-413.

WHITE, G.N. & DIXON, J.B.(1997): Mineralogical, Physical and Chemical Properties of a Bentonite from Minas de Gádor, Spain. Informe. Clay Mineralogy Laboratory. Soil and Crop Science Departement. *Texas A&M University*. Texas. 18 pp.

WILKINSON, W.B. & SHIPLEY, E.L.(1972): Vertical and horizontal laboratory permeability measurements in clay soils. In: IAHR(Ed.): Fundamentals of transport phenomena in porous media. *Developments in Soil Science* 2. Elsevier. 285-297.

WIND, G.P.(1966): Capillary conductivity data estimated by a simple method. *Proc. UNESCO/IASH Symp. Water in the Unsturated Zone*. Wageningen. 181-191.

WONG, H.Y. & YONG, R.N.(1975): Unsaturated flow mechanics in low swelling clays. *Soil Science* 120(5): 339-348.

WOODBURN, J.A.; HOLDEN, J. & PETER, P.(1993): The transistor psychrometer: a new instrument for measuring soil suction. In: HOUSTO & WRAY (eds.): Unsaturated Soils. *Geotechnical Special Publications ASCE* nº39. Dallas. 91-102.

WOODING, R.A.(1968): Steady infiltration from a shallow circular pond. *Water Resour. Res*. 4: 1259-1273.

YONG, R.N.; BOONSINSUK, P. & WONG, G.(1986): Formulation of backfill material for a nuclear fuel waste disposal vault. *Can. Geotech. J*. 23: 216-228.

YONG, R.N.; MOHAMED, A.M.O. & WARKENTIN, B.P. (1992): Principles of contaminant transport in soils. *Developments in Geotechnical Engineering* 73. *Elsevier*. Amsterdam. 327 pp.

YOSHIMI, Y. & OSTERBERG, J.O.(1963): Compression of partially saturated cohesive soils. *J. Soil Mechanics and Foundations Division*. ASCE 89, SM 4: 1-24.

PUBLICACIONES TÉCNICAS

1991

01 *REVISIÓN SOBRE LOS MODELOS NUMÉRICOS RELACIONADOS ON EL ALMACENAMIENTO DE RESIDUOS RADIACTIVOS.*

02 *REVISIÓN SOBRE LOS MODELOS NUMÉRICOS RELACIONADO CON EL ALMACENAMIENTO DE RESIDUOS RADIACTIVOS. ANEXO 1. Guía de códigos aplicables.*

03 *PRELIMINARY SOLUBILITY STUDIES OF URANIUM DIOXIDE UNDER THE CONDITIONS EXPECTED IN A SALINE REPOSITORY.*

04 *GEOESTADÍSTICA PARA EL ANÁLISIS DE RIESGOS. Una introducción a la Geoestadística no paramétrica.*

05 *SITUACIONES SINÓPTICAS Y CAMPOS DE VIENTOS ASOCIADOS EN "EL CABRIL".*

06 *PARAMETERS, METHODOLOGIES AND PRIORITIES OF SITE SELECTION FOR RADIOACTIVE WASTE DISPOSAL IN ROCK SALT FORMATIONS.*

1992

01 *STATE OF THE ART REPORT: DISPOSAL OF RADIACTIVE WASTE IN DEEP ARGILLACEOUS FORMATIONS.*

02 *ESTUDIO DE LA INFILTRACIÓN A TRAVÉS DE LA COBERTERA DE LA FUA.*

03 *SPANISH PARTICIPATION IN THE INTERNATIONAL INTRAVAL PROJECT.*

04 *CARACTERIZACIÓN DE ESMECTITAS MAGNÉSICAS DE LA CUENCA DE MADRID COMO MATERIALES DE SELLADO. Ensayos de alteración hidrotermal.*

05 *SOLUBILITY STUDIES OF URANIUM DIOXIDE UNDER THE CONDITIONS EXPECTED IN A SALINE REPOSITORY. Phase II*

06 *REVISIÓN DE MÉTODOS GEOFÍSICOS APLICABLES AL ESTUDIO Y CARACTERIZACIÓN DE EMPLAZAMIENTOS PARA ALMACENAMIENTO DE RESIDUOS RADIACTIVOS DE ALTA ACTIVIDAD EN GRANITOS, SALES Y ARCILLAS.*

07 *COEFICIENTES DE DISTRIBUCIÓN ENTRE RADIONUCLEIDOS.*

08 *CONTRIBUTION BY CTN-UPM TO THE PSACOIN LEVEL-S EXERCISE.*

09 *DESARROLLO DE UN MODELO DE RESUSPENSIÓN DE SUELOS CONTAMINADOS. APLICACIÓN AL ÁREA DE PALOMARES.*

10 *ESTUDIO DEL CÓDIGO FFSM PARA CAMPO LEJANO. IMPLANTACIÓN EN VAX.*

11 *LA EVALUACIÓN DE LA SEGURIDAD DE LOS SISTEMAS DE ALMACENAMIENTO DE RESIDUOS RADIACTIVOS. UTILIZACIÓN DE MÉTODOS PROBABILISTAS.*

12 *METODOLOGÍA CANADIENSE DE EVALUACIÓN DE LA SEGURIDAD DE LOS ALMACENAMIENTOS DE RESIDUOS RADIACTIVOS.*

13 *DESCRIPCIÓN DE LA BASE DE DATOS WALKER.*

Publicaciones no periódicas

PONENCIAS E INFORMES, 1988-1991.
SEGUNDO PLAN DE I+D, 1991-1995. TOMOS I, II Y III.
SECOND RESEARCH AND DEVELOPMENT PLAN, 1991-1995, VOLUME I.

1993

01 *INVESTIGACIÓN DE BENTONITAS COMO MATERIALES DE SELLADO PARA ALMACENAMIENTO DE RESIDUOS RADIACTIVOS DE ALTA ACTIVIDAD. ZONA DE CABO DE GATA, ALMERÍA.*

02 *TEMPERATURA DISTRIBUTION IN A HYPOTHETICAL SPENT NUCLEAR FUEL REPOSITORY IN A SALT DOME.*

03 *ANÁLISIS DEL CONTENIDO EN AGUA EN FORMACIONES SALINAS. Su aplicación al almacenamiento de residuos radiactivos*

04 *SPANISH PARTICIPATION IN THE HAW PROJECT. Laboratory Investigations on Gamma Irradiation Effects in Rock Salt.*

05 *CARACTERIZACIÓN Y VALIDACIÓN INDUSTRIAL DE MATERIALES ARCILLOSOS COMO BARRERA DE INGENIERÍA.*

06 *CHEMISTRY OF URANIUM IN BRINES RELATED TO THE SPENT FUEL DISPOSAL IN A SALT REPOSITORY (I).*

07 *SIMULACIÓN TÉRMICA DEL ALMACENAMIENTO EN GALERÍA-TSS.*

08 *PROGRAMAS COMPLEMENTARIOS PARA EL ANÁLISIS ESTOCÁSTICO DEL TRANSPORTE DE RADIONUCLEIDOS.*

09 *PROGRAMAS PARA EL CÁLCULO DE PERMEABILIDADES DE BLOQUE.*

10 *METHODS AND RESULTS OF THE INVESTIGATION OF THE THERMOMECHANICAL BEAVIOUR OF ROCK SALT WITH REGARD TO THE FINAL DISPOSAL OF HIGH-LEVEL RADIOACTIVE WASTES.*

Publicaciones no periódicas

SEGUNDO PLAN DE I+D. INFORME ANUAL 1992.

PRIMERAS JORNADAS DE I+D EN LA GESTIÓN DE RESIDUOS RADIACTIVOS. TOMOS I Y II.

1994

01 *MODELO CONCEPTUAL DE FUNCIONAMIENTO DE LOS ECOSISTEMAS EN EL ENTORNO DE LA FÁBRICA DE URANIO DE ANDÚJAR.*

02 *CORROSION OF CANDIDATE MATERIALS FOR CANISTER APPLICATIONS IN ROCK SALT FORMATIONS.*

03 *STOCHASTIC MODELING OF GROUNDWATER TRAVEL TIMES*

04 *THE DISPOSAL OF HIGH LEVEL RADIOACTIVE WASTE IN ARGILLACEOUS HOST ROCKS. Identification of parameters, constraints and geological assessment priorities.*

05 *EL OESTE DE EUROPA Y LA PENÍNSULA IBÉRICA DESDE HACE -120.000 AÑOS HASTA EL PRESENTE. Isostasia glaciar, paleogeografías paleotemperaturas.*

06 *ECOLOGÍA EN LOS SISTEMAS ACUÁTICOS EN EL ENTORNO DE EL CABRIL.*

07 *ALMACENAMIENTO GEOLÓGICO PROFUNDO DE RESIDUOS RADIACTIVOS DE ALTA ACTIVIDAD (AGP). Conceptos preliminares de referencia.*

08 *UNIDADES MÓVILES PARA CARACTERIZACIÓN HIDROGEOQUÍMICA*

09 *EXPERIENCIAS PRELIMINARES DE MIGRACIÓN DE RADIONUCLEIDOS CON MATERIALES GRANÍTICOS. EL BERROCAL, ESPAÑA.*

10 *ESTUDIOS DE DESEQUILIBRIOS ISOTÓPICOS DE SERIES RADIACTIVAS NATURALES EN UN AMBIENTE GRANÍTICO: PLUTÓN DE EL BERROCAL (TOLEDO).*

11 *RELACION ENTRE PARAMETROS GEOFISICOS E HIDROGEOLOGICOS. Una revisión de literatura.*

12 *DISEÑO Y CONSTRUCCIÓN DE LA COBERTURA MULTICAPA DEL DIQUE DE ESTÉRILES DE LA FÁBRICA DE URANIO DE ANDÚJAR.*

Publicaciones no periódicas

SEGUNDO PLAN I+D 1991-1995. INFORME ANUAL 1993.

1995

01 *DETERMINACIÓN DEL MÓDULO DE ELASTICIDAD DE FORMACIONES ARCILLOSAS PROFUNDAS.*

02 *UO_2 LEACHING AND RADIONUCLIDE RELEASE MODELLING UNDER HIGH AND LOW IONIC STRENGTH SOLUTION AND OXIDATION CONDITIONS.*

03 *THERMO-HYDRO-MECHANICAL CHARACTERIZATION OF THE SPANISH REFERENCE CLAY MATERIAL FOR ENGINEERED BARRIER FOR GRANITE AND CLAY HLW REPOSITORY: LABORATORY AND SMALL MOCK UP TESTING.*

04 *DOCUMENTO DE SÍNTESIS DE LA ASISTENCIA GEOTÉCNICA AL DISEÑO AGP-ARCILLA. Concepto de referencia.*

05 *DETERMINACIÓN DE LA ENERGÍA ACUMULADA EN LAS ROCAS SALINAS FUERTEMENTE IRRADIADAS MEDIANTE TÉCNICAS DE TERMOLUMINISCENCIA. Aplicación al análisis de repositorios de residuos radiactivos de alta actividad.*

06 *PREDICCIÓN DE FENÓMENOS DE TRANSPORTE EN CAMPO PRÓXIMO Y LEJANO. Interacción en fases sólidas.*

07 *ASPECTOS RELACIONADOS CON LA PROTECCIÓN RADIOLÓGICA DURANTE EL DESMANTELAMIENTO Y CLAUSURA DE LA FÁBRICA DE ANDÚJAR.*

08 *ANALYSIS OF GAS GENERATION MECHANISMS IN UNDERGROUND RADIACTIVE WASTE REPOSITORIES. (Pegase Project).*

09 *ENSAYOS DE LIXIVIACIÓN DE EMISORES BETA PUROS DE LARGA VIDA.*

10 *2º PLAN DE I+D. DESARROLLOS METODOLÓGICOS, TECNOLÓGICOS, INSTRUMENTALES Y NUMÉRICOS EN LA GESTIÓN DE RESIDUOS RADIACTIVOS.*

11 *PROYECTO AGP- ALMACENAMIENTO GEOLÓGICO PROFUNDO. FASE 2.*

12 *IN SITU INVESTIGATION OF THE LONG-TERM SEALING SYSTEM AS COMPONENT OF DAM CONSTRUCTION (DAM PROJECT). Numerical simulator: Code-Bright.*

Publicaciones no periódicas

TERCER PLAN DE I+D 1995-1999.

SEGUNDAS JORNADAS DE I+D. EN LA GESTIÓN DE RESIDUOS RADIACTIVOS. TOMOS I Y II.

1996

01 *DESARROLLO DE UN PROGRAMA INFORMÁTICO PARA EL ASESORAMIENTO DE LA OPERACIÓN DE FOCOS EMISORES DE CONTAMINANTES GASEOSOS.*

02 *FINAL REPORT OF PHYSICAL TEST PROGRAM CONCERNING SPANISH CLAYS (SAPONITES AND BENTONITES).*

03 *APORTACIONES AL CONOCIMIENTO DE LA EVOLUCIÓN PALEOCLIMÁTICA Y PALEOAMBIENTAL EN LA PENÍNSULA IBÉRICA DURANTE LOS DOS ÚLTIMOS MILLONES DE AÑOS A PARTIR DEL ESTUDIO DE TRAVERTINOS Y ESPELEOTEMAS.*

04 *MÉTODOS GEOESTADÍSTICOS PARA LA INTEGRACIÓN DE INFORMACIÓN.*

05 *ESTUDIO DE LONGEVIDAD EN BENTONITAS: ESTABILIDAD HIDROTERMAL DE SAPONITAS.*

06 *ALTERACIÓN HIDROTERMAL DE LAS BENTONITAS DE ALMERÍA.*

07 *MAYDAY. UN CÓDIGO PARA REALIZAR ANÁLISIS DE INCERTIDUMBRE Y SENSIBILIDAD. Manuales.*

Publicaciones no periódicas

EL BERROCAL PROJECT. VOLUME I. GEOLOGICAL STUDIES.

EL BERROCAL PROJECT. VOLUME II. HYDROGEOCHEMISTRY.

EL BERROCAL PROJECT. VOLUME III. LABORATORY MIGRATION TESTS AND IN SITU TRACER TEST.

EL BERROCAL PROJECT. VOLUME IV. HYDROGEOLOGICAL MODELLING AND CODE DEVELOPMENT.

1997

01 *CONSIDERACIÓN DEL CAMBIO MEDIOAMBIENTAL EN LA EVALUACIÓN DE LA SEGURIDAD. ESCENARIOS CLIMÁTICOS A LARGO PLAZO EN LA PENÍNSULA IBÉRICA.*

02 *METODOLOGÍA DE EVALUACIÓN DE RIESGO SÍSMICO EN SEGMENTOS DE FALLA.*

03 *DETERMINACIÓN DE RADIONUCLEIDOS PRESENTES EN EL INVENTARIO DE REFERENCIA DEL CENTRO DE ALMACENAMIENTO DE EL CABRIL.*

04 *ALMACENAMIENTO DEFINITIVO DE RESIDUOS DE RADIACTIVIDAD ALTA. Caracterización y comportamiento a largo plazo de los combustibles nucleares irradiados (I).*

05 *METODOLOGÍA DE ANÁLISIS DE LA BIOSFERA EN LA EVALUACIÓN DE ALMACENAMIENTOS GEOLÓGICOS PROFUNDOS DE RESIDUOS RADIACTIVOS DE ALTA ACTIVIDAD ESPECÍFICA.*

06 *EVALUACIÓN DEL COMPORTAMIENTO Y DE LA SEGURIDAD DE UN ALMACENAMIENTO GEOLÓGICO PROFUNDO EN GRANITO. Marzo 1997*

07 *SÍNTESIS TECTOESTRATIGRÁFICA DEL MACIZO HESPÉRICO. VOLUMEN I.*

Títulos publicados

08 *IIIas JORNADAS DE I+D Y TECNOLOGÍAS DE GESTIÓN DE RESIDUOS RADIACTIVOS. Pósters descriptivos de los proyectos de I+D y evaluación de la seguridad a largo plazo.*

09 *FEBEX. ETAPA PREOPERACIONAL. INFORME DE SÍNTESIS.*

10 *METODOLOGÍA DE GENERACIÓN DE ESCENARIOS PARA LA EVALUACIÓN DEL COMPORTAMIENTO DE LOS ALMACENAMIENTOS DE RESIDUOS RADIACTIVOS.*

11 *MANUAL DE CESARR V.2. Código para la evaluación de seguridad de un almacenamiento superficial de residuos radiactivos de baja y media actividad.*

1998

01 *FEBEX. PRE-OPERATIONAL STAGE. SUMMARY REPORT.*

02 *PERFORMANCE ASSESSMENT OF A DEEP GEOLOGICAL REPOSITORY IN GRANITE. March 1997.*

03 *FEBEX. DISEÑO FINAL Y MONTAJE DEL ENSAYO "IN SITU" EN GRIMSEL.*

04 *FEBEX. BENTONITA: ORIGEN, PROPIEDADES Y FABRICACIÓN DE BLOQUES.*

05 *FEBEX. BENTONITE: ORIGIN, PROPERTIES AND FABRICATION OF BLOCKS.*

06 *TERCERAS JORNADAS DE I+D Y TECNOLOGÍAS DE GESTIÓN DE RESIDUOS RADIACTIVOS. 24-29 Noviembre, 1997. Volumen I*

07 *TERCERAS JORNADAS DE I+D Y TECNOLOGÍAS DE GESTION DE RESIDUOS RADIACTIVOS. 24-29 Noviembre, 1997. Volumen II*

08 *MODELIZACIÓN Y SIMULACIÓN DE BARRERAS CAPILARES.*

09 *FEBEX. PREOPERATIONAL THERMO-HYDRO-MECHANICAL (THM) MODELLING OF THE "IN SITU" TEST.*

10 *FEBEX. PREOPERATIONAL THERMO-HYDRO-MECHANICAL (THM) MODELLING OF THE "MOCK UP" TEST.*

11 *DISOLUCIÓN DEL $UO_2(s)$ EN CONDICIONES REDUCTORAS Y OXIDANTES.*

12 *FEBEX. FINAL DESIGN AND INSTALLATION OF THE "IN SITU" TEST AT GRIMSEL.*

1999

01 *MATERIALES ALTERNATIVOS DE LA CÁPSULA DE ALMACENAMIENTO DE RESDIUOS RADIACTIVOS DE ALTA ACTIVIDAD.*

02 *INTRAVAL PROJECT PHASE 2: STOCHASTIC ANALYSIS OF RADIONUCLIDES TRAVEL TIMES AT THE WASTE ISOLATION PILOT PLANT (WIPP), IN NEW MEXICO (U.S.A.).*

03 *EVALUACIÓN DEL COMPORTAMIENTO Y DE LA SEGURIDAD DE UN ALMACENAMIENTO PROFUNDO EN ARCILLA. Febrero 1999.*

04 *ESTUDIOS DE CORROSIÓN DE MATERIALES METÁLICOS PARA CÁPSULAS DE ALMACENAMIENTO DE RESIDUOS DE ALTA ACTIVIDAD.*

05 *MANUAL DEL USUARIO DEL PROGRAMA VISUAL BALAN V. 1.0. CÓDIGO INTERACTIVO PARA LA REALIZACION DE BALANCES HIDROLÓGICOS Y LA ESTIMACIÓN DE LA RECARGA.*

06 *COMPORTAMIENTO FÍSICO DE LAS CÁPSULAS DE ALMACENAMIENTO.*

07 *PARTICIPACIÓN DEL CIEMAT EN ESTUDIOS DE RADIOECOLOGÍA EN ECOSISTEMAS MARINOS EUROPEOS.*

08 *PLAN DE INVESTIGACIÓN Y DESARROLLO TECNOLÓGICO PARA LA GESTIÓN DE RESIDUOS RADIACTIVOS 1999-2003. OCTUBRE 1999.*

09 *ESTRATIGRAFÍA BIOMOLECULAR. LA RACEMIZACIÓN/EPIMERIZACIÓN DE AMINOACIDOS COMO HERRAMIENTA GEOCRONOLÓGICA Y PALEOTERMOMÉTRICA.*

10 *CATSIUS CLAY PROJECT. Calculation and testing of behaviour of unsaturarted clay as barrier in radioactive waste repositories. STAGE 1: VERIFICATION EXERCISES.*

11 *CATSIUS CLAY PROJECT. Calculation and testing of behaviour of unsaturarted clay as barrier in radioactive waste repositories. STAGE 2: VALIDATION EXERCISES AT LABORATORY SCALE.*

12 *CATSIUS CLAY PROJECT. Calculation and testing of behaviour of unsaturarted clay as barrier in radioactive waste repositories. STAGE 3: VALIDATION EXERCISES AT LARGE "IN SITU" SCALE.*

2000

01 *FEBEX PROJECT. FULL-SCALE ENGINEERED BARRIERS EXPERIMENT FOR A DEEP GEOLOGICAL REPOSITORY FOR HIGH LEVEL RADIOACTIVE WASTE IN CRYISTALLINE HOST ROCK. FINAL REPORT.*

02 *CÁLCULO DE LA GENERACIÓN DE PRODUCTOS RADIOLÍTICOS EN AGUA POR RADIACIÓN α. DETERMINACIÓN DE LA VELOCIDAD DE ALTERACIÓN DE LA MATRIZ DEL COMBUSTIBLE NUCLEAR GASTADO.*

03 *LIBERACIÓN DE RADIONUCLEIDOS E ISÓTOPOS ESTABLES CONTENIDOS EN LA MATRIZ DEL COMBUSTIBLE. MODELO CONCEPTUAL Y MODELO MATEMÁTICO DEL COMPORTAMIENTO DEL RESIDUO.*

04 *DESARROLLO DE UN MODELO GEOQUÍMICO DE CAMPO PRÓXIMO.*

05 *ESTUDIOS DE DISOLUCIÓN DE ANÁLOGOS NATURALES DE COMBUSTIBLE NUCLEAR IRRADIADO Y DE FASES DE (U)VI-SILICIO REPRESENTATIVAS DE UN PROCESO DE ALTERACIÓN OXIDATIVA.*

06 *CORE2D. A CODE FOR NON-ISOTHERMAL WATER FLOW AND REACTIVE SOLUTE TRANSPORT. USERS MANUAL VERSION 2.*

07 *ANÁLOGOS ARQUEOLÓGICOS E INDUSTRIALES PARA ALMACENAMIENTOS PROFUNDOS: ESTUDIO DE PIEZAS ARQUEOLÓGICAS METÁLICAS.*

08 *PLAN DE INVESTIGACIÓN Y DESARROLLO TECNOLÓGICO PARA LA GESTIÓNDE RESIDUOS RADIACTIVOS 1999-2003. REVISIÓN 2000.*

09 *IV JORNADAS DE INVESTIGACIÓN Y DESARROLLO TECNOLÓGICO EN GESTIÓN DE RESIDUOS RADIACTIVOS. POSTERS DIVULGATIVOS.*

10 *IV JORNADAS DE INVESTIGACIÓN Y DESARROLLO TECNOLÓGICO EN GESTIÓN DE RESIDUOS RADIACTIVOS. POSTERS TÉCNICOS.*

11 *PROGRAMA DE INVESTIGACIÓN PARA ESTUDIAR LOS EFECTOS DE LA RADIACIÓN GAMMA EN BENTONITAS CÁLCICAS ESPAÑOLAS.*

12 *CARACTERIZACIÓN Y LIXIVIACIÓN DE COMBUSTIBLES NUCLEARES IRRADIADOS Y DE SUS ANÁLOGOS QUÍMICOS.*

2001

01 *MODELOS DE FLUJO MULTIFÁSICO NO ISOTERMO Y DE TRANSPORTE REACTIVO MULTICOMPONENTE EN MEDIOS POROSOS.*

02 *IV JORNADAS DE INVESTIGACIÓN Y DESARROLLO TECNOLÓGICO EN GESTIÓN DE RESIDUOS RADIACTIVOS. RESÚMENES Y ABSTRACTS.*

03 *ALMACENAMIENTO DEFINITIVO DE RESIDUOS DE RADIACTIVIDAD ALTA. CARACTERIZACIÓN Y COMPORTAMIENTO A LARGO PLAZO DE LOS COMBUSTIBLES NUCLEARES IRRADIADOS (II).*

04 *CONSIDERATIONS ON POSSIBLE SPENT FUEL AND HIGH LEVEL WASTE MANAGEMENT OPTIONS.*

05 *LA PECHBLENDA DE LA MINA FE (CIUDAD RODRIGO, SALAMANCA), COMO ANÁLOGO NATURAL DEL COMPORTAMIENTO DEL COMBUSTIBLE GASTADO. Proyecto Matrix I.*

06 *TESTING AND VALIDATION OF NUMERICAL MODELS OF GROUNDWATER FLOW, SOLUTE TRANSPORT AND CHEMICAL REACTIONS IN FRACTURED GRANITES: A QUANTITATIVE STUDY OF THE HYDROGEOLOGICAL AND HYDROCHEMICAL IMPACT PRODUCED.*

07 *IV JORNADAS DE INVESTIGACIÓN Y DESARROLLO TECNOLÓGICO EN GESTIÓN DE RESIDUOS RADIACTIVOS. Volumen I.*

08 *IV JORNADAS DE INVESTIGACIÓN Y DESARROLLO TECNOLÓGICO EN GESTIÓN DE RESIDUOS RADIACTIVOS. Volumen II.*

09 *IV JORNADAS DE INVESTIGACIÓN Y DESARROLLO TECNOLÓGICO EN GESTIÓN DE RESIDUOS RADIACTIVOS. Volumen III*

10 *IV JORNADAS DE INVESTIGACIÓN Y DESARROLLO TECNOLÓGICO EN GESTIÓN DE RESIDUOS RADIACTIVOS. Volumen IV*

2002

01 *FABRICACIÓN DE BLANCOS PARA LA TRANSMUTACIÓN DE AMERICIO: SÍNTESIS DE MATRICES INERTES POR EL MÉTODO SOL-GEL. ESTUDIO DEL PROCEDIMIENTO DE INFILTRACIÓN DE DISOLUCIONES RADIACTIVAS.*

02 *ESTUDIO GEOQUÍMICO DE LOS PROCESOS DE INTERACCIÓN AGUA-ROCA SOBRE SISTEMAS GEOTERMALES DE AGUAS ALCALINAS GRANITOIDES.*

03 *ALTERACIÓN ALCALINA HIDROTERMAL DE LA BARRERA DE BENTONITA POR AGUAS INTERSTICIALES DE CEMENTOS.*

Thermo-hydro-mechanical characterisation of a bentonite from Cabo de Gata

A study applied to the use of bentonite as sealing material in high level radioactive waste repositories

PUBLICACIÓN TÉCNICA 04/2002

Para más información, dirigirse a:

enresa

Dirección de Comunicación
C/ Emilio Vargas, 7
28043 MADRID

http://www.enresa.es

Abril 2002